A sight for sore eyes

Assessing oncogenic functions of Hdmx and reactivation of p53 as a potential cancer treatment

Proefschrift

ter verkrijging van

de graad van Doctor aan de Universiteit Leiden,

op gezag van Rector Magnificus prof. Mr. P.F. van der Heijden,

volgens besluit van het College voor Promoties

te verdedigen op woensdag 9 mei 2012

klokke 13:45 uur

door

Job de Lange

geboren te Zwolle

in 1982

Promotiecommissie:

Promotor:	Prof. P. Ten Dijke
Co-promotor	Dr. A.G. Jochemsen

Overige leden:

Prof. Dr. B.M. Burgering, UMC Utrecht

Dr. P.A. Van der Velden

Dr. H. Van Attikum

Table of Contents

Chapter 1

General Introduction

The p53 protein was discovered over thirty years ago as a target of the Large T-antigen of the oncogenic DNA virus SV40 [1;2]. Initial observations that p53 possesses oncogenic activity suggested that p53 functions as an oncogene, but it soon became evident that this was due to mutations in the initially isolated cDNAs and that normal p53 rather acts as a tumor suppressor [3]. The p53 protein provides essential protection against malignancies; mice deficient for p53 are prone to develop cancer [4;5] and the p53 gene is mutated in approximately 50% of all human tumors [6;7]. Germ line p53 mutations cause a rare type of cancer predisposition known as Li-Fraumeni Syndrome [8]. Because of its prominent role in cancer, p53 has been the subject of extensive research to understand the different aspects of its regulation and function in different cellular settings. A complex picture has emerged, of which the core message is that p53 functions to cease the growth of damaged cells by regulating the required responses to cellular insults, in order to prevent tumorigenesis. The anti-proliferative functions of p53 are primarily based on its ability to regulate transcription of genes involved in cell cycle arrest, apoptosis, senescence, DNA repair and prevention of angiogenesis [9]. Importantly, 95% of p53 mutations are located in the DNA binding domain, emphasizing the key role of p53 as a transcription factor [10]. However, also transcription-independent activities have been reported, including direct regulation of apoptosis at the mitochondria [11] and regulation of miRNA processing [12]. Interestingly, from an evolutionary perspective it has been argued that p53 was not selected for its tumor suppressor function [13], and p53 is probably involved in many other biological processes as well, such as stem cell homeostasis [14] and fertility [15].

The human p53 protein can be divided into several functional domains (Figure 1). It contains two N-terminal transactivation domains, that allow p53 to interact with transcriptional cofactors [16;17]. The N-terminus also contains the main Hdm2 and Hdmx binding site (see below). The central region of p53 holds a well-conserved DNA binding domain [18]. An oligomerization domain just C-terminal of the DNA binding domain mediates p53 tetramerization, which is crucial for target gene transactivation [19]. A nuclear localization signal [20] and a nuclear export domain [21] are located within the oligomerization domain. The carboxy-terminus consists of a basic domain, which is subject to distinct post-translational modifications and is considered to be a major regulator of p53 transcriptional activity [22]. The p53 tetramer binds to a p53 responsive element (RE) in promoter or intronic sequences of the target gene. A p53 RE consists of two copies of a 10 base-pair motif, separated by a 0-13 base-pair spacer [23]. The exact p53 RE composition determines the binding efficiency, thereby providing a possible mechanism for differential gene regulation by p53 [24].

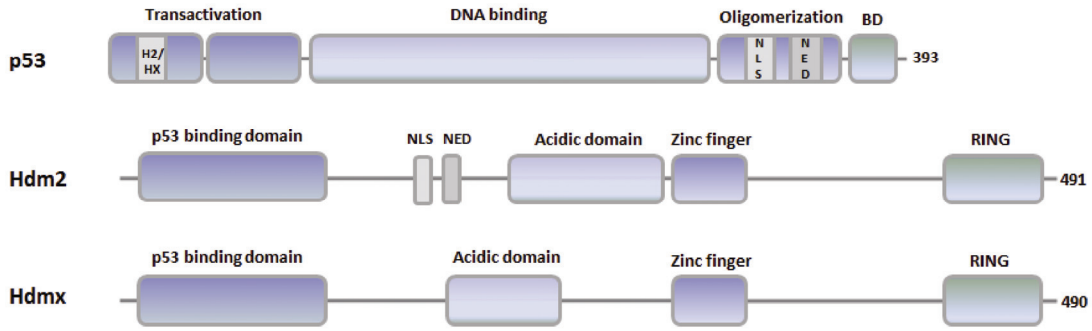

Figure 1 Domain architecture of p53, Hdm2 and Hdmx proteins. H2/HX, Hdm2/Hdmx binding site; NLS, nuclear localization signal; NED, nuclear export domain; BD, basic domain; RING, really interesting new gene.

P53 regulation by Hdm2 and Hdmx

Cells need to keep their p53 activity in check in order to proliferate. Two critical negative regulators of p53 are Mdm2 and Mdmx, in humans mostly referred to as Hdm2 and Hdmx. Mdm2 (murine double minute clone 2) was originally cloned from purified acentric chromosomes, also known as double minutes, which often contain amplified genes that contribute to cellular proliferation and tumorigenesis [25]. Mdm2 was found to directly bind p53, thereby abrogating its transcription regulatory properties [26;27]. The rescue of early embryonic lethality of Mdm2 deficient mice by simultaneous p53 knockout strongly established the importance of Mdm2 in p53 inhibition [28;29]. Later on, another protein showing sequence similarity with Mdm2 was identified to interact with p53 and named Mdmx [30]. Similar to Mdm2, loss of Mdmx also caused p53-dependent embryonic lethality, although occurring somewhat later (E10.5 vs. E4.5) in embryogenesis [31-33]. This indicates that Mdm2 and Mdmx are essential, non-redundant regulators of p53 during embryonic development. In adult tissues, the currently available data indicate that Mdm2 loss is almost invariably lethal, whereas Mdmx loss can be tolerated in some cases [34-39]. Thus, the contribution of Mdm2 and Mdmx to p53 regulation *in vivo* may be cell type-specific.

The human Hdm2 and Hdmx proteins (depicted in Figure 1) show great structural similarities [40]. Best conserved is their N-terminal hydrophobic pocket, which binds to an N-terminal alpha-helix of p53. This binding shields p53's transcription activation domain, thereby inhibiting its activity [41]. In addition, Hdm2 has E3 ubiquitin ligase activity that can target p53 for proteasomal degradation via poly-ubiquitination, for which a central acidic domain as well as a C-terminal RING finger are necessary. Hdmx has no detectable

E3 ligase activity for p53 (or any other substrate), despite the presence of both the acidic domain and the RING finger [42-44]. Hdmx and Hdm2 dimerize via their RING finger domains [45]. The Hdm2-Hdmx hetero-oligomer promotes Hdm2 stability and is a more effective E3 ligase for p53 than the Hdm2 homo-dimer [46;47]. Because the ratio between Hdm2 and Hdmx levels strongly determines p53 stability, it is subject of tight regulation. Besides degrading p53, Hdm2 can also ubiquitinate itself [48;49] and Hdmx [50-52], thereby building positive feedback loops into this system. Moreover, ubiquitinations of Hdm2, Hdmx and p53 can all be counteracted by multiple deubiquitinating enzymes, such as HAUSP [53;54] and USP42 [55]. In addition to the long list of p53 target genes that execute the required biological responses to cellular stress, p53 also transactivates the Hdm2 gene. Since Hdm2 inhibits the p53 response, this provides an important negative feedback loop [56], resulting in out of phase oscillation of p53 and Hdm2 protein levels [57]. More recently, a p53 RE in the first intron of the Hdmx gene has been described. This initiates transcription from an alternative promoter (P2), resulting in an alternative first exon (1β) in the Hdmx mRNA and the synthesis of a slightly longer protein (Hdmx-L), which also contributes to the attenuation phase of the p53 response [58-60].

The p53 pathway as a protective mechanism against cancer

Multiple stress signals can induce the p53 network (Figure 2). These stresses are in many ways related to carcinogenesis and include for example double-strand DNA breaks, DNA replication stress, telomere erosion, oncogene activation, oxidative stress, nitric oxide, hypoxia, ribonucleotide depletion and mitotic apparatus dysfunction [61]. One of the most extensively studied p53 activating triggers is DNA damage. Diverse types of DNA damage lead to the activation of the ataxia-telangiectasia mutated (ATM) and the ataxia-telangiectasia and Rad3-related (ATR) kinases, which subsequently phosphorylate a multitude of proteins, including the checkpoint kinases Chk1 and Chk2 [62]. ATM, ATR, Chk1 and Chk2 have all been reported to directly mediate N-terminal phosphorylations on p53, including the transactivation domain and the Hdm2/Hdmx binding alpha helix [63-65]. These phosphorylations weaken the interaction with Hdm2 and Hdmx, allowing some p53 to escape from functional inhibition. Many other p53 modifications may occur sequentially following phosphorylation [66]. For example, p53 Ser15 phosphorylation stimulates the recruitment of factors involved in transcription, including the acetyl-transferases p300 and CBP [67;68]. This leads to the acetylation of a number of C-terminal lysines, several of which are also ubiquitination sites, thereby contributing to the stabilization of p53 [69]. In addition to p53 modifications, DNA damage signaling also induces the phosphorylation of Hdm2 and Hdmx, resulting in their ubiquitination and degradation [49;70-73].

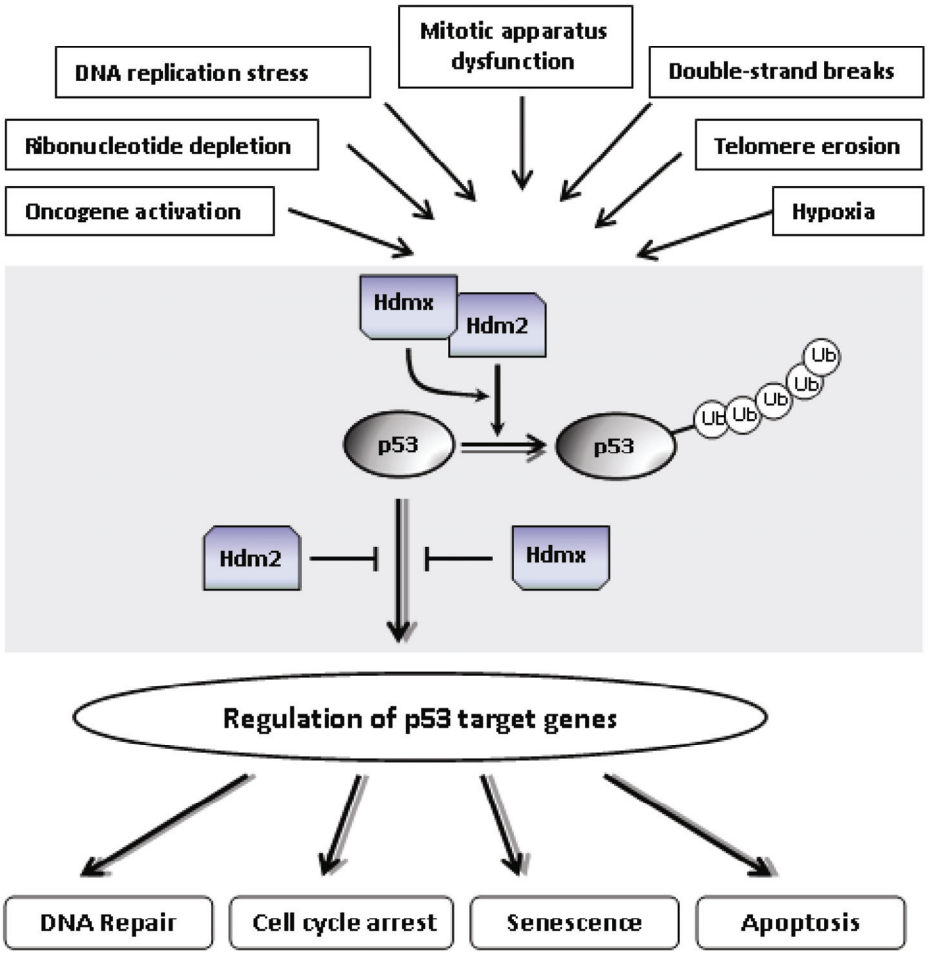

Figure 2 Simplified scheme of the p53 tumor suppressor pathway. Multiple stress signals act upon the inhibitory activities of Hdm2 and Hdmx toward p53. This results in the release and activation of p53, regulation of p53 target genes and the induction of the required cellular response.

Another major p53 activating mechanism involves the deregulation of various mitogenic signaling pathways. The induction of p53 by aberrant activation of oncogenes such as Ras [74], c-myc [75], E2F1 [76], and adenovirus E1A [77] mostly relies on the tumor suppressor protein $p14^{ARF}$. $p14^{ARF}$ (alternative reading frame) is the product of an alternative transcript of the CDKN2A locus which also encodes another tumor suppressor, $p16^{INK4A}$ [78]. $p14^{ARF}$ interacts with Hdm2, thereby directly inhibiting the E3 ligase activity of Hdm2 and also sequestering Hdm2 in the nucleolus [79-81]. This stimulates p53-mediated cellular responses, thereby serving as protection against the tumorigenic consequences of oncogene activation. Loss of this signaling pathway may predispose cells to malignant transformation. Although the resulting tumor cells are no longer growth inhibited by oncogene-induced p53, p53 reactivation might still be achieved through alternative pathways, which could be beneficial for targeting a subset of cancers.

The p53 pathway as target for tumor therapy

As mentioned, about half of all human cancers contain p53 mutations. Mutant p53 can exert tumor-promoting effects, owing to dominant-negative inactivation of wild-type p53 function, as well as to certain oncogenic gain-of-function activities [82]. There is considerable variation of p53 mutation frequency among different cancer types. For instance, p53 mutation occurs in up to 70% of ovarian [83], colorectal [84] and head and neck [85] cancers, whereas it is rare in leukemia's [86], retinoblastoma [87] and melanoma's [88]. The tumors that retain wild-type p53 are assumed to have other defects in p53 regulation or downstream signaling that impede a proper p53 response [89]. For example, some cancers harbor Hdm2 amplification [90], and others show upregulation of Hdmx expression, mostly correlating with wild-type p53 status [91-93].

The pivotal position of p53 in tumor suppression makes it a potentially attractive target for cancer treatment. Several low-molecular-mass compounds aiming at specific reactivation of p53 function have been developed, in order to aid or substitute conventional cancer therapies. For example PRIMA1 [94] has been designed to interact with mutant p53, thereby altering its conformation and restoring p53 activity. This thesis mostly focuses on tumors that express wild-type, but functionally impaired p53. Reactivation of p53 in these tumors may be achieved by inhibiting the p53-Hdm2 interaction. This strategy is exemplified by the small molecule Nutlin-3, which binds Hdm2 in its p53-binding pocket, thereby releasing, stabilizing and activating p53 [95]. Nutlin-3 is a non-genotoxic p53 activator and normal (non-tumor) cells are relatively insensitive to Nutlin-3 induced apoptosis [96]. The biological outcome of p53 activation by Nutlin-3 is highly dependent on the cellular context. Factors contributing to apoptosis induction may include the status of Hdmx [97-99] and E2F1 [100]. Nutlin-3 appeared promising in retinoblastoma treatment, especially when combined with the topoisomerase I inhibitor Topotecan [101]. The use of Nutlin-3 in combination with chemotherapeutics may enhance their effectiveness and allow such drugs to be administered at lower doses [102-105]. Other examples of Hdm2 antagonists include Benzodiazepinedione [106], MI-63 and MI-219 [107]. Hdmx antagonists have also been described, including SJ172550 [108] and SAH-p53-8 [109], and recently a compound was identified that activated p53 through inhibition of Hdmx transcription [110]. In addition to these Hdm2 and Hdmx targeting drugs, RITA (reactivation of p53 and induction of tumor cell apoptosis) was identified to suppress *in vivo* growth of transformed cells in a p53-dependent manner [111], supposedly by direct binding to p53. In addition to p53 stabilization, other effects are likely to contribute to the

activation of a pro-apoptotic program by RITA in tumor cells [112], although the exact mechanisms are still unclear and require further investigations.

Scope of thesis

Much of the work described in this thesis is centered on two types of eye cancer that typically express a wild-type p53 protein: retinoblastoma and uveal melanoma. Retinoblastoma is a rare childhood cancer (approximately 1-2 cases per million people per year [113]) initiating in the retina, a specialized light-sensitive stack of neuronal layers at the back of the eye. Mutations in the RB1 gene, encoding the Rb tumor suppressor protein, are responsible for most cases of retinoblastoma [114]. Loss of Rb in the developing retina activates the tumor surveillance pathway mediated by $p14^{ARF}$, Hdm2 and p53. Interestingly, a particularly high proportion of retinoblastomas apparently select for increased Hdmx levels as a mechanism to suppress the p53 response in Rb-deficient cells [101]. Although most primary melanoma's originate from melanocytes in the skin, in some cases (5.3%) the eye is affected [115]. This type of tumor arises in the uveal tract, comprising iris, ciliary body and choroid. The annual incidence of uveal melanoma in the western world is 6-8 cases per million people [116]. Metastases occur in up to 50% of patients, mostly to the liver, but also to other distant sites such as the lung, bone and skin [117-119]. Prognosis is poor when the tumor has metastasized; median survival is about 10 - 18 months [120;121]. Interestingly, p53 mutations are infrequent in uveal melanoma [122-125].

This thesis presents novel studies regarding the role of Hdmx in p53 inactivation during tumorigenesis, as well as the use of specific drugs for p53 reactivation as cancer treatment. Chapter 2 shows that constitutive Hdmx over-expression contributes to the neoplastic transformation of human fibroblasts and embryonic retinoblasts, thereby functionally resembling loss of p53. Chapter 3 establishes the importance of Hdmx as an oncogene in a subset of uveal melanomas. Importantly, the results described in this chapter extend the function of Hdmx beyond p53 inhibition. Chapter 4 evaluates the use of the specific p53 activating drugs Nutlin-3 and RITA in synergy studies as potential therapy for uveal melanoma. Chapter 5 is a more detailed analysis of the cellular responses to RITA. In particular, Chk2 is shown to be an essential mediator of the RITA-induced effects. Chapter 6 is a general discussion of the results presented in this thesis, and their implications for clinical exploitation and future research.

Reference List

1. Lane,D.P. and Crawford,L.V. (1979) T antigen is bound to a host protein in SV40-transformed cells. *Nature*, **278**, 261-263.

2. Linzer,D.I. and Levine,A.J. (1979) Characterization of a 54K dalton cellular SV40 tumor antigen present in SV40-transformed cells and uninfected embryonal carcinoma cells. *Cell*, **17**, 43-52.

3. Nigro,J.M., Baker,S.J., Preisinger,A.C., Jessup,J.M., Hostetter,R., Cleary,K., Bigner,S.H., Davidson,N., Baylin,S., and Devilee,P. (1989) Mutations in the p53 gene occur in diverse human tumour types. *Nature*, **342**, 705-708.

4. Donehower,L.A., Harvey,M., Slagle,B.L., McArthur,M.J., Montgomery,C.A., Jr., Butel,J.S., and Bradley,A. (1992) Mice deficient for p53 are developmentally normal but susceptible to spontaneous tumours. *Nature*, **356**, 215-221.

5. Jacks,T., Remington,L., Williams,B.O., Schmitt,E.M., Halachmi,S., Bronson,R.T., and Weinberg,R.A. (1994) Tumor spectrum analysis in p53-mutant mice. *Curr.Biol.*, **4**, 1-7.

6. Hainaut,P. and Hollstein,M. (2000) p53 and human cancer: the first ten thousand mutations. *Adv.Cancer Res.*, **77**, 81-137.

7. Hollstein,M., Sidransky,D., Vogelstein,B., and Harris,C.C. (1991) p53 mutations in human cancers. *Science*, **253**, 49-53.

8. Malkin,D., Li,F.P., Strong,L.C., Fraumeni,J.F., Jr., Nelson,C.E., Kim,D.H., Kassel,J., Gryka,M.A., Bischoff,F.Z., Tainsky,M.A., and . (1990) Germ line p53 mutations in a familial syndrome of breast cancer, sarcomas, and other neoplasms. *Science*, **250**, 1233-1238.

9. Vogelstein,B., Lane,D., and Levine,A.J. (2000) Surfing the p53 network. *Nature*, **408**, 307-310.

10. Olivier,M., Eeles,R., Hollstein,M., Khan,M.A., Harris,C.C., and Hainaut,P. (2002) The IARC TP53 database: new online mutation analysis and recommendations to users. *Hum.Mutat.*, **19**, 607-614.

11. Moll,U.M., Wolff,S., Speidel,D., and Deppert,W. (2005) Transcription-independent pro-apoptotic functions of p53. *Curr.Opin.Cell Biol.*, **17**, 631-636.

12. Suzuki,H.I., Yamagata,K., Sugimoto,K., Iwamoto,T., Kato,S., and Miyazono,K. (2009) Modulation of microRNA processing by p53. *Nature*, **460**, 529-533.

13. Aranda-Anzaldo,A. and Dent,M.A. (2007) Reassessing the role of p53 in cancer and ageing from an evolutionary perspective. *Mech.Ageing Dev.*, **128**, 293-302.

14. Pearson,B.J. and Sanchez,A.A. (2010) A planarian p53 homolog regulates proliferation and self-renewal in adult stem cell lineages. *Development*, **137**, 213-221.

15. Kang,H.J., Feng,Z., Sun,Y., Atwal,G., Murphy,M.E., Rebbeck,T.R., Rosenwaks,Z., Levine,A.J., and Hu,W. (2009) Single-nucleotide polymorphisms in the p53 pathway regulate fertility in humans. *Proc.Natl.Acad.Sci.U.S.A*, **106**, 9761-9766.

16. Lill,N.L., Grossman,S.R., Ginsberg,D., DeCaprio,J., and Livingston,D.M. (1997) Binding and modulation of p53 by p300/CBP coactivators. *Nature*, **387**, 823-827.

17. Van Orden,K., Giebler,H.A., Lemasson,I., Gonzales,M., and Nyborg,J.K. (1999) Binding of p53 to the KIX domain of CREB binding protein. A potential link to human T-cell leukemia virus, type I-associated leukemogenesis. *J.Biol.Chem.*, **274**, 26321-26328.

18. Cho,Y., Gorina,S., Jeffrey,P.D., and Pavletich,N.P. (1994) Crystal structure of a p53 tumor suppressor-DNA complex: understanding tumorigenic mutations. *Science*, **265**, 346-355.

19. Chene,P. (2001) The role of tetramerization in p53 function. *Oncogene*, **20**, 2611-2617.

20. Liang,S.H. and Clarke,M.F. (1999) A bipartite nuclear localization signal is required for p53 nuclear import regulated by a carboxyl-terminal domain. *J.Biol.Chem.*, **274**, 32699-32703.

21. Stommel,J.M., Marchenko,N.D., Jimenez,G.S., Moll,U.M., Hope,T.J., and Wahl,G.M. (1999) A leucine-rich nuclear export signal in the p53 tetramerization domain: regulation of subcellular localization and p53 activity by NES masking. *EMBO J.*, **18**, 1660-1672.

22. Scoumanne,A., Harms,K.L., and Chen,X. (2005) Structural basis for gene activation by p53 family members. *Cancer Biol.Ther.*, **4**, 1178-1185.

23. el-Deiry,W.S., Kern,S.E., Pietenpol,J.A., Kinzler,K.W., and Vogelstein,B. (1992) Definition of a consensus binding site for p53. *Nat.Genet.*, **1**, 45-49.

24. Qian,H., Wang,T., Naumovski,L., Lopez,C.D., and Brachmann,R.K. (2002) Groups of p53 target genes involved in specific p53 downstream effects cluster into different classes of DNA binding sites. *Oncogene*, **21**, 7901-7911.

25. Cahilly-Snyder,L., Yang-Feng,T., Francke,U., and George,D.L. (1987) Molecular analysis and chromosomal mapping of amplified genes isolated from a transformed mouse 3T3 cell line. *Somat.Cell Mol.Genet.*, **13**, 235-244.

26. Barak,Y. and Oren,M. (1992) Enhanced binding of a 95 kDa protein to p53 in cells undergoing p53-mediated growth arrest. *EMBO J.*, **11**, 2115-2121.

27. Momand,J., Zambetti,G.P., Olson,D.C., George,D., and Levine,A.J. (1992) The mdm-2 oncogene product forms a complex with the p53 protein and inhibits p53-mediated transactivation. *Cell*, **69**, 1237-1245.

28. Jones,S.N., Roe,A.E., Donehower,L.A., and Bradley,A. (1995) Rescue of embryonic lethality in Mdm2-deficient mice by absence of p53. *Nature*, **378**, 206-208.

29. Montes de Oca,L.R., Wagner,D.S., and Lozano,G. (1995) Rescue of early embryonic lethality in mdm2-deficient mice by deletion of p53. *Nature*, **378**, 203-206.

30. Shvarts,A., Steegenga,W.T., Riteco,N., van Laar,T., Dekker,P., Bazuine,M., van Ham,R.C., van der Houven van Oordt,W., Hateboer,G., van der Eb,A.J., and Jochemsen,A.G. (1996) MDMX: a novel p53-binding protein with some functional properties of MDM2. *EMBO J.*, **15**, 5349-5357.

31. Finch,R.A., Donoviel,D.B., Potter,D., Shi,M., Fan,A., Freed,D.D., Wang,C.Y., Zambrowicz,B.P., Ramirez-Solis,R., Sands,A.T., and Zhang,N. (2002) mdmx is a negative regulator of p53 activity in vivo. *Cancer Res.*, **62**, 3221-3225.

32. Migliorini,D., Lazzerini,D.E., Danovi,D., Jochemsen,A.G., Capillo,M., Gobbi,A., Helin,K., Pelicci,P.G., and Marine,J.C. (2002) Mdm4 (Mdmx) regulates p53-induced growth arrest and neuronal cell death during early embryonic mouse development. *Mol.Cell Biol.*, **22**, 5527-5538.

33. Parant,J., Chavez-Reyes,A., Little,N.A., Yan,W., Reinke,V., Jochemsen,A.G., and Lozano,G. (2001) Rescue of embryonic lethality in Mdm4-null mice by loss of Trp53 suggests a nonoverlapping pathway with MDM2 to regulate p53. *Nat.Genet.*, **29**, 92-95.

34. Francoz,S., Froment,P., Bogaerts,S., De,C.S., Maetens,M., Doumont,G., Bellefroid,E., and Marine,J.C. (2006) Mdm4 and Mdm2 cooperate to inhibit p53 activity in proliferating and quiescent cells in vivo. *Proc.Natl.Acad.Sci.U.S.A*, **103**, 3232-3237.

35. Grier,J.D., Xiong,S., Elizondo-Fraire,A.C., Parant,J.M., and Lozano,G. (2006) Tissue-specific differences of p53 inhibition by Mdm2 and Mdm4. *Mol.Cell Biol.*, **26**, 192-198.

36. Maetens,M., Doumont,G., Clercq,S.D., Francoz,S., Froment,P., Bellefroid,E., Klingmuller,U., Lozano,G., and Marine,J.C. (2007) Distinct roles of Mdm2 and Mdm4 in red cell production. *Blood*, **109**, 2630-2633.

37. Ringshausen,I., O'Shea,C.C., Finch,A.J., Swigart,L.B., and Evan,G.I. (2006) Mdm2 is critically and continuously required to suppress lethal p53 activity in vivo. *Cancer Cell*, **10**, 501-514.

38. Valentin-Vega,Y.A., Okano,H., and Lozano,G. (2008) The intestinal epithelium compensates for p53-mediated cell death and guarantees organismal survival. *Cell Death.Differ.*, **15**, 1772-1781.

39. Valentin-Vega,Y.A., Box,N., Terzian,T., and Lozano,G. (2009) Mdm4 loss in the intestinal epithelium leads to compartmentalized cell death but no tissue abnormalities. *Differentiation*, **77**, 442-449.

40. Marine,J.C. and Jochemsen,A.G. (2004) Mdmx and Mdm2: brothers in arms? *Cell Cycle*, **3**, 900-904.

41. Bottger,V., Bottger,A., Garcia-Echeverria,C., Ramos,Y.F., van der Eb,A.J., Jochemsen,A.G., and Lane,D.P. (1999) Comparative study of the p53-mdm2 and p53-MDMX interfaces. *Oncogene*, **18**, 189-199.

42. Haupt,Y., Barak,Y., and Oren,M. (1996) Cell type-specific inhibition of p53-mediated apoptosis by mdm2. *EMBO J.*, **15**, 1596-1606.

43. Kawai,H., Wiederschain,D., and Yuan,Z.M. (2003) Critical contribution of the MDM2 acidic domain to p53 ubiquitination. *Mol.Cell Biol.*, **23**, 4939-4947.

44. Meulmeester,E., Frenk,R., Stad,R., de Graaf,P., Marine,J.C., Vousden,K.H., and Jochemsen,A.G. (2003) Critical role for a central part of Mdm2 in the ubiquitylation of p53. *Mol.Cell Biol.*, **23**, 4929-4938.

45. Sharp,D.A., Kratowicz,S.A., Sank,M.J., and George,D.L. (1999) Stabilization of the MDM2 oncoprotein by interaction with the structurally related MDMX protein. *J.Biol.Chem.*, **274**, 38189-38196.

46. Gu,J., Kawai,H., Nie,L., Kitao,H., Wiederschain,D., Jochemsen,A.G., Parant,J., Lozano,G., and Yuan,Z.M. (2002) Mutual dependence of MDM2 and MDMX in their functional inactivation of p53. *J.Biol.Chem.*, **277**, 19251-19254.

47. Linares,L.K., Hengstermann,A., Ciechanover,A., Muller,S., and Scheffner,M. (2003) HdmX stimulates Hdm2-mediated ubiquitination and degradation of p53. *Proc.Natl.Acad.Sci.U.S.A*, **100**, 12009-12014.

48. Fang,S., Jensen,J.P., Ludwig,R.L., Vousden,K.H., and Weissman,A.M. (2000) Mdm2 is a RING finger-dependent ubiquitin protein ligase for itself and p53. *J.Biol.Chem.*, **275**, 8945-8951.

49. Stommel,J.M. and Wahl,G.M. (2004) Accelerated MDM2 auto-degradation induced by DNA-damage kinases is required for p53 activation. *EMBO J.*, **23**, 1547-1556.

50. de Graaf,P., Little,N.A., Ramos,Y.F., Meulmeester,E., Letteboer,S.J., and Jochemsen,A.G. (2003) Hdmx protein stability is regulated by the ubiquitin ligase activity of Mdm2. *J.Biol.Chem.*, **278**, 38315-38324.

51. Kawai,H., Wiederschain,D., Kitao,H., Stuart,J., Tsai,K.K., and Yuan,Z.M. (2003) DNA damage-induced MDMX degradation is mediated by MDM2. *J.Biol.Chem.*, **278**, 45946-45953.

52. Pan,Y. and Chen,J. (2003) MDM2 promotes ubiquitination and degradation of MDMX. *Mol.Cell Biol.*, **23**, 5113-5121.

53. Li,M., Brooks,C.L., Kon,N., and Gu,W. (2004) A dynamic role of HAUSP in the p53-Mdm2 pathway. *Mol.Cell*, **13**, 879-886.

54. Meulmeester,E., Maurice,M.M., Boutell,C., Teunisse,A.F., Ovaa,H., Abraham,T.E., Dirks,R.W., and Jochemsen,A.G. (2005) Loss of HAUSP-mediated deubiquitination contributes to DNA damage-induced destabilization of Hdmx and Hdm2. *Mol.Cell*, **18**, 565-576.

55. Hock,A.K., Vigneron,A.M., Carter,S., Ludwig,R.L., and Vousden,K.H. (2011) Regulation of p53 stability and function by the deubiquitinating enzyme USP42. *EMBO J.*.

56. Momand,J., Zambetti,G.P., Olson,D.C., George,D., and Levine,A.J. (1992) The mdm-2 oncogene product forms a complex with the p53 protein and inhibits p53-mediated transactivation. *Cell*, **69**, 1237-1245.

57. Pigolotti,S., Krishna,S., and Jensen,M.H. (2007) Oscillation patterns in negative feedback loops. *Proc.Natl.Acad.Sci.U.S.A*, **104**, 6533-6537.

58. Li,B., Cheng,Q., Li,Z., and Chen,J. (2010) p53 inactivation by MDM2 and MDMX negative feedback loops in testicular germ cell tumors. *Cell Cycle*, **9**, 1411-1420.

59. Phillips,A., Teunisse,A., Lam,S., Lodder,K., Darley,M., Emaduddin,M., Wolf,A., Richter,J., De Lange,J., Verlaan-de,V.M., Lenos,K., Bohnke,A., Bartel,F., Blaydes,J.P., and Jochemsen,A.G. (2010) HDMX-L is expressed from a functional p53-responsive promoter in the first intron of the HDMX gene and participates in an autoregulatory feedback loop to control p53 activity. *J.Biol.Chem.*, **285**, 29111-29127.

60. Wei,C.L., Wu,Q., Vega,V.B., Chiu,K.P., Ng,P., Zhang,T., Shahab,A., Yong,H.C., Fu,Y., Weng,Z., Liu,J., Zhao,X.D., Chew,J.L., Lee,Y.L., Kuznetsov,V.A., Sung,W.K., Miller,L.D., Lim,B., Liu,E.T.,

Yu,Q., Ng,H.H., and Ruan,Y. (2006) A global map of p53 transcription-factor binding sites in the human genome. *Cell*, **124**, 207-219.

61. Levine,A.J. and Oren,M. (2009) The first 30 years of p53: growing ever more complex. *Nat.Rev.Cancer*, **9**, 749-758.

62. Smith,J., Tho,L.M., Xu,N., and Gillespie,D.A. (2010) The ATM-Chk2 and ATR-Chk1 pathways in DNA damage signaling and cancer. *Adv.Cancer Res.*, **108**, 73-112.

63. Banin,S., Moyal,L., Shieh,S., Taya,Y., Anderson,C.W., Chessa,L., Smorodinsky,N.I., Prives,C., Reiss,Y., Shiloh,Y., and Ziv,Y. (1998) Enhanced phosphorylation of p53 by ATM in response to DNA damage. *Science*, **281**, 1674-1677.

64. Lakin,N.D., Hann,B.C., and Jackson,S.P. (1999) The ataxia-telangiectasia related protein ATR mediates DNA-dependent phosphorylation of p53. *Oncogene*, **18**, 3989-3995.

65. Shieh,S.Y., Ahn,J., Tamai,K., Taya,Y., and Prives,C. (2000) The human homologs of checkpoint kinases Chk1 and Cds1 (Chk2) phosphorylate p53 at multiple DNA damage-inducible sites. *Genes Dev.*, **14**, 289-300.

66. Meek,D.W. (2009) Tumour suppression by p53: a role for the DNA damage response? *Nat.Rev.Cancer*, **9**, 714-723.

67. Dornan,D. and Hupp,T.R. (2001) Inhibition of p53-dependent transcription by BOX-I phospho-peptide mimetics that bind to p300. *EMBO Rep.*, **2**, 139-144.

68. Lambert,P.F., Kashanchi,F., Radonovich,M.F., Shiekhattar,R., and Brady,J.N. (1998) Phosphorylation of p53 serine 15 increases interaction with CBP. *J.Biol.Chem.*, **273**, 33048-33053.

69. Ito,A., Kawaguchi,Y., Lai,C.H., Kovacs,J.J., Higashimoto,Y., Appella,E., and Yao,T.P. (2002) MDM2-HDAC1-mediated deacetylation of p53 is required for its degradation. *EMBO J.*, **21**, 6236-6245.

70. Khosravi,R., Maya,R., Gottlieb,T., Oren,M., Shiloh,Y., and Shkedy,D. (1999) Rapid ATM-dependent phosphorylation of MDM2 precedes p53 accumulation in response to DNA damage. *Proc.Natl.Acad.Sci.U.S.A*, **96**, 14973-14977.

71. Maya,R., Balass,M., Kim,S.T., Shkedy,D., Leal,J.F., Shifman,O., Moas,M., Buschmann,T., Ronai,Z., Shiloh,Y., Kastan,M.B., Katzir,E., and Oren,M. (2001) ATM-dependent phosphorylation of Mdm2 on serine 395: role in p53 activation by DNA damage. *Genes Dev.*, **15**, 1067-1077.

72. Chen,L., Gilkes,D.M., Pan,Y., Lane,W.S., and Chen,J. (2005) ATM and Chk2-dependent phosphorylation of MDMX contribute to p53 activation after DNA damage. *EMBO J.*, **24**, 3411-3422.

73. LeBron,C., Chen,L., Gilkes,D.M., and Chen,J. (2006) Regulation of MDMX nuclear import and degradation by Chk2 and 14-3-3. *EMBO J.*, **25**, 1196-1206.

74. Palmero,I., Pantoja,C., and Serrano,M. (1998) p19ARF links the tumour suppressor p53 to Ras. *Nature*, **395**, 125-126.

75. Zindy,F., Eischen,C.M., Randle,D.H., Kamijo,T., Cleveland,J.L., Sherr,C.J., and Roussel,M.F. (1998) Myc signaling via the ARF tumor suppressor regulates p53-dependent apoptosis and immortalization. *Genes Dev.*, **12**, 2424-2433.

76. Bates,S., Phillips,A.C., Clark,P.A., Stott,F., Peters,G., Ludwig,R.L., and Vousden,K.H. (1998) p14ARF links the tumour suppressors RB and p53. *Nature*, **395**, 124-125.

77. De Stanchina E., McCurrach,M.E., Zindy,F., Shieh,S.Y., Ferbeyre,G., Samuelson,A.V., Prives,C., Roussel,M.F., Sherr,C.J., and Lowe,S.W. (1998) E1A signaling to p53 involves the p19(ARF) tumor suppressor. *Genes Dev.*, **12**, 2434-2442.

78. Quelle,D.E., Zindy,F., Ashmun,R.A., and Sherr,C.J. (1995) Alternative reading frames of the INK4a tumor suppressor gene encode two unrelated proteins capable of inducing cell cycle arrest. *Cell*, **83**, 993-1000.

79. Honda,R. and Yasuda,H. (1999) Association of p19(ARF) with Mdm2 inhibits ubiquitin ligase activity of Mdm2 for tumor suppressor p53. *EMBO J.*, **18**, 22-27.

80. Tao,W. and Levine,A.J. (1999) P19(ARF) stabilizes p53 by blocking nucleo-cytoplasmic shuttling of Mdm2. *Proc.Natl.Acad.Sci.U.S.A*, **96**, 6937-6941.

81. Weber,J.D., Taylor,L.J., Roussel,M.F., Sherr,C.J., and Bar-Sagi,D. (1999) Nucleolar Arf sequesters Mdm2 and activates p53. *Nat.Cell Biol.*, **1**, 20-26.

82. Brosh,R. and Rotter,V. (2009) When mutants gain new powers: news from the mutant p53 field. *Nat.Rev.Cancer*, **9**, 701-713.

83. Schuijer,M. and Berns,E.M. (2003) TP53 and ovarian cancer. *Hum.Mutat.*, **21**, 285-291.

84. Iacopetta,B. (2003) TP53 mutation in colorectal cancer. *Hum.Mutat.*, **21**, 271-276.

85. Blons,H. and Laurent-Puig,P. (2003) TP53 and head and neck neoplasms. *Hum.Mutat.*, **21**, 252-257.

86. Peller,S. and Rotter,V. (2003) TP53 in hematological cancer: low incidence of mutations with significant clinical relevance. *Hum.Mutat.*, **21**, 277-284.

87. Kato,M.V., Shimizu,T., Ishizaki,K., Kaneko,A., Yandell,D.W., Toguchida,J., and Sasaki,M.S. (1996) Loss of heterozygosity on chromosome 17 and mutation of the p53 gene in retinoblastoma. *Cancer Lett.*, **106**, 75-82.

88. Houben,R., Hesbacher,S., Schmid,C.P., Kauczok,C.S., Flohr,U., Haferkamp,S., Muller,C.S., Schrama,D., Wischhusen,J., and Becker,J.C. (2011) High-level expression of wild-type p53 in melanoma cells is frequently associated with inactivity in p53 reporter gene assays. *PLoS.One.*, **6**, e22096.

89. Vousden,K.H. and Lu,X. (2002) Live or let die: the cell's response to p53. *Nat.Rev.Cancer*, **2**, 594-604.

90. Momand,J., Jung,D., Wilczynski,S., and Niland,J. (1998) The MDM2 gene amplification database. *Nucleic Acids Res.*, **26**, 3453-3459.

91. Danovi,D., Meulmeester,E., Pasini,D., Migliorini,D., Capra,M., Frenk,R., de Graaf,P., Francoz,S., Gasparini,P., Gobbi,A., Helin,K., Pelicci,P.G., Jochemsen,A.G., and Marine,J.C. (2004) Amplification of Mdmx (or Mdm4) directly contributes to tumor formation by inhibiting p53 tumor suppressor activity. *Mol.Cell Biol.*, **24**, 5835-5843.

92. Riemenschneider,M.J., Knobbe,C.B., and Reifenberger,G. (2003) Refined mapping of 1q32 amplicons in malignant gliomas confirms MDM4 as the main amplification target. *Int.J.Cancer*, **104**, 752-757.

93. Ramos,Y.F., Stad,R., Attema,J., Peltenburg,L.T., van der Eb,A.J., and Jochemsen,A.G. (2001) Aberrant expression of HDMX proteins in tumor cells correlates with wild-type p53. *Cancer Res.*, **61**, 1839-1842.

94. Bykov,V.J., Issaeva,N., Shilov,A., Hultcrantz,M., Pugacheva,E., Chumakov,P., Bergman,J., Wiman,K.G., and Selivanova,G. (2002) Restoration of the tumor suppressor function to mutant p53 by a low-molecular-weight compound. *Nat.Med.*, **8**, 282-288.

95. Vassilev,L.T., Vu,B.T., Graves,B., Carvajal,D., Podlaski,F., Filipovic,Z., Kong,N., Kammlott,U., Lukacs,C., Klein,C., Fotouhi,N., and Liu,E.A. (2004) In vivo activation of the p53 pathway by small-molecule antagonists of MDM2. *Science*, **303**, 844-848.

96. Vassilev,L.T. (2007) MDM2 inhibitors for cancer therapy. *Trends Mol.Med.*, **13**, 23-31.

97. Hu,B., Gilkes,D.M., Farooqi,B., Sebti,S.M., and Chen,J. (2006) MDMX overexpression prevents p53 activation by the MDM2 inhibitor Nutlin. *J.Biol.Chem.*, **281**, 33030-33035.

98. Patton,J.T., Mayo,L.D., Singhi,A.D., Gudkov,A.V., Stark,G.R., and Jackson,M.W. (2006) Levels of HdmX expression dictate the sensitivity of normal and transformed cells to Nutlin-3. *Cancer Res.*, **66**, 3169-3176.

99. Wade,M., Wong,E.T., Tang,M., Stommel,J.M., and Wahl,G.M. (2006) Hdmx modulates the outcome of p53 activation in human tumor cells. *J.Biol.Chem.*, **281**, 33036-33044.

100. Kitagawa,M., Aonuma,M., Lee,S.H., Fukutake,S., and McCormick,F. (2008) E2F-1 transcriptional activity is a critical determinant of Mdm2 antagonist-induced apoptosis in human tumor cell lines. *Oncogene*, **27**, 5303-5314.

101. Laurie,N.A., Donovan,S.L., Shih,C.S., Zhang,J., Mills,N., Fuller,C., Teunisse,A., Lam,S., Ramos,Y., Mohan,A., Johnson,D., Wilson,M., Rodriguez-Galindo,C., Quarto,M., Francoz,S., Mendrysa,S.M., Guy,R.K., Marine,J.C., Jochemsen,A.G., and Dyer,M.A. (2006) Inactivation of the p53 pathway in retinoblastoma. *Nature*, **444**, 61-66.

102. Coll-Mulet,L., Iglesias-Serret,D., Santidrian,A.F., Cosialls,A.M., de Frias,M., Castano,E., Campas,C., Barragan,M., de Sevilla,A.F., Domingo,A., Vassilev,L.T., Pons,G., and Gil,J. (2006) MDM2 antagonists activate p53 and synergize with genotoxic drugs in B-cell chronic lymphocytic leukemia cells. *Blood*, **107**, 4109-4114.

103. Lam,S., Lodder,K., Teunisse,A.F., Rabelink,M.J., Schutte,M., and Jochemsen,A.G. (2010) Role of Mdm4 in drug sensitivity of breast cancer cells. *Oncogene*.

104. Kojima,K., Konopleva,M., McQueen,T., O'Brien,S., Plunkett,W., and Andreeff,M. (2006) Mdm2 inhibitor Nutlin-3a induces p53-mediated apoptosis by transcription-dependent and transcription-independent mechanisms and may overcome Atm-mediated resistance to fludarabine in chronic lymphocytic leukemia. *Blood*, **108**, 993-1000.

105. Barbieri,E., Mehta,P., Chen,Z., Zhang,L., Slack,A., Berg,S., and Shohet,J.M. (2006) MDM2 inhibition sensitizes neuroblastoma to chemotherapy-induced apoptotic cell death. *Mol.Cancer Ther.*, **5**, 2358-2365.

106. Grasberger,B.L., Lu,T., Schubert,C., Parks,D.J., Carver,T.E., Koblish,H.K., Cummings,M.D., LaFrance,L.V., Milkiewicz,K.L., Calvo,R.R., Maguire,D., Lattanze,J., Franks,C.F., Zhao,S., Ramachandren,K., Bylebyl,G.R., Zhang,M., Manthey,C.L., Petrella,E.C., Pantoliano,M.W., Deckman,I.C., Spurlino,J.C., Maroney,A.C., Tomczuk,B.E., Molloy,C.J., and Bone,R.F. (2005) Discovery and cocrystal structure of benzodiazepinedione HDM2 antagonists that activate p53 in cells. *J.Med.Chem.*, **48**, 909-912.

107. Ding,K., Lu,Y., Nikolovska-Coleska,Z., Wang,G., Qiu,S., Shangary,S., Gao,W., Qin,D., Stuckey,J., Krajewski,K., Roller,P.P., and Wang,S. (2006) Structure-based design of spiro-

oxindoles as potent, specific small-molecule inhibitors of the MDM2-p53 interaction. *J.Med.Chem.*, **49**, 3432-3435.

108. Reed,D., Shen,Y., Shelat,A.A., Arnold,L.A., Ferreira,A.M., Zhu,F., Mills,N., Smithson,D.C., Regni,C.A., Bashford,D., Cicero,S.A., Schulman,B.A., Jochemsen,A.G., Guy,R.K., and Dyer,M.A. (2010) Identification and characterization of the first small molecule inhibitor of MDMX. *J.Biol.Chem.*, **285**, 10786-10796.

109. Bernal,F., Wade,M., Godes,M., Davis,T.N., Whitehead,D.G., Kung,A.L., Wahl,G.M., and Walensky,L.D. (2010) A stapled p53 helix overcomes HDMX-mediated suppression of p53. *Cancer Cell*, **18**, 411-422.

110. Wang,H. and Yan,C. (2011) A Small-Molecule p53 Activator Induces Apoptosis through Inhibiting MDMX Expression in Breast Cancer Cells. *Neoplasia.*, **13**, 611-619.

111. Issaeva,N., Bozko,P., Enge,M., Protopopova,M., Verhoef,L.G., Masucci,M., Pramanik,A., and Selivanova,G. (2004) Small molecule RITA binds to p53, blocks p53-HDM-2 interaction and activates p53 function in tumors. *Nat.Med.*, **10**, 1321-1328.

112. Enge,M., Bao,W., Hedstrom,E., Jackson,S.P., Moumen,A., and Selivanova,G. (2009) MDM2-dependent downregulation of p21 and hnRNP K provides a switch between apoptosis and growth arrest induced by pharmacologically activated p53. *Cancer Cell*, **15**, 171-183.

113. Kivela,T. (2009) The epidemiological challenge of the most frequent eye cancer: retinoblastoma, an issue of birth and death. *Br.J.Ophthalmol.*, **93**, 1129-1131.

114. Dyer,M.A. and Bremner,R. (2005) The search for the retinoblastoma cell of origin. *Nat.Rev.Cancer*, **5**, 91-101.

115. Chang,A.E., Karnell,L.H., and Menck,H.R. (1998) The National Cancer Data Base report on cutaneous and noncutaneous melanoma: a summary of 84,836 cases from the past decade. The American College of Surgeons Commission on Cancer and the American Cancer Society. *Cancer*, **83**, 1664-1678.

116. Virgili,G., Gatta,G., Ciccolallo,L., Capocaccia,R., Biggeri,A., Crocetti,E., Lutz,J.M., and Paci,E. (2007) Incidence of uveal melanoma in Europe. *Ophthalmology*, **114**, 2309-2315.

117. Bedikian,A.Y., Kantarjian,H., Young,S.E., and Bodey,G.P. (1981) Prognosis in metastatic choroidal melanoma. *South.Med.J.*, **74**, 574-577.

118. Char,D.H. (1978) Metastatic choroidal melanoma. *Am.J.Ophthalmol.*, **86**, 76-80.

119. Lorigan,J.G., Wallace,S., and Mavligit,G.M. (1991) The prevalence and location of metastases from ocular melanoma: imaging study in 110 patients. *AJR Am.J.Roentgenol.*, **157**, 1279-1281.

120. Kivela,T., Eskelin,S., and Kujala,E. (2006) Metastatic uveal melanoma. *Int.Ophthalmol.Clin.*, **46**, 133-149.

121. Augsburger,J.J., Correa,Z.M., and Shaikh,A.H. (2009) Effectiveness of treatments for metastatic uveal melanoma. *Am J Ophthalmol.*, **148**, 119-127.

122. Brantley,M.A., Jr. and Harbour,J.W. (2000) Deregulation of the Rb and p53 pathways in uveal melanoma. *Am J Pathol.*, **157**, 1795-1801.

123. Chana,J.S., Wilson,G.D., Cree,I.A., Alexander,R.A., Myatt,N., Neale,M., Foss,A.J., and Hungerford,J.L. (1999) c-myc, p53, and Bcl-2 expression and clinical outcome in uveal melanoma. *Br.J Ophthalmol.*, **83**, 110-114.

124. Hussein,M.R. (2005) The relationships between p53 protein expression and the clinicopathological features in the uveal melanomas. *Cancer Biol.Ther.*, **4**, 57-59.

125. Sun,Y., Tran,B.N., Worley,L.A., Delston,R.B., and Harbour,J.W. (2005) Functional analysis of the p53 pathway in response to ionizing radiation in uveal melanoma. *Invest Ophthalmol.Vis.Sci.*, **46**, 1561-1564.

Chapter 2

Oncogenic functions of hMDMX in *in vitro* transformation of primary human fibroblasts and embryonic retinoblasts

Kristiaan Lenos*, Job de Lange*, Amina Teunisse, Kirsten Lodder, Matty Verlaan-de Vries, Eliza Wiercinska, Marja van der Burg, Karoly Szuhai, Aart Jochemsen

Department of Molecular Cell Biology, Leiden University Medical Center, 2300 RC Leiden, The Netherlands

*These authors contributed equally to this work

Molecular Cancer 2011 Sep 12; 10(1):111

Abstract

Background: In around 50% of all human cancers the tumor suppressor p53 is mutated. It is generally assumed that in the remaining tumors the wild-type p53 protein is functionally impaired. The two main inhibitors of p53, Hdm2 (Mdm2) and Hdmx (Mdmx/Mdm4) are frequently overexpressed in wild-type p53 tumors. Whereas the main activity of Hdm2 is to degrade p53 protein, its close homolog Hdmx does not degrade p53, but it represses its transcriptional activity. Here we study the role of Hdmx in the neoplastic transformation of human fibroblasts and embryonic retinoblasts, since a high number of retinoblastomas contain elevated Hdmx levels.

Methods: We made use of an in vitro transformation model using a retroviral system of RNA interference and gene overexpression in primary human fibroblasts and embryonic retinoblasts. Consecutive knockdown of Rb and p53, overexpression of SV40-small t, oncogenic HRasV12 and HA-Hdmx resulted in a number of stable cell lines representing different stages of the transformation process, enabling a comparison between loss of p53 and Hdmx overexpression. The cell lines were tested in various assays to assess their oncogenic potential.

Results: Both p53-knockdown and Hdmx overexpression accelerated proliferation and prevented growth suppression induced by introduction of oncogenic Ras, which was required for anchorage-independent growth and the ability to form tumors in vivo. Furthermore, we found that Hdmx overexpression represses basal p53 activity to some extent. Transformed fibroblasts with very high levels of Hdmx became largely resistant to the p53 reactivating drug Nutlin-3. The Nutlin-3 response of Hdmx transformed retinoblasts was intact and resembled that of retinoblastoma cell lines.

Conclusions: Our studies show that Hdmx has the essential properties of an oncogene. Its constitutive expression contributes to the oncogenic phenotype of transformed human cells. Its main function appears to be p53 inactivation. Therefore, developing new drugs targeting Hdmx is a valid approach to obtain new treatments for a subset of human tumors expressing wild-type p53.

Background

In approximately 50% of all human cancers mutations are found in the TP53 gene, encoding the tumor suppressor protein p53 [1, 2], whereas it is assumed that in tumors expressing wild-type p53 the tumor suppressing activity of p53 is attenuated [3]. Normal, non-stressed cells maintain relatively low p53 protein levels. Upon various stress signals like DNA damage or oncogenic stress, p53 is stabilized and activated. Activated p53 affects various processes, including cell cycle progression, DNA repair, senescence and apoptosis [4]. Two main negative regulators of p53 are MDM2 and MDMX, also called hMDM2 and hMDMX. MDM2, an E3 ubiquitin ligase, inhibits p53 via poly-ubiquitination [5] and by binding to p53's N-terminus, thereby shielding its transcription activation domain. Since the MDM2 gene is also a p53 target, a negative feedback-loop is established [6]. The importance of MDM2 in p53 regulation was best shown by the p53-dependent embryonic lethality of MDM2 -/- mice [7, 8]. Similarly, MDMX -/- mice are embryonic lethal in a p53-dependent manner [9-11], indicating that both MDM2 and MDMX fulfill an essential, non-redundant function in p53-regulation. Despite great structural similarities between MDM2 and MDMX [12], including the RING finger domain needed for MDM2 E3 ligase activity, MDMX has no detectable E3 ligase activity. MDMX functions mostly by inhibiting p53 activity through interaction with its transcription activation domain [13, 14]. Furthermore, MDMX and MDM2 dimerize via their RING finger domains [15], thereby stabilizing MDM2 and promoting its E3 ligase activity towards p53 [16, 17].

hMDM2 is overexpressed in 5-10% of all human tumors, revealing hMDM2 as an oncogene [18]. Similar observations were made regarding hMDMX. A study of common tumor types showed increased hMDMX mRNA expression in 20% of these tumors [19], and a subset of gliomas contained hMDMX gene amplification [20]. Furthermore, Ramos et al. showed upregulated or aberrant hMDMX expression in a large number of human tumor cell lines, mostly correlating with wild-type p53 status [21]. A particularly high proportion of retinoblastomas contain hMDMX gene amplification [22]. hMDMX knockdown in p53 wild-type tumor cells has been shown to induce p53-dependent growth inhibition [19, 22].

The first evidence for direct oncogenic activity of MDMX was provided by Danovi et al. [19]. MDMX overexpression in early cultures of mouse embryonic fibroblasts resulted in immortalization and neoplastic transformation when combined with HRasV12 overexpression. This suggests that MDMX overexpression is sufficient to inactivate the p53 tumor suppressor pathway. However, such an oncogene function of hMDMX has not yet been directly shown in human cells.

Human primary cells require a specific set of genetic changes for neoplastic transformation. By expression of the human Telomerase reverse transcriptase subunit (hTERT), oncogenic HRasV12, and the early region of SV40, encoding the viral large and small T antigens (LT and st), primary human cells can be immortalized and transformed. LT is needed to inactivate Rb and p53, since functional loss of both genes is required for tumor formation [23, 24]. By combining this transformation model with specific RNA interference, the tumor-suppressive functions of p14ARF and p16INK4A were assessed by Voorhoeve and Agami [25]. They also showed that directly targeting p53 and RB could replace LT expression. Here we use a retroviral system of RNA interference and gene overexpression to establish an in vitro transformation model for assessing the contribution of hMDMX to the transformation of human primary cells.

Results

Generation of transformed human skin fibroblasts and human embryonic retinoblasts, including hMDMX as a potential oncogene

To investigate whether hMDMX can function as an oncogene in the transformation of human primary cells, we applied a previously described in vitro transformation model [25] to two different cell types: human foreskin fibroblasts (VH10) and human embryonic retinoblasts (HER).

The generation of the VH10 transformation model is depicted in Figure 1a. Sequential retroviral transductions resulted in a panel of stable polyclonal cell lines, representing different stages of the transformation process. This enabled a pair-wise comparison between hMDMX overexpression and p53-knockdown. Stable cell lines with shRB-HA-hMDMX, or shRB alone, could not be established, suggesting that RB reduction is growth limiting in these cells. Oncogenic HRasV12 without concomitant p53-knockdown or HA-hMDMX overexpression induced a senescent-like crisis blocking proliferation of most cells, followed by expansion of single colonies. This suggests the occurrence of additional selection bypassing the HRas-V12-induced growth inhibition. RB knockdown was not sufficient to rescue HRasV12-induced growth inhibition. Therefore, the cell lines VH10-shRB-HRasV12 and VH10-HRasV12 could not be established. We monitored the effectiveness of the transductions by western blotting (Figure 1b) and found strong overexpression of hMDMX, somewhat increased HRas levels and marked reductions of p53 and RB, correlating with the respective transductions. Interestingly, endogenous HRas level

was slightly increased upon p53-knockdown or hMDMX overexpression, correlating with accelerated growth. HRasV12 has been reported to induce p16-dependent senescence in human fibroblasts [4, 25, 26]. Indeed, HRas-V12-transformed as well as p53-knockdown cells expressed higher p16 protein levels (Figure 1b), although we observed no signs of senescence. This suggests that during the transformation process the pathway downstream of p16 is somehow impaired. Alternatively, p53 inactivation may prevent HRasV12-induced senescence, which was indeed described for hMDMX overexpression [27].

For HER transformation, we initially used a comparable approach. However, HRas-V12-transformed cells could not be established without p53-knockdown or HA-hMDMX overexpression, which prompted us to modify the scheme (Figure 1c). Transformation of HER-hTERT-shRB or HER-hTERT cells with an empty puromycin vector and subsequent puromycin selection resulted in initial colony formation, but these colonies eventually

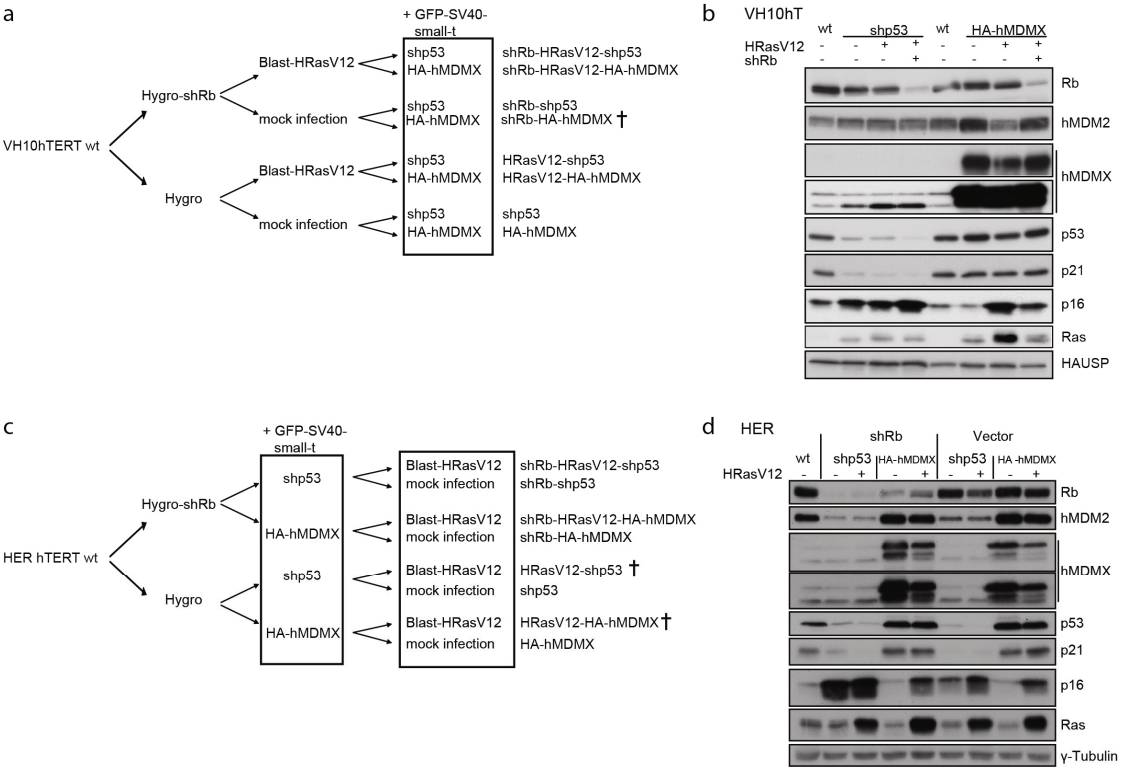

Figure 1 Generation of panels of transformed human skin fibroblasts and human embryonic retinoblasts. (**a**) Schematic representation of the transformation process. Primary human fibroblasts (VH10) were immortalized with human Telomerase (hTERT). In subsequent rounds of retroviral infection using the indicated constructs, followed by selection, several stable cell lines were created. (**b**) Total cell extracts from all transformed fibroblast cell lines were analyzed by immunoblotting with the indicated antibodies. (**c**) Human Embryonic Retinoblasts (HER) were similarly transformed according to the scheme. (**d**) Total cell extracts from all transformed HER cell lines were analyzed by immunoblotting with the indicated antibodies.

Table 1: mRNA expression levels in VH10 and HER cell lines.

VH10	p21	hMDM2 ex2	PUMA
VH10 wt	1,00 ± 0,16	1,00 ± 0,17	1,00 ± 0,23
shp53	0,24 ± 0,03	0,20 ± 0,03	0,49 ± 0,11
HRasV12-shp53	0,15 ± 0,03	0,32 ± 0,07	0,44 ± 0,15
shRb-HRasV12-shp53	0,63 ± 0,11	0,41 ± 0,15	1,54 ± 0,32
HA-hMDMX	0,47 ± 0,09	0,61 ± 0,08	0,41 ± 0,08
HRasV12-HA-hMDMX	0,76 ± 0,12	1,05 ± 0,17	0,53 ± 0,14
shRb-HRasV12-HA-hMDMX	1,05 ± 0,12	1,14 ± 0,15	0,28 ± 0,07
HER	**p21**	**hMDM2 ex2**	**PUMA**
HER wt	1,00 ± 0,16	1,00 ± 0,15	1,00 ± 0,19
shp53	0,11 ± 0,03	0,01 ± 0,01	0,46 ± 0,13
shRb-shp53	0,23 ± 0,05	0,02 ± 0,00	0,36 ± 0,06
shRb-HRasV12-shp53	0,05 ± 0,02	0,01 ± 0,00	0,15 ± 0,04
HA-hMDMX	1,51 ± 0,26	1,43 ± 0,28	0,67 ± 0,30
shRb-HA-hMDMX	1,01 ± 0,16	0,62 ± 0,13	0,34 ± 0,11
shRb-HRasV12-HA-hMDMX	2,52 ± 0,70	0,61 ± 0,17	0,60 ± 0,17

Total RNA of each cell line was isolated and expression levels of the indicated genes were determined by qRT-PCR and normalized for the housekeeping genes *CAPNS1* and *TBP*; levels are shown relative to wild-type cells.

stopped growing. This suggests that in HER cells, in contrast to VH10, inactivation of p53 is essential for establishing immortalized cell lines. Protein levels of RB, hMDMX, p53 and HRas correlated with the applied transductions (Figure 1d), although the RB depletion was less efficient in HA-hMDMX cells (lane 4 and 5). Similar to the observations in VH10 cells, HRasV12 expression induced p16 protein levels in HER cells. This did not affect growth of RB-knockdown cells, whereas HER cells without RB-knockdown eventually stopped proliferating upon HRasV12 overexpression. Likely, HRasV12 activated a p16- and RB-dependent mechanism resulting in growth suppression (also illustrated by large, flattened cells, Figure 2c), which could not be rescued by p53-knockdown or hMDMX overexpression. Therefore, these cells could not be used in further experiments.

hMDMX overexpression and p53-knockdown were analyzed with qRT-PCR, showing ~ 90% reduction of p53 and 10-fold increase of hMDMX mRNA expression in VH10 cells (Table 1 and not shown). Expression of p53 target genes p21, PUMA and hMDM2-p2 was significantly decreased upon p53-knockdown in VH10 and HER cells, and also hMDMX overexpression slightly decreased basal levels of some of these genes (Table 1). Reduced p21 protein levels upon p53-knockdown (Figure 1b and 1d), in line with the qRT-PCR data, indicate impaired basal p53 activity. hMDMX overexpression did slightly reduce basal p21 protein levels in VH10 cells (Table 2). In addition, in HA-hMDMX cells the protein levels of p53 were slightly increased, most likely by protein stabilization.

Immunofluorescence analysis revealed abundant GFP throughout the entire cell in all HER and VH10 cell lines, which confirmed SV40-st expression (Supplementary Figure 1a and 1c). Exogenous hMDMX showed mainly cytoplasmic localization in VH10 cells, but nuclear hMDMX was also observed (Supplementary Figure 1a). In HER cells, the main localization

Table 2: Protein levels, relative to untreated VH10 wt cells, corrected for HAUSP expression.

Cell line	Nutlin-3 treatment (h)	p53	p21	hMDM2
VH10 wt	0	1.00	1.00	1.00
	6	4.96	6.68	82.32
	24	7.82	11.16	149.60
shp53	0	0.35	0.20	0.27
	6	0.87	0.65	0.30
	24	1.25	2.26	4.54
HRasV12-shp53	0	0.28	0.03	0.33
	6	0.30	0.09	0.78
	24	0.44	0.33	0.74
shRb-HRasV12- shp53	0	0.45	1.01	2.51
	6	0.49	1.24	4.55
	24	0.74	2.85	9.17
HA-hMDMX	0	6.99	0.56	0.87
	6	9.72	2.86	47.81
	24	11.70	2.10	17.19
HRasV12-HA-hMDMX	0	1.63	0.63	0.69
	6	4.13	2.88	36.75
	24	5.01	3.07	29.42
shRb-HRasV12-HA-hMDMX	0	1.07	1.45	2.79
	6	2.38	5.37	132.80
	24	1.76	4.28	79.91

Band intensities shown in figure 3b were quantified using the Odyssey 2.1 analysis software (LI-COR Biosciences) and the relative protein levels were calculated using HAUSP expression as an internal control. Basal protein levels in VH10 wild-type cells were set at 1.0.

was nuclear (Supplementary Figure 1b). High levels of cytoplasmic hMDMX were reported to prevent p53 nuclear localization [28]. However, we found no alterations in p53 localization upon hMDMX overexpression (Supplementary Figure 1b and 1d). hMDM2 protein, irrespective of hMDMX levels, was detected in the nucleus, although it could be observed in the cytoplasm as well. The cytoplasmic signal of hMDM2 is relatively underrepresented since the protein is diffused throughout the relatively large cytoplasmic surface, but is certainly present, as reported before [29] (Supplementary Figure 1b and 1d).

Since p53 contributes to the maintenance of genomic stability [4], the various cell lines were analyzed for chromosomal abnormalities using COBRA-FISH [30]. Wild-type VH10hTERT cells (Supplementary Figure 2a) showed a normal 46, XY karyogram in 20% of the analyzed cells. The remaining cells harboured a Robertsonian translocation [31], which results in loss of the short arms of two acrocentric chromosomes. As these contain the ribosomal gene cassettes, this translocation has no further consequences at the cellular level. The observed rob(13;22) chromosome was lost during the transformation process. The transformed VH10 cell lines showed heterogeneous populations of mainly diploid and chromosomal stable cells, with low percentage random translocations or polyploidy. The

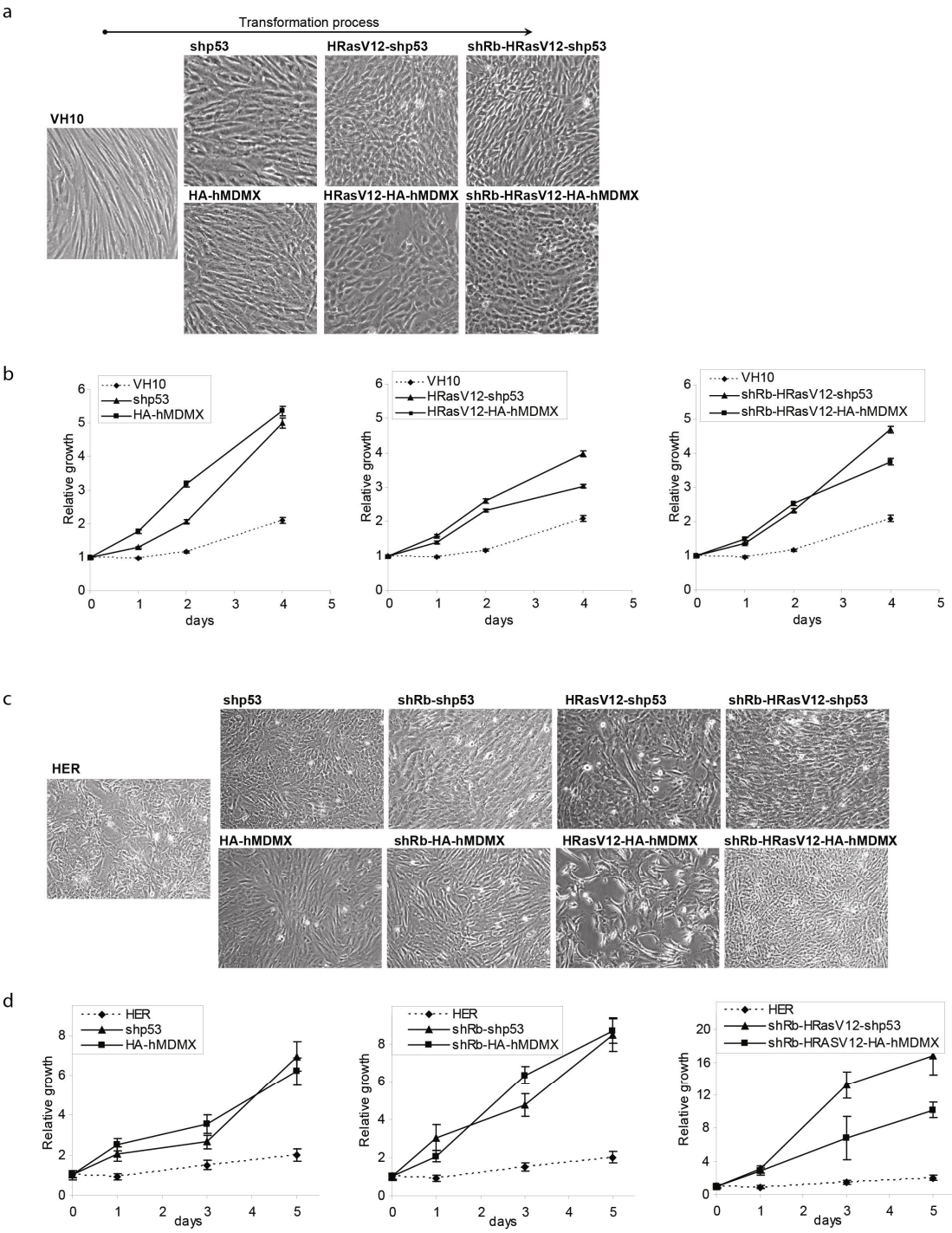

Figure 2 Transformation alters cell morphology and growth rate. Phase-contrast photographs of the transformed VH10 (**a**) and HER (**c**) cell lines (10x magnification, Olympus CKX41) showing morphology changes during the transformation process. Growth rates of VH10 (**b**) and HER (**d**) cell lines were measured using WST-1 proliferation assays.

HER cells showed more chromosomal aberrations and translocations (Supplementary Figure 2b). Most notably, loss of chromosome 13, harbouring the RB gene, was found in four out of six cell lines. The fact that it was not found in the HA-hMDMX and shRB-HA-hMDMX-HRasV12 cell line suggests that loss of this chromosome occurred independently in those four cell lines (see Figure 1c for transformation scheme). Two unlinked cell lines (shp53 and shRB-HA-hMDMX-HRasV12) lost one X-chromosome, whereas loss of chromosome 22 and gain of chromosome 8 in shRB-shp53 and shRB-shp53-HRasV12 is likely to have been passed on from their shared parental cell line. In addition, several random translocations and fusions were observed, however, none was found in more than one cell line. In conclusion, transformation of VH10 and HER cells did not induce wide-spread genomic instability and aneuploidy.

Alterations in morphology and proliferation rate during transformation process

Cell morphology changed during the transformation process. Whereas normal VH10hTERT cells are extended, fibroblastic cells aligning orderly in the dish, during the sequential transformation stages the cells became apparently smaller and rounder (Figure 2a). HRasV12 induced a disordered way of growing and showed loss of contact inhibition. hMDMX-overexpressing and p53-knockdown cells showed similar morphology changes. Both shp53 and HA-hMDMX cells obviously proliferated faster than wild-type VH10hTERT cells, a property that was not further enhanced by additional HRasV12 expression. This was confirmed in short-term growth (WST-1) assays (Figure 2b), suggesting that hMDMX overexpression is sufficient to inhibit p53-dependent growth control, similar to p53-knockdown.

Morphology changes in transformed HER cells were comparable to those observed in VH10 cells (Figure 2c). In addition, both p53-knockdown and hMDMX overexpression accelerated growth as compared to wild-type HER cells (Figure 2d). HRasV12 even further enhanced growth rate in shRB-shp53 cells, but not in shRB-HA-hMDMX cells.

Effect of hMDMX overexpression on anchorage-independent growth

Anchorage-independent growth is a vital feature of tumorigenic cells. Therefore, we investigated the growth potential of the different cell lines in soft agar (Figure 3a).

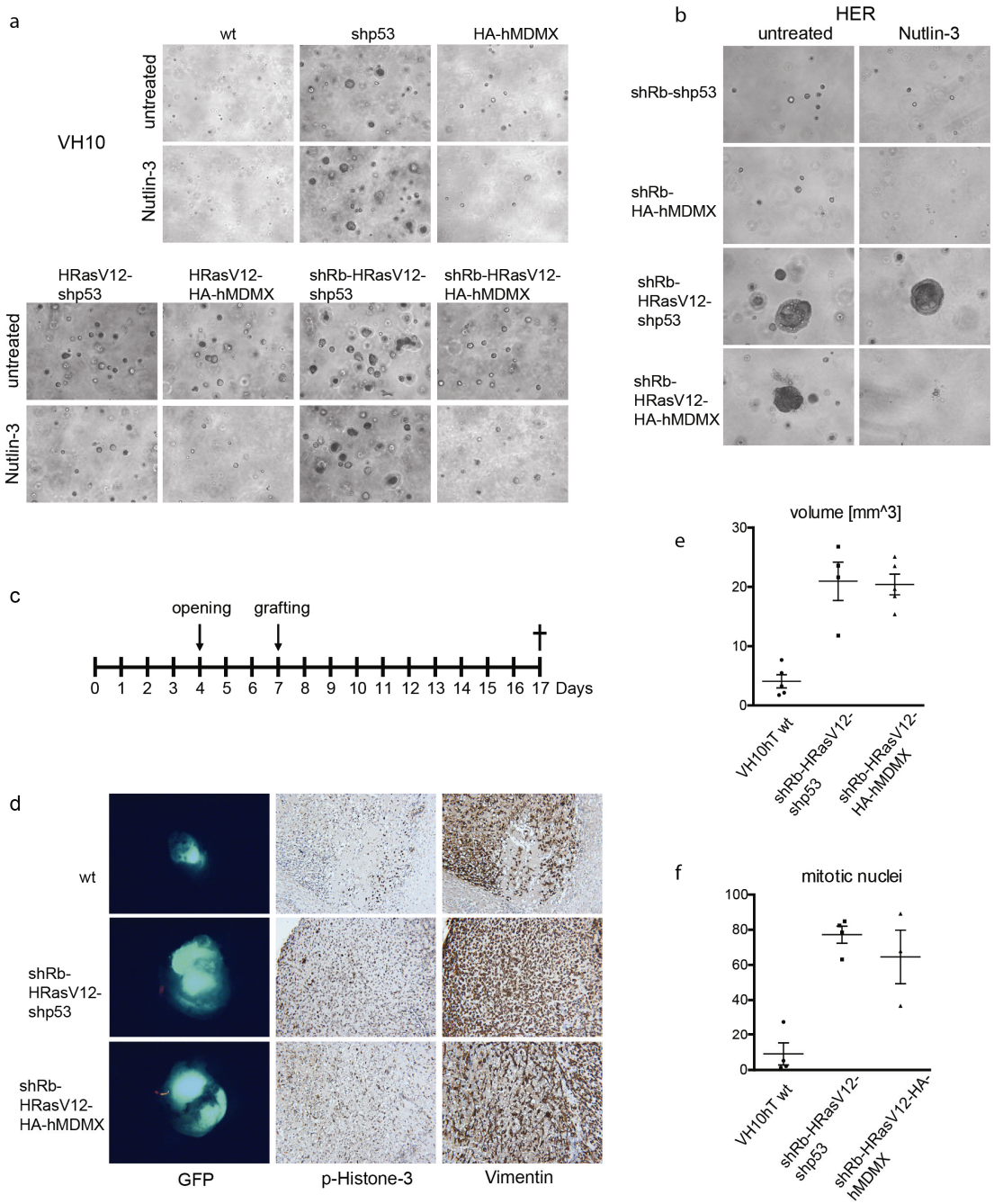

Figure 3 hMDMX overexpression promotes anchorage-independent growth and tumor growth *in vivo*. (**a**, **b**) Various VH10hTERT and HER cell lines were embedded in 0.3 % agarose on a 0.6% agarose bottom-layer, with additional normal growth medium or growth medium containing 10 µM Nutlin-3 on top of the agarose. Colony outgrowth was monitored 18 days (VH10) and 4 weeks (HER) after seeding. Representative pictures of several independent experiments are shown. (**c**) Schedule for investigating *in vivo* growth of parental and transformed VH10 cells using the shell-less chicken CAM model. At embryonic development day (EDD) 7, 2.5 million cells were grafted onto a chicken CAM. Tumors were harvested at EDD17. (**d**) Representative pictures of GFP-positive tumors, P-Histone-3 staining and vimentin staining. (**e**) Tumor volumes of VH10hTERT control (N=5), shRB-HRasV12-shp53 (N=4) and shRB-HRasV12-HA-hMDMX (N=5). F. Quantification of the number of mitotic (P-Histone-3 positive) cells. Statistical analysis was performed by one-way ANOVA followed by Bonferroni's Multiple Comparison Test. $P < 0.05$ was considered statistically significant.

Control VH10hTERT cells did not grow, but both p53-knockdown and hMDMX overexpression induced formation of some small colonies. HRasV12 expression clearly increased the size and the number of colonies. However, this was more pronounced in p53-knockdown cells than in hMDMX-overexpressing cells. Interestingly, hMDMX overexpression did not prevent the growth inhibitory effect of Nutlin-3, in contrast to experiments in 2D-culture (see below). These findings suggest that hMDMX cannot fully inhibit the function of p53 in soft agar growth.

Untransformed HER cells did not grow at all in soft agar, and neither hMDMX overexpression nor p53-knockdown alone was able to induce colony formation (not shown). Additional RB knockdown induced formation of very small colonies, only HRasV12 expression dramatically increased colony size and number (Figure 3b). Similar to the observations in VH10 cells, colony formation was more efficient in p53-knockdown cells than in hMDMX-overexpressing cells. Furthermore, Nutlin-3 inhibited colony formation of hMDMX-overexpressing cells, whereas p53-knockdown cells were unaffected.

Role of hMDMX in tumorigenicity *in vivo*.

We tested the *in vivo* tumorigenic potential of the transformed VH10 cells by subcutaneous injection into Balb/c nu/nu mice. Unfortunately, no tumor formation could be detected. The lack of tumor growth could possibly be explained by the immune response still present in nu/nu mice; however, similar results were obtained in NOD/SCID mice. Therefore, we switched to the shell-less chick CAM assay [32] (Figure 3c-f). Ten days after grafting both shRB-HRasV12-HA-hMDMX- and shRB-HRasV12-shp53 tumors were significantly larger (4-5 fold) than those formed by wild-type VH10 cells ($P < 0.05$, Bonferroni's Multiple Comparison Test; Figure 3d left and 3e). Interestingly, the transformed cell lines showed equal tumor volumes, indicating that hMDMX overexpression and p53-knockdown have similar effects on tumor growth. Moreover, tumors from the transformed cells contained significantly ($P < 0.05$) more mitotic cells than wild-type tumors as revealed with P-Histone-3 staining, with no detectable difference between hMDMX-overexpressing and p53-knockdown cells (Figure 3d middle and 3f. Staining with fibroblast marker vimentin showed the fibroblastic origin of the tumors (Figure 3d right).

The *in vivo* growth capacity of transformed HER cells was tested in a previously described murine model [33], by injection into the anterior eye chamber of Balb/c nu/nu mice. Both tested cell lines showed similar, but limited *in vivo* growth potential. The hMDMX-

expressing cells showed growth in 2/5 cases, however growth stopped when the eye chamber was filled up to 50% with tumor cells. The p53-knockdown cells started tumor growth in 4/5 cases, but stopped when the eye chamber was filled up to 20% (2x), 30% (1x) or 50% (1x). Altogether, it is clear that hMDMX overexpression promotes *in vivo* tumor growth and in that respect largely mimics p53-knockdown in the same cells.

hMDMX overexpression inhibits the Nutlin-3 induced p53 response in VH10 skin fibroblasts.

We next investigated whether hMDMX overexpression prevents p53 activation in VH10 cells. The various cell lines were treated with the small-molecule p53-activator Nutlin-3 [34]. Nutlin-3 reduced survival of normal human fibroblasts (Figure 4a), whereas p53-knockdown cells were not affected. hMDMX overexpression also prevented Nutlin-3 induced growth inhibition. In wild-type VH10hTERT cells, the Nutlin-3 response is marked by increased p53, hMDM2 and p21 and decreased hMDMX protein levels (Figure 4b). This response was diminished upon p53-knockdown, reaching levels slightly above basal expression in wild-type cells (Table 2). HA-hMDMX overexpression also attenuated the induction of p53 and its target genes. Notably, exogenous HA-hMDMX levels remained relatively high, despite some Nutlin-3 induced degradation. Levels of the p53-responsive transcripts of hMDM2-p2, p21 and PUMA correlated with protein levels (Figure 4c). Furthermore, hMDMX overexpression partially rescued the reduction of the anti-apoptotic gene SURVIVIN by Nutlin-3 [35]. Table 3 shows fold changes of p53, hMDM2, hMDMX and the p53 targets hMDM2-p2, p21, PUMA, GADD45-alpha and SURVIVIN, for each cell line separately. As expected, p53 and hMDMX mRNA levels did not significantly change upon Nutlin-3 treatment.

hMDMX overexpression in HER cells is not sufficient to inhibit the Nutlin-3 induced p53 response.

Similar to the observations in VH10, in HER cells Nutlin-3 increased p53, hMDM2 and p21 and reduced hMDMX protein levels, which was efficiently blocked by p53-knockdown (Figure 5a). Surprisingly however, hMDMX overexpression hardly rescued these effects. Although at the mRNA level (Figure 5b) the inductions of p53 targets hMDM2-p2, p21 and PUMA were indeed slightly attenuated, this appeared to be insufficient to prevent Nutlin-3 induced growth inhibition, as illustrated by reduced survival (Figure 5c) and S-phase depletion (Figure 5d).

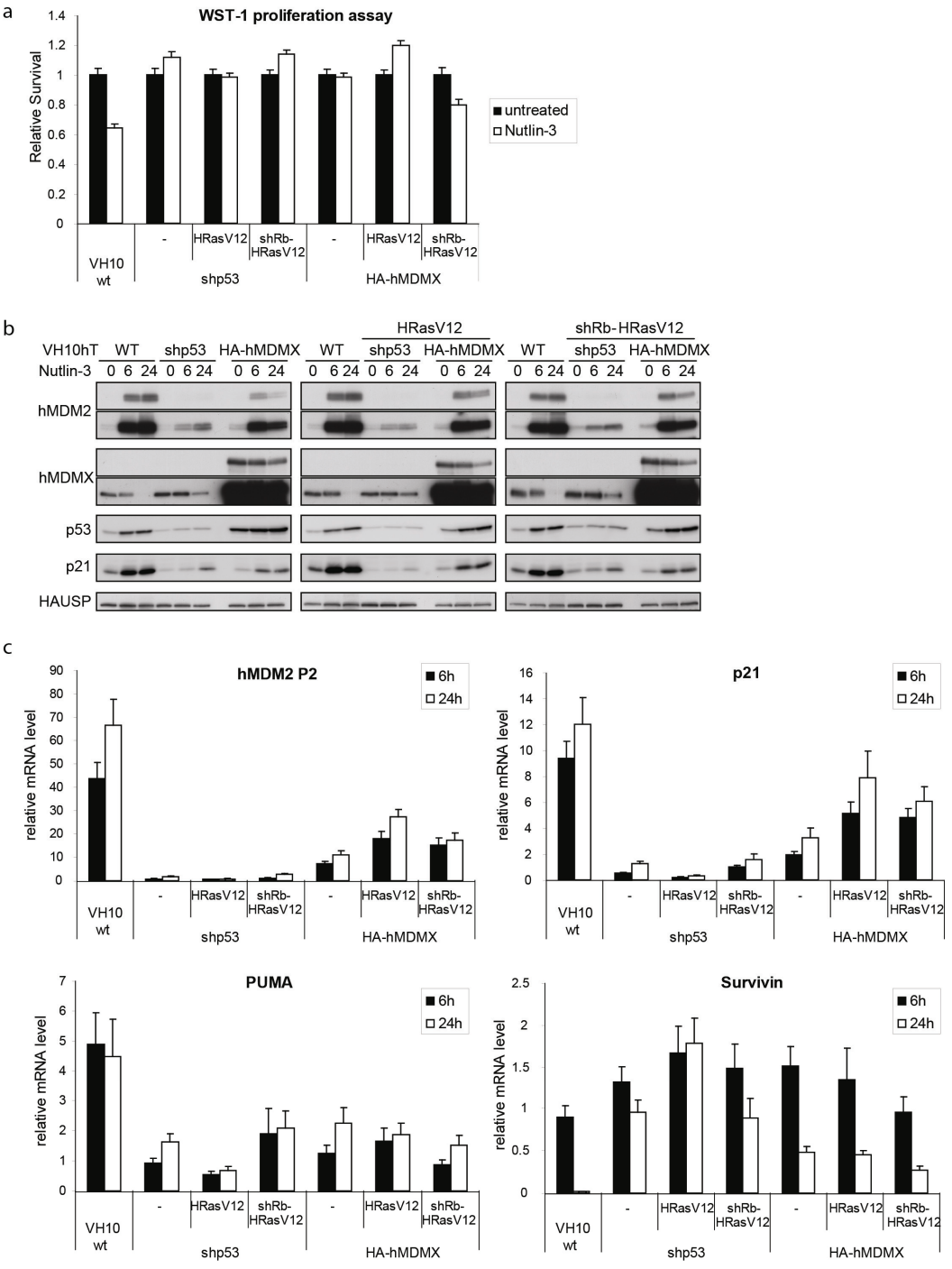

Figure 4 hMDMX overexpression inhibits Nutlin-3 mediated p53 activation in human fibroblasts. (**a**) Various VH10hTERT cell lines were continuously treated with 10 µM Nutlin-3 and proliferation was measured after 96 hours using a WST-1 assay. Relative cell numbers are displayed as survival relative to untreated cells. (**b**) Various VH10hTERT cell lines were treated for the indicated times with 10 µM Nutlin-3, and protein levels were analyzed with immunoblotting using the indicated antibodies. (**c**) qRT-PCR analysis of cells treated as in (**b**). Expression levels of hMDM2-p2, p21, PUMA and SURVIVIN are shown as the fold induction relative to untreated wild-type VH10 cells.

To explain the differences between the hMDMX-overexpressing VH10 and HER cells in their Nutlin-3 response, we compared protein and mRNA levels side-by-side (Figure 5e and 5f). Strikingly, HA-hMDMX was clearly higher expressed in VH10 cells than in HER cells, while endogenous p53, hMDM2 and p21 levels were comparable. As Nutlin-3 not only binds hMDM2 but also hMDMX, albeit with much lower affinity [22], the levels of hMDMX may affect Nutlin-3 sensitivity. In HER cells, the remaining hMDMX levels after Nutlin-3 treatment may not be sufficient to prevent p53 activity. Importantly, we found that hMDMX levels in transformed HER cells were comparable to the levels in retinoblastoma cell lines Y79 and Weri1 (Figure 5G). We have previously shown that in these retinoblastoma cells p53 is inhibited via high hMDMX expression, and that they are sensitive to Nutlin-3 [22]. These findings indicate that the transformed retinoblasts provide a representative model for retinoblastoma.

The response to Nutlin-3 may also be determined by E2F1 activity, which activates p73. Kitagawa et al. [36] reported that Nutlin-3 induced downregulation of E2F1 correlates with relative Nutlin-3 resistance, and they suggested that cells lacking RB activity are much more prone to entering Nutlin-3-induced apoptosis. Therefore, we compared RB and E2F1 levels in a

selected panel of VH10 and HER cell lines (Figure 5e). As reported before [37], Nutlin-3 decreased total and hyper-phosphorylated (upper band) RB. However, the amount of hypo-RB (lower band) was hardly affected. Moreover, after Nutlin-3 treatment, the hypo-RB levels in normal and RB-knockdown cells were comparable, and the differences between VH10 and HER cells were rather small. E2F1 reduction at the protein (Figure 5e) and mRNA level (Supplementary Figure 3a, upper panel) as observed in the parental VH10 and HER cells was attenuated in the transformed cells. The mRNA levels of the E2F1 target gene CDC25a followed a similar pattern. Nutlin-3 also reduced the expression of both total p73 (Supplementary Figure 3a, lower panel) and TA-p73 (not shown) in the parental cells. Strikingly, basal p73 expression was strongly reduced upon transformation. However, transformed VH10 and HER cells showed comparable E2F1 regulation and p73 expression, so this cannot explain the observed differences in Nutlin-3 sensitivity. Therefore, these dissimilarities are more likely the result of different HA-hMDMX levels.

hMDMX overexpression in VH10 cells also inhibited p53 activation by 5-FU and etoposide on both mRNA and protein level (Supplementary Figure 3b and 3c), similar as observed with Nutlin-3 treatments. However, reduced proliferation in response to these drugs occurred mainly through p53-independent pathways, because neither p53-knockdown nor

hMDMX overexpression rescued the growth inhibitory effect (Supplementary Figure 3d). Nevertheless, FACS analysis showed different responses between wild-type, hMDMX-overexpressing and p53-knockdown VH10 cells (data not shown). Upon etoposide treatment, wild-type and hMDMX-overexpressing cells showed a two-fold reduction of G1 phase and an increased G2 fraction. The G2 arrest in p53-knockdown cells was much more severe, with less than 10% remaining in G1. 5-FU induced S-phase accumulation and G2 reduction in wild-type and HA-hMDMX expressing cells, whereas p53-knockdown cells strongly accumulated in G1.

Discussion

In this study, we analyzed the putative oncogenic function of hMDMX in the neoplastic transformation of normal human skin fibroblasts and Human Embryonic Retinoblasts. We chose retinoblasts since hMDMX is frequently overexpressed and/or amplified in retinoblastoma development. Retinoblastoma's, like most other human tumors with increased hMDMX levels, retain wild-type p53 [19-22], suggesting that the oncogenic function of hMDMX is based upon p53 inhibition. After RB inactivation, E2F1 is activated resulting in elevated p14ARF levels, repression of hMDM2 and activation of p53. Since hMDMX is not inhibited by p14ARF, hMDMX-overexpressing cells escape the p53-mediated cell death [38].

Indeed, we find that constitutive expression of hMDMX in foreskin fibroblasts functionally strongly resembles p53-knockdown cells. In combination with other defined genetic changes, hMDMX expression contributes to neoplastic transformation. In transformed cells, hMDMX overexpression reduces basal mRNA and protein levels of p53 targets, with exception of hMDM2 protein levels which are increased most likely via hMDMX-mediated stabilization. Vice versa, the expression of p53-repressed genes, like SURVIVIN, is increased. The ultimately obtained transformed cells show anchorage-independent growth, and can form tumors in an *in vivo* model.
Similarly, hMDMX-expressing HER cells largely resemble p53-knockdown HER cells regarding transformed properties, although hMDMX is less able to counteract the oncogenic HRas-induced growth inhibition, even in RB-knockdown cells. The ultimately obtained transformed cells, with either hMDMX overexpression or p53-knockdown, show *in vivo* growth capacity, although limited.

Our results support the idea that the hMDMX overexpression, which is found in a subset of human tumors [19-22], is an important step in the development of that tumor, and that its

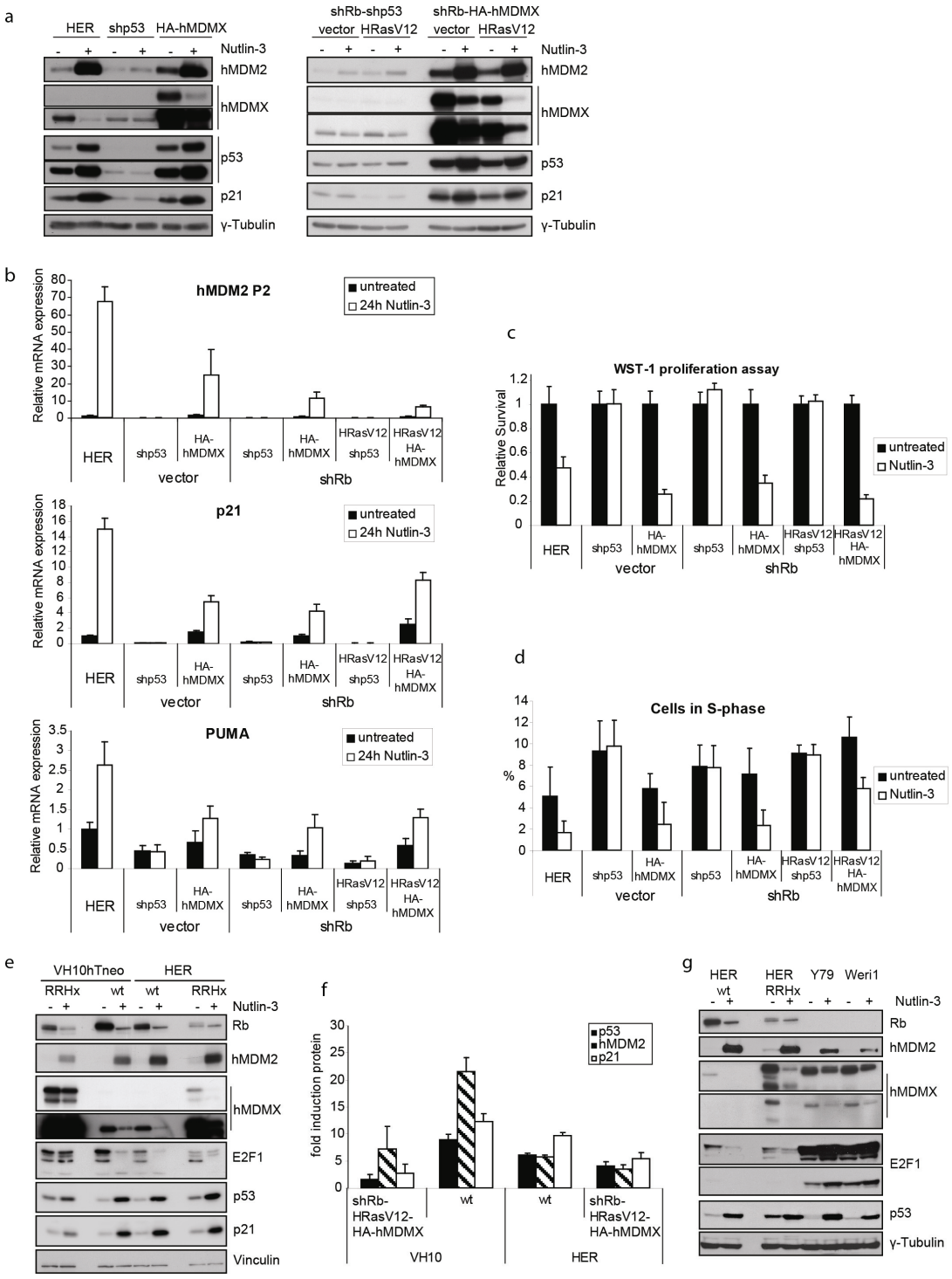

Figure 5 hMDMX overexpression in HER cells is not sufficient to prevent the Nutlin-3 induced p53-activation, which resembles retinoblastoma cell lines. (**a**) The various HER cell lines were treated with 10 µM Nutlin-3 for 24 hours, and protein levels were analyzed with immunoblotting using the indicated antibodies. (**b**) qRT-PCR analysis of cells treated as in (**a**). Expression levels of hMDM2-p2, p21 and PUMA are shown as the fold induction relative to untreated wild-type HER cells. (**c**) The various HER cell lines were continuously treated with 10 µM Nutlin-3 and proliferation was measured after 120 hours using a WST-1 assay. Relative cell numbers are displayed as survival relative to untreated cells. (**d**) Cells were treated with 10 µM Nutlin-3 for 24

hours and analyzed by flow cytometry. Percentages of cells in S-phase are displayed as indicative for cell proliferation. (**e**) Parental and shRB-HRasV12-HA-hMDMX (RRHx) transformed VH10 and HER cells were treated with 10 µM Nutlin-3 for 24 hours and analyzed with immunoblotting using the indicated antibodies. (**f**) Quantification of the indicated protein levels using Odyssey 2.1 analysis software (LI-COR Biosciences) for at least two different exposures. Relative protein levels were calculated using Vinculin expression as an internal control and indicated as fold induction relative to untreated cells. (**g**) Parental and RRHx transformed HER cells and the retinoblastoma cell lines Y79 and Weri1 were treated with 10 µM Nutlin-3 for 24 hours, and analyzed with immunoblotting using the indicated antibodies.

Table 3: Fold induction mRNA per cell line after Nutlin-3 treatment.

Cell line	Nutlin-3 treatment (h)	p53	p21	hMDM2	hMDM2 ex2	hMDMX	PUMA	GADD45a	Survivin
	0	1.00 ± 0.19	1.00 ± 0.16	1.00 ± 0.16	1.00 ± 0.17	1.00 ± 0.16	1.00 ± 0.23	1.00 ± 0.38	1.00 ± 0.16
VH10 wt	6	1.10 ± 0.18	9.36 ± 1.34	28.62 ± 5.40	43.93 ± 6.93	1.38 ± 0.21	4.90 ± 1.06	5.17 ± 1.45	0.90 ± 0.14
	24	0.79 ± 0.18	11.98 ± 2.09	26.42 ± 5.42	66.60 ± 11.19	0.95 ± 0.16	4.49 ± 1.25	4.89 ± 1.79	0.02 ± 0.00
	0	1.00 ± 0.09	1.00 ± 0.11	1.00 ± 0.25	1.00 ± 0.09	1.00 ± 0.09	1.00 ± 0.23	1.00 ± 0.11	1.00 ± 0.13
shp53	6	0.85 ± 0.17	2.24 ± 0.24	1.56 ± 0.31	4.26 ± 0.43	0.91 ± 0.17	1.84 ± 0.35	1.46 ± 0.28	1.18 ± 0.14
	24	0.63 ± 0.54	5.36 ± 0.45	4.08 ± 0.92	9.46 ± 0.73	1.00 ± 0.12	3.29 ± 0.54	1.28 ± 0.12	0.85 ± 0.11
HRasV12-	0	1.00 ± 0.35	1.00 ± 0.27	1.00 ± 0.32	1.00 ± 0.28	1.00 ± 0.29	1.00 ± 0.41	1.00 ± 0.28	1.00 ± 0.23
shp53	6	0.81 ± 0.24	1.34 ± 0.33	1.29 ± 0.39	1.97 ± 0.56	1.09 ± 0.41	1.19 ± 0.40	1.14 ± 0.30	0.99 ± 0.22
	24	0.84 ± 0.28	2.11 ± 0.50	1.44 ± 0.36	2.37 ± 0.66	1.18 ± 0.30	1.53 ± 0.47	1.37 ± 0.32	1.06 ± 0.22
shRb-	0	1.00 ± 0.24	1.00 ± 0.18	1.00 ± 0.22	1.00 ± 0.48	1.00 ± 0.19	1.00 ± 0.18	1.00 ± 0.18	1.00 ± 0.18
HRasV12-	6	0.88 ± 0.24	1.54 ± 0.30	1.16 ± 0.30	2.61 ± 0.97	1.22 ± 0.24	1.22 ± 0.54	1.49 ± 0.63	1.00 ± 0.20
shp53	24	0.98 ± 0.27	2.49 ± 0.67	1.68 ± 0.66	6.32 ± 2.59	1.18 ± 0.38	1.35 ± 0.35	1.76 ± 0.48	0.59 ± 0.16
	0	1.00 ± 0.17	1.00 ± 0.22	1.00 ± 0.03	1.00 ± 0.08	1.00 ± 0.34	1.00 ± 0.14	1.00 ± 0.09	1.00 ± 0.58
HA-hMDMX	6	0.74 ± 0.23	4.14 ± 0.67	3.47 ± 1.26	11.83 ± 1.00	1.42 ± 0.36	3.05 ± 0.49	1.25 ± 0.58	1.52 ± 0.64
	24	1.63 ± 0.25	6.86 ± 1.71	11.92 ± 1.36	18.14 ± 2.03	1.80 ± 0.58	5.45 ± 1.00	2.88 ± 0.93	0.48 ± 0.20
HRasV12-	0	1.00 ± 0.14	1.00 ± 0.16	1.00 ± 0.16	1.00 ± 0.16	1.00 ± 0.22	1.00 ± 0.29	1.00 ± 0.14	1.00 ± 0.16
HA-hMDMX	6	0.90 ± 0.16	6.78 ± 1.16	9.01 ± 1.83	17.33 ± 2.97	1.09 ± 0.22	3.09 ± 0.91	1.27 ± 0.21	0.79 ± 0.22
	24	0.79 ± 0.10	10.38 ± 2.76	12.08 ± 1.58	26.21 ± 2.95	0.74 ± 0.11	3.50 ± 0.85	1.69 ± 0.19	0.26 ± 0.03
shRb-	0	1.00 ± 0.10	1.00 ± 0.05	1.00 ± 0.09	1.00 ± 0.07	1.00 ± 0.05	1.00 ± 0.26	1.00 ± 0.05	1.00 ± 0.06
HRasV12-	6	1.04 ± 0.13	4.57 ± 0.46	6.46 ± 1.61	13.53 ± 2.08	1.01 ± 0.13	3.10 ± 0.63	1.73 ± 0.26	0.81 ± 0.13
HA-hMDMX	24	0.99 ± 0.14	5.76 ± 0.92	6.55 ± 0.94	15.36 ± 2.04	0.96 ± 0.14	5.33 ± 1.27	1.71 ± 0.28	0.23 ± 0.03

VH10 cells were treated with 10 µM Nutlin-3 for the indicated times and analyzed using qRT-PCR. Expression was normalized for the housekeeping genes *CAPNS1* and *TBP*. The induction of mRNA expression upon Nutlin-3 treatment per cell line is shown for *p53*, *p21*, *hMDM2*, *hMDM2-p2*, *hMDMX*, *PUMA*, *GADD45alpha* and *SURVIVIN*. For each cell line the basal mRNA expression is set at 1.0.

main function is to inactivate p53. Interestingly, recently two transgenic mouse models have been described that widely overexpress MDMX [39, 40]. Surprisingly, the phenotypes were very different. Whereas mice from the Lozano lab spontaneously developed tumors upon MDMX overexpression [39], no spontaneous tumor formation nor cooperation with Eµ-Myc-induced tumors was observed in the mice from the Marine lab [40]. In both cases the MDMX-overexpressing MEFs or thymocytes showed an attenuated p53 response upon Nutlin-3 and IR treatment, respectively, suggesting the expression of a functional MDMX protein. It will be important to carefully examine these two mouse models to understand the distinct phenotype. This might teach us more about functions of MDMX in tumorigenesis.

In line with these studies, we find that hMDMX overexpression attenuates the Nutlin-3 mediated p53 activation and growth inhibition in skin fibroblasts. Nutlin-3 has a much lower affinity for hMDMX compared to hMDM2 [22, 41], so the effect of hMDMX overexpression is probably caused by direct p53 inhibition. Similarly, hMDMX overexpression reduces p53 activation by etoposide and 5-FU.

More strikingly, the hMDMX-overexpressing HER cells are still sensitive to Nutlin-3. The p53-response is hardly affected, both regarding regulation of p53 target genes and inhibition of cell proliferation. This difference with hMDMX-transformed VH10 cells is probably due to the lower hMDMX levels in HER-hMDMX cells, which are even further reduced by Nutlin-3. In that respect, the Nutlin-3 response of the transformed retinoblasts resembles that of retinoblastoma cell lines. As we have shown before, these retinoblastoma cell lines are still sensitive to Nutlin-3 and even show an apoptotic response, despite high levels of hMDMX [22].

High hMDMX expression has been reported to attenuate the Nutlin-3 response [42-44]. In a study by Patton and colleagues [43], human embryonic lung fibroblasts were transformed using hTERT, E1A, and oncogenic Ras, with either hMDMX or hMDM2 overexpression, or p53-knockdown, and Nutlin-3 sensitivity was assessed. They found that hMDMX overexpression, in contrast to hMDM2, prevented p53 activation upon Nutlin-3 treatment, which fits most of our data. Nutlin-3 did not inhibit soft agar growth of hMDMX-overexpressing cells in their study. By contrast, we found partial inhibition of soft agar growth by Nutlin-3, whereas growth in a monolayer was not affected at all. Possibly, in 3D additional stress is posed upon the cells, causing super-activation of p53 that cannot be completely counteracted by hMDMX proteins.
The discussed fibroblast models also show a different Nutlin-3 response: IMR-90 cells entered apoptosis, whereas in VH10 cells Nutlin-3 mainly inhibited cell growth without induction of apoptosis (data not shown). Notably, IMR-90 cells are embryonic lung cells; embryonic cells are less differentiated and can be more easily transformed. Furthermore, Patton et al. used adenovirus E1A for RB inactivation, but E1A proteins have additional growth affecting functions, including attenuation of the p53 response by interacting with p300/CBP [45, 46]. Therefore, a clean appreciation of the effects of hMDMX on the p53 response in the presence of E1A is difficult.

Beside hMDMX levels, also other factors may be involved in determining the outcome of Nutlin-3 treatment. Kitagawa et al. [36] have shown that RB status and E2F1 activity are important contributors. However, we found only minor changes in E2F1 activity in our model, which cannot explain the differences in Nutlin-3 sensitivity. Interestingly, the E2F1 target TA-p73 was dramatically decreased upon transformation. This might be a result of HRasV12 activity; oncogenic Ras has been described to switch the expression from TA-p73 to the antagonistic ΔN-p73, an important step during transformation. TA-p73 was reported to prevent anchorage-independent growth via activation of KCNK1 [47]. However, since

transformed fibroblasts as well as retinoblasts express low levels of p73, this does not provide an explanation for the differential Nutlin-3 responses.

Conclusions

In conclusion, we find that hMDMX overexpression can replace loss of p53 during the transformation process of human fibroblasts and embryonic retinoblasts. In addition, very high hMDMX levels, as observed in VH10 cells, can prevent p53 activation by Nutlin-3. However, lower hMDMX levels like in the HER cells can no longer inhibit p53 after Nutlin-3 treatment, because hMDMX protein is mostly degraded by elevated hMDM2 levels, as previously shown in other tumor cells [48]. The Nutlin-3 response of the transformed HER cells resembles that of retinoblastoma cell lines, indicating that this is a physiologically relevant model. A combination therapy using Nutlin-3 and a specific hMDMX inhibitor, possibly a low dose of a DNA damaging agent leading to hMDMX degradation, might result in more effective treatment of tumors expressing wild-type p53 and high levels of hMDMX.

Methods

Generation of stably transformed human cell lines

Primary human fibroblasts (VH10) and Human Embryonic Retinoblasts (HER) were immortalized by introducing human Telomerase (hTERT). Cells were maintained in DMEM supplemented with 10% FBS, 1% glutamine, antibiotics, amino-acids, glucose and vitamins. Stably transformed cell lines were generated in subsequent retroviral infection rounds according to the transformation schemes in Figure 1A and 1C. pRetroSuper-shRB-Hygro and pRS-Hygro [25] were used for RB-knockdown or control cell lines, followed by hygromycin selection (50 µg/ml). pMSCV-blast-Ras or pMSCV-blast [25] were used for HRasV12 overexpression or control cell lines, followed by blasticidin selection (5 µg/ml). pBABE-HA-hMDMX-puro or pRS-shp53-puro [25] were used for hMDMX overexpression or p53-knockdown, both combined with pMSCV-GFP-st [25] for SV40-small-t expression, followed by puromycin selection (0.5 µg/ml). Cell lines were maintained under selection pressure.

Immunoblotting

Cells were lysed in Giordano 250 buffer (50 mM Tris-HCl, pH 7.4, 250 mM NaCl, 0.1% Triton X-100, 5 mM EDTA), with protease- and phosphatase inhibitors. Proteins were separated by SDS-PAGE, transferred onto polyvinyldene difluoride membranes (Immobilon-P, Millipore) and incubated with the appropriate primary (listed in Supplementary Table 1) and HRP-conjugated secondary antibody (Jackson Laboratories). Bands were visualized by enhanced chemiluminescence (Super Signal; Pierce). Alternatively, membranes were incubated with secondary antibodies coupled to IRdye-680 and IRdye-800 near Infrared dyes (LI-COR Biosciences), and analyzed with the Odyssey Infrared

Imager (LI-COR Biosciences). Signals were quantified using the Odyssey 2.1 analysis software (LI-COR Biosciences).

Immunofluorescence

Cells were fixed with 4% paraformaldehyde for 10 min, permeabilized with 0.2 % Triton X-100 for 10 min, blocked with 5% Normal Goat Serum (NGS) for 1 hour and incubated with primary antibodies for 1.5 hours and anti-mouse-Rhodamine secondary antibody (Jackson Laboratories) for 30 min. Coverslips were mounted onto microscope slides using DAPI-DABCO mounting solution.

RNA isolation, qRT-PCR

RNA was isolated using the SV Total RNA isolation kit (Promega, Madison, WI). cDNA was synthesized using 1.0 µg RNA in Reverse Transcriptase reaction mixture (Promega). Samples were analyzed in triplicate using SYBR Green mix (Roche Biochemicals, Indianapolis, IN) in a 7900ht Fast Real-Time PCR System (Applied Biosystems, Foster City, CA). For normalization the geometric mean of at least two housekeeping genes was used. Primer sequences are available in Supplementary Table 2.

Growth assay, soft agar assay

For growth assays, 1000 cells were seeded in triplicate in 96-wells plates; treatments were started 24 hours after seeding. Cells were incubated with WST-1 reagent (Roche) for 1-4 hours and absorbance (450 nm) was measured in a microplate reader (Victor3 Multilabel Counter 1420-042, Perkin-Elmer).

Soft agar assays were performed in 96-well plates (VH10) or 6-well plates (HER) coated with a 0.6 % agarose bottom-layer. Per well, 5000 VH10 or 20.000 HER cells were seeded in 0.3 % agarose. Colony outgrowth was monitored (10x magnification, Olympus CKX41) and pictures were taken at several time points.

Flow cytometry

Cells were harvested, washed with PBS and fixed ice-cold 70 % ethanol. Cells were washed in PBS and incubated in PBS containing 50 µg/ml propidium iodide and 50 µg/ml RNase. Flow cytometry was performed in a BD LSR II system (BD Biosciences).

Cytogenetic methods and combined binary ratio fluorescence in situ hybridization (COBRA-FISH)

Culturing, harvest conditions and karyotyping were performed according to standard protocols [49]. Slides with metaphase chromosomes were hybridized using a multicolor FISH approach. Staining, digital imaging, and analysis were performed as described previously [30]. Hybridizations with individual libraries labeled with single fluorochromes were used to confirm the detected rearrangements. Chromosomal breakpoints were assigned by using inverted images counterstained with 4',6-diamidino-2-phenylindole (DAPI; Downers Grove, IL) together with the information derived from the short- and long-arm specific hybridization during COBRA-FISH. Karyotypes were described according to ISCN 2009.

Shell-less Chicken Chorioallantoic Membrane (CAM) assay

Fertilised chicken eggs were incubated at 37°C in humidified atmosphere. After 4 days they were cracked open into plastic dishes. At day 7, two-and-half million cells transduced with turbo-GFP lentiviral construct (SHC003, Sigma-Aldrich) were mixed with 50 µl basement membrane matrix (BD Biosciences) and grafted onto the CAM. At day 17, tumors with surrounding CAM were removed and the size was measured. GFP-positive tumors were photographed using a fluorescence stereomicroscope. Tumors were embedded in paraffin, sectioned and stained with anti-Vimentin, clone V9 (Santa Cruz) and anti-phospho-Histone-3 (Upstate, Millipore). Percentage of proliferating cells was calculated by quantifying phospho-Histone-3 positive nuclei of on average 500 nuclei from 5 random pictures per sample.

Acknowledgements

The authors would like to thank Dr. Levine and Madelon Maurice for the gift of anti-Mdm2 4B2 and anti-HAUSP monoclonal antibody, respectively. The help of Long Ly with the intraocular injections of the transformed retinoblasts is gratefully acknowledged. This work was supported by grants from the Dutch Cancer Society (UL-2006-3595) and by EC FP6 funding (contract 503576). This publication reflects the authors' views and not necessarily those of the European Community. The EC is not liable for any use that may be made of the information contained.

Authors' contributions

KLe and JdL performed the transformations of the human cells, performed all growth assays and contributed to the protein and mRNA analyses and immunofluorescence data. KLo and EW performed the *in vivo* tumorigenicity studies. AT, KLo and MVdV performed protein and mRNA analyses and contributed to the immunofluorescence data. MvdB and KS performed and interpreted the COBRA-FISH analyses. KLe, JdL and AGJ designed and coordinated the study and drafted the manuscript.

References

1. Hainaut P, Hollstein M: p53 and human cancer: the first ten thousand mutations. *Adv Cancer Res* 2000, 77:81-137.
2. Hollstein M, Sidransky D, Vogelstein B, Harris CC: p53 mutations in human cancers. *Science* 1991, 253:49-53.
3. Vogelstein B, Lane D, Levine AJ: Surfing the p53 network. *Nature* 2000, 408:307-310.
4. Lane DP: Cancer. p53, guardian of the genome. *Nature* 1992, 358:15-16.
5. Haupt Y, Barak Y, Oren M: Cell type-specific inhibition of p53-mediated apoptosis by mdm2. *EMBO J* 1996, 15:1596-1606.

6. Momand J, Zambetti GP, Olson DC, George D, Levine AJ: The mdm-2 oncogene product forms a complex with the p53 protein and inhibits p53-mediated transactivation. *Cell* 1992, 69:1237-1245.
7. Montes de Oca LR, Wagner DS, Lozano G: Rescue of early embryonic lethality in mdm2-deficient mice by deletion of p53. *Nature* 1995, 378:203-206.
8. Jones SN, Roe AE, Donehower LA, Bradley A: Rescue of embryonic lethality in Mdm2-deficient mice by absence of p53. *Nature* 1995, 378:206-208.
9. Parant J, Chavez-Reyes A, Little NA, Yan W, Reinke V, Jochemsen AG, Lozano G: Rescue of embryonic lethality in Mdm4-null mice by loss of Trp53 suggests a nonoverlapping pathway with MDM2 to regulate p53. *Nat Genet* 2001, 29:92-95.
10. Migliorini D, Lazzerini Denchi E., Danovi D, Jochemsen A, Capillo M, Gobbi A, Helin K, Pelicci PG, Marine JC: Mdm4 (Mdmx) regulates p53-induced growth arrest and neuronal cell death during early embryonic mouse development. *Mol Cell Biol* 2002, 22:5527-5538.
11. Finch RA, Donoviel DB, Potter D, Shi M, Fan A, Freed DD, Wang CY, Zambrowicz BP, Ramirez-Solis R, Sands AT, Zhang N: mdmx is a negative regulator of p53 activity in vivo. *Cancer Res* 2002, 62:3221-3225.
12. Marine JC, Jochemsen AG: Mdmx and Mdm2: brothers in arms? *Cell Cycle* 2004, 3:900-904.
13. Marine JC, Jochemsen AG: Mdmx as an essential regulator of p53 activity. *Biochem Biophys Res Commun* 2005, 331:750-760.
14. Shvarts A, Steegenga WT, Riteco N, van Laar T., Dekker P, Bazuine M, van Ham RC, van der Houven van Oordt, Hateboer G, van der Eb AJ, Jochemsen AG: MDMX: a novel p53-binding protein with some functional properties of MDM2. *EMBO J* 1996, 15:5349-5357.
15. Sharp DA, Kratowicz SA, Sank MJ, George DL: Stabilization of the MDM2 oncoprotein by interaction with the structurally related MDMX protein. *J Biol Chem* 1999, 274:38189-38196.
16. Gu J, Kawai H, Nie L, Kitao H, Wiederschain D, Jochemsen AG, Parant J, Lozano G, Yuan ZM: Mutual dependence of MDM2 and MDMX in their functional inactivation of p53. *J Biol Chem* 2002, 277:19251-19254.
17. Linares LK, Hengstermann A, Ciechanover A, Muller S, Scheffner M: HdmX stimulates Hdm2-mediated ubiquitination and degradation of p53. *Proc Natl Acad Sci U S A* 2003, 100:12009-12014.
18. Momand J, Wu HH, Dasgupta G: MDM2--master regulator of the p53 tumor suppressor protein. *Gene* 2000, 242:15-29.
19. Danovi D, Meulmeester E, Pasini D, Migliorini D, Capra M, Frenk R, de Graaf P., Francoz S, Gasparini P, Gobbi A, Helin K, Pelicci PG, Jochemsen AG, Marine JC: Amplification of Mdmx (or Mdm4) directly contributes to tumor formation by inhibiting p53 tumor suppressor activity. *Mol Cell Biol* 2004, 24:5835-5843.
20. Riemenschneider MJ, Knobbe CB, Reifenberger G: Refined mapping of 1q32 amplicons in malignant gliomas confirms MDM4 as the main amplification target. *Int J Cancer* 2003, 104:752-757.

21. Ramos YF, Stad R, Attema J, Peltenburg LT, van der Eb AJ, Jochemsen AG: Aberrant expression of HDMX proteins in tumor cells correlates with wild-type p53. *Cancer Res* 2001, 61:1839-1842.
22. Laurie NA, Donovan SL, Shih CS, Zhang J, Mills N, Fuller C, Teunisse A, Lam S, Ramos Y, Mohan A, Johnson D, Wilson M, Rodriguez-Galindo C, Quarto M, Francoz S, Mendrysa SM, Guy RK, Marine JC, Jochemsen AG, Dyer MA: Inactivation of the p53 pathway in retinoblastoma. *Nature* 2006, 444:61-66.
23. Hahn WC, Counter CM, Lundberg AS, Beijersbergen RL, Brooks MW, Weinberg RA: Creation of human tumour cells with defined genetic elements. *Nature* 1999, 400:464-468.
24. Hahn WC, Dessain SK, Brooks MW, King JE, Elenbaas B, Sabatini DM, DeCaprio JA, Weinberg RA: Enumeration of the simian virus 40 early region elements necessary for human cell transformation. *Mol Cell Biol* 2002, 22:2111-2123.
25. Voorhoeve PM, Agami R: The tumor-suppressive functions of the human INK4A locus. *Cancer Cell* 2003, 4:311-319.
26. Brookes S, Rowe J, Ruas M, Llanos S, Clark PA, Lomax M, James MC, Vatcheva R, Bates S, Vousden KH, Parry D, Gruis N, Smit N, Bergman W, Peters G: INK4a-deficient human diploid fibroblasts are resistant to RAS-induced senescence. *EMBO J* 2002, 21:2936-2945.
27. Miller KR, Kelley K, Tuttle R, Berberich SJ: HdmX overexpression inhibits oncogene induced cellular senescence. *Cell Cycle* 2010, 9.
28. Ghosh M, Huang K, Berberich SJ: Overexpression of Mdm2 and MdmX fusion proteins alters p53 mediated transactivation, ubiquitination, and degradation. *Biochemistry* 2003, 42:2291-2299.
29. Wang YV, Wade M, Wong E, Li YC, Rodewald LW, Wahl GM: Quantitative analyses reveal the importance of regulated Hdmx degradation for p53 activation. *Proc Natl Acad Sci U S A* 2007, 104:12365-12370.
30. Szuhai K, Tanke HJ: COBRA: combined binary ratio labeling of nucleic-acid probes for multi-color fluorescence in situ hybridization karyotyping. *Nat Protoc* 2006, 1:264-275.
31. Therman E, Susman B, Denniston C: The nonrandom participation of human acrocentric chromosomes in Robertsonian translocations. *Ann Hum Genet* 1989, 53:49-65.
32. Dohle DS, Pasa SD, Gustmann S, Laub M, Wissler JH, Jennissen HP, Dunker N: Chick ex ovo culture and ex ovo CAM assay: how it really works. *J Vis Exp* 2009.
33. Ly LV, Baghat A, Versluis M, Jordanova ES, Luyten GP, van Rooijen N., van Hall T., van der Velden PA, Jager MJ: In aged mice, outgrowth of intraocular melanoma depends on proangiogenic M2-type macrophages. *J Immunol* 2010, 185:3481-3488.
34. Vassilev LT, Vu BT, Graves B, Carvajal D, Podlaski F, Filipovic Z, Kong N, Kammlott U, Lukacs C, Klein C, Fotouhi N, Liu EA: In vivo activation of the p53 pathway by small-molecule antagonists of MDM2. *Science* 2004, 303:844-848.
35. Mirza A, McGuirk M, Hockenberry TN, Wu Q, Ashar H, Black S, Wen SF, Wang L, Kirschmeier P, Bishop WR, Nielsen LL, Pickett CB, Liu S: Human survivin is negatively regulated by wild-type p53 and participates in p53-dependent apoptotic pathway. *Oncogene* 2002, 21:2613-2622.

36. Kitagawa M, Aonuma M, Lee SH, Fukutake S, McCormick F: E2F-1 transcriptional activity is a critical determinant of Mdm2 antagonist-induced apoptosis in human tumor cell lines. *Oncogene* 2008, 27:5303-5314.
37. Du W, Wu J, Walsh EM, Zhang Y, Chen CY, Xiao ZX: Nutlin-3 affects expression and function of retinoblastoma protein: role of retinoblastoma protein in cellular response to nutlin-3. *J Biol Chem* 2009, 284:26315-26321.
38. Marine JC, Dyer MA, Jochemsen AG: MDMX: from bench to bedside. *J Cell Sci* 2007, 120:371-378.
39. Xiong S, Pant V, Suh YA, Van Pelt CS, Wang Y, Valentin-Vega YA, Post SM, Lozano G: Spontaneous tumorigenesis in mice overexpressing the p53-negative regulator Mdm4. *Cancer Res* 2010, 70:7148-7154.
40. de Clercq S, Gembarska A, Denecker G, Maetens M, Naessens M, Haigh K, Haigh JJ, Marine JC: Widespread overexpression of epitope tagged-Mdm4 does not accelerate tumor formation in vivo. *Mol Cell Biol* 2010.
41. Joseph TL, Madhumalar A, Brown CJ, Lane DP, Verma C: Differential binding of p53 and nutlin to MDM2 and MDMX: Computational studies. *Cell Cycle* 2010, 9.
42. Hu B, Gilkes DM, Farooqi B, Sebti SM, Chen J: MDMX overexpression prevents p53 activation by the MDM2 inhibitor Nutlin. *J Biol Chem* 2006, 281:33030-33035.
43. Patton JT, Mayo LD, Singhi AD, Gudkov AV, Stark GR, Jackson MW: Levels of HdmX expression dictate the sensitivity of normal and transformed cells to Nutlin-3. *Cancer Res* 2006, 66:3169-3176.
44. Wade M, Wong ET, Tang M, Stommel JM, Wahl GM: Hdmx modulates the outcome of p53 activation in human tumor cells. *J Biol Chem* 2006, 281:33036-33044.
45. Steegenga WT, van Laar T., Riteco N, Mandarino A, Shvarts A, van der Eb AJ, Jochemsen AG: Adenovirus E1A proteins inhibit activation of transcription by p53. *Mol Cell Biol* 1996, 16:2101-2109.
46. Somasundaram K, El-Deiry WS: Inhibition of p53-mediated transactivation and cell cycle arrest by E1A through its p300/CBP-interacting region. *Oncogene* 1997, 14:1047-1057.
47. Beitzinger M, Hofmann L, Oswald C, Beinoraviciute-Kellner R, Sauer M, Griesmann H, Bretz AC, Burek C, Rosenwald A, Stiewe T: p73 poses a barrier to malignant transformation by limiting anchorage-independent growth. *EMBO J* 2008, 27:792-803.
48. Xia M, Knezevic D, Tovar C, Huang B, Heimbrook DC, Vassilev LT: Elevated MDM2 boosts the apoptotic activity of p53-MDM2 binding inhibitors by facilitating MDMX degradation. *Cell Cycle* 2008, 7:1604-1612.
49. Szuhai K, Ijszenga M, Tanke HJ, Taminiau AH, de Schepper A., van Duinen SG, Rosenberg C, Hogendoorn PC: Detection and molecular cytogenetic characterization of a novel ring chromosome in a histological variant of Ewing sarcoma. *Cancer Genet Cytogenet* 2007, 172:12-22.

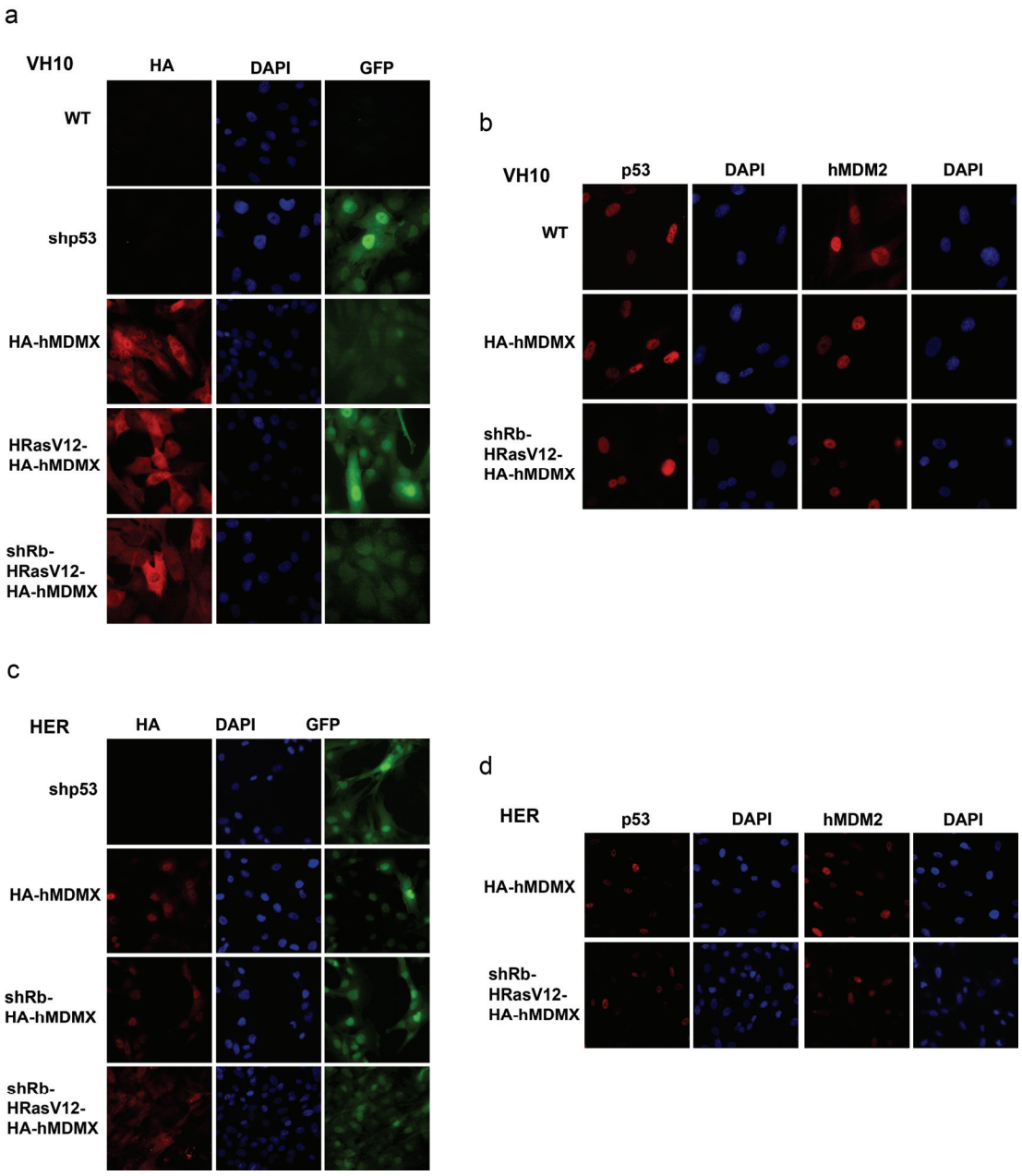

Supplementary Figure 1 Overexpressed HA-hMDMX is localised both nuclear and cytoplasmic and does not alter p53 and hMDM2 localisation. Localisation of hMDMX, hMDM2 and p53 in various VH10 (**a**,**b**) and HER (**c**,**d**) cell lines was determined by immunofluorescence using the indicated antibodies. DAPI staining was used to visualise nuclei, GFP signal represents SV-40 small-t expression.

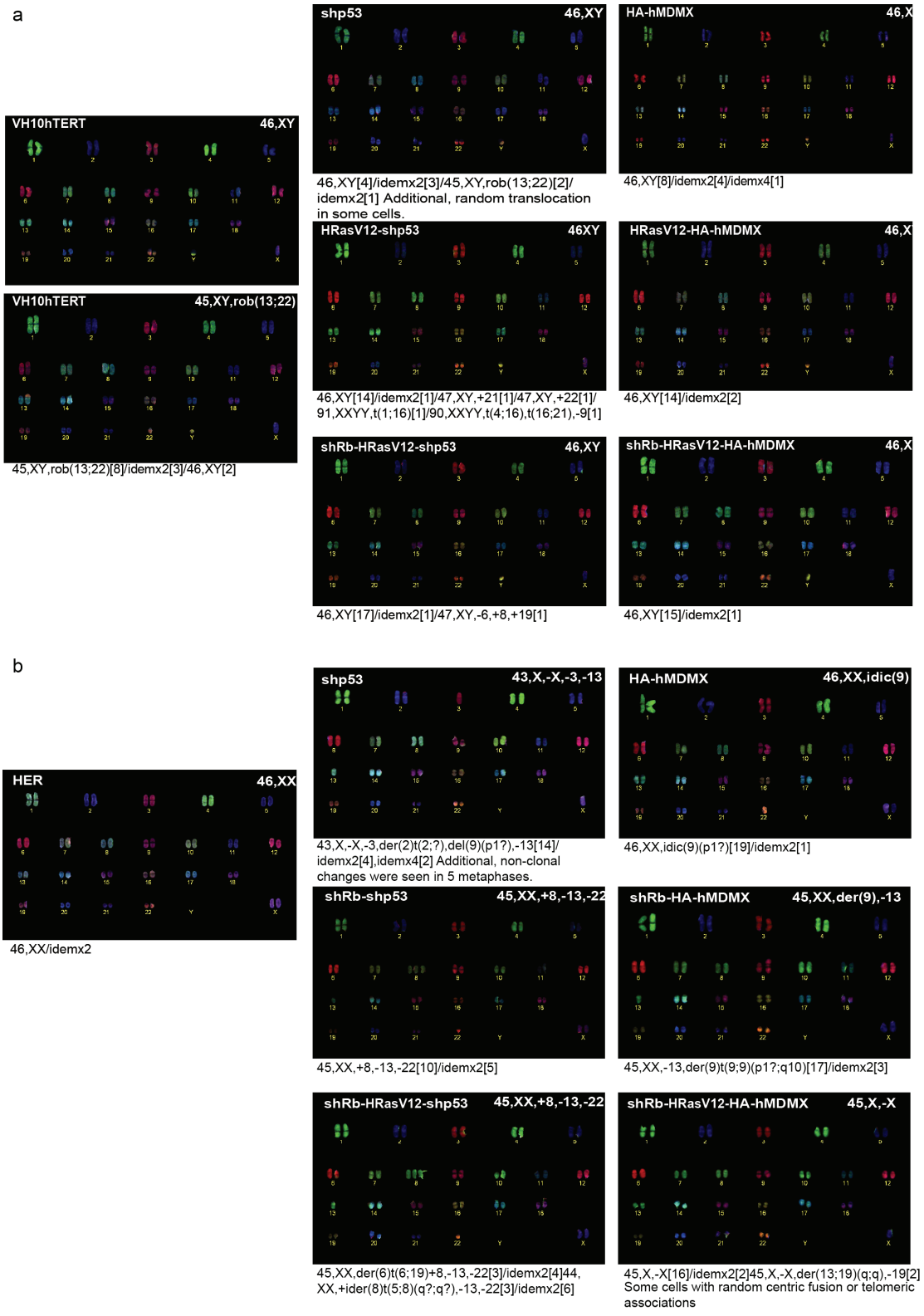

Supplementary Figure 2 Karyotyping of VH10 and HER cell lines. Karyotypes of transformed VH10 (**a**) and HER (**b**) cell lines using combined binary ratio labeling-fluorescence in situ hybridization (COBRA-FISH). Representative karyograms after COBRA-FISH hybridization are shown for each cell line.

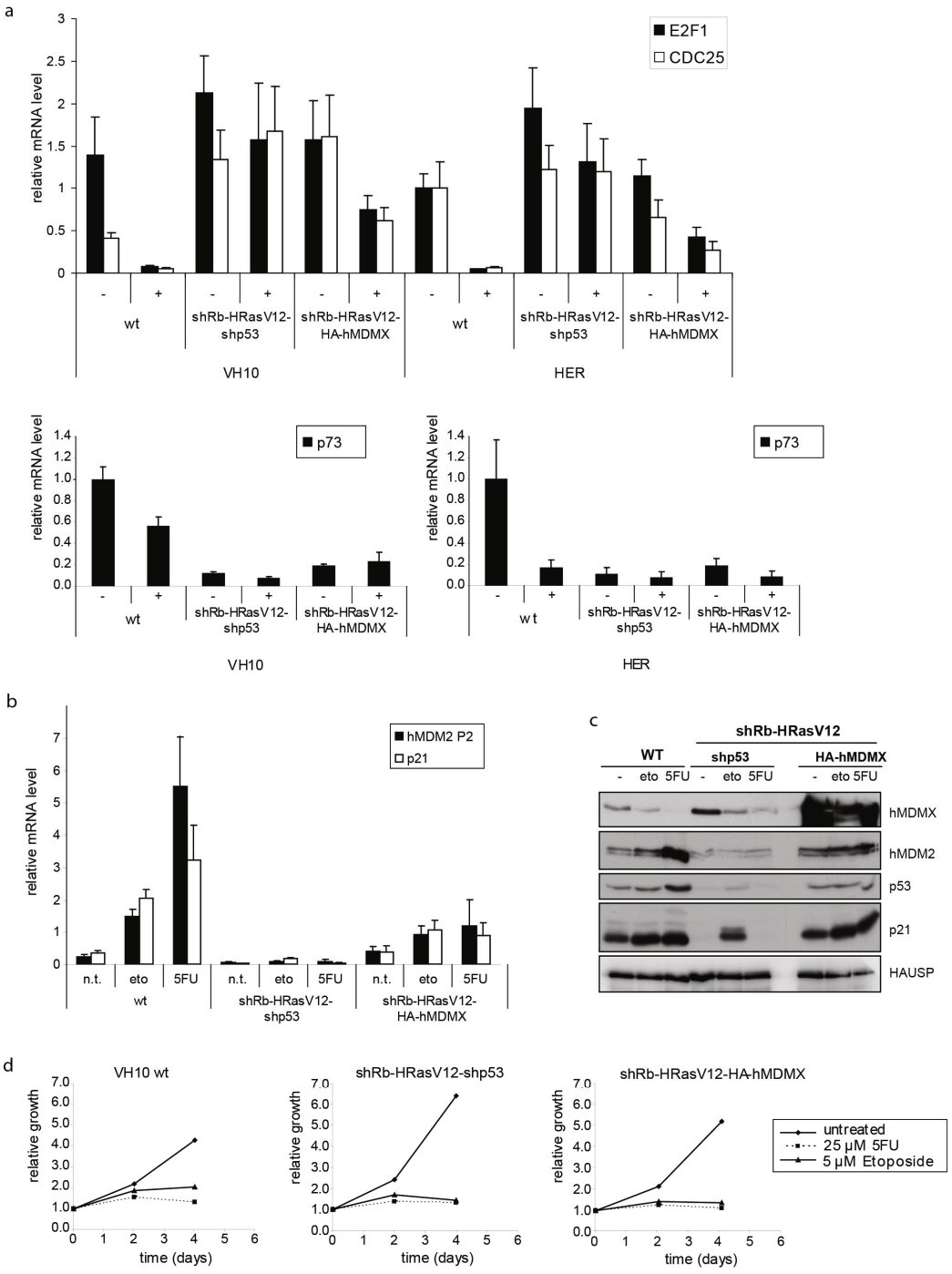

Supplementary Figure 3 hMDMX overexpression inhibits p53 response but does not rescue the growth inhibition induced by 5-fluoro-uracil or etoposide in human fibroblasts. (**a**) The indicated VH10 and HER cell lines were treated with 10 µM Nutlin-3 for 24 hours and analyzed with qRT-PCR. Expression levels of E2F1, CDC25a (upper panel) and p73 (lower panel) were normalized for housekeeping genes RPS11 and CAPNS1. (**b**) Indicated VH10 cell lines were treated for 24 hours with 25 µM 5-FU, 5 µM etoposide or mock treated, and analyzed with qRT-PCR. Expression levels of hMDM2-p2 and p21 were normalized for housekeeping genes CAPNS1 and SRPR. (**c**) Protein levels of cells treated as in (**b**) were analyzed with immunoblotting using the indicated antibodies. (**d**) Cell growth was monitored using WST-1 proliferation assays. 24 hours after seeding the cells were treated for 24 hours with the indicated drugs. Cell proliferation was measured at day 0, 2 and 4 after treatment.

Supplementary Table 1: List of used antibodies.

Protein	Name/ cat. #	Company
hMDMX	A300-287A	Bethyl Laboratories, Montgomery TX, USA
hMDM2	6B1A	Ref 1
HA-tag	HA.11	Covance, Princeton, New Jersey, USA
HA-tag	ab9110	Abcam, Cambridge, UK
p53 °	DO-1 / sc-126	Santa Cruz Biotechnology, Santa Cruz, CA, USA
p53 °	18O1 / sc-98	Santa Cruz Biotechnology, Santa Cruz, CA, USA
p53	FL-393	Santa Cruz Biotechnology, Santa Cruz, CA, USA
hMDM2 * / MDM2	4B2	Ref 2
hMDM2 *	SMP14 sc-6965	Santa Cruz Biotechnology, Santa Cruz, CA, USA
p21	CP74 / 05-655	Upstate Biotechnology, Lake Placid, NY, USA
Rb	G3-245 / 554136	BD Pharmingen, Franklin Lakes, New Jersey, USA
HRas	Y13-259	Ref 3
HAUSP USP7	A300-033A	Bethyl Laboratories, Montgomery TX, USA
HAUSP USP7	7G9	Ref 4
p21	CP74 / 05-655	Upstate Biotechnology, Lake Placid, NY, USA
γ-Tubulin	GTU-88 / T6557	Sigma-Aldrich, St Louis, MO, USA

For detection of human p53 we used a mix of DO-1 and 1801 (°), for detection of human hMDM2 we used a mix of 4B2 and SMP14 (*).

Ref 1) Stad R *et al.* **Hdmx stabilizes Mdm2 and p53**. *J Biol Chem* 2000, **275:**28039-28044.
Ref 2) Chen J *et al.* **Mapping of the p53 and mdm-2 interaction domains**. *Mol Cell Biol* 1993, **13:**4107-4114.
Ref 3) Furth ME *et al.* **Monoclonal antibodies to the 21 products of the transformation gene of Harvey murine sarcoma virus and of the cellular ras gene family.** *J. Virol.* 1982, **43**, 293-304.
Ref 4) Kessler BM *et al.* **Proteome changes induced by knock-down of the deubiquitylating enzyme HAUSP/USP7**. *J Proteome Res* 2007, 6:4163-4172.

Supplementary Table 2: Sequences of qRT-PCR primers.

hMDM2-P2 Fw	5'-acgcacgccacttttctct- 3'
hMDM2-P2 Rv	5'-tccgaagctggaatctgtgag- 3'
P53 Fw	5'-ctctccccagccaaagaagaa- 3'
P53 Rv	5'-tccaaggcctcattcagctct- 3'
hMDMX Fw	5'-aggtgcgcaaggtgaaatgt- 3'
hMDMX Rv	5'-ccatatgctgctcctgctgat- 3'
PUMA Fw	5'-gacctcaacgcacagta- 3'
PUMA Rv	5'-ctaattgggctccatct- 3'
p21 Fw	5'-agcagaggaagaccatgtgga- 3'
p21 Rv	5'-aatctgtcatgctggtctgcc- 3'
SURVIVIN Fw	5'-gagacagaatagagtgatagg- 3'
SURVIVIN Rv	5'-gacagatgtgaaggttgg- 3'
GADD45a Fw	5'-gcgacctgcagtttgcaata- 3'
GADD45a Rv	5'-atcccccaccttatccatcct- 3'
CAPNS1 Fw	5'-atggttttggcattgacacatg- 3'
CAPNS1 Rv	5'-gcttgcctgtggtgtcgc- 3'
TBP Fw	5'-cacgaaccacggcactgatt- 3'
TBP Rv	5'-ttttcttgctgccagtctggac- 3'
RPS11 Fw	5'-aagcagccgaccatctttca- 3'
RPS11 Rv	5'-cgggagcttctccttgcc- 3'
SRPR Fw	5'-cattgcttttgcacgtaaccaa- 3'
SRPR Rv	5'-attgtcttgcatgcggcc- 3'
CDC25A Fw	5'-ctccgagtcaacagattcagg- 3'
CDC25A Rv	5'-ttcaaggttttctttactgtccaa- 3'

Chapter 3

High levels of Hdmx promote cell growth in a subset of uveal melanomas

J. de Lange[1], A.F.A.S. Teunisse[1], M. Verlaan-de Vries[1], K. Lodder[1], S. Lam[1], G.P.M. Luyten[2], M.J. Jager[2], A.G. Jochemsen[1]

[1] Department of Molecular Cell Biology, Leiden University Medical Center, 2300 RC Leiden, The Netherlands
[2] Department of Ophtalmology, Leiden University Medical Center, 2300 RC Leiden, The Netherlands

Abstract

The p53 tumor suppressor pathway is inactivated in cancer either via direct mutation or via deregulation of upstream regulators or downstream effectors. P53 mutations are rare in uveal melanoma. Here we investigated the role of the p53 inhibitor Hdmx in uveal melanoma. We found Hdmx over-expression in a subset of uveal melanoma cell lines and fresh-frozen tumor samples. Hdmx depletion resulted in cell-line dependent growth inhibition, apparently correlating with differential Hdm2 levels. Surprisingly, p53 knockdown hardly rescued cell cycle arrest and apoptosis induction upon Hdmx knockdown when using three different shRNA constructs, whereas it effectively prevented growth suppression induced by the potent p53 activator Nutlin-3. These findings suggest a novel, growth-promoting function of Hdmx that does not rely on its ability to inhibit p53. We provide evidence for a contribution of p27 protein induction to the observed p53-independent G1 arrest in response to Hdmx knockdown. In conclusion, our study establishes the importance of Hdmx as an oncogene in a subset of uveal melanomas and widens the spectrum of its function beyond p53 inhibition.

Introduction

After skin, primary melanoma most commonly affects the eye [1]. Uveal melanoma arises in the uveal tract, which comprises the iris, ciliary body, and the choroid. Current treatments mostly involve plaque radiotherapy (brachytherapy), proton beam irradiation or enucleation [2]. However, these local treatments do not prevent distant metastases. Up to 50% of patients with uveal melanoma develop metastases after the initial diagnosis and treatment, most frequently in the liver. Prognosis is poor when the tumor has metastasized; metastases are only sporadically curable and median survival is about 10 - 18 months [3;4]. Therefore, a better understanding of the molecular mechanisms underlying uveal melanomagenesis is needed to develop more efficient treatment modalities.

The molecular pathogenesis of uveal melanoma is different from that in cutaneous melanoma. For example, mutations of NRAS, BRAF and CDKN2A (the gene encoding $p16^{INK4A}$ and $p14^{ARF}$) are frequently observed in cutaneous melanoma, but not in uveal melanoma [5-7]. Uveal melanomas have been reported to show frequent loss of chromosome 3, correlating with poor prognosis [8]; over-expression of Cyclin D1 [9;10] and inactivating mutation of BAP1 [11], both associated with metastasis; activating mutations of GNAQ and GNA11 [12;13] and promoter methylation of the tumor suppressors $p16^{INK4A}$ [14] and RassF1A [15]. Interestingly, mutations of p53 are uncommon both in cutaneous melanoma [16] and in uveal melanoma [17-19]. DNA damage induces p53 stabilization in uveal melanoma cell lines, although downstream functional defects may be common [20].

Functional inactivation of the p53 tumor suppressor pathway is believed to be involved in virtually all human cancers [21]. Direct gene mutation is found in about 50% of tumors [22;23], whereas those retaining wild type p53 contain other genetic changes preventing p53's tumor suppressor function [24]. P53 maintains genomic integrity following a variety of stress signals by orchestrating the cellular responses, including cell cycle arrest, DNA repair, senescence and apoptosis [25]. Controlled p53 activation requires tight regulation of the main p53 inhibitors, Hdm2 and Hdmx [26]. Hdm2 ubiquitinates p53 to target it for degradation [27], whereas Hdmx functions mostly by inhibiting p53 activity through interaction with its transcription activation domain [28;29]. Furthermore, Hdmx and Hdm2 dimerize via their RING finger domains [30], which promotes Hdm2's E3 ligase activity towards p53 [31;32].

About 5-10% of all human tumors show Hdm2 overexpression [33]. In addition, increased Hdmx mRNA levels in 20% of common tumor types [34] and Hdmx gene amplification and overexpression in high percentage of retinoblastomas [35] and in a subset gliomas [36] indicate an oncogene function for Hdmx. Aberrant Hdmx expression in a large number of human tumor cell lines correlated with wild-type p53 status [37]. In addition, a few reports suggested p53-independent activities for Hdmx. For example, Hdmx has been implicated to suppress transcriptional activity of E2F1 [38] and Smad proteins [39;40], and to downregulate p21 protein levels [41]. However, p53 remains its major cellular target. Since uveal melanomas usually harbor wild-type p53, a subset of these cancers probably relies on increased levels of Hdm2 or Hdmx. To investigate this, we evaluated the status of the p53 pathway in uveal melanoma, with particular focus on Hdmx. Interestingly, when performing functional analysis of Hdmx in several selected uveal melanoma cell lines we encountered a growth promoting function of Hdmx that is independent of p53 inhibition. Our findings suggest that a novel p53-independent function of Hdmx is relevant in uveal melanoma and that targeting Hdmx may be beneficial in a subset of these tumors.

Results

Hdmx is over-expressed in a subset of uveal melanomas

A panel of ten uveal melanoma cell lines was analyzed for basal levels of several key proteins in the p53 pathway (Figure 1a). The levels of p53 itself were found to be more or less constant in all cell lines and they were comparable to the wild-type p53 expressing osteosarcoma cell line U2OS that we used as control, suggesting the absence of p53 mutations. The double band pattern observed in some lanes most likely represents the p53 codon 72 polymorphism [44]. The levels of Hdm2 and Hdmx varied greatly between cell lines, with most cell lines showing increased levels of at least one of these proteins.

In addition to OCM8, especially the cell lines derived from a metastasis (Omm1, Omm2.3 and Omm2.5) show very low levels of Hdmx protein. Recently, we found that especially in later stage tumors the relative expression of an alternative splice variant of Hdmx, Hdmx-S is increased accompanied with lower Hdmx protein levels, correlating with lower survival of patients (Lenos *et al.*, in preparation). Therefore, we investigated the levels of Hdmx and Hdmx-S mRNA in the panel of uveal melanoma cell lines. Indeed, the results revealed that all three metastasis-derived cell lines express relatively high levels of Hdmx-S mRNA (Figure 1b). We also analyzed Hdm2 and Hdmx protein levels in lysates of fresh-frozen uveal melanoma tumor tissue and compared these with normal uveal melanocytes (NUM),

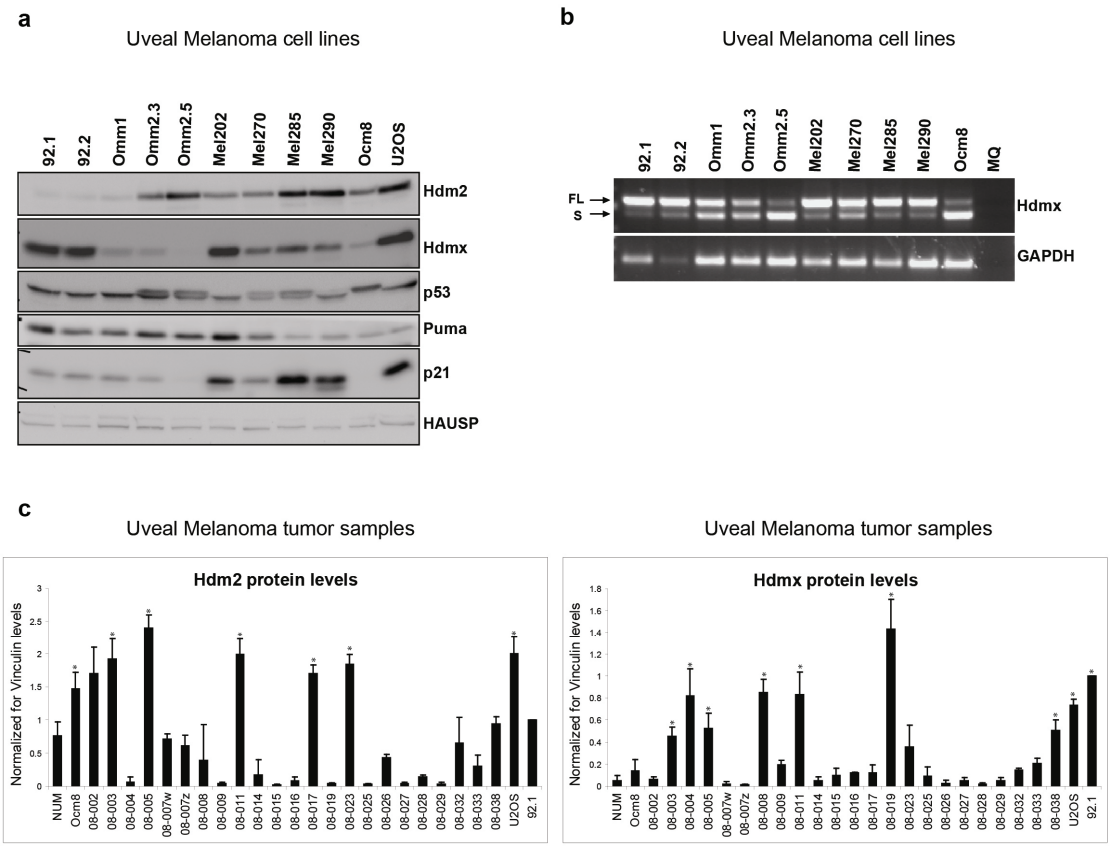

Figure 1 High expression of Hdmx in a subset of uveal melanomas. (**a**) Total lysates of ten uveal melanoma cell lines and the osteosarcoma cell line U2OS were analyzed by western blot using the indicated antibodies. (**b**) RT-PCR analysis of the mRNA levels of Hdmx (exon 3 – exon 8) and GAPDH. FL = full length Hdmx; S = short splice variant. (**c**) Protein extracts of 23 fresh-frozen uveal melanoma tumor samples were analyzed for Hdm2, Hdmx and Vinculin protein levels by western blot. Band intensities were quantified from two different blots using Image J software. For all samples, the expression levels of Hdm2 and Hdmx were calculated relative to 92.1, which was loaded on each gel, and corrected for Vinculin levels on each blot. Statistical comparison of each sample with NUM levels was performed using a two-tailed t-test; an asterisk indicates $p < 0.05$.

OCM8, 92.1 and U2OS lysates, representing low and high level Hdm2 and Hdmx controls (Figure 1c and Supplementary Figure 1). Hdm2 levels were significantly elevated in 5 out of 23 tumor samples (22%) compared to NUM. In 7 samples (30%) we found increased levels of Hdmx; 3 of these tumor samples overlapped. These findings suggest that Hdm2 and Hdmx over-expression control p53 activity in a subset of uveal melanomas.

Cell line-dependent growth inhibition upon Hdmx knockdown

To investigate whether high Hdmx expression indeed contributes to the growth of uveal melanoma cell lines, we selected three cell lines from the panel based on their differential expression of Hdmx and Hdm2. The 92.1 cells express high levels of Hdmx and low Hdm2, Mel202 cells express high levels of Hdmx and moderate Hdm2, and Mel285 cells express

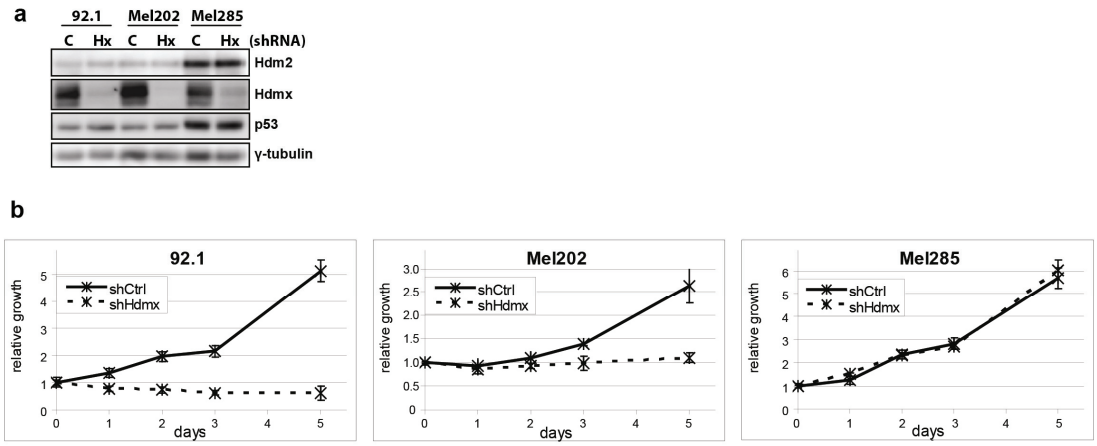

Figure 2 Cell line-dependent growth inhibition upon Hdmx knockdown. (**a**) 92.1, Mel202 and Mel285 cells were transduced with shCtrl or shHdmx#1 RNAs, and protein extracts were analyzed by western blot using the indicated antibodies. (**b**) Cells were counted and seeded for WST-1 proliferation assay, and cell viability was measured at several time points during five days.

moderate levels of Hdmx and high Hdm2. We reduced Hdmx expression using shRNA and analyzed cell proliferation/survival. Hdmx knockdown strongly suppressed growth of both 92.1 and Mel202 cells, whereas the growth of Mel285 cells was largely unaffected (Figure 2). This difference in sensitivity is most likely the result of differences in Hdm2 levels, which are highest in Mel285 cells. We have previously shown that Mel285 cells are sensitive to Nutlin-3 treatment, precluding the argument that p53 is not wild-type in Mel285 cells [45].

P53-independent growth inhibition upon Hdmx knockdown

To investigate whether the growth inhibitory effect of Hdmx knockdown was p53-dependent, we generated stable shp53 and shCtrl cell lines, which were transduced with shCtrl or three different shHdmx RNAs (Figure 3a). Surprisingly, p53 depletion did not rescue the effects of Hdmx knockdown in a 5-day growth assay, for none of the knockdown constructs (Figure 3b). We further evaluated the biological effects of Hdmx depletion by flow cytometry and found a clear G1 arrest, which was largely p53-independent (Figure 3c). Notably, a proportion of cells did not arrest in G1 upon Hdmx knockdown, as visualized by BrdU incorporation (Supplementary Figure 2a, left). Analysis 16h after BrdU removal indicated that a fraction of shHdmx cells still managed to enter the cell cycle and replicated at similar rate compared to the shCtrl cells (Supplementary Figure 2a, middle). This could be due to incomplete Hdmx knockdown in this cell fraction. Indeed, we found a selection for cells in which the knockdown was weaker: after 5 weeks culturing under puromycin selection, Hdmx expression returned to normal levels (Supplementary Figure 2b) and proliferation was no longer affected (Supplementary Figure 2a, right). In addition to cell cycle arrest, loss of Hdmx also resulted in a modest increase of Sub-G1 fraction (Figure 3d)

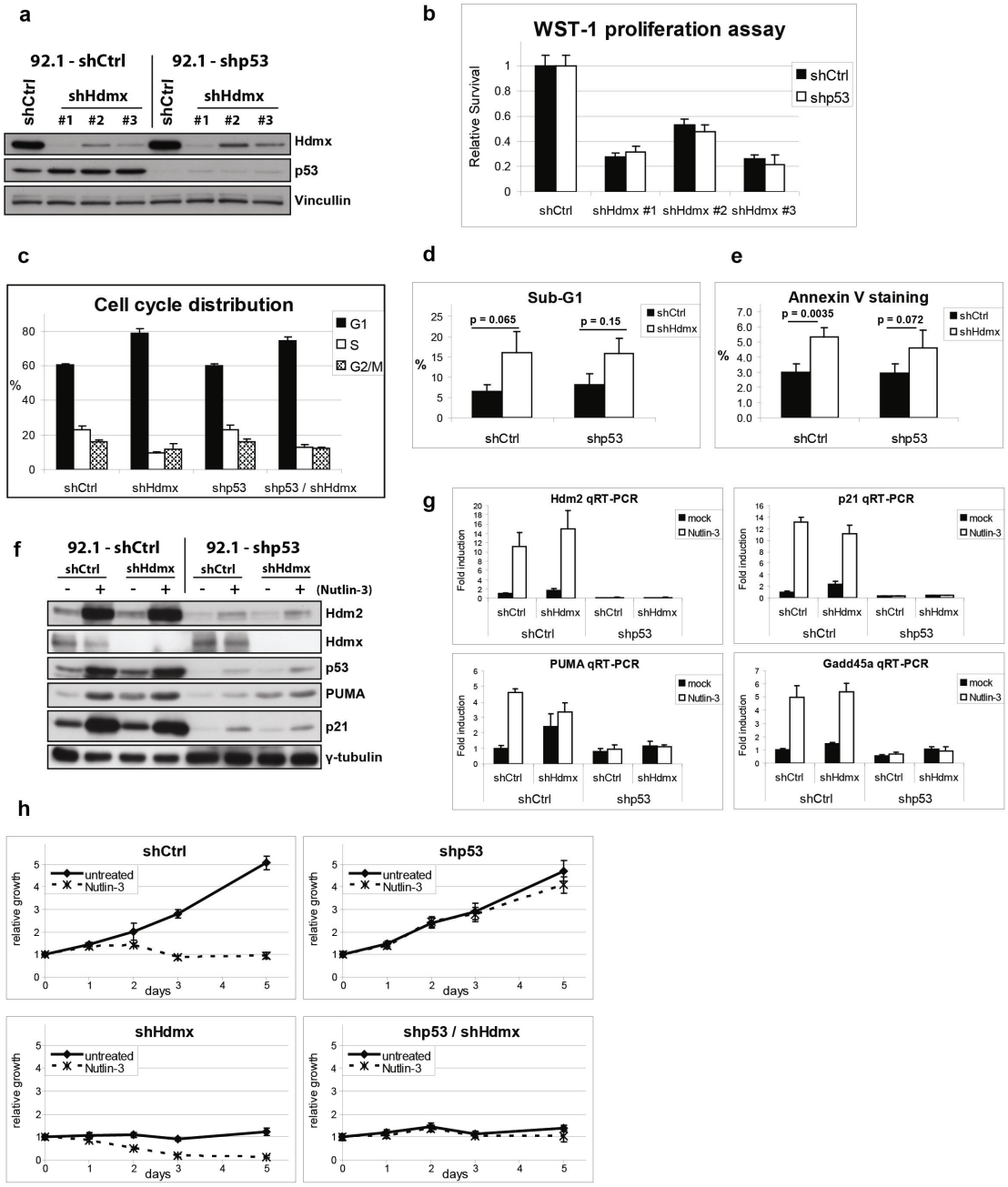

Figure 3 p53-independent growth inhibition upon Hdmx knockdown. (**a**) 92.1 cells were stably transduced using shCtrl or shp53 RNAs. The resulting cell lines were transduced with shCtrl or with three different shHdmx RNAs, and protein extracts were analyzed by western blot using the indicated antibodies. (**b**) Cells were counted and seeded for WST-1 proliferation assay, and cell viability was measured after five days. (**c**) Stable 92.1-shCtrl and 92.1-shp53 cells were transiently transduced with shCtrl or shHdmx#1 RNA and after six days, cell cycle profiles were analyzed by flow cytometry. Bars represent the mean and s.e. of two independent experiments. (**d,e**) Evaluation of Sub-G1 fractions and Annexin V staining, four days after transduction. Bars represent the mean and s.e. of three independent experiments. Statistical analysis was performed using a two-tailed t-test. (**f-h**) Stable 92.1-shCtrl and 92.1-shp53 cells were transiently transduced with shCtrl or shHdmx#1 RNA and subsequently mock-treated or treated with 10 μM Nutlin-3 for 24h. (**f**) Protein extracts were analyzed by western blot using the indicated antibodies. (**g**) qRT-PCR analysis of the expression levels of Hdm2, PUMA, p21 and Gadd45α, normalized for the geometric mean of CAPNS1, GAPDH and ARP. (**h**) Cells were counted and seeded for WST-1 proliferation assay. Cells were mock-treated or treated with 10 μM Nutlin-3, and cell viability was measured at several time points during five days.

and of Annexin V staining (Figure 3e). These results indicate some increased apoptosis upon Hdmx knockdown, in part p53-dependent, although the inductions were borderline significant.

The above described effects of Hdmx depletion in shp53 cells would be easily explained if the knockdown of p53 would be far from complete. In that case, Hdmx knockdown would still lead to p53 reactivation and p53-dependent growth inhibition. Therefore, we tested the efficiency of p53 knockdown by treating the cells with Nutlin-3, a potent activator of p53 [46]. Nutlin-3 was designed to bind Hdm2, but it also binds Hdmx albeit with lower affinity [35;47]. As shown in Figure 3f, 24h Nutlin-3 treatment strongly induced the protein levels of p53 and its target genes Hdm2, PUMA and p21 in shCtrl cells. We also found inductions of Hdm2, PUMA, p21 and Gadd45α at the mRNA level (Figure 3g). Of note, Hdmx knockdown in shCtrl cells also affected the expression of p53 targets, indicating some p53 activation in response to Hdmx depletion in these cells. Nutlin-3 strongly suppressed cell proliferation, and the growth inhibiting effect of Hdmx knockdown was further enhanced (Figure 3h). Importantly, the shp53 cells showed strongly reduced effects of Nutlin-3 on protein levels, mRNA levels and cell proliferation, indicating that the p53 knockdown was indeed sufficient to prevent p53 activation by Nutlin-3. In addition, FACS analysis revealed that Nutlin-3 treatment in shCtrl cells caused G1 arrest and increased Sub-G1 fractions, and it further enhanced the effects of Hdmx knockdown, whereas these effects were largely absent in shp53 cells (Supplementary Figure 3). Importantly, we observed similar p53-independent effects of Hdmx depletion on protein levels, mRNA levels, proliferation, and cell cycle profiles in Mel202 cells (Supplementary Figure 4a-d). Together, these findings indicate that the growth inhibition upon Hdmx knockdown is at least in part due to a novel function of Hdmx that stretches beyond p53 inhibition.

Reducing the expression of the retinoblastoma gene fails to rescue growth inhibition upon Hdmx knockdown

To characterize the aforementioned p53-independent function of Hdmx, we investigated the involvement of a few obvious candidates. First, we reasoned that in addition to p53, also the p53 homolog p73 might be bound and inhibited by Hdmx. Release of this inhibition would then result in p73-dependent growth suppression. However, we have not been able to detect p73 protein in these cells (not shown), making it unlikely that p73 reactivation is responsible for the observed effects of Hdmx knockdown. Next, we investigated a putative involvement of the tumor suppressor protein Rb. We hypothesized that, similar to the reported activity of Hdm2 towards Rb [48], Hdmx may also function via

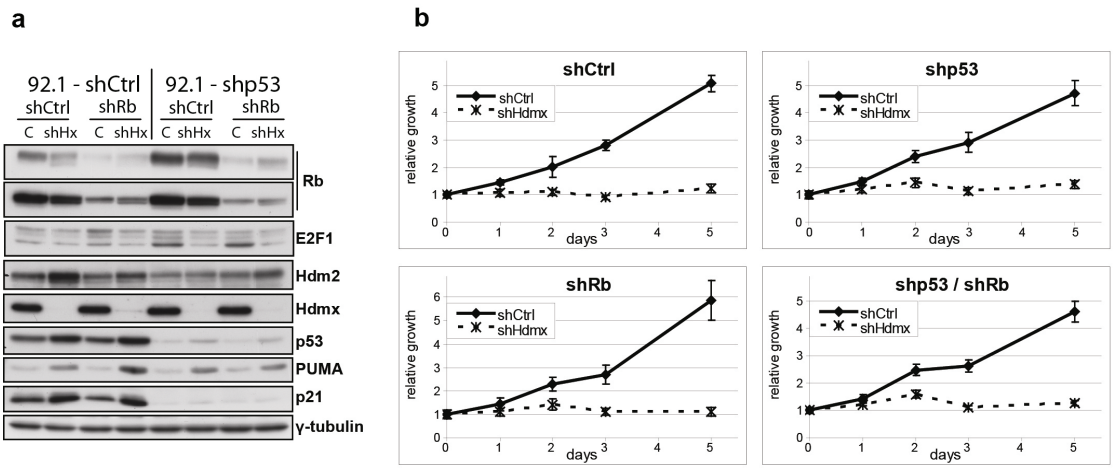

Figure 4 Rb knockdown fails to rescue growth inhibition upon Hdmx knockdown. (**a**) 92.1 cells were stably transduced with shCtrl, shp53, shRb or with a combination of shp53 and shRb RNAs. The four resulting cell lines were transduced with shCtrl or shHdmx#1 RNAs and after four days protein extracts were analyzed by western blot using the indicated antibodies. (**b**) Cells from (**a**) were counted and seeded for WST-1 proliferation assay, and cell viability was measured at several time points during five days.

Rb inhibition. We stably reduced Rb expression via shRNA expression (Figure 4a) and investigated the effect of Hdmx knockdown on proliferation (Figure 4b). We found that reduced Rb levels failed to rescue the growth suppression upon Hdmx knockdown, although in this particular experiment the Rb knockdown is not very effective (Figure 4a).

Analysis of Hdmx knockdown-induced changes in expression of apoptosis-related genes

To search for genes that contribute to p53-independent apoptosis induction, we used a RT^2 Profiler PCR Array, which analyses the expression of 84 genes involved in apoptosis. Six genes showed more than 1.5 fold increased mRNA expression in both shCtrl and shp53 cells (Supplementary Figure 5a), of which four (BCL2L11, Caspase 4, Caspase 9 and TNFRSF1A) were annotated as apoptosis promoting genes. Seven genes showed more than 1.5 fold reduction of mRNA expression in both shCtrl and shp53 cells (Supplementary Figure 5b), of which three (Akt1, TRAF2 and BCL2L2) were annotated as apoptosis suppressing genes. Unfortunately, for none of these genes subsequent experiments could validate their expression to correlate with Hdmx knockdown (data not shown). This suggests that the p53-independent induction of apoptosis in response to Hdmx knockdown does not occur via transcriptional regulation, at least as far as the 84 genes represented on the array are concerned.

Survivin over-expression fails to rescue growth inhibition upon Hdmx knockdown

Interestingly, Hdmx knockdown reduced the mRNA expression of the inhibitor of apoptosis (IAP) family member Survivin, which was not included in the RT^2 Profiler PCR Array (Supplementary Figure 6a). This reduction was partially p53-dependent as indicated by the effects of Nutlin-3. However, there may also be a p53-independent effect, as the Survivin expression was also somewhat reduced upon Hdmx knockdown in the shp53 cells. At the protein level, we found similar effects of Hdmx knockdown, using two shRNAs targeting Hdmx (Supplementary Figure 6b). We investigated a putative contribution of Survivin to the growth inhibiting effect of Hdmx knockdown by stable Survivin over-expression. However, despite high levels of exogenous Survivin (Supplementary Figure 6c), this could not rescue the negative effects of Hdmx knockdown on proliferation (Supplementary Figure 6d).

Induction of p27 protein levels upon Hdmx knockdown occurs independently of p53 and contributes to G1 arrest

The G1 arrest that is induced by Hdmx knockdown could be caused by increased levels of Cdk inhibitor(s). For example, p21 has been reported to interact with Hdmx, which leads to p21 degradation [41]. However, we found strongly reduced mRNA and protein levels of p21 in shp53 cells as compared to shCtrl cells (Figure 3f and 3g and Supplementary Figure 4a and 4b). Especially since the p21 levels in shp53-shHdmx cells were much lower than in shCtrl cells, a functional contribution of p21 to the observed effects of Hdmx knockdown is highly unlikely.

Another Cdk inhibitor that might be involved in the growth inhibiting effects of Hdmx knockdown is p27. Interestingly, p27 is a transcriptional target of FOXO proteins, and Hdm2 has been reported to inhibit activity of FOXO proteins by inducing the poly-ubiquitination of FOXO1 and FOXO3A [49] and mono-ubiquitination of FOXO4 [50]. Therefore, Hdmx might also function via regulation of FOXO proteins. Indeed, we observed an induction of p27 protein levels after Hdmx knockdown in 92.1 (Figure 5A) and Mel202 cells (Supp Figure 4A), irrespective of p53 levels. However, p27 mRNA was not induced (Figure 5B) indicating that the increased p27 levels in response to Hdmx knockdown does not occur at the transcriptional level. Importantly, we found p27 protein induction already one day after Hdmx knockdown (Figure 5C), a time frame during which the G1 arrest is not yet maximal (not shown), suggesting that the increased p27 protein level is not a secondary effect of cell cycle arrest [51-53]. To further examine the relevance of p27

induction in the responses to Hdmx knockdown, we reduced p27 expression by shRNA (Figure 5A) and analyzed cell cycle progression. Interestingly, the reduction of cells in S-phase (Figure 5D) as well as the amount of BrdU positive cells (Figure 5E) upon Hdmx knockdown was partially rescued by p27 depletion. A summary of these experiments (Figure 5F) illustrates that p27 knockdown partially prevents the G1 arrest induced by Hdmx knockdown, on top of a partial rescue by p53 depletion.

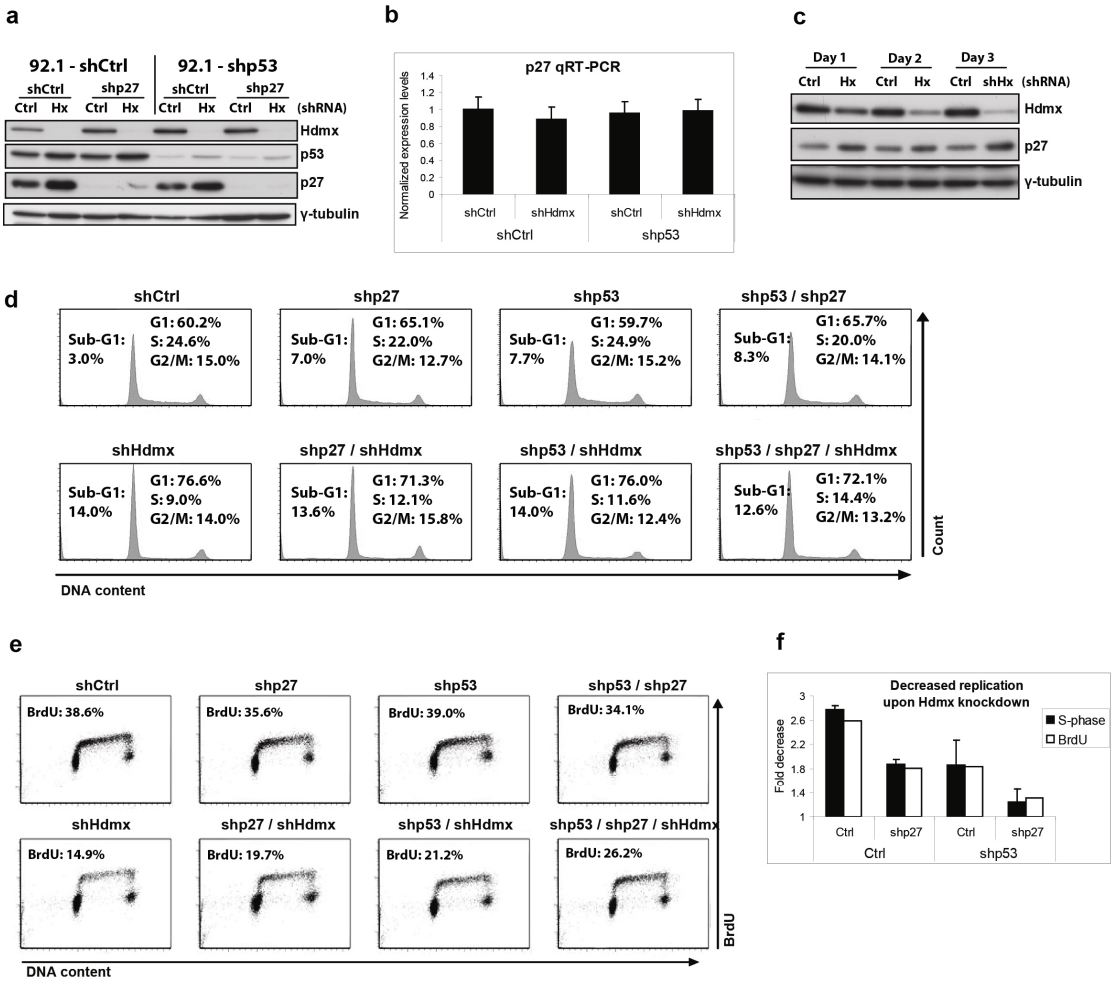

Figure 5 Induction of p27 protein levels upon Hdmx knockdown occurs independently of p53 and contributes to G1 arrest. A, 92.1 cells were stably transduced with shCtrl, shp53, shp27 or with a combination of shp53 and shp27 RNAs. The resulting cell lines were transduced with shCtrl or shHdmx#1 RNAs and after four days protein extracts were analyzed by western blot using the indicated antibodies. B, Cells were transduced as indicated and analyzed by qRT-PCR for p27 expression levels, normalized for the geometric mean of CAPNS1, ARP and RPS11. C, 92.1-shp53 cells were transduced with shCtrl or shHdmx#1 RNAs. Protein extracts were isolated at the indicated time-points and analyzed by western blot using the indicated antibodies. D, Cells transduced as in A were analyzed by flow cytometry. E, Cells transduced as in A were incubated with 20 µM BrdU for 2 hrs and analyzed by flow cytometry. F, Quantification of D and E. Graphs indicate the fold reductions upon Hdmx knockdown of S-phase cells (mean and s.e. of two independent experiments) and BrdU positive cells.

Discussion

Hdmx over-expression is found in a subset of human cancers, generally correlating with the presence of wild-type p53 protein [34-37]. Constitutive Hdmx over-expression contributes to the oncogenic transformation of cultured cells, thereby functionally resembling loss of p53 [34;54]. These findings emphasize that Hdmx over-expression in cancer mainly serves to block p53 activity. Indeed, in this study we show Hdmx over-expression in a subset of cell lines and fresh-frozen tumor samples from uveal melanoma, which rarely contain p53 mutations. Increased levels of Hdm2 were also observed in some cell lines and tumor samples, although the extent of over-expression was not impressive when compared to normal uveal melanocytes. Interestingly, our experiments in uveal melanoma cell lines also suggest the existence of an additional growth promoting function of Hdmx. Of note, we used three different Hdmx knockdown constructs and observed comparable effects on proliferation in 92.1 and Mel202 cells, whereas Mel285 cells remained largely unaffected. This indicates that a subset of uveal melanomas depends on Hdmx over-expression. In addition, the resistance of Mel285 cells reduces the likelihood of non-specific effects caused by the Hdmx knockdown constructs in 92.1 and Mel202 cells. Importantly, the lack of growth inhibition by Nutlin-3 in shp53 cells confirmed the efficiency of the p53 knockdown, indicating that Hdmx promotes uveal melanoma growth partially through p53-independent pathways.

At first sight this finding is a little surprising, particularly in light of the complete rescue of the embryonic lethality of Mdmx deletion by loss of p53 [55;56], which would argue against the importance of p53-independent effects of Hdmx. On the other hand, the physiological role of basal Hdmx levels during development may not be identical to the pathological effects of Hdmx over-expression during tumorigenesis. In addition, it is becoming increasingly clear that Hdm2 activity, and especially pathologically high levels of Hdm2, is not restricted to p53 regulation. Because of the homology between Hdm2 and Hdmx, our search for the mechanisms underlying p53-independent activities of Hdmx was primarily based on known functions of Hdm2. Enhanced Hdm2 activity has been reported to inhibit Rb function via ubiquitin-dependent degradation [48]. The Rb tumor suppressor protein represses E2F1 transcriptional activity via direct protein-protein interaction. Once released from Rb, resulting from Cyclin-Cdk mediated Rb phosphorylations, E2F1 transcriptionally activates genes involved in G1-S transition. A putative inhibiting function of Hdmx towards Rb might, therefore, explain the growth suppressing effect of Hdmx knockdown, as loss of such inhibition would subsequently lead to Rb reactivation.

However, the lack of rescue in our Rb knockdown experiments suggests that Rb is not responsible for the observed effects of Hdmx knockdown.

Interestingly, our results point at p27 protein induction as being one of the factors contributing to the growth inhibiting effects of Hdmx knockdown. Although p27 may exert some functions that are potentially oncogenic, it is generally considered to be a tumor suppressor [57]. The main role of p27 is to regulate the G0/G1 to S transition by binding and inhibiting cyclin E/CDK2 and cyclin D/CDK4,6 complexes. P27 itself is highly regulated at multiple levels, including transcription, translation, phosphorylation and ubiquitination [57;58]. P27 protein levels are maximal during G0 and early G1, mainly due to differences in cap-independent translation [59] and ubiquitin-dependent proteolysis [60] in different stages of the cell cycle. However, the induction of p27 protein levels in response to Hdmx knockdown probably occurred too quickly to be a secondary event of the G1 arrest. Moreover, p27 knockdown partially prevented the G1 arrest in response to Hdmx knockdown. This indicates that Hdmx somehow prevents p27 from inhibiting cell proliferation, via an unknown mechanism. Interestingly, Hdm2 can target FOXO proteins [49;50] and FOXO proteins regulate p27. Therefore, a reduction of Hdmx might lead to increased activity of FOXO proteins towards p27. Although we detected no changes in p27 mRNA expression, p27 regulation by FOXO proteins may exceed transcription. For instance, FOXO4 inhibits Akt1 to promote p27 nuclear translocation [61], and FOXM1 increases p27 stability [62]. Therefore, a closer examination of the involvement of FOXO proteins might still be rewarding.

Our search for genes contributing to apoptosis induction upon Hdmx knockdown turned out to be disappointing. Overall, the changes in mRNA expression of the 84 genes on the profiler array were rather small, which on itself might fit with the rather modest apoptosis induction in response to Hdmx knockdown. However, none of the ‘hits’ could be validated in additional tests. Thus, either the responsible gene(s) were not represented on the array, or the induction of apoptosis is transcription-independent. We further looked into the inhibitor of apoptosis (IAP) family member Survivin, since it is aberrantly expressed in a variety of human cancers [63]. Furthermore, a few reports suggest that this also includes uveal melanoma. A comparative transcriptomic analysis of uveal melanoma and normal uveal melanocytes revealed an upregulation of BIRC5 (the gene encoding Survivin) [64], whereas another study reported elevated expression of Survivin in several uveal melanoma cell lines, including 92.1, correlating with enhanced cisplatin resistance [65]. However, Survivin over-expression did not affect the outcome of Hdmx knockdown experiments, despite the reduction of endogenous levels. Indeed, Survivin transcription is

regulated in a cell cycle-dependent manner, peaking at mitosis [66;67], so the reduced Survivin levels may have been an indirect effect of Hdmx knockdown-induced G1 arrest.

In conclusion, Hdmx over-expression is present in a subset of uveal melanomas, most likely to promote tumorigenesis by inhibiting p53, which is rarely mutated in this type of tumors. Interestingly, however, we show that Hdmx also has an important p53-independent role in promoting cell proliferation and survival. It will be important to analyze the relevance of this role of Hdmx in other cell types as well. Our attempts to uncover the molecular basis of a p53-independent function of Hdmx have revealed a contribution for p27 in the induction of G1 arrest. Future studies are required to provide more insights into the mechanism by which Hdmx affects p27 protein levels. However, our data strongly suggest the involvement of additional, yet unknown factors, although unraveling these factors thus far proved difficult. In this respect, it may be worthwhile to investigate the involvement of proteins reported to interact with Hdm2, but not tested in this study, since they might interact with Hdmx as well. Alternatively, a mass spectrometry screen for Hdmx binding partners and functional characterization of newly found interactions might open new avenues to clarify p53-independent activities of Hdmx. Together this will improve our understanding of Hdmx over-expressing tumors and ultimately may lead to the development of new therapeutic strategies to target such tumors.

Materials and Methods

Cell lines, lentiviral transductions, drug treatments

Human uveal melanoma cell lines 92.1 [42], Mel202 and Mel285 were cultured in RPMI + F10 medium (1:1 ratio) with 10% fetal bovine serum (FBS) and antibiotics. Lentiviral constructs (listed in Supp Table 1) were described before [43] or obtained from the Mission shRNA library (Sigma-Aldrich, St Louis, MO). For lentiviral transductions, cells were seeded at a density of $4.0*10^5$ (92.1 and Mel285) or $6.0*10^5$ (Mel202) cells per 6 cm dish. The next day, cells were transduced using MOI = 1.0 in medium containing 8.0 µg/mL polybrene and were puromycin-selected for stable expression. Nutlin-3 was used at a final concentration of 10 µM and was purchased from Cayman Chemical (Ann Arbor, MI, USA).

Immunoblotting

Cells were lysed in Giordano buffer (50 mM Tris-HCl, pH 7.4, 250 mM NaCl, 0.1% Triton X-100, 5 mM EDTA) with protease- and phosphatase inhibitors. Proteins were separated by SDS-PAGE, blotted onto Polyvinylidene Fluoride Transfer membranes, incubated with the appropriate primary (listed in

Supp Table 2) and secondary antibodies, and bands were visualized by chemoluminescence (West Dura, Pierce Biotechnology, Rockford, IL).

RNA isolation, qRT-PCR

RNA was isolated using the SV Total RNA isolation kit (Promega, Madison, WI). cDNA was synthesized using 2.0 µg RNA in a total volume of 30 µL reverse transcriptase reaction mixture (Promega). Samples were analyzed in triplicate using SYBR Green mix (Roche Biochemicals, Indianapolis, IN) in a 7900ht Fast Real-Time PCR System (Applied Biosystems, Foster City, CA). For normalization the geometric mean of at least two housekeeping genes was used. Primer sequences are listed in Supp. Table 3.

Flow cytometry

Cells were harvested, washed in PBS and fixed in ice-cold 70% EtOH. Prior to FACS analysis, cells were washed in PBS and resuspended in PBS containing 50 µg/mL RNase A and 50 µg/mL propidium iodide (PI). Flow cytometry was performed in the BD LSR II system (BD Biosciences). For Annexin V staining, cells were washed twice in PBS and resuspended in Annexin V-binding buffer containing Fluorescein isothyocyanate (FITC)-labeled Annexin-V (Sigma-Aldrich) and PI. After 10 min RT incubation cells were analyzed by flow cytometry. Positive PI staining, indicating necrotic or late apoptotic cells, were excluded from the analysis. PI-negative, Annexin V-positive cells represent early apoptotic cells. For bromodeoxyuridine (BrdU) incorporation, we added BrdU to the culture medium at a final concentration of 20 µM for 2h. Cells were harvested, washed in PBS and fixed in ice-cold 70% EtOH. Subsequently, cells were treated with 50 µg/ml RNase A (30 min 37 °C), washed and resuspended in 5 M HCl / 0.5% Triton (20 min RT). Cells were then neutralized in 1 M Tris/HCl pH 7.5, washed in PBS and incubated with anti-BrdU-FITC antibody (50 µg 11 202 693 001, Roche) in PBS/Tween with 1% BSA (30 min RT). Cells were washed twice in PBS/Tween, resuspended in PBS containing 50 µg/mL PI and analyzed by flow cytometry to detect BrdU and PI staining.

WST-1 proliferation assay

Cells were counted and seeded in triplicate in 96-well plates at a density of 3000 (92.1 and Mel285) or 6000 (Mel202) cells per well, in a total volume of 100 µL culture medium. To determine the survival/cell growth, 10 µL WST-1 (Roche) was added to the wells and absorbance (450 nm) was measured 2 hrs later in a microplate reader (Victor; Perkin Elmer).

Acknowledgements

We thank Prof. B.R. Ksander for providing the Mel cell lines, Dr. A. Levine for providing anti-Mdm2 antibody and Martijn Rabelink for help with the shRNA viruses.

Reference List

1. Chang,A.E., Karnell,L.H., and Menck,H.R. (1998) The National Cancer Data Base report on cutaneous and noncutaneous melanoma: a summary of 84,836 cases from the past decade. The American College of Surgeons Commission on Cancer and the American Cancer Society. *Cancer*, **83**, 1664-1678.

2. Shields,C.L. and Shields,J.A. (2009) Ocular melanoma: relatively rare but requiring respect. *Clin.Dermatol.*, **27**, 122-133.

3. Kivela,T., Eskelin,S., and Kujala,E. (2006) Metastatic uveal melanoma. *Int.Ophthalmol.Clin.*, **46**, 133-149.

4. Augsburger,J.J., Correa,Z.M., and Shaikh,A.H. (2009) Effectiveness of treatments for metastatic uveal melanoma. *Am J Ophthalmol.*, **148**, 119-127.

5. Cruz,F., III, Rubin,B.P., Wilson,D., Town,A., Schroeder,A., Haley,A., Bainbridge,T., Heinrich,M.C., and Corless,C.L. (2003) Absence of BRAF and NRAS mutations in uveal melanoma. *Cancer Res.*, **63**, 5761-5766.

6. Rimoldi,D., Salvi,S., Lienard,D., Lejeune,F.J., Speiser,D., Zografos,L., and Cerottini,J.C. (2003) Lack of BRAF mutations in uveal melanoma. *Cancer Res.*, **63**, 5712-5715.

7. Goldstein,A.M., Stacey,S.N., Olafsson,J.H., Jonsson,G.F., Helgason,A., Sulem,P., Sigurgeirsson,B., Benediktsdottir,K.R., Thorisdottir,K., Ragnarsson,R., Kjartansson,J., Kostic,J., Masson,G., Kristjansson,K., Gulcher,J.R., Kong,A., Thorsteinsdottir,U., Rafnar,T., Tucker,M.A., and Stefansson,K. (2008) CDKN2A mutations and melanoma risk in the Icelandic population. *J.Med.Genet.*, **45**, 284-289.

8. Prescher,G., Bornfeld,N., Hirche,H., Horsthemke,B., Jockel,K.H., and Becher,R. (1996) Prognostic implications of monosomy 3 in uveal melanoma. *Lancet*, **347**, 1222-1225.

9. Coupland,S.E., Bechrakis,N., Schuler,A., Anagnostopoulos,I., Hummel,M., Bornfeld,N., and Stein,H. (1998) Expression patterns of cyclin D1 and related proteins regulating G1-S phase transition in uveal melanoma and retinoblastoma. *Br.J.Ophthalmol.*, **82**, 961-970.

10. Coupland,S.E., Anastassiou,G., Stang,A., Schilling,H., Anagnostopoulos,I., Bornfeld,N., and Stein,H. (2000) The prognostic value of cyclin D1, p53, and MDM2 protein expression in uveal melanoma. *J.Pathol.*, **191**, 120-126.

11. Harbour,J.W., Onken,M.D., Roberson,E.D., Duan,S., Cao,L., Worley,L.A., Council,M.L., Matatall,K.A., Helms,C., and Bowcock,A.M. (2010) Frequent mutation of BAP1 in metastasizing uveal melanomas. *Science*, **330**, 1410-1413.

12. Van Raamsdonk,C.D., Bezrookove,V., Green,G., Bauer,J., Gaugler,L., O'Brien,J.M., Simpson,E.M., Barsh,G.S., and Bastian,B.C. (2009) Frequent somatic mutations of GNAQ in uveal melanoma and blue naevi. *Nature*, **457**, 599-602.

13. Van Raamsdonk,C.D., Griewank,K.G., Crosby,M.B., Garrido,M.C., Vemula,S., Wiesner,T., Obenauf,A.C., Wackernagel,W., Green,G., Bouvier,N., Sozen,M.M., Baimukanova,G., Roy,R., Heguy,A., Dolgalev,I., Khanin,R., Busam,K., Speicher,M.R., O'Brien,J., and Bastian,B.C. (2010) Mutations in GNA11 in uveal melanoma. *N.Engl.J.Med.*, **363**, 2191-2199.

14. van der Velden,P.A., Metzelaar-Blok,J.A., Bergman,W., Monique,H., Hurks,H., Frants,R.R., Gruis,N.A., and Jager,M.J. (2001) Promoter hypermethylation: a common cause of reduced p16(INK4a) expression in uveal melanoma. *Cancer Res.*, **61**, 5303-5306.

15. Maat,W., Beiboer,S.H., Jager,M.J., Luyten,G.P., Gruis,N.A., and van der Velden,P.A. (2008) Epigenetic regulation identifies RASEF as a tumor-suppressor gene in uveal melanoma. *Invest Ophthalmol.Vis.Sci.*, **49**, 1291-1298.

16. Houben,R., Hesbacher,S., Schmid,C.P., Kauczok,C.S., Flohr,U., Haferkamp,S., Muller,C.S., Schrama,D., Wischhusen,J., and Becker,J.C. (2011) High-level expression of wild-type p53 in melanoma cells is frequently associated with inactivity in p53 reporter gene assays. *PLoS.One.*, **6**, e22096.

17. Brantley,M.A., Jr. and Harbour,J.W. (2000) Deregulation of the Rb and p53 pathways in uveal melanoma. *Am.J.Pathol.*, **157**, 1795-1801.

18. Chana,J.S., Wilson,G.D., Cree,I.A., Alexander,R.A., Myatt,N., Neale,M., Foss,A.J., and Hungerford,J.L. (1999) c-myc, p53, and Bcl-2 expression and clinical outcome in uveal melanoma. *Br.J.Ophthalmol.*, **83**, 110-114.

19. Hussein,M.R. (2005) The relationships between p53 protein expression and the clinicopathological features in the uveal melanomas. *Cancer Biol.Ther.*, **4**, 57-59.

20. Sun,Y., Tran,B.N., Worley,L.A., Delston,R.B., and Harbour,J.W. (2005) Functional analysis of the p53 pathway in response to ionizing radiation in uveal melanoma. *Invest Ophthalmol.Vis.Sci.*, **46**, 1561-1564.

21. Vogelstein,B., Lane,D., and Levine,A.J. (2000) Surfing the p53 network. *Nature*, **408**, 307-310.

22. Hainaut,P. and Hollstein,M. (2000) p53 and human cancer: the first ten thousand mutations. *Adv.Cancer Res.*, **77**, 81-137.

23. Hollstein,M., Sidransky,D., Vogelstein,B., and Harris,C.C. (1991) p53 mutations in human cancers. *Science*, **253**, 49-53.

24. Wynford-Thomas,D. and Blaydes,J. (1998) The influence of cell context on the selection pressure for p53 mutation in human cancer. *Carcinogenesis*, **19**, 29-36.

25. Lane,D.P. (1992) Cancer. p53, guardian of the genome. *Nature*, **358**, 15-16.

26. Wade,M., Wang,Y.V., and Wahl,G.M. (2010) The p53 orchestra: Mdm2 and Mdmx set the tone. *Trends Cell Biol.*, **20**, 299-309.

27. Haupt,Y., Barak,Y., and Oren,M. (1996) Cell type-specific inhibition of p53-mediated apoptosis by mdm2. *EMBO J.*, **15**, 1596-1606.

28. Marine,J.C. and Jochemsen,A.G. (2005) Mdmx as an essential regulator of p53 activity. *Biochem.Biophys.Res.Commun.*, **331**, 750-760.

29. Shvarts,A., Steegenga,W.T., Riteco,N., van Laar,T., Dekker,P., Bazuine,M., van Ham,R.C., van der Houven van Oordt,W., Hateboer,G., van der Eb,A.J., and Jochemsen,A.G. (1996) MDMX: a novel p53-binding protein with some functional properties of MDM2. *EMBO J.*, **15**, 5349-5357.

30. Sharp,D.A., Kratowicz,S.A., Sank,M.J., and George,D.L. (1999) Stabilization of the MDM2 oncoprotein by interaction with the structurally related MDMX protein. *J.Biol.Chem.*, **274**, 38189-38196.

31. Gu,J., Kawai,H., Nie,L., Kitao,H., Wiederschain,D., Jochemsen,A.G., Parant,J., Lozano,G., and Yuan,Z.M. (2002) Mutual dependence of MDM2 and MDMX in their functional inactivation of p53. *J.Biol.Chem.*, **277**, 19251-19254.

32. Linares,L.K., Hengstermann,A., Ciechanover,A., Muller,S., and Scheffner,M. (2003) HdmX stimulates Hdm2-mediated ubiquitination and degradation of p53. *Proc.Natl.Acad.Sci.U.S.A*, **100**, 12009-12014.

33. Momand,J., Wu,H.H., and Dasgupta,G. (2000) MDM2--master regulator of the p53 tumor suppressor protein. *Gene*, **242**, 15-29.

34. Danovi,D., Meulmeester,E., Pasini,D., Migliorini,D., Capra,M., Frenk,R., de,G.P., Francoz,S., Gasparini,P., Gobbi,A., Helin,K., Pelicci,P.G., Jochemsen,A.G., and Marine,J.C. (2004) Amplification of Mdmx (or Mdm4) directly contributes to tumor formation by inhibiting p53 tumor suppressor activity. *Mol.Cell Biol.*, **24**, 5835-5843.

35. Laurie,N.A., Donovan,S.L., Shih,C.S., Zhang,J., Mills,N., Fuller,C., Teunisse,A., Lam,S., Ramos,Y., Mohan,A., Johnson,D., Wilson,M., Rodriguez-Galindo,C., Quarto,M., Francoz,S., Mendrysa,S.M., Guy,R.K., Marine,J.C., Jochemsen,A.G., and Dyer,M.A. (2006) Inactivation of the p53 pathway in retinoblastoma. *Nature*, **444**, 61-66.

36. Riemenschneider,M.J., Knobbe,C.B., and Reifenberger,G. (2003) Refined mapping of 1q32 amplicons in malignant gliomas confirms MDM4 as the main amplification target. *Int.J.Cancer*, **104**, 752-757.

37. Ramos,Y.F., Stad,R., Attema,J., Peltenburg,L.T., van der Eb,A.J., and Jochemsen,A.G. (2001) Aberrant expression of HDMX proteins in tumor cells correlates with wild-type p53. *Cancer Res.*, **61**, 1839-1842.

38. Wunderlich,M., Ghosh,M., Weghorst,K., and Berberich,S.J. (2004) MdmX represses E2F1 transactivation. *Cell Cycle*, **3**, 472-478.

39. Kadakia,M., Brown,T.L., McGorry,M.M., and Berberich,S.J. (2002) MdmX inhibits Smad transactivation. *Oncogene*, **21**, 8776-8785.

40. Yam,C.H., Siu,W.Y., Arooz,T., Chiu,C.H., Lau,A., Wang,X.Q., and Poon,R.Y. (1999) MDM2 and MDMX inhibit the transcriptional activity of ectopically expressed SMAD proteins. *Cancer Res.*, **59**, 5075-5078.

41. Jin,Y., Zeng,S.X., Sun,X.X., Lee,H., Blattner,C., Xiao,Z., and Lu,H. (2008) MDMX promotes proteasomal turnover of p21 at G1 and early S phases independently of, but in cooperation with, MDM2. *Mol.Cell Biol.*, **28**, 1218-1229.

42. De Waard-Siebinga,I., Blom,D.J., Griffioen,M., Schrier,P.I., Hoogendoorn,E., Beverstock,G., Danen,E.H., and Jager,M.J. (1995) Establishment and characterization of an uveal-melanoma cell line. *Int.J.Cancer*, **62**, 155-161.

43. Lam,S., Lodder,K., Teunisse,A.F., Rabelink,M.J., Schutte,M., and Jochemsen,A.G. (2010) Role of Mdm4 in drug sensitivity of breast cancer cells. *Oncogene*.

44. Matlashewski,G.J., Tuck,S., Pim,D., Lamb,P., Schneider,J., and Crawford,L.V. (1987) Primary structure polymorphism at amino acid residue 72 of human p53. *Mol.Cell Biol.*, **7**, 961-963.

45. De Lange,J., Ly,L.V., Lodder,K., Verlaan-de Vries,M., Teunisse,A.F., Jager,M.J., and Jochemsen,A.G. (2011) Synergistic growth inhibition based on small-molecule p53 activation as treatment for intraocular melanoma. *Oncogene*.

46. Vassilev,L.T., Vu,B.T., Graves,B., Carvajal,D., Podlaski,F., Filipovic,Z., Kong,N., Kammlott,U., Lukacs,C., Klein,C., Fotouhi,N., and Liu,E.A. (2004) In vivo activation of the p53 pathway by small-molecule antagonists of MDM2. *Science*, **303**, 844-848.

47. Joseph,T.L., Madhumalar,A., Brown,C.J., Lane,D.P., and Verma,C.S. (2010) Differential binding of p53 and nutlin to MDM2 and MDMX: computational studies. *Cell Cycle*, **9**, 1167-1181.

48. Uchida,C., Miwa,S., Kitagawa,K., Hattori,T., Isobe,T., Otani,S., Oda,T., Sugimura,H., Kamijo,T., Ookawa,K., Yasuda,H., and Kitagawa,M. (2005) Enhanced Mdm2 activity inhibits pRB function via ubiquitin-dependent degradation. *EMBO J.*, **24**, 160-169.

49. Fu,W., Ma,Q., Chen,L., Li,P., Zhang,M., Ramamoorthy,S., Nawaz,Z., Shimojima,T., Wang,H., Yang,Y., Shen,Z., Zhang,Y., Zhang,X., Nicosia,S.V., Zhang,Y., Pledger,J.W., Chen,J., and Bai,W. (2009) MDM2 acts downstream of p53 as an E3 ligase to promote FOXO ubiquitination and degradation. *J.Biol.Chem.*, **284**, 13987-14000.

50. Brenkman,A.B., de Keizer,P.L., van den Broek,N.J., Jochemsen,A.G., and Burgering,B.M. (2008) Mdm2 induces mono-ubiquitination of FOXO4. *PLoS.One.*, **3**, e2819.

51. Carrano,A.C., Eytan,E., Hershko,A., and Pagano,M. (1999) SKP2 is required for ubiquitin-mediated degradation of the CDK inhibitor p27. *Nat.Cell Biol.*, **1**, 193-199.

52. Sheaff,R.J., Groudine,M., Gordon,M., Roberts,J.M., and Clurman,B.E. (1997) Cyclin E-CDK2 is a regulator of p27Kip1. *Genes Dev.*, **11**, 1464-1478.

53. Sutterluty,H., Chatelain,E., Marti,A., Wirbelauer,C., Senften,M., Muller,U., and Krek,W. (1999) p45SKP2 promotes p27Kip1 degradation and induces S phase in quiescent cells. *Nat.Cell Biol.*, **1**, 207-214.

54. Lenos,K., De Lange,J., Teunisse,A.F., Lodder,K., Verlaan-de Vries M., Wiercinska E., Van der Burg,M.J.M., Szuhai,K., and Jochemsen,A.G. (2011) Oncogenic functions of Hdmx in *in vitro* transformation of primary human fibroblasts and embryonic retinoblasts. *Mol.Cancer*, **2011**, 10-111.

55. Jones,S.N., Roe,A.E., Donehower,L.A., and Bradley,A. (1995) Rescue of embryonic lethality in Mdm2-deficient mice by absence of p53. *Nature*, **378**, 206-208.

56. Montes de Oca Luna,R., Wagner,D.S., and Lozano,G. (1995) Rescue of early embryonic lethality in mdm2-deficient mice by deletion of p53. *Nature*, **378**, 203-206.

57. Chu,I.M., Hengst,L., and Slingerland,J.M. (2008) The Cdk inhibitor p27 in human cancer: prognostic potential and relevance to anticancer therapy. *Nat.Rev.Cancer*, **8**, 253-267.

58. Kedde,M., van,K.M., Zwart,W., Oude Vrielink,J.A., Elkon,R., and Agami,R. (2010) A Pumilio-induced RNA structure switch in p27-3' UTR controls miR-221 and miR-222 accessibility. *Nat.Cell Biol.*, **12**, 1014-1020.

59. Miskimins,W.K., Wang,G., Hawkinson,M., and Miskimins,R. (2001) Control of cyclin-dependent kinase inhibitor p27 expression by cap-independent translation. *Mol.Cell Biol.*, **21**, 4960-4967.

60. Nakayama,K.I. and Nakayama,K. (2006) Ubiquitin ligases: cell-cycle control and cancer. *Nat.Rev.Cancer*, **6**, 369-381.

61. Yang,H., Zhao,R., Yang,H.Y., and Lee,M.H. (2005) Constitutively active FOXO4 inhibits Akt activity, regulates p27 Kip1 stability, and suppresses HER2-mediated tumorigenicity. *Oncogene*, **24**, 1924-1935.

62. Wang,X., Krupczak-Hollis,K., Tan,Y., Dennewitz,M.B., Adami,G.R., and Costa,R.H. (2002) Increased hepatic Forkhead Box M1B (FoxM1B) levels in old-aged mice stimulated liver regeneration through diminished p27Kip1 protein levels and increased Cdc25B expression. *J.Biol.Chem.*, **277**, 44310-44316.

63. Ambrosini,G., Adida,C., and Altieri,D.C. (1997) A novel anti-apoptosis gene, survivin, expressed in cancer and lymphoma. *Nat.Med.*, **3**, 917-921.

64. An,J., Wan,H., Zhou,X., Hu,D.N., Wang,L., Hao,L., Yan,D., Shi,F., Zhou,Z., Wang,J., Hu,S., Yu,J., and Qu,J. (2011) A comparative transcriptomic analysis of uveal melanoma and normal uveal melanocyte. *PLoS.One.*, **6**, e16516.

65. Li,H., Niederkorn,J.Y., Neelam,S., and Alizadeh,H. (2006) Downregulation of survivin expression enhances sensitivity of cultured uveal melanoma cells to cisplatin treatment. *Exp.Eye Res.*, **83**, 176-182.

66. Altieri,D.C. (2006) The case for survivin as a regulator of microtubule dynamics and cell-death decisions. *Curr.Opin.Cell Biol.*, **18**, 609-615.

67. Lens,S.M., Vader,G., and Medema,R.H. (2006) The case for Survivin as mitotic regulator. *Curr.Opin.Cell Biol.*, **18**, 616-622.

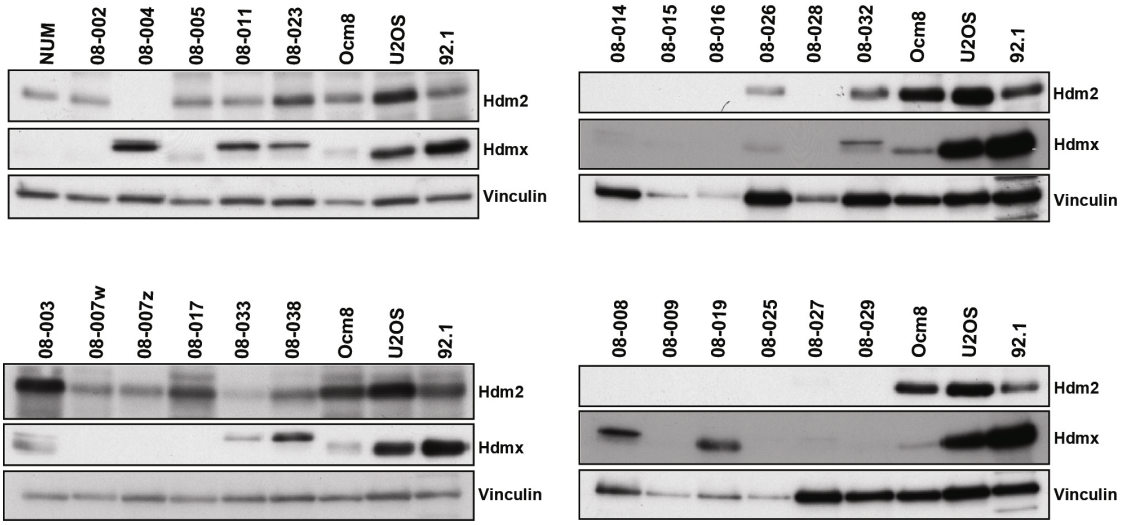

Supplementary Figure 1 Hdmx is over-expressed in a subset of uveal melanomas. Protein extracts of 23 fresh-frozen uveal melanoma tumor samples were analyzed for Hdmx and Vinculin protein levels by western blot, in comparison with the levels in NUM (Normal Uveal melanocytes) and Ocm8 cells (low Hdmx levels), 92.1 and U2OS cells, (high Hdmx). Quantifications of these blots are shown in Figure 1b.

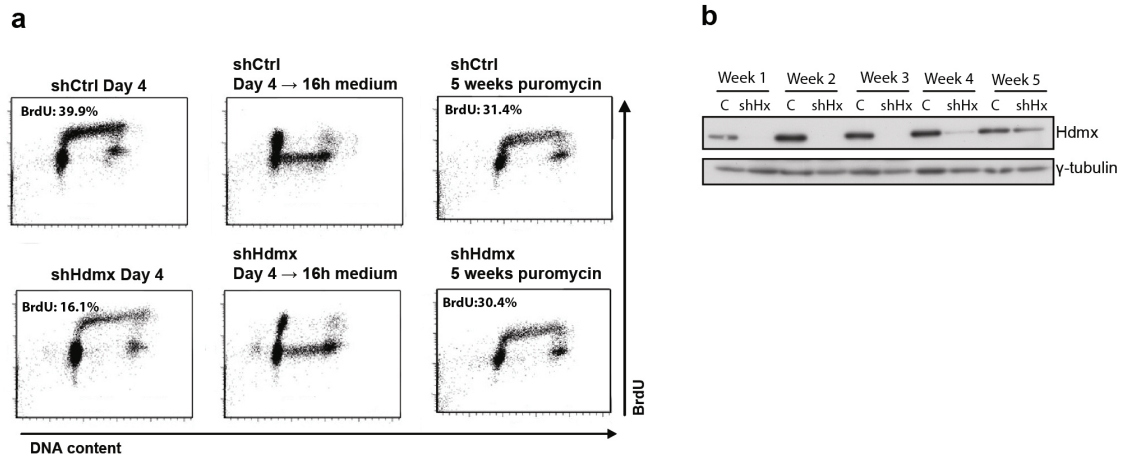

Supplementary Figure 2 The partial G1 arrest upon Hdmx knockdown is lost after several weeks of puromycin selection. 92.1 cells were transduced with shCtrl or shHdmx#1 RNAs and after four days they were incubated with 20 μM BrdU for 2h. Subsequently, cells were immediately harvested (**a**, left panel), or harvested 16h after replacing the culture medium with medium lacking BrdU (**a**, middle panel) and cells were analyzed by flow cytometry. In addition, one dish for each transduction was maintained and propagated under puromycin selection. After 5 weeks, the surviving cells were incubated with 20 μM BrdU for 2h and analyzed by flow cytometry (**a**, right panel). Protein extracts were isolated every week and analyzed by western blot for Hdmx and γ-tubulin levels (**b**).

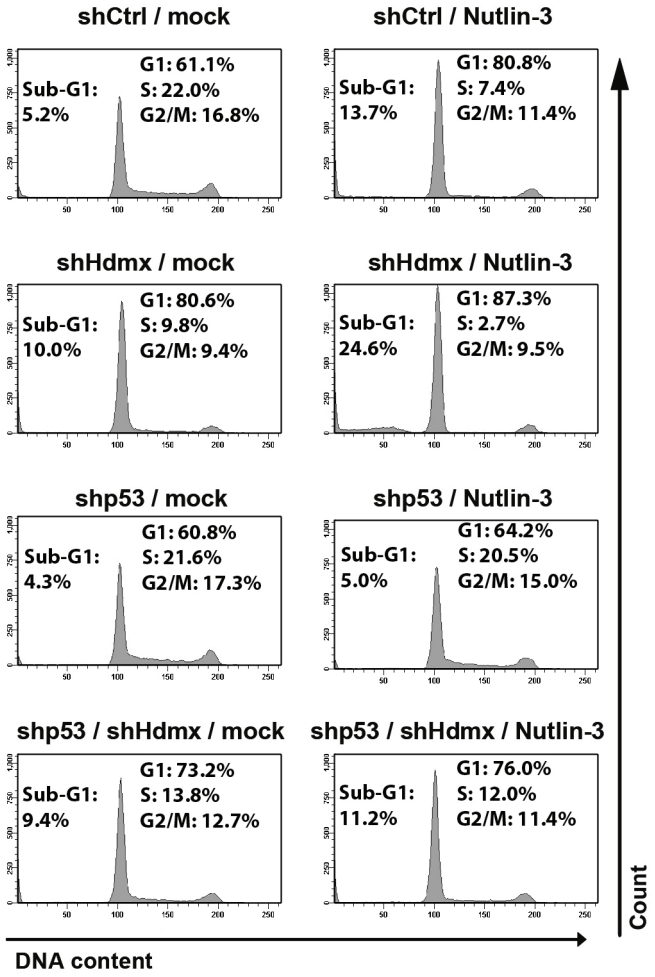

Supplementary Figure 3 p53 knockdown is sufficient to prevent Nutlin-3 induced growth inhibition. Stable 92.1-shCtrl and 92.1-shp53 cells were transiently transduced with shCtrl or shHdmx#1 RNA. Subsequently, cells were mock-treated or treated with 10 µM Nutlin-3 for 24h and analyzed by flow cytometry.

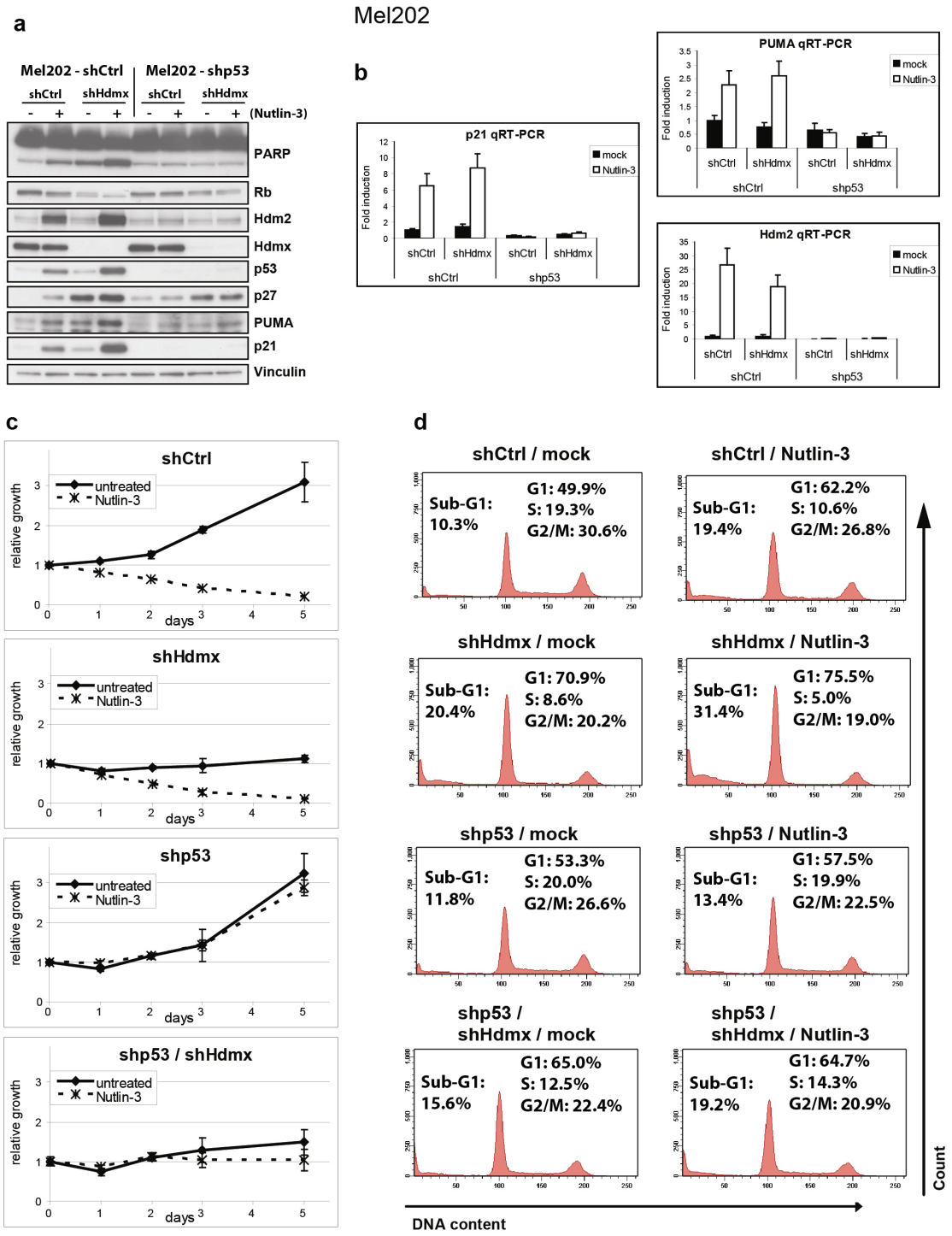

Supplementary Figure 4 p53-independent growth inhibition upon Hdmx knockdown in Mel202 cells. A, Mel202 cells were stably transduced using shCtrl or shp53 RNAs. The resulting cell lines were transduced with shCtrl or shHdmx#1 RNAs. Four days after transduction, cells were treated with 10 µM Nutlin-3 for 24h and analyzed by western blot using the indicated antibodies. B, Cells were transduced and treated as mentioned in A and RNA expression was analyzed by qRT-PCR. Expression levels of Hdm2, PUMA and p21 were normalized for the geometric mean of CAPNS1, GAPDH and ARP. C, Cells were transduced as mentioned in A, counted and seeded for WST-1 proliferation assay. Cells were mock treated or treated with 10 µM Nutlin-3, and cell viability was measured at several time points during five days. D, Cells were transduced and treated as mentioned in A and analyzed by flow cytometry.

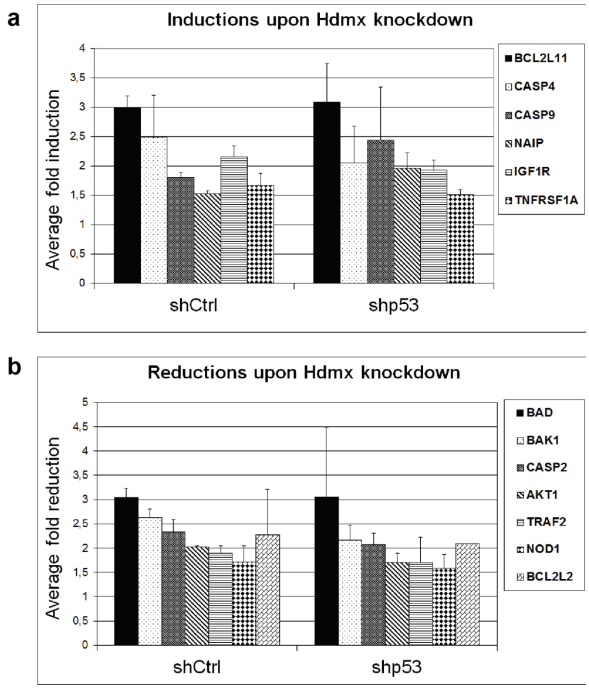

Supplementary Figure 5 Analysis of Hdmx knockdown-induced changes in expression of apoptosis-related genes. Stable 92.1-shCtrl and 92.1-shp53 cells were transduced with shCtrl or shHdmx#1 RNAs and total RNA was extracted four days post-transduction. Gene expression of 84 genes involved in apoptosis (and five housekeeping genes for normalization: B2M, HPRT1, RPL13A, GAPDH and ACTB) was assessed using the RT^2 Profiler^{TM} PCR Array (SABiosciences) according to the manufacturer's instructions. Two independent experiments were averaged and genes demonstrating a 1.5-fold or greater increase (A) or decrease (B) are shown.

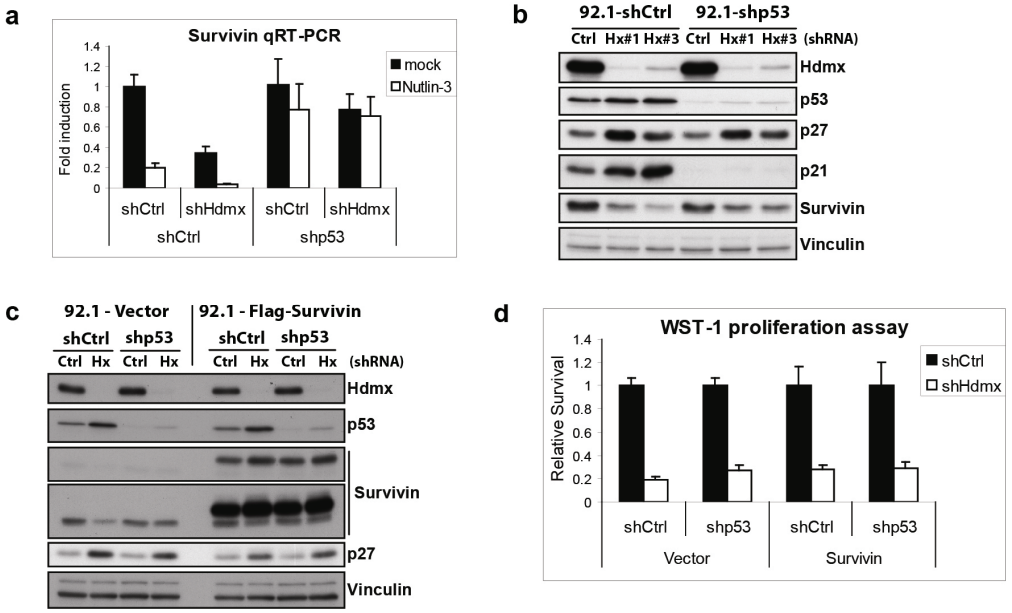

Supplementary Figure 6 Survivin over-expression fails to rescue growth inhibition upon Hdmx knockdown. A, Stable 92.1-shCtrl and 92.1-shp53 cells were transduced with shCtrl or shHdmx#1 RNAs and analyzed by qRT-PCR four day post-transduction. Expression levels of Survivin were normalized for the geometric mean of CAPNS1, GAPDH and ARP. B, Stable 92.1-shCtrl and 92.1-shp53 cells were transduced with shCtrl, shHdmx#1 or shHdmx#3 RNAs. Four day post-transduction, protein extracts were analyzed by western blot using the indicated antibodies. C, Stable 92.1-shCtrl and 92.1-shp53 cells were transduced with an empty vector or with a Flag-tagged Survivin expression vector, and neomycin selected to obtain stable cell lines. The resulting cell lines were transduced with shCtrl or shHdmx#1 RNAs. Four days post-transduction, protein extracts were analyzed by western blot using the indicated antibodies. D, Cells from C were counted and seeded for WST-1 proliferation assay, and cell viability was measured after five days.

Supplementary Table 1: List of shRNA sequences and TRCN numbers

shRNA	Oligo sequences / TRCN numbers
shCtrl	Fw: gatccg**GAATCTTGTTACATCAGCT** ttcaagaga**AGCTGATGTAACAAGATTC** ttttt ggaaa
	Rv: agcttttccaaaaa**GAATCTTGTTACATCAGCT** tctcttgaa**AGCTGATGTAACAAGATTC** ggg
shp53	Fw: gatccg**GACTCCAGTGGTAATCTAC** ttcaagaga**GTAGATTACCACTGGAGTC** ttttt ggaaa
	Rv: agcttttccaaaaa**GACTCCAGTGGTAATCTAC** tctcttgaa**GTAGATTACCACTGGAGTC** ggg
shHdmx#1	Fw: gatccg**GTGCAGAGGAAAGTTCCAC** ttcaagaga**GTGGAACTTTCCTCTGCAC** ttttt ggaaa
	Rv: agcttttccaaaaa**GTGCAGAGGAAAGTTCCAC** tctcttgaa**GTGGAACTTTCCTCTGCAC** ggg
shHdmx#2	Fw: gatccg**AGTCAAGCAACTGAAGC** ttcaagaga**GCTTCAGTTGCTTGACT** ttttt ggaaa
(Exon 6 #2)	Rv: agcttttccaaaaa**AGTCAAGCAACTGAAGC** tctcttgaa**GCTTCAGTTGCTTGACT** ggg
shHdmx#3	Fw: gatccg**GTGCAGTGAGTCAAGATTG** ttcaagaga**CAATCTTGACTCACTGCAC** ttttt ggaaa
(3'UTR)	Rv: agcttttccaaaaa**GTGCAGTGAGTCAAGATTG** tctcttgaa**CAATCTTGACTCACTGCAC** ggg
shRb	ccgg**CCACATTATTTCTAGTCCAAA** ctcgag**TTTGGACTAGAAATAATGTGG** ttttg / TRCN0000040163
shp27	ccgg**GCGCAAGTGGAATTTCGATTT** ctcgag**AAATCGAAATTCCACTTGCGC** ttttg / TRCN0000039930

Supplementary Table 2: List of antibodies

Protein	Name/ cat. #	Company
PARP	9542	Cell signalling Technology, Beverly, MA, USA
Hdm2 *	4B2	Chen *et al*., 1993
Hdm2 *	SMP14 sc-6965	Santa Cruz Biotechnology, Santa Cruz, CA, USA
Hdmx	A300-287A	Bethyl Laboratories, Montgomery TX, USA
p-p53 Ser46	2190-1 / EP42Y	Epitomics,California, USA
p-p53 Ser15	9284	Cell signalling Technology, Beverly, MA, USA
p53 °	DO-1 / sc-126	Santa Cruz Biotechnology, Santa Cruz, CA, USA
p53 °	PAb1801 / sc-98	Santa Cruz Biotechnology, Santa Cruz, CA, USA
PUMA N-terminal	P4743	Sigma-Aldrich, St Louis, MO, USA
p21	CP74 / 05-655	Upstate Biotechnology, Lake Placid, NY, USA
RB	G3-245 / 554136	BD Pharmingen, Franklin Lakes, New Jersey, USA
E2F1	KH95 / sc-251	Santa Cruz Biotechnology, Santa Cruz, CA, USA
p27/Kip1 (C-terminal)	1591-1	Epitomics,California, USA
Survivin	71G4B7 / 2808	Cell signalling Technology, Beverly, MA, USA
γ-Tubulin	GTU-88 / T6557	Sigma-Aldrich, St Louis, MO, USA
Vinculin	hVIN-1 / V9131	Sigma-Aldrich, St Louis, MO, USA
HAUSP USP7	A300-033A	Bethyl Laboratories, Montgomery TX, USA

For detection of human hMDM2 we used a mix of 4B2 and SMP14 (*), for detection of human p53 we used a mix of DO-1 and 1801 (°).

Ref) Chen J *et al.* Mapping of the p53 and mdm-2 interaction domains. *Mol Cell Biol* 1993, **13:**4107-4114.

Supplementary Table 3: Primer sequences used for qRT-PCR reactions.

Gene	Forward primer	Reverse primer
HDM2	5'-ACGCACGCCACTTTTTCTCT-3'	5'-TCCGAAGCTGGAATCTGTGAG-3'
PUMA	5'-GACCTCAACGCACAGTA-3'	5'-CTAATTGGGCTCCATCT-3'
p21	5'-AGCAGAGGAAGACCATGTGGA-3'	5'-AATCTGTCATGCTGGTCTGCC-3'
GADD45α	5'-GCGACCTGCAGTTTGCAATA-3'	5'-ATCCCCCACCTTATCCATCCT-3'
p27	5'-CAAATGCCGGTTCTGTGGAG-3'	5'-TCCATTCCATGAAGTCAGCGATA-3'
Survivin	5'-GAGACAGAATAGAGTGATAGG- 3'	5'-GACACATGTGAAGGTTGG- 3'
CAPNS1	5'-ATGGTTTTGGCATTGACACATG-3'	5'-GCTTGCCTGTGGTGTCGC-3'
GAPDH	5'-TGCCATGTAGACCCCTTGAAG-3'	5'-ATGGTACATGACAAGGTGCGG-3'
ARP	5'-CACCATTGAAATCCTGAGTGATGT-3'	5'-ACCAGCCGAAAGGAGAAG-3'
RPS11	5'-AAGCAGCCGACCATCTTTCA-3'	5'-CGGGAGCTTCTCCTTGCC-3'
Hdmx exon 3	5'-TGCATGCAGCAGGTGCG-3'	
Hdmx exon 8		5'-CATTACTTCTAGGTGTAT-3'

Chapter 4

Synergistic growth inhibition based on small-molecule p53 activation as treatment for intraocular melanoma

J. de Lange[1], L.V. Ly[2], K. Lodder[1], M. Verlaan - de Vries[1], A.F.A.S. Teunisse[1], M.J. Jager[1], A.G. Jochemsen[1]

[1] Department of Molecular Cell Biology, Leiden University Medical Center, 2300 RC Leiden, The Netherlands
[2] Department of Ophtalmology, Leiden University Medical Center, 2300 RC Leiden, The Netherlands

Oncogene 2012 Mar 1;31(9):1105-16

Abstract

The prognosis for patients with uveal melanoma is poor. Because of the limited efficacy of current treatments, new therapeutic strategies need to be developed. Because p53 mutations are uncommon in uveal melanoma, reactivation of p53 may be used to achieve tumor regression. We investigated the use of combination therapies for intraocular melanoma, based on the p53 activators Nutlin-3 and reactivation of p53 and induction of tumor cell apoptosis (RITA) and the topoisomerase I inhibitor Topotecan. Nutlin-3 treatment induced p53-dependent growth inhibition in human uveal melanoma cell lines. The sensitivity to Nutlin-3 of the investigated cell lines did not correlate with basal Hdm2 or Hdmx levels. Nutlin-3 synergized with RITA and Topotecan to induce apoptosis in uveal melanoma cell lines and short term cultures. Drug synergy correlated with enhanced induction of p53-Ser46 phosphorylation, which was attenuated by ATM inhibition. Nutlin-3 and Topotecan also significantly delayed tumor growth *in vivo* in a murine B16F10 model for ocular melanoma. Combination treatment appeared to inhibit tumor growth slightly more efficient than either drug alone. Nutlin-3, RITA and Topotecan lead to comparable p53 activation and growth inhibition under normoxia and hypoxia. Treatment with Nutlin-3 or RITA had no effect on HIF-1α induction by hypoxia, whereas the combination of these two drugs did inhibit hypoxia-induced HIF-1α. Also Topotecan, alone or in combination with Nutlin-3, reduced HIF-1α protein levels, suggesting that a certain level of DNA damage response is required for p53-mediated down-regulation of HIF-1α. In conclusion, combination treatments based on small-molecule induced p53 activation may have clinical potential for uveal melanoma.

Introduction

The eye is the second most common site of malignant melanoma, comprising 5.3% of all melanoma cases (Chang *et al.*, 1998). Up to 50% of patients with uveal melanoma may develop metastases. Prognosis is poor when the tumor has metastasized; median survival is about 10 - 18 months (Kivela *et al.*, 2006; Augsburger *et al.*, 2009). Functional inactivation of the p53 tumor suppressor pathway is believed to be involved in virtually all human cancers. The *p53* gene is directly mutated in about 50% of human malignancies, whereas tumors retaining wild type p53 contain other genetic aberrations that prevent p53's tumor suppressor function (Wynford-Thomas and Blaydes 1998). It is generally assumed that p53 mutations in uveal melanoma are rare. The presence of wild type, but functionally impaired p53 and intact downstream signaling may provide an attractive therapeutic strategy to target tumor cells by restoring p53 activity. To this end, small-molecule compounds have been developed, such as the Hdm2 antagonist Nutlin-3 (Vassilev *et al.*, 2004). Specifically, Nutlin-3 binds Hdm2 in its p53-binding pocket, thereby inhibiting Hdm2-p53 interaction, which releases, stabilizes and activates p53. Nutlin-3 activates p53 without inducing DNA damage, making it a non-genotoxic agent (Vassilev, 2007). Normal cells are relatively insensitive to Nutlin-3-induced apoptosis. The p53-binding molecule RITA (reactivation of p53 and induction of tumor cell apoptosis) was described to induce p53-dependent apoptosis and to inhibit tumor growth *in vivo* (Issaeva *et al.*, 2004). RITA was proposed to induce conformational changes in p53, leading to reduced p53-Hdm2 binding. Although this mechanism was questioned by a later study (Krajewski *et al.*, 2005), a more recent report supports it (Enge *et al.*, 2009).

Several groups included Nutlin-3 in combination treatments, mostly together with genotoxic drugs, to enhance their effectiveness and allow such drugs to be administered at lower doses (Coll-Mulet *et al.*, 2006; Lam *et al.*, 2010; Kojima *et al.*, 2006; Barbieri *et al.*, 2006). Those studies showed that in certain experimental settings, synergistic induction of apoptosis can be achieved. The use of Nutlin-3 appeared promising in retinoblastoma treatment (Laurie *et al.*, 2006). Notably, subconjunctival delivery of Nutlin-3, especially in combination with Topotecan, strongly inhibited growth of Y79 human retinoblastoma cells injected into the eyes of newborn rats. Topotecan, frequently used as chemotherapeutic agent, is a topoisomerase I inhibitor that induces double-strand DNA breaks, stimulates p53 phosphorylation, but also triggers apoptosis in p53-deficient cells (Tomicic *et al.*, 2010). The results with retinoblastoma suggest that subconjunctival delivery of Nutlin-3 and Topotecan may also be used in uveal melanoma.

We investigated the use of p53-activating drugs as treatment for uveal melanoma. Our data show that Nutlin-3 induces p53-dependent growth inhibition and synergizes with both RITA and Topotecan to induce apoptosis in uveal melanoma cell lines and short-term cultures. Furthermore, Nutlin-3 and Topotecan inhibited *in vivo* growth of B16F10 cells in a murine model for ocular melanoma. We found similar p53 activation by the various treatments under normoxic and hypoxic conditions. Together, our results indicate that p53 activators have promise in treating primary uveal melanoma and its metastases.

Results

Nutlin-3 activates p53 and inhibits cell growth in uveal melanoma cell lines

To examine whether Nutlin-3 can inhibit the growth of uveal melanoma cell lines 92.1 and Mel202 in a p53-dependent manner, we first generated stable shp53 and shCtrl cell lines. We treated the resulting cell lines with Nutlin-3 and analyzed protein (Figure 1a) and mRNA (Figure 1b) levels. In shCtrl cells, treatment with Nutlin-3 resulted in increased p53 protein levels and upregulation of p53 target genes *Hdm2*, *PUMA* and *p21* at both mRNA and protein level, as expected. In shp53 cells, expressing much lower p53 levels, induction of p53 targets was strongly diminished, showing that the effect of Nutlin-3 is p53 dependent. We examined cell growth using a WST-1 proliferation assay. Nutlin-3 significantly inhibited growth of shCtrl cells, whereas shp53 cells were largely unaffected (Figure 1c).

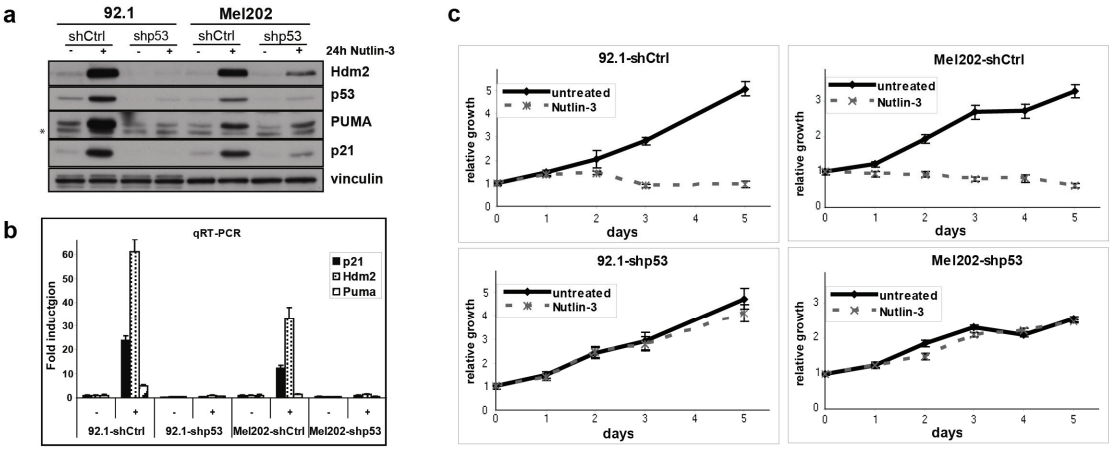

Figure 1 Nutlin-3 activates p53 and inhibits cell growth in uveal melanoma cell lines. The 92.1 and Mel202 cells stably expressing shCtrl or shp53 RNAs were treated with 10 μM Nutlin-3 for 24 h, followed by western blot analysis (**a**) and qRT-PCR (**b**). * Non-specific background staining. (**c**) Cells were counted, seeded for WST-1 proliferation assay and treated with 10 μM Nutlin-3. Cell viability was measured at 0, 24, 48, 72, 96, and 120 h upon Nutlin-3 addition.

In an earlier examination of levels of several proteins in uveal melanoma cell lines, we had observed relatively high levels of Hdmx in 92.1 and Mel202, whereas Mel285 and Mel270 contain high levels of Hdm2 compared with Mel202 and 92.1 cells (Supplementary Figure 1a). Because Hdm2 and Hdmx levels may affect the sensitivity to Nutlin-3 (Patton *et al.*, 2006; Wade *et al.*, 2006; Hu *et al.*, 2006), we tested whether this also applies for uveal

a

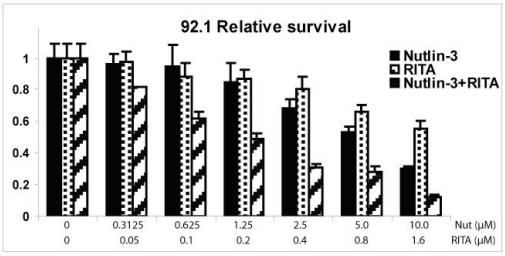

Nutlin-3 Dose (μM)	Effect	RITA Dose (μM)	Effect	Combination N+R Effect	CI
0.3125	0.036	0.05	0.024	0.182	0.356
0.625	0.052	0.1	0.115	0.382	0.276
1.25	0.155	0.2	0.134	0.516	0.338
2.5	0.318	0.4	0.194	0.691	0.348
5	0.470	0.8	0.343	0.718	0.620
10	0.700	1.6	0.445	0.875	0.509
IC50	5.15 μM	IC50	1.74 μM		
m	1.23	m	0.91		
r	0.994	r	0.960		

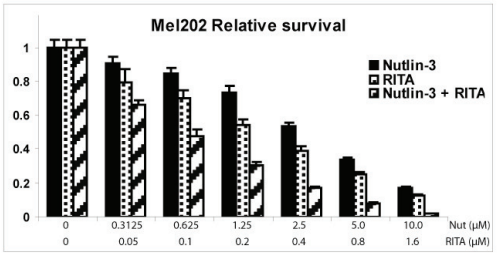

Nutlin-3 Dose (μM)	Effect	RITA Dose (μM)	Effect	Combination N+R Effect	CI
0.3125	0.092	0.05	0.208	0.336	0.653
0.625	0.155	0.1	0.297	0.525	0.599
1.25	0.265	0.2	0.458	0.696	0.583
2.5	0.467	0.4	0.609	0.825	0.567
5	0.664	0.8	0.751	0.919	0.476
10	0.827	1.6	0.876	0.982	0.212
IC50	2.71 μM	IC50	0.23 μM		
m	1.12	m	0.95		
r	0.997	r	0.997		

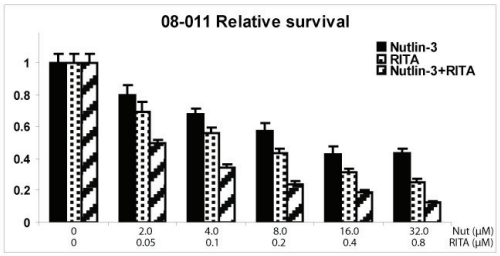

Nutlin-3 Dose (μM)	Effect	RITA Dose (μM)	Effect	Combination N+R Effect	CI
2	0.200	0.05	0.304	0.504	0.467
4	0.319	0.1	0.439	0.657	0.367
8	0.425	0.2	0.569	0.759	0.354
16	0.571	0.4	0.684	0.814	0.441
32	0.569	0.8	0.750	0.872	0.463
IC50	14.49 μM	IC50	0.15 μM		
m	0.63	m	0.7		
r	0.969	r	0.995		

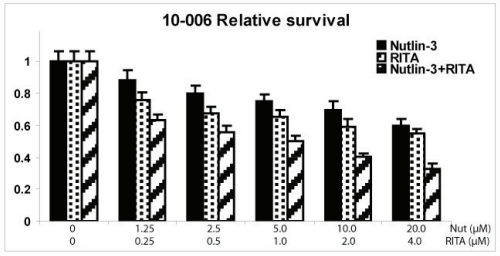

Nutlin-3 Dose (μM)	Effect	RITA Dose (μM)	Effect	Combination N+R Effect	CI
1.25	0.114	0.25	0.239	0.364	0.293
2.5	0.197	0.5	0.323	0.443	0.258
50	0.248	1	0.345	0.500	0.284
10	0.305	2	0.411	0.596	0.226
20	0.404	4	0.450	0.674	0.211
IC50	38.88 μM	IC50	6.46 μM		
m	0.56	m	0.33		
r	0.987	r	0.981		

Figure 2 Synergistic growth inhibition by Nutlin-3 in combination with RITA or Topotecan. The 92.1, Mel202, 08-011 and 10-006 cells were counted and seeded for WST-1 proliferation assay. Cells were treated as indicated with different concentrations, alone or in constant ratio combinations, of Nutlin-3 and RITA (**a**) or Nutlin-3 and Topotecan (**b**). Cell viability was measured after 72 h treatment. The effects of drug treatment as

melanoma. In a WST-1 proliferation assay (Supplementary Figure 1b) we observed comparable Nutlin-3 responses in Mel285 and Mel270 as those found in 92.1 and Mel202. In 92.1, Mel202 and Mel270, but not in Mel285, morphology changes suggested apoptosis induction in a proportion of cells (Supplementary Figure 1c). These findings indicate a lack of correlation between basal Hdm2 or Hdmx levels and sensitivity to Nutlin-3 in the cells examined.

b

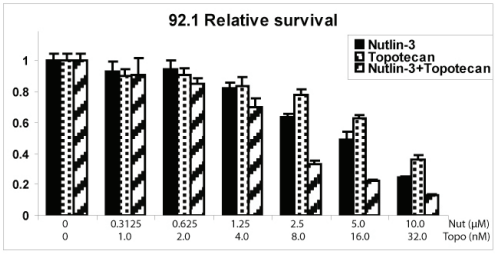

Nutlin-3 Dose (μM)	Effect	Topotecan Dose (nM)	Effect	Combination N+T Effect	CI
0.3125	0.071	1	0.096	0.093	1.164
0.625	0.059	2	0.093	0.152	1.276
1.25	0.176	4	0.161	0.298	1.045
2.5	0.369	8	0.219	0.667	0.444
5	0.513	16	0.370	0.779	0.513
10	0.753	32	0.641	0.872	0.548
IC50	4.38 μM	IC50	25.78 nM		
m	1.15	m	0.81		
r	0.976	r	0.957		

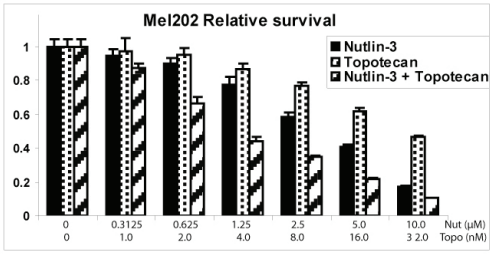

Nutlin-3 Dose (μM)	Effect	Topotecan Dose (nM)	Effect	Combination N+T Effect	CI
0.3125	0.054	1	0.025	0.123	0.670
0.625	0.097	2	0.047	0.333	0.475
1.25	0.221	4	0.130	0.557	0.446
2.5	0.413	8	0.230	0.649	0.652
5	0.596	16	0.382	0.783	0.755
10	0.829	32	0.534	0.896	0.747
IC50	3.28 μM	IC50	25.42 nM		
m	1.28	m	1.12		
r	0.997	r	0.996		

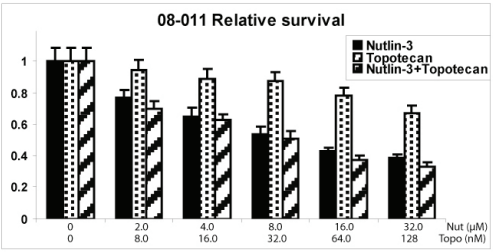

Nutlin-3 Dose (μM)	Effect	Topotecan Dose (nM)	Effect	Combination N+T Effect	CI
2	0.229	8	0.057	0.303	0.708
4	0.348	16	0.108	0.373	0.864
8	0.461	32	0.122	0.490	0.807
16	0.573	64	0.217	0.627	0.667
32	0.617	128	0.327	0.670	0.993
IC50	11.88 μM	IC50	376.27 nM		
m	0.62	m	0.72		
r	0.986	r	0.987		

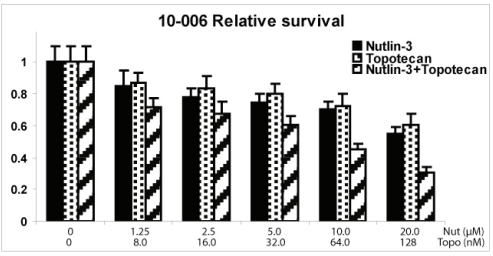

Nutlin-3 Dose (μM)	Effect	Topotecan Dose (nM)	Effect	Combination N+T Effect	CI
1.25	0.149	8	0.129	0.282	0.343
2.5	0.220	16	0.165	0.327	0.454
50	0.256	32	0.200	0.397	0.506
10	0.300	64	0.277	0.550	0.303
20	0.452	128	0.394	0.692	0.186
IC50	37.25 μM	IC50	357.90 nM		
m	0.51	m	0.52		
r	0.976	r	0.987		

fraction of mock-treated control cells were calculated. The dose-response values IC50 (dose required for median effect), *m* (slope signifying the shape of the dose-response curve) and *r* (linear correlation coefficient; *r* = 1 indicates perfect fit) for each single drug were derived using Compusyn software (Chou and Martin, 2007). Based on these values, the CI was derived for each drug combination, reflecting the extent of synergy or antagonism for two drugs. CI<0.9, synergy; 0.9<CI<1.1, additive effect; CI>1.1, antagonism.

Synergistic growth inhibition by Nutlin-3 in combination with RITA or Topotecan

The use of Nutlin-3 alone may not be sufficient to achieve full tumor regression. Combination with other drugs could well enhance the effectiveness of treatment. We analyzed the sensitivity of 92.1 and Mel202 cells to combinations of Nutlin-3 with either RITA or Topotecan. We performed synergy studies using the method of Chou (Chou, 2006). Dose-effect analyses are shown in Figure 2. Nutlin-3 and RITA synergized in both cell lines, with synergy confirmed by calculation of the CI. This is in line with recent findings in multiple myeloma (Saha *et al*., 2010). Nutlin-3 and Topotecan combinations also showed synergistic growth inhibition at most concentrations, except when using low doses in 92.1 cells. We extended our studies to two short-term uveal melanoma cultures, because these should more closely resemble 'real' tumor behavior than fully established cell lines. Short-term cultures 10-006 and 08-011 were also synergistically inhibited by the combination treatments (Figure 2 and Supplementary Figure 2).

To further investigate the cellular responses to the different treatments, we applied flow cytometry (Figure 3a). Nutlin-3 mainly induced G1 arrest, whereas RITA preferentially increased the G2/M fraction. When applied as single treatment, the used doses of Nutlin-3 and RITA only induced a modest sub-G1 increase. This was significantly enhanced in the combination treatment. Topotecan treatment resulted in a G1 reduction and in more cells in S and G2/M phase. A closer examination of the kinetics of this response (Supplementary Figure 3) showed that Topotecan treatment slows down the process of DNA replication. We observed no sustained S-phase arrest, but cells eventually arrested in G2. Combining Topotecan with Nutlin-3 maintained a substantial G1 fraction, and prevented a robust G2 arrest. The increasing S-phase may reflect a 'real' S-arrest or, more likely, dying G2 cells that form a so-called 'sub-G2' fraction. Importantly, sub-G1 fractions were strongly increased in the combination treatment compared with the single treatments. In addition to the enhanced sub-G1 fractions, we found increased Annexin V staining in Nutlin-3 + RITA and Nutlin-3 + Topotecan-treated cells, confirming enhanced induction of apoptosis (Figure 3b).

We analyzed the levels of a number of proteins by western blot (Figure 3c). The levels of various markers of apoptosis, including cleaved PARP, cleaved caspase 3 and p53-Ser46 phosphorylation, were elevated in the combination treated cells, further underscoring that the combination treatments shifted the cellular response from cell cycle arrest to apoptosis. Combination treatments also induced p53-Ser46 phosphorylation in short-term cultures 08-011 and 10-006 (Supplementary Figure 2). Tightly controlled phosphorylation

events are crucial for modulating the p53 response; specifically phosphorylation of serine 46 is believed to result in apoptosis induction (Bulavin *et al.*, 1999; Saito *et al.*, 2002). Therefore, identifying the kinase(s) involved in p53-Ser46 phosphorylation may provide more insight in how apoptosis is triggered. Because RITA has been reported to increase HIPK2 levels, a kinase for p53-Ser46 (D'Orazi *et al.*, 2002; Rinaldo *et al.*, 2009), HIPK2 could be involved. However, in our settings RITA treatment did not lead to HIPK2 induction (Figure 3c). Therefore, the kinase activity of HIPK2 is probably not required for the observed effects.

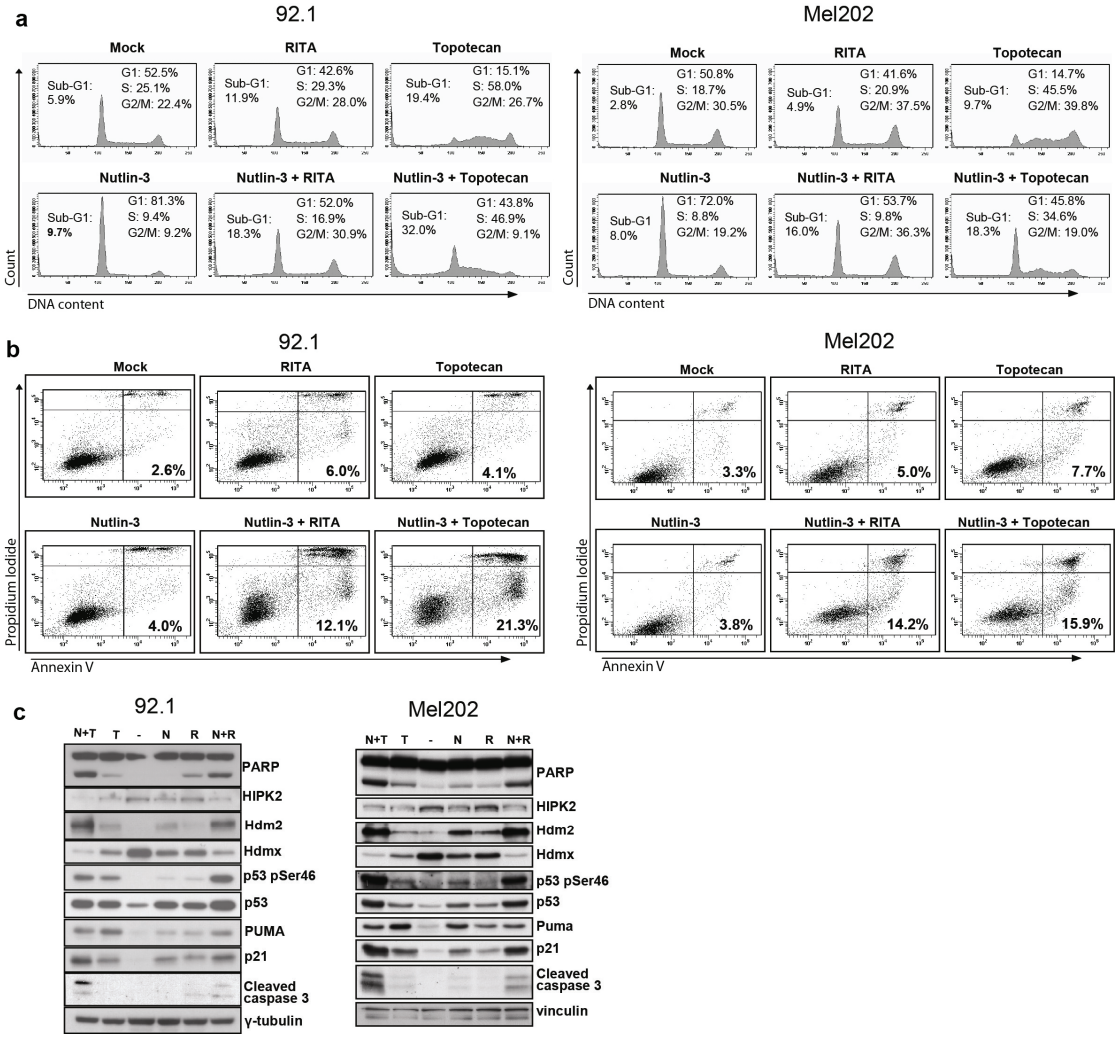

Figure 3 Enhanced apoptosis induction by Nutlin-3 in combination with RITA or Topotecan. Single or combination treatments were performed in 92.1 using 2.0 µM Nutlin-3, 0.7 µM RITA and 25 nM Topotecan and in Mel202 using 3.0 µM Nutlin-3, 0.25 µM RITA and 25 nM Topotecan. (**a**) Flow cytometry analysis after 24 h treatment as indicated. (**b**) Annexin V staining after 48 h treatment as indicated. (**c**) Western blots after 48 h treatment as indicated. N, Nutlin-3; R, RITA; T, Topotecan.

ATM inhibition attenuates p53-Ser46 phosphorylation upon combination treatments without rescuing the induction of apoptosis

We continued the search for the kinase(s) responsible for p53-Ser46 phosphorylation by using a set of specific kinase inhibitors. P53-Ser46 phosphorylation and p53 stabilization was efficiently blocked by Caffeine and by the ATM-specific inhibitor KU55933 (Figure 4a), suggesting a role for the DNA damage sensor kinase ATM. This notion prompted us to investigate the contribution of the DNA damage response more thoroughly. Single Topotecan treatment induced phosphorylation of ATM and its substrates Kap1 and p53-Ser15 (Figure 4b). Addition of Nutlin-3 did not affect p-ATM levels, but slightly reduced p-Kap1, whereas p-p53-Ser15 was elevated in Mel202 cells, correlating with stabilization of p53. Thus, Nutlin-3 might modulate the Topotecan-induced ATM activity. RITA treatment resulted in induction of p-ATM, p-Kap1 and p-p53-Ser15, although to a much lesser extent as compared with Topotecan-treated cells. Combination with Nutlin-3 slightly enhanced ATM and Kap1 phosphorylations in Mel202, but not in 92.1. Increased pSer15-p53 in response to RITA plus Nutlin-3, compared with RITA alone, appears to correlate with extra stabilization of total p53, which is similar to the findings in short-term cultures 08-011 and 10-006 (Supplementary Figure 2).
To investigate the involvement of ATM in more detail, we inhibited ATM activity either by knocking down ATM levels with two different shRNAs (Figures 4c-e), or by using KU55933 (Supplementary Figure 4). Indeed ATM inhibition caused a substantial decrease of the Nutlin-3 plus RITA-induced phosphorylations of p53-Ser15, p53-Ser46, Kap1 and ATM (Figure 4c and Supplementary Figure 4a) as well as the Nutlin-3 plus Topotecan-induced phosphorylations of ATM, Kap1, Chk2, p53-Ser46 and p53-Ser15 (Figure 4d and Supplementary Figure 4b). However, ATM inhibition resulted in even enhanced PARP cleavage, indicating apoptosis induction in the absence of functional ATM. Cell death was confirmed by dramatic increases of sub-G1 cells (Figure 4e and Supplementary Figure 4c). Apparently, inhibiting ATM activity by itself is incompatible with survival of these cells. Therefore, we cannot conclude whether ATM is somehow involved in the mechanism underlying the synergy as found in the combination therapies.

***In vivo* tumor protection by Nutlin-3 and Topotecan**

To investigate the *in vivo* applicability of the treatments, we used mouse melanoma B16F10, a wt-p53 cell line that has frequently been used as model for ocular melanoma, in particular for *in vivo* experiments (Ly *et al.*, 2010). First, we generated stable B16F10 shp53 and shCtrl cell lines to analyze Nutlin-3-mediated p53 activation. In B16-shCtrl, p53 protein

levels and Mdm2 and p21 protein and mRNA levels were induced already after 4 h Nutlin-3 treatment (Supplementary Figure 5a and b), accompanied by reduced cell viability (Supplementary Figure 5c). The observed p53 response and growth inhibition were significantly weaker in B16-shp53, although this was only a partial reduction. Most likely,

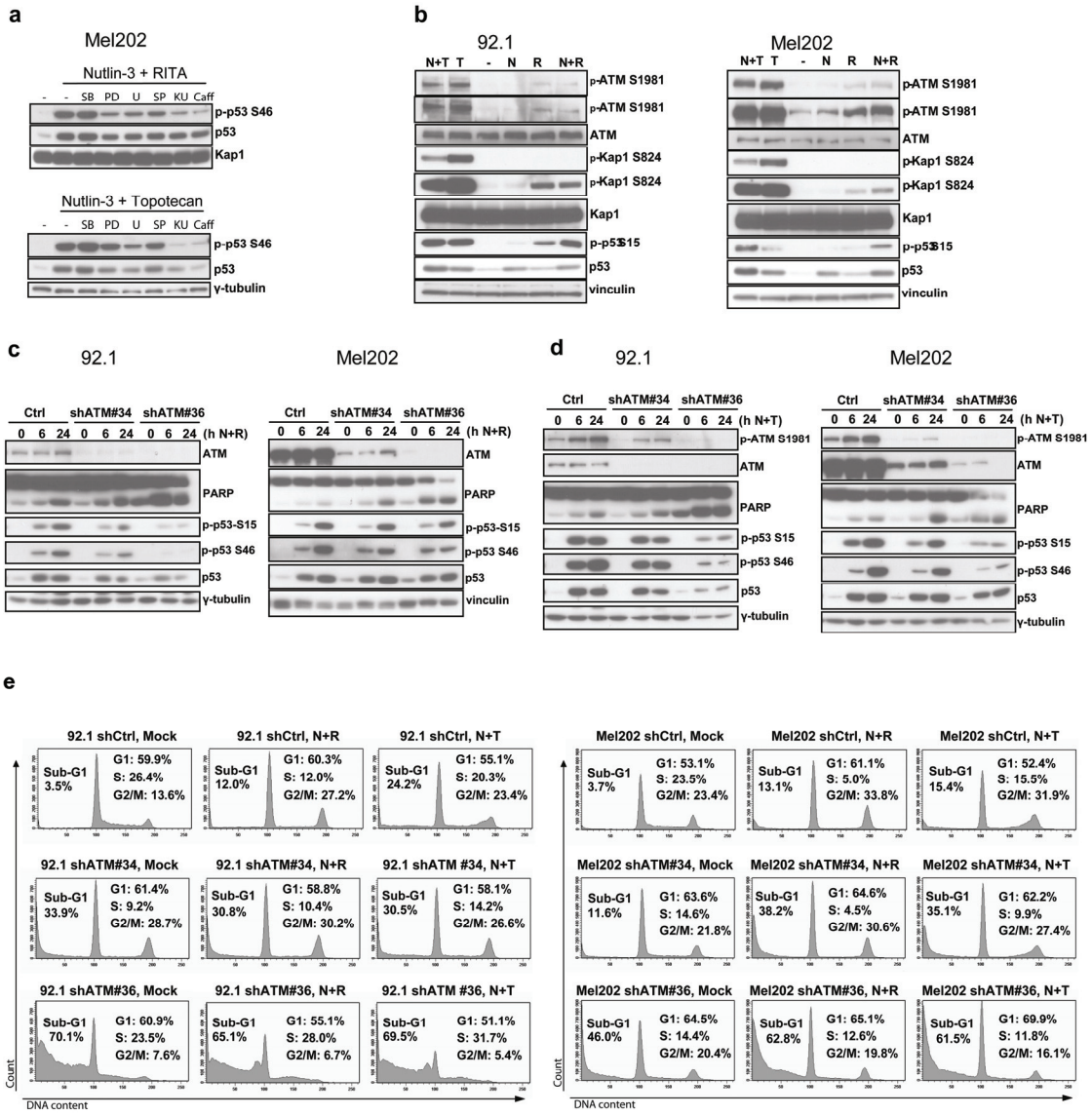

Figure 4 ATM inhibition attenuates p53-Ser46 phosphorylation upon combination treatments without rescuing the induction of apoptosis. (**a**) Western blots of Mel202 cells treated with 3.0 µM Nutlin-3 and 0.25 µM RITA (upper panel) or 3.0 µM Nutlin-3 and 25 nM Topotecan (lower panel) for 24h in the presence of the indicated kinase inhibitors. SB = 10 µM SB203580 (p38 inhibitor), PD = 15 µM PD98059 (MEK1 inhibitor), U = 10 µM U0126 (MEK1 and MEK2 inhibitor), SP = 20 µM SP600125 (JNK1 and JNK2 inhibitor), KU = 10 µM KU55933 (ATM inhibitor), Caff = 10 µM Caffeine (PIKK inhibitor). (**b**) Western blots of 92.1 and Mel202 cells treated for 24 h as in Figure 3. (**c, d**) The 92.1 and Mel202 cells were transduced with shCtrl or shATM RNAs, treated as indicated and analyzed by western blotting. (**e**) Flow cytometry analysis of 92.1 and Mel202 cells transduced with shCtrl or shATM RNAs and treated for 24 h as indicated.

this is because of incomplete p53 knockdown that still enables Nutlin-3 to elicit a reduced effect. We also examined the effect of Nutlin-3 on soft agar growth (Supplementary Figure 5d). Mock-treated B16-shCtrl and B16-shp53 formed colonies in soft agar. Nutlin-3 inhibited colony formation of B16-shCtrl, whereas it only partially affected B16-shp53, indicating that inhibition of anchorage-independent growth by Nutlin-3 is mostly mediated via p53.

Because RITA binds murine p53 very inefficiently (Issaeva *et al.*, 2004), we could only investigate the use of Topotecan in B16F10. Combination of Nutlin-3 and Topotecan resulted in synergistic growth inhibition (Figure 5a) and enhanced p53 activation (Figure 5b). Analogous to the cell cycle profiles in human uveal melanomas (Figure 3a and Supplementary Figure 3), in B16F10 we also observed Nutlin-3-induced G1 arrest, Topotecan-induced G2 arrest and upon combination treatment an additional peak in (late) S-phase, possibly a 'sub-G2' fraction (Figure 5c). Importantly, the sub-G1 fraction was higher after combination treatment compared with single treatments. Next, we used a murine model for ocular melanoma, in which B16F10 cells are injected into the anterior eye chamber (AC) of C57Bl/6 mice. Cells started to form tumors 6-8 days after implantation. Survival (Figure 5d) is defined as the percentage of mice with <80% tumor occupation in their AC; mice were killed upon exceeding this threshold. Subconjunctival delivery of Nutlin-3, Topotecan, or the combination of both (upper graphs) all delayed tumor growth significantly compared with the control group. Although the combination treatment seemed to inhibit tumor growth slightly more efficiently than either drug alone, these differences were not significant (lower graphs).

Equal sensitivity of uveal melanoma cells to treatments under normoxia and hypoxia

At certain stages during tumor development tumor cells are confronted with low-oxygen conditions, which may influence drug sensitivity (Moeller *et al.*, 2005). We investigated responses to the various treatments during hypoxia in 92.1 (Figure 6) and Mel202 (Supplementary Figure 6). Culturing shCtrl and shp53 cells in hypoxia (1% O2) resulted in clear induction of HIF-1α and HIF-2α protein levels (Figure 6a and Supplementary Figure 6a) and increased the expression of the HIF target genes *VEGF*, *Glut1* and *Enolase-γ* (Figure 6b and Supplementary Figure 6b, left panels). These activations appear to be p53 independent, as we observed no major differences between shCtrl and shp53 cells. As expected, Nutlin-3 treatment induced p53 protein levels and enhanced p21, Hdm2 and PUMA protein and mRNA levels in shCtrl, but not in shp53 (Figure 6a and Supplementary Figure 6a and right panels of Figure 6b and Supplementary Figure 6b). Hdmx protein levels

were downregulated upon Nutlin-3 treatment in a p53-dependent manner, as observed in other cell lines (Patton *et al.*, 2006; Wade *et al.*, 2006). Importantly, the inductions of p53, Hdm2, p21 and PUMA by Nutlin-3 were comparable under normoxic and hypoxic conditions.

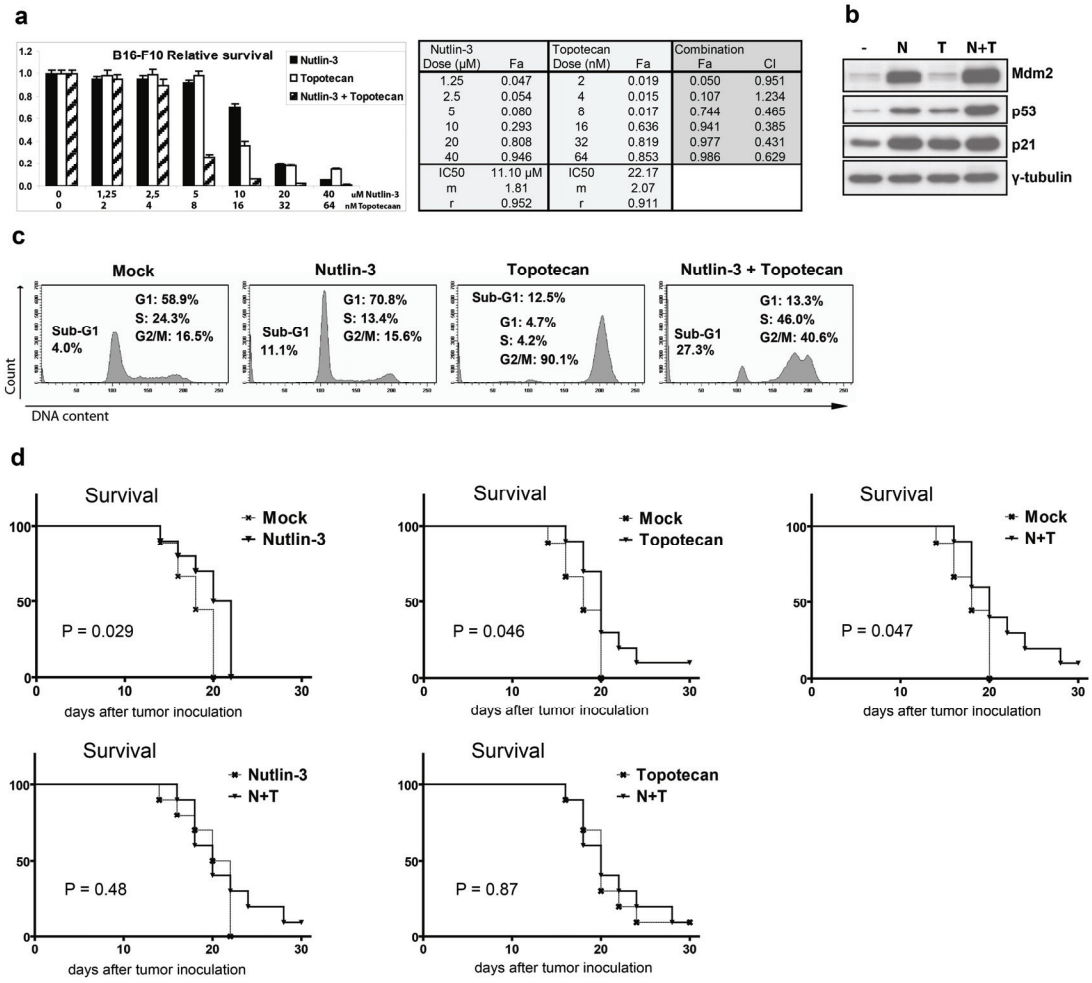

Nutlin-3 Dose (μM)	Fa	Topotecan Dose (nM)	Fa	Combination Fa	CI
1.25	0.047	2	0.019	0.050	0.951
2.5	0.054	4	0.015	0.107	1.234
5	0.080	8	0.017	0.744	0.465
10	0.293	16	0.636	0.941	0.385
20	0.808	32	0.819	0.977	0.431
40	0.946	64	0.853	0.986	0.629
IC50	11.10 μM	IC50	22.17		
m	1.81	m	2.07		
r	0.952	r	0.911		

Figure 5 B16F10 growth inhibition in cell culture and *in vivo* by Nutlin-3 and Topotecan. (**a**) B16F10 cells were counted and seeded for WST-1 proliferation assay. Cells were treated as indicated with different concentrations, alone or in constant ratio combinations, of Nutlin-3 and Topotecan. Cell viability was measured after 72 h treatment, and the effects of drug treatments as fraction of untreated control cells were calculated. The dose-response values IC50, *m* and *r* for each single drug as well as the CI for each drug combination were derived using Compusyn software (Chou and Martin, 2007). CI<0.9, synergy; 0.9<CI<1.1, additive effect; CI>1.1, antagonism. (**b**) Western blot of B16F10 cells treated for 24 h as indicated. N= 10 μM Nutlin-3; T = 25 nM Topotecan. (**c**) Flow cytometry of B16F10 cells treated for 24 h as indicated. (**d**) B16F10 cells were injected into the AC of C57BL/6 mice and animals were either mock treated or treated as described. *In vivo* tumor growth was monitored every 2 days and mice were killed when the AC was filled for 80-100% with tumor cells. The Kaplan-Meyer curves represent percentage survival, defined as the percentage of mice that have <80% tumor occupation in their AC. Log-rank tests were used to determine statistically significant differences between two curves.

We also applied RITA and Topotecan treatments, alone or with Nutlin-3, in hypoxia. At the RITA concentrations we used, no downregulation of HIF-1α was observed in 92.1 and Mel202 cells, in contrast to what was previously described for HCT116 cells (Yang *et al.*, 2009). Interestingly, HIF-1α protein levels were clearly lower in cells treated with Topotecan or with either combination, which partially seemed to correlate with increased levels of HIF-2α (Figure 6c and Supplementary Figure 6c). At mRNA level, the hypoxic inductions of Glut1 (in both cells) and VEGF (Mel202) were unaffected by the treatments, whereas Enolase-γ (in both cells) and VEGF (in 92.1) loosely followed the same trend as HIF-1α protein levels (Figure 6d and Supplementary Figure 6d, left panels). These data suggest that HIF-2α may partially compensate for loss of HIF-1α activity. In line with the results obtained with Nutlin-3 treatment in hypoxia, also RITA, Topotecan and the combination treatments led to comparable inductions of p53, Hdm2, p21 and PUMA in normoxia and hypoxia (Figure 6c, Supplementary Figure 6c and right panels of Figure 6d and Supplementary Figure 6d). Thus, in uveal melanoma cell lines, p53 activation by Nutlin-3, RITA and Topotecan is independent of oxygen level, and is not impaired by altered levels of HIF-1α and HIF-2α. In addition, in B16F10 cells Nutlin-3 was equally efficient in stabilizing p53 and activating Mdm2 and p21 in normoxia and hypoxia (Supplementary Figure 7).

We further investigated the biological treatment responses in hypoxia. Nutlin-3 induced similar growth inhibition in hypoxia and normoxia (Figure 6e and Supplementary Figure 6e). Flow cytometry (Figure 6f and Supplementary Figure 6f) showed that incubation at 1% O_2 for 48h slightly increased G1 fractions, which was p53 dependent (not shown) indicating that hypoxia alone may indeed trigger a minor p53 response (An *et al.*, 1998). All single or combination treatments induced similar patterns when comparing cell cycle profiles in normoxia and hypoxia. Altogether, these data indicate that Nutlin-3, RITA and Topotecan lead to efficient p53 activation in normoxia and hypoxia. This should allow the efficient treatment of cells growing in hypoxic tumor areas.

Discussion

For developing novel cancer therapies, much work has focused on specific reactivation of p53, which is functionally inactivated in virtually all human tumors. About half of the tumors still express a wt-p53 protein that might be reactivated by chemotherapeutic agents. The design of non-genotoxic, small-molecule compounds is potentially attractive as they may target tumors without severely damaging healthy tissues. Uveal melanoma is an example of a cancer generally lacking p53 mutations. Therefore, we investigated the use of

p53-activating drugs as treatment for uveal melanoma. Nutlin-3 specifically disrupts the Hdm2-p53 interaction and has already shown therapeutic potential in both *in vitro* and *in vivo* experiments (Vassilev *et al.*, 2004). In our studies, Nutlin-3 efficiently induced p53-dependent growth inhibition in uveal melanoma cell lines, confirming the presence of wt-p53 and intact down-stream signaling. Interestingly, both 92.1 and Mel202 over-express Hdmx, which is probably responsible for p53 inactivation in these tumor cells. Compared with other uveal melanoma cell lines with low Hdmx, 92.1 and Mel202 showed similar

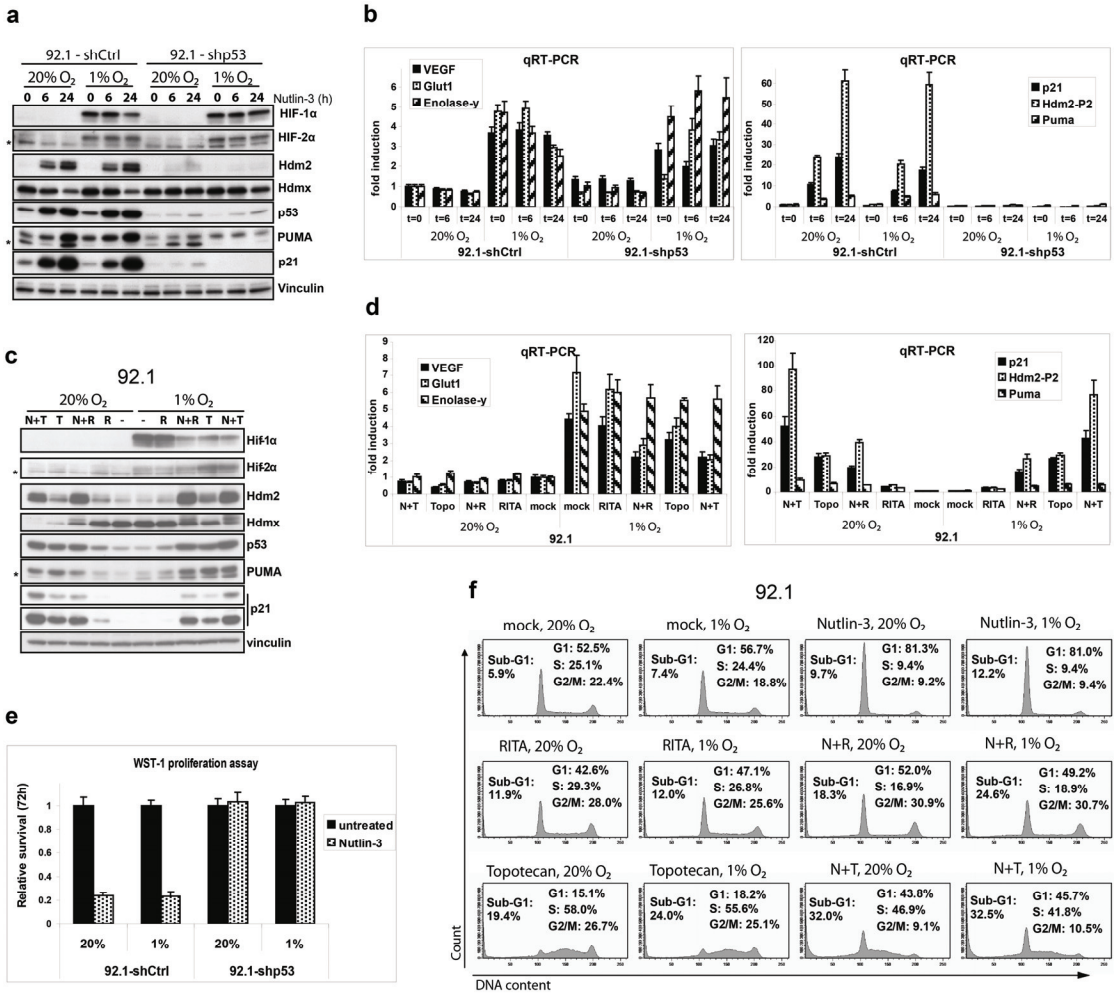

Figure 6 Similar p53 activation and growth inhibition in normoxia and hypoxia by Nutlin-3, RITA and Topotecan in 92.1 cells. The 92.1 cells stably expressing shCtrl or shp53 RNAs were incubated at 20% or 1% O_2 for 48 h and treated with 10 μM Nutlin-3 during the last 6 or 24 h as indicated, followed by western blot analysis (**a**) and qRT-PCR (**b**). Single or combination treatments (24 h) in 92.1 cells incubated at 20% or 1% O_2 for 48 h were performed as indicated using 2.0 μM Nutlin-3, 0.7 μM RITA and 25 nM Topotecan, followed by western blot analysis (**c**) and qRT-PCR (**d**). *Non-specific background staining. (**e**) The 92.1 cells stably expressing shCtrl or shp53 RNAs were counted and seeded for WST-1 proliferation assay. Cells were incubated at 20 or 1% O_2 as indicated, treated with 10 μM Nutlin-3 and cell viability was measured 72 h after treatment. (**f**) The 92.1 cells were incubated at 20 or 1% O_2 for 48 h and treated as indicated during the last 24 h, followed by flow cytometry analysis. Concentrations used: 2.0 μM Nutlin-3, 0.7 μM RITA and 25 nM Topotecan.

sensitivity to Nutlin-3, re-evaluating the idea that Hdmx expression *per se* is an important determinant for the efficacy of Nutlin-3 treatment (Patton *et al.*, 2006; Wade *et al.*, 2006; Hu *et al.*, 2006).

Because p53 can induce both cell cycle arrest and apoptosis, it is crucial to direct the cellular response toward the clinically more desirable apoptosis. In many cell types, however, including the uveal melanoma cells we examined, Nutlin-3 mainly induces G1 arrest. Nutlin-3 may be more effective when used in combination therapy, which ideally results in synergistic growth inhibition. Furthermore, this may reduce the dosage of genotoxic drugs (thus minimizing side effects) and decrease the chance of resistance-conferring mutations. In this study, we show that Nutlin-3 synergizes with both the topoisomerase I inhibitor Topotecan and with the small-molecule p53-activator RITA to inhibit uveal melanoma growth. Importantly, synergy was observed in established cell lines as well as in short-term cultures. The biological basis for synergistic growth inhibition is presumably enhanced apoptosis induction, evidenced by increased sub-G1 fractions, Annexin V staining and cleaved PARP and Caspase 3 levels. How this is achieved mechanistically is more speculative. A potential clue could be the enhanced phosphorylation of p53-Ser46, believed to result in apoptosis induction. Despite earlier reports that RITA activates HIPK2 by reducing Hdm2 (Rinaldo *et al.*, 2009), possibly contributing to RITA-induced apoptosis, we found no evidence for HIPK2 involvement in these cells. Nutlin-3 either alone or in combination with RITA, but not RITA alone, slightly reduced HIPK2 protein levels. HIPK2 reduction correlated with Hdm2 increase, but also with enhanced p53-Ser46 phosphorylation, indicating that a kinase other than HIPK2 is responsible for p53-S46 phosphorylation.

A quick search for the kinase(s) responsible for p53-Ser46 phosphorylation suggested a role for the DNA damage sensor kinase ATM. Several factors support a putative involvement of the DNA damage response. First, multiple kinases involved in p53-Ser46 phosphorylation, including ATM (Saito *et al.*, 2002; Kodama *et al.*, 2010), are induced by DNA damage. Moreover, Topotecan directly leads to double strand-breaks. Recently, also RITA has been indicated to induce a DNA damage response, via a p53-dependent mechanism (Yang *et al.*, 2009). We also found RITA induced phosphorylation of ATM, Kap1 and p53-Ser15, although these were much weaker compared with those induced by Topotecan, when the drugs were used at around IC50 concentrations. Precisely how RITA acts mechanistically remains poorly understood, but its activity clearly stretches beyond p53 stabilization. It is interesting to note that, although both were developed as p53-activating molecules, Nutlin-3 and RITA have very different effects on the cell cycle (G1 vs G2 arrest). This may be an important contribution to the synergy, as only a stronger

activation of the same pathway would be expected to be additive, not synergistic. The involvement of ATM in p53-Ser46 phosphorylation was confirmed by drugs and shRNAs. However, ATM inhibition was incompatible with survival, suggesting that these cells are sensitive to loss of checkpoint activation. Such effects of ATM inhibition have also been described by others (White *et al.*, 2008; Li and Yang 2010). Although by itself this is an intriguing observation and may provide another starting point for developing anti-cancer strategies, it prevents us from concluding whether ATM is involved in the synergy as found in the combination therapies. Further research is necessary to address the relevance of p53-Ser46 phosphorylation. It is noteworthy that also the MEK-inhibitors and the JNK inhibitor affected p53-Ser46 phosphorylation, although less than caffeine or KU55933. It indicates that multiple pathways are activated upon RITA and Topotecan treatment, which might collaborate to obtain the observed biological effects.

For *in vivo* testing of the treatments we switched to mouse melanoma B16F10, given its ability to form tumors when injected into the AC of murine eyes (Ly *et al.*, 2010). Because RITA has very low affinity for mouse p53, we only investigated the use of Nutlin-3 and Topotecan in this model. We confirmed efficient p53 activation by Nutlin-3 and showed synergistic growth inhibition by Nutlin-3 and Topotecan in B16F10. Importantly, both Nutlin-3 and Topotecan delayed *in vivo* tumor growth, albeit only limited. Combination treatment seemed to inhibit tumor growth slightly more efficient, although this trend was not significant. Possibly the experimental conditions need to be further optimized to achieve clear synergy. An important issue may be the fact that drug synergy can be dose dependent. The *in vitro* synergy studies already indicated that in 92.1 and B16F10, Nutlin-3 and Topotecan did not synergize at very low doses. Thus, if the drug delivery in our experimental settings was not sufficient, no synergy might be expected. Final drug concentrations in tumors are difficult to control. When drugs are over-diluted or washed away too quickly, cells will hardly be affected. A solution might be the use of intra-cameral instead of subconjunctival injections.

Notably, our experiment protocol forced us to stop treatments after day 10 following tumor cell inoculation. Around this time-point, the tumors in the combination treatment group were indeed much smaller. Possibly, even the combination treatment does not kill all tumor cells, and upon ending the treatments the surviving cells start growing and initial group differences are lost.

As most tumors at a certain stage face a hypoxic environment, any treatment must be still functional under hypoxic conditions. We mimicked this by culturing cells in 1% O_2 and

found that Nutlin-3, RITA and Topotecan, as well as both combination treatments, induced p53 and subsequent growth inhibition that was equally efficient as in cells cultured at 20% O_2. This predicts that fluctuating oxygen levels *in vivo* will not interfere with the efficacy of the proposed treatments.

Several other investigators examined whether small-molecule activation of p53 potentially mediates anti-angiogenic effects via attenuating HIF-1α mediated transcription. The interplay between the p53 and HIF pathways is not entirely clear. HIF-1α may stabilize p53 through inhibition of Hdm2-mediated p53 ubiquitination (An *et al.*, 1998); in turn, p53 may destabilize HIF-1α by promoting Hdm2-mediated HIF-1α ubiquitination (Ravi *et al.*, 2000). In contrast, direct association of Hdm2 with HIF-1α would increase HIF-1α activity (LaRusch *et al.*, 2007). The use of Nutlin-3 might, therefore, result in p53-dependent degradation of HIF-1α and/ or p53-independent inactivation of HIF-1α by preventing interaction with Hdm2 (Lee *et al.*, 2009). However, we found no evidence for direct inhibition of the hypoxic induction of HIF-1α by Nutlin-3 alone. Perhaps the (impact of Nutlin-3 on) regulation of HIF-1α stability and activity is not universal. A putative direct regulation of HIF-1α by Hdm2 may depend on the cellular context, like high levels of Hdmx as found in the cells we examined. Beside Nutlin-3, also RITA has been implicated in HIF-1α inhibition, supposedly through inducing a DNA damage response and suppressing protein synthesis via phosphorylation of eIF-2α (Yang *et al.*, 2009). In our experiments, RITA alone did not change HIF-1α levels. However, the combination of RITA and Nutlin-3, as well as Topotecan alone or in combination with Nutlin-3, indeed decreased HIF-1α protein levels. These findings would fit into a model in which a certain level of DNA damage response is required for p53-mediated down-regulation of HIF-1α (Kaluzova *et al.*, 2004). Interestingly, HIF-2α seemed to partially compensate for loss of HIF-1α. This implies that for anti-angiogenic therapies also the contribution of HIF-2α needs to be taken into account.

Altogether, our data suggest that synergistic growth inhibition based on small-molecule p53 activation may have clinical potential for ocular melanoma. However, future studies in a clinical setting are necessary to address the utility of p53 activators and possible advantages over the current standard therapies.

Materials and Methods

Cell lines, lentiviral transductions

Human uveal melanoma cell lines 92.1 (De Waard-Siebinga *et al.*, 1995), Mel202, Mel270 and Mel285 and short-term cultures 10-006 and 08-011 were cultured in RPMI + F10 medium (1:1 ratio)

with 10% fetal bovine serum and antibiotics. B16F10 cells were cultured in Dulbecco's modified eagle medium supplemented with 10% fetal bovine serum and antibiotics. Lentiviral constructs (listed in Supplementary Table 1) were described before (Lam *et al.*, 2010) or obtained from the Mission shRNA library (Sigma-Aldrich, St Louis, MO, USA). Cells were transduced using MOI = 1.0 in medium containing 8.0 µg/ml polybrene and puromycin selected for stable expression.

Immunoblotting

Cells were lysed in Giordano buffer (50 mM Tris-HCl, pH 7.4, 250 mM NaCl, 0.1% Triton X-100, 5 mM ethylenediaminetetraacetic acid) with protease- and phosphatase inhibitors. Proteins were separated by sodium dodecyl sulfate-polyacrylamide gel electrophoresis, blotted onto polyvinylidene fluoride transfer membranes, incubated with the appropriate primary (listed in Supplementary Table 2) and secondary antibodies, and bands were visualized by chemoluminescence (West Dura, Pierce Biotechnology, Rockford, IL, USA).

RNA isolation, reverse transcriptase-PCR (RT-PCR)

RNA was isolated using the SV Total RNA isolation kit (Promega, Madison, WI, USA). Complementary DNA was synthesized using 2.0 µg RNA in a total volume of 30 µL reverse transcriptase reaction mixture (Promega). Samples were analyzed in triplicate using SYBR Green mix (Roche Biochemicals, Indianapolis, IN, USA) in a 7900ht Fast Real-Time PCR System (Applied Biosystems, Foster City, CA, USA). For normalization the geometric mean of at least two housekeeping genes was used. Primer sequences are listed in Supplementary Table 3.

Flow cytometry

Cells were harvested, washed in phosphate buffered saline (PBS) and fixed in ice-cold 70% EtOH. Before fluorescence-activated cell sorter analysis, cells were washed in PBS and resuspended in PBS containing 50 µg/mL RNase A and 50 µg/mL propidium iodide. Flow cytometry was performed in the BD LSR II system (BD Biosciences, Sparks, MD, USA). For Annexin V staining, cells were washed twice in PBS and resuspended in Annexin V-binding buffer containing Fluorescein isothyocyanate-labeled Annexin-V (Sigma-Aldrich) and propidium iodide. After 10 min RT incubation cells were analyzed by flow cytometry. Positive propidium iodide staining, indicating necrotic or late apoptotic cells, were excluded from the analysis. Propidium iodide-negative, Annexin V-positive cells represent early apoptotic cells.

WST-1 proliferation assay, calculation of synergism

Cells were counted and seeded in triplicate in 96-well plates at a density of 1500 (B16F10), 3000 (92.1, Mel285 and Mel270) or 6000 (Mel202) cells per well, in a total volume of 100 µL medium. Cells were incubated with 10 µL WST-1 (Roche) for 2 h and absorbance (450 nm) was measured in a microplate reader (Victor; Perkin Elmer, San Jose, CA, USA). For synergy studies, drug effects were calculated as 'affected fraction' of treated vs untreated cells. Dose-effect analyses and calculation of

combination index (CI) were performed using CompuSyn software (Chou and Martin, 2007). CI reflects the extent of synergy or antagonism for two drugs: CI<0.9, synergy; 0.9<CI<1.1, additive effect; CI>1.1, antagonism.

Soft agar assay

Trypsinized cells were counted and resuspended in 0.3% agarose medium containing 10% fetal bovine serum with 10 μM Nutlin-3. 50,000 cells were plated in triplicate over a 0.6% agarose bottom layer with 10 μM Nutlin-3. Medium with Nutlin-3 was replaced every 3-4 days. Colony outgrowth was monitored during 18 days using light microscopy.

***In vivo* tumor growth and treatments**

Authors confirm adherence to the ARVO Statement for use of animals in Ophthalmic and Vision Research. Mice were inoculated with 25,000 cells/ 4 μL B16F10 cells in the anterior chamber (AC) under anaesthesia; a 1:1 mixture of Xylazine (Rompun 2%, Bayer, Leverkussen, Germany) and Ketamine Hydrochloride (Aescoket, Aesculaap bv, Boxtel, The Netherlands), given intraperitoneally. A previously described technique for deposition of tumor cells into the AC was applied (Ly *et al.*, 2010). Treatment was performed on days 2, 4, 6, 8 and 10 after tumor inoculation by subconjunctival injection of 16 μl PBS, 16 μl 100 μM Nutlin-3, or 16 μl 200nM Topotecan, or of 16 μl combination of both drugs, in four different subconjunctival sites, creating a bleb. The eyes were examined every 2 days under a dissecting microscope and tumor volume was recorded as percentage of AC occupied by tumor. Mice were killed when the tumor occupied 80–100% of the AC.

Acknowledgements

We thank Dr PA van der Velden and M Versluis for the primer sets to detect the expression of the HIF target genes and the early cultures of primary uveal melanoma cells, Dr A Vertegaal for the antibodies detecting HIF-1α and HIF-2α proteins, Prof BR Ksander for providing the Mel cell lines, Dr G Selivanova for providing RITA and Dr A Levine for providing anti-Mdm2 antibody. This study was supported by grants from Netherlands Organization for Scientific Research NWO (Mozaiek grant 017.003.059) and by EC FP6 funding (contract 503576).

Reference List

An WG, Kanekal M, Simon MC, Maltepe E, Blagosklonny MV, Neckers LM. (1998). Stabilization of wild-type p53 by hypoxia-inducible factor 1alpha. *Nature* **392;** 405-408.

Augsburger JJ, Correa ZM, Shaikh AH. (2009). Effectiveness of treatments for metastatic uveal melanoma. *Am J Ophthalmol* **148;** 119-127.

Barbieri E, Mehta P, Chen Z, Zhang L, Slack A, Berg S *et al*. (2006). MDM2 inhibition sensitizes neuroblastoma to chemotherapy-induced apoptotic cell death. *Mol Cancer Ther* **5;** 2358-2365.

Bulavin DV, Saito S, Hollander MC, Sakaguchi K, Anderson CW, Appella E *et al*. (1999). Phosphorylation of human p53 by p38 kinase coordinates N-terminal phosphorylation and apoptosis in response to UV radiation. *EMBO J* **18;** 6845-6854.

Chang AE, Karnell LH, Menck HR. (1998). The National Cancer Data Base report on cutaneous and noncutaneous melanoma: a summary of 84,836 cases from the past decade. The American College of Surgeons Commission on Cancer and the American Cancer Society. *Cancer* **83;** 1664-1678.

Chou TC. (2006). Theoretical basis, experimental design, and computerized simulation of synergism and antagonism in drug combination studies. *Pharmacol Rev* **58;** 621-681.

Chou, T. C. and Martin, N. CompuSyn software for drug combinations and for general dose-effect analysis, and user's guide. 9-2-2007. ComboSyn, Inc.Paramus, NJ. 2007.
Ref Type: Computer Program

Coll-Mulet L, Iglesias-Serret D, Santidrian AF, Cosialls AM, de FM, Castano E *et al*. (2006). MDM2 antagonists activate p53 and synergize with genotoxic drugs in B-cell chronic lymphocytic leukemia cells. *Blood* **107;** 4109-4114.

D'Orazi G, Cecchinelli B, Bruno T, Manni I, Higashimoto Y, Saito S *et al*. (2002). Homeodomain-interacting protein kinase-2 phosphorylates p53 at Ser 46 and mediates apoptosis. *Nat Cell Biol* **4;** 11-19.

De Waard-Siebinga I, Blom DJ, Griffioen M, Schrier PI, Hoogendoorn E, Beverstock G *et al*. (1995). Establishment and characterization of an uveal-melanoma cell line. *Int J Cancer* **62;** 155-161.

Enge M, Bao W, Hedstrom E, Jackson SP, Moumen A, Selivanova G. (2009). MDM2-dependent downregulation of p21 and hnRNP K provides a switch between apoptosis and growth arrest induced by pharmacologically activated p53. *Cancer Cell* **15;** 171-183.

Hu B, Gilkes DM, Farooqi B, Sebti SM, Chen J. (2006). MDMX overexpression prevents p53 activation by the MDM2 inhibitor Nutlin. *J Biol Chem* **281;** 33030-33035.

Issaeva N, Bozko P, Enge M, Protopopova M, Verhoef LG, Masucci M *et al*. (2004). Small molecule RITA binds to p53, blocks p53-HDM-2 interaction and activates p53 function in tumors. *Nat Med* **10;** 1321-1328.

Kaluzova M, Kaluz S, Lerman MI, Stanbridge EJ. (2004). DNA damage is a prerequisite for p53-mediated proteasomal degradation of HIF-1alpha in hypoxic cells and downregulation of the hypoxia marker carbonic anhydrase IX. *Mol Cell Biol* **24;** 5757-5766.

Kivela T, Eskelin S, Kujala E. (2006). Metastatic uveal melanoma. *Int Ophthalmol Clin* **46;** 133-149.

Kodama M, Otsubo C, Hirota T, Yokota J, Enari M, Taya Y. (2010). Requirement of ATM for rapid p53 phosphorylation at Ser46 without Ser/Thr-Gln sequences. *Mol Cell Biol* **30;** 1620-1633.

Kojima K, Konopleva M, McQueen T, O'Brien S, Plunkett W, Andreeff M. (2006). Mdm2 inhibitor Nutlin-3a induces p53-mediated apoptosis by transcription-dependent and transcription-independent mechanisms and may overcome Atm-mediated resistance to fludarabine in chronic lymphocytic leukemia. *Blood* **108;** 993-1000.

Krajewski M, Ozdowy P, D'Silva L, Rothweiler U, Holak TA. (2005). NMR indicates that the small molecule RITA does not block p53-MDM2 binding in vitro. *Nat Med* **11;** 1135-1136.

Lam S, Lodder K, Teunisse AF, Rabelink MJ, Schutte M, Jochemsen AG. (2010). Role of Mdm4 in drug sensitivity of breast cancer cells. *Oncogene*.

LaRusch GA, Jackson MW, Dunbar JD, Warren RS, Donner DB, Mayo LD. (2007). Nutlin3 blocks vascular endothelial growth factor induction by preventing the interaction between hypoxia inducible factor 1alpha and Hdm2. *Cancer Res* **67;** 450-454.

Laurie NA, Donovan SL, Shih CS, Zhang J, Mills N, Fuller C *et al*. (2006). Inactivation of the p53 pathway in retinoblastoma. *Nature* **444;** 61-66.

Lee YM, Lim JH, Chun YS, Moon HE, Lee MK, Huang LE *et al*. (2009). Nutlin-3, an Hdm2 antagonist, inhibits tumor adaptation to hypoxia by stimulating the FIH-mediated inactivation of HIF-1alpha. *Carcinogenesis* **30;** 1768-1775.

Li Y, Yang DQ. (2010). The ATM inhibitor KU-55933 suppresses cell proliferation and induces apoptosis by blocking Akt in cancer cells with overactivated Akt. *Mol Cancer Ther* **9;** 113-125.

Ly LV, Baghat A, Versluis M, Jordanova ES, Luyten GP, van RN *et al*. (2010). In aged mice, outgrowth of intraocular melanoma depends on proangiogenic M2-type macrophages. *J Immunol* **185;** 3481-3488.

Moeller BJ, Dreher MR, Rabbani ZN, Schroeder T, Cao Y, Li CY *et al*. (2005). Pleiotropic effects of HIF-1 blockade on tumor radiosensitivity. *Cancer Cell* **8;** 99-110.

Patton JT, Mayo LD, Singhi AD, Gudkov AV, Stark GR, Jackson MW. (2006). Levels of HdmX expression dictate the sensitivity of normal and transformed cells to Nutlin-3. *Cancer Res* **66;** 3169-3176.

Ravi R, Mookerjee B, Bhujwalla ZM, Sutter CH, Artemov D, Zeng Q *et al*. (2000). Regulation of tumor angiogenesis by p53-induced degradation of hypoxia-inducible factor 1alpha. *Genes Dev* **14;** 34-44.

Rinaldo C, Prodosmo A, Siepi F, Moncada A, Sacchi A, Selivanova G *et al*. (2009). HIPK2 regulation by MDM2 determines tumor cell response to the p53-reactivating drugs nutlin-3 and RITA. *Cancer Res* **69;** 6241-6248.

Saito S, Goodarzi AA, Higashimoto Y, Noda Y, Lees-Miller SP, Appella E *et al*. (2002). ATM mediates phosphorylation at multiple p53 sites, including Ser(46), in response to ionizing radiation. *J Biol Chem* **277;** 12491-12494.

Tomicic MT, Christmann M, Kaina B. (2010). Topotecan triggers apoptosis in p53-deficient cells by forcing degradation of XIAP and survivin thereby activating caspase-3-mediated Bid cleavage. *J Pharmacol Exp Ther* **332;** 316-325.

Vassilev LT. (2007). MDM2 inhibitors for cancer therapy. *Trends Mol Med* **13;** 23-31.

Vassilev LT, Vu BT, Graves B, Carvajal D, Podlaski F, Filipovic Z *et al*. (2004). In vivo activation of the p53 pathway by small-molecule antagonists of MDM2. *Science* **303;** 844-848.

Wade M, Wong ET, Tang M, Stommel JM, Wahl GM. (2006). Hdmx modulates the outcome of p53 activation in human tumor cells. *J Biol Chem* **281;** 33036-33044.

White JS, Choi S, Bakkenist CJ. (2008). Irreversible chromosome damage accumulates rapidly in the absence of ATM kinase activity. *Cell Cycle* **7;** 1277-1284.

Wynford-Thomas D, Blaydes J. (1998). The influence of cell context on the selection pressure for p53 mutation in human cancer. *Carcinogenesis* **19;** 29-36.

Yang J, Ahmed A, Poon E, Perusinghe N, de Haven BA, Box G *et al*. (2009). Small-molecule activation of p53 blocks hypoxia-inducible factor 1alpha and vascular endothelial growth factor expression in vivo and leads to tumor cell apoptosis in normoxia and hypoxia. *Mol Cell Biol* **29;** 2243-2253.

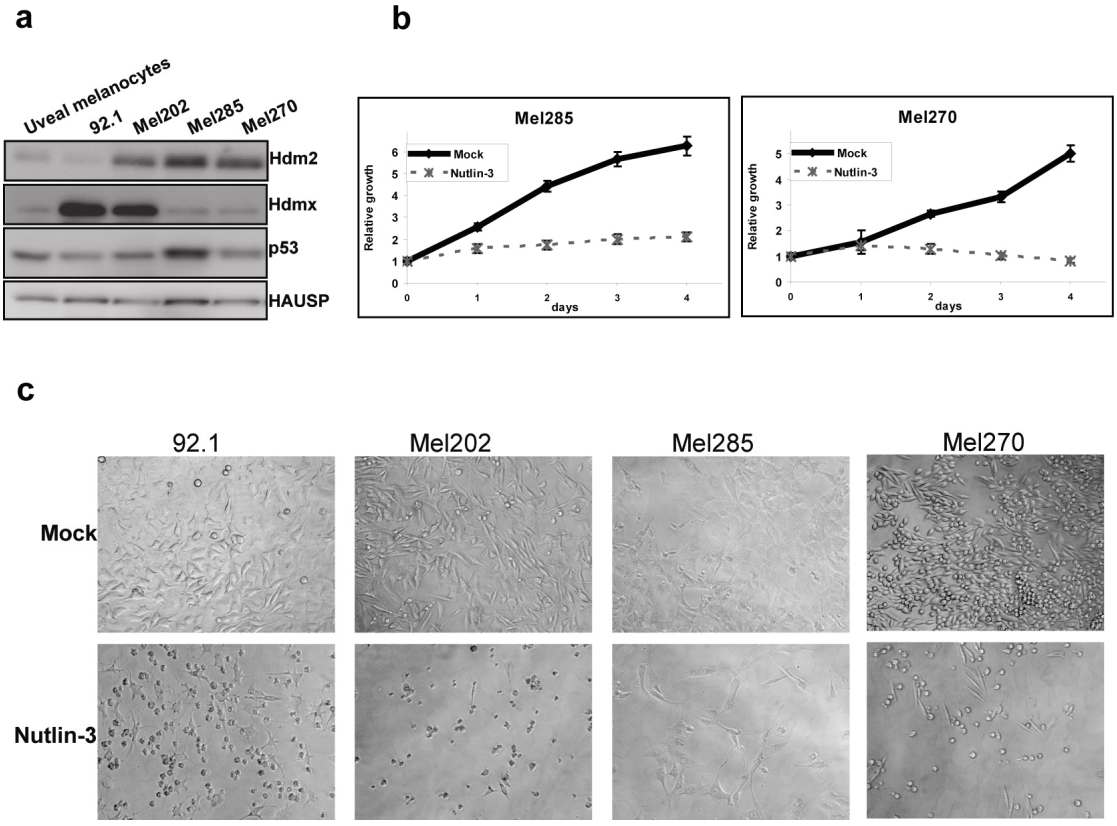

Supplementary Figure 1 No correlation between basal Hdmx and Hdm2 levels and sensitivity to Nutlin-3. (**a**) Four uveal melanoma cell lines and uveal melanocytes as control were analyzed by Western blot for the indicated protein levels. (**b**) Mel285 and Mel270 cells were counted, seeded for WST-1 proliferation assay, and treated with 10 µM Nutlin-3. Cell viability was measured at 0, 24, 48, 72, and 96 h after treatment. (**c**) 72 h after addition of Nutlin-3, pictures were taken from the 96-wells plates from panel (**b**).

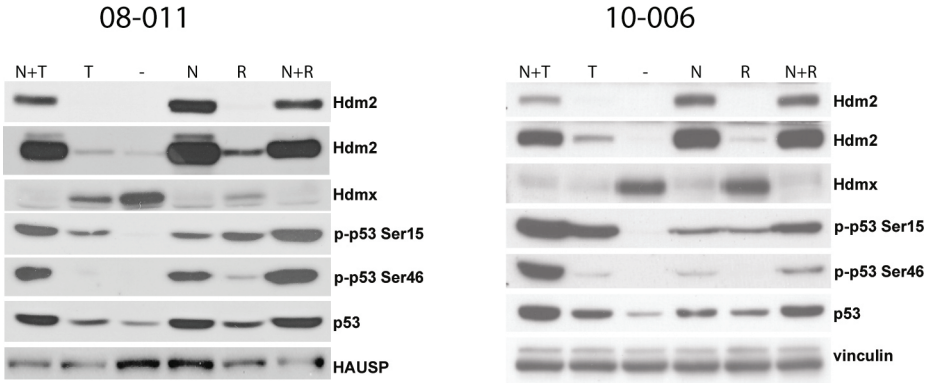

Supplementary Figure 2 Enhanced p53 phosphorylation and stabilization in short-term uveal melanoma cultures upon treatment with Nutlin-3 in combination with RITA or Topotecan. Western blots were performed after 24 h single or combination treatments in short-term uveal melanoma cultures 08-011 and 10-006 as indicated. Treatments in 08-011: N, 12 µM Nutlin-3; R, 0.2 µM RITA; T, 100 nM Topotecan. Treatments in 10-006: N, 8 µM Nutlin-3; R, 1 µM RITA, T, 100 nM Topotecan.

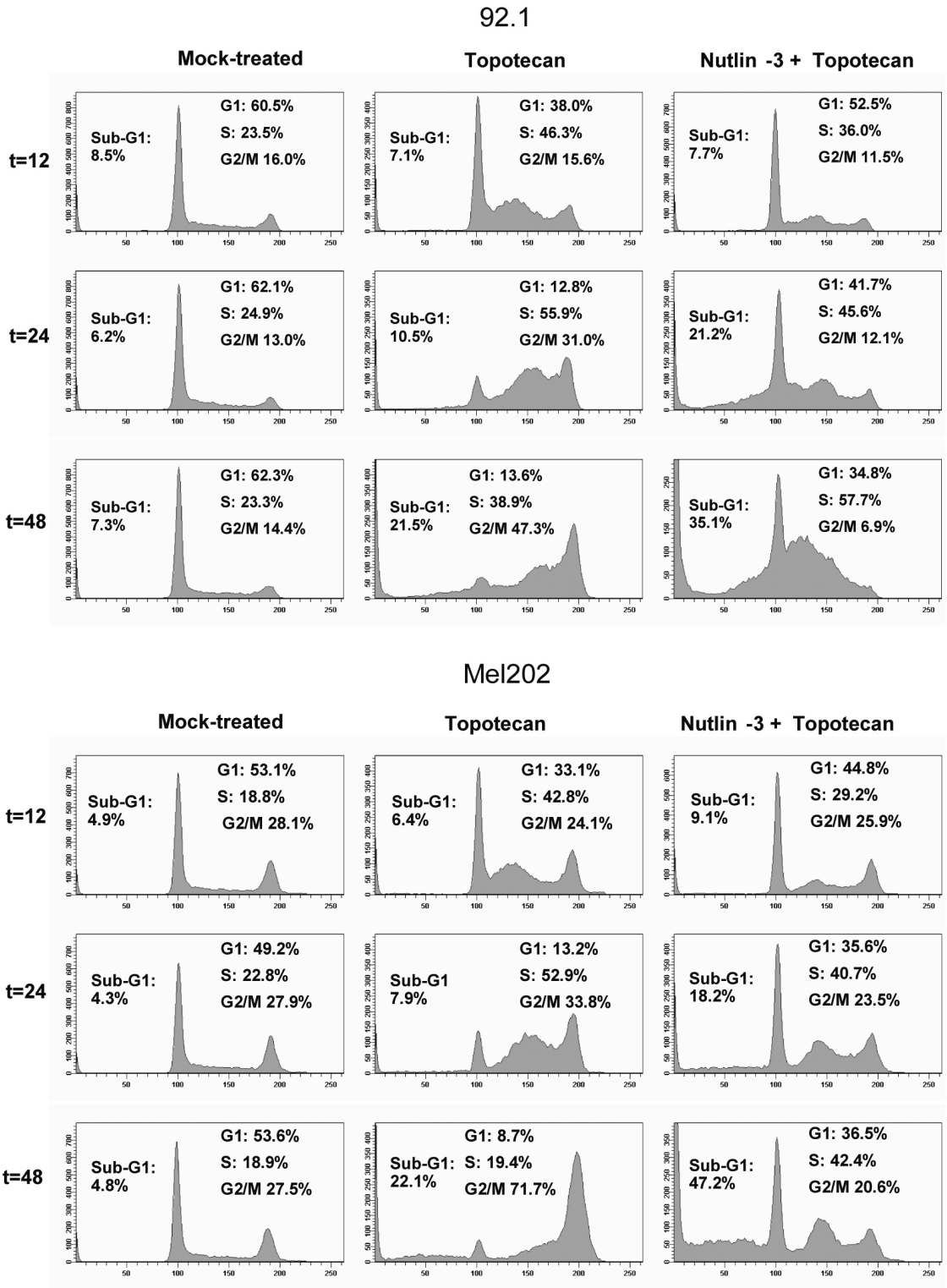

Supplementary Figure 3 Kinetic analysis of the cell cycle in response to Topotecan alone or in combination with Nutlin-3. Flow cytometry analysis of 92.1 and Mel202 cells treated for 12 h, 24 h or 48 h as indicated. Used concentrations in 92.1: 2.0 µM Nutlin-3, 25 nM Topotecan. Used concentrations in Mel202: 3.0 µM Nutlin-3 and 25 nM Topotecan.

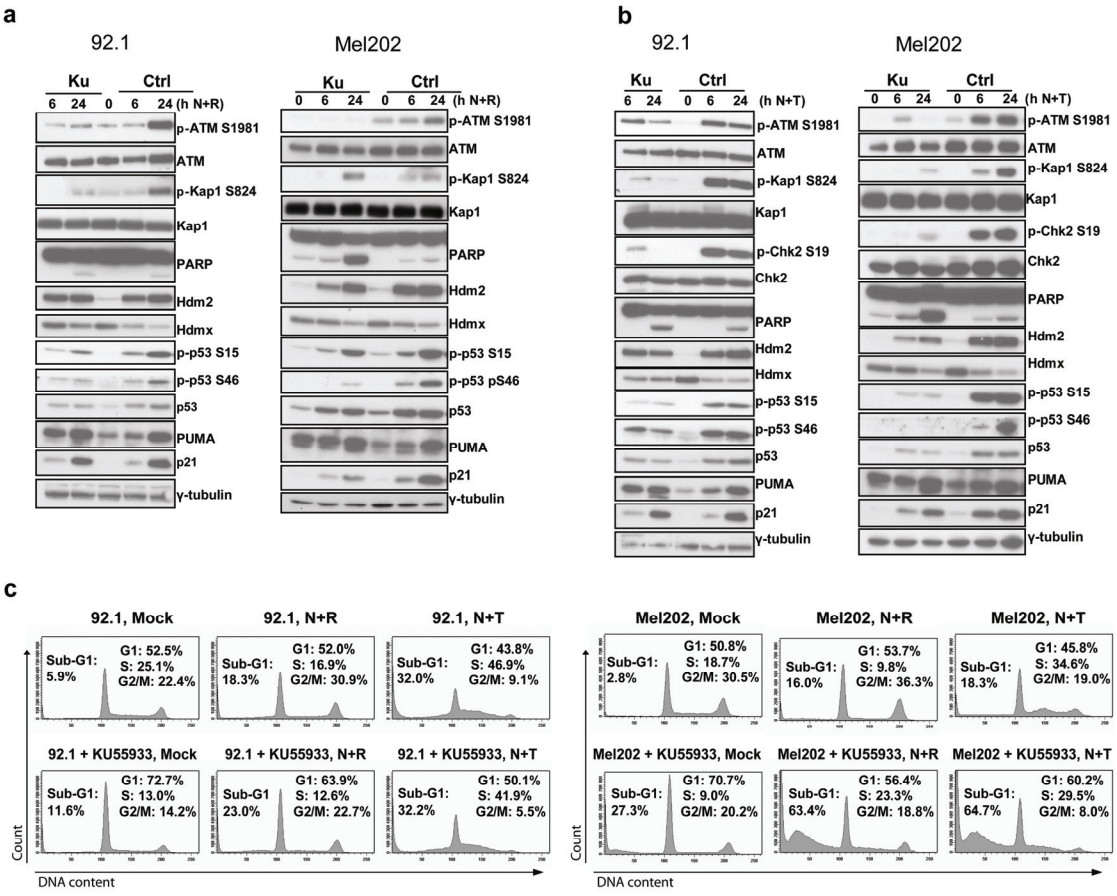

Supplementary Figure 4 ATM inhibition attenuates p53-Ser46 phosphorylation upon combination treatments without rescuing the induction of apoptosis. 92.1 and Mel202 cells were 2 h pre-treated with 10 µM KU55933, treated for 24 h as indicated and analyzed by Western blot (**a**, **b**) and flow cytometry (**c**). Used concentrations in 92.1: 2.0 µM Nutlin-3, 0.7 µM RITA, 25 nM Topotecan. Used concentrations in Mel202: 3.0 µM Nutlin-3, 0.25 µM RITA, 25 nM Topotecan.

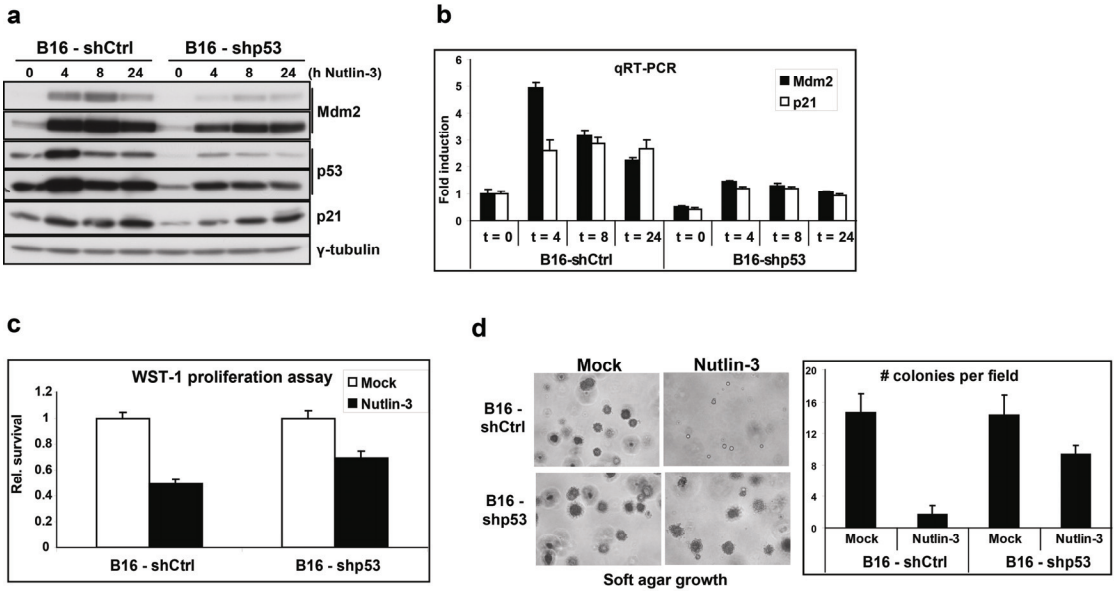

Supplementary Figure 5 Nutlin-3 activates p53 and inhibits cell growth in B16F10 cells. B16F10 cells stably expressing shCtrl or shp53 RNAs were treated with 10 µM Nutlin-3 for the indicated times and analyzed by Western blot (**a**) and qRT-PCR (**b**). (**c**) Cells were counted and seeded for WST-1 proliferation assay and treated with 10 µM Nutlin-3. Cell viability was measured 72 h after treatment. (**d**) B16F10 cells stably expressing shCtrl or shp53 RNAs were counted and seeded in triplicate in soft agar containing 10 µM Nutlin-3. Medium with Nutlin-3 was replaced every 3-4 days. Colony outgrowth was monitored with light microscopy and after 18 days the colonies were counted (one microscope field per well). Representative pictures and a quantification of the results are shown.

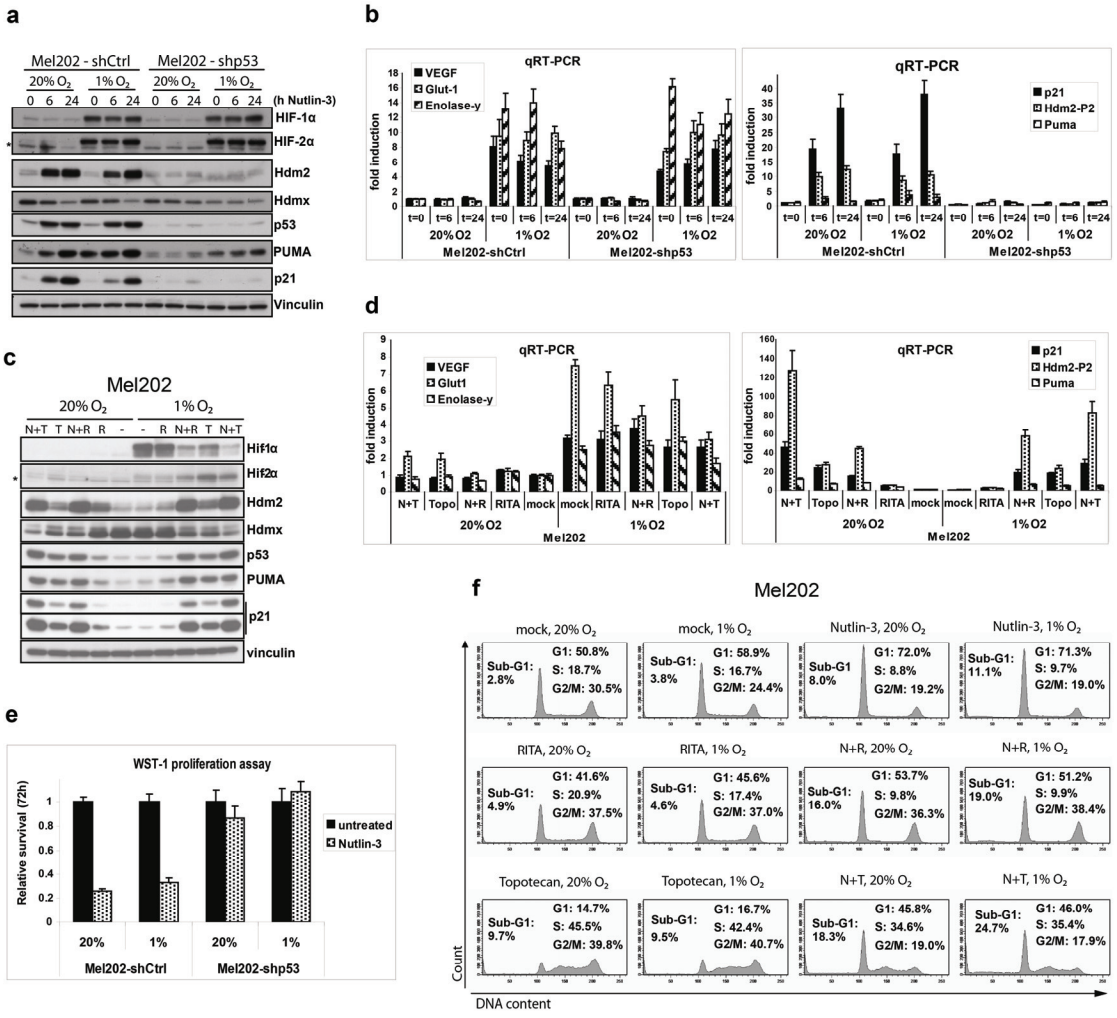

Supplementary Figure 6 Similar p53 activation and growth inhibition in normoxia and hypoxia by Nutlin-3, RITA and Topotecan in Mel202 cells. Mel202 cells stably expressing shCtrl or shp53 RNAs were incubated at 20% or 1% O_2 for 48 h and treated with 10 µM Nutlin-3 during the last 6 or 24 h as indicated, followed by Western blot analysis (**a**) and qRT-PCR (**b**). Single or combination treatments (24 h) in Mel202 cells incubated at 20% or 1% O_2 for 48 h were performed as indicated using 3.0 µM Nutlin-3, 0.25 µM RITA and 25 nM Topotecan, followed by Western blot analysis (**c**) and qRT-PCR (**d**). *Non-specific background staining. (**e**) Mel202 cells stably expressing shCtrl or shp53 RNAs were counted and seeded for WST-1 proliferation. Cells were incubated at 20 or 1% O_2 as indicated, treated with 10 µM Nutlin-3 and cell viability was measured 72 h after treatment. (**f**) The Mel202 cells were incubated at 20% or 1% O_2 for 48 h and treated as indicated during the last 24 h, followed by flow cytometry analysis. Concentrations used: 3.0 µM Nutlin-3, 0.25 µM RITA and 25 nM Topotecan.

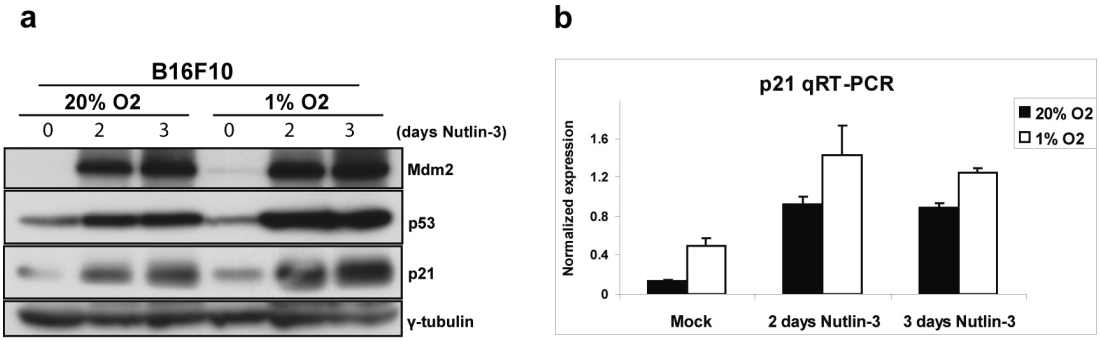

Supplementary Figure 7 Similar Nutlin-3 induced p53 activation under normoxic and hypoxic conditions in B16F10 cells. B16F10 cells were cultured at 1% or 20% O_2 for 72 h and treated with Nutlin-3 for the final 2 or 3 days, followed by Western blot analysis (**a**) and qRT-PCR (**b**).

Supplementary Table 1: List of shRNA sequences

shRNA	Target sequences
human shCtrl	GAATCTTGTTACATCAGCT
human shp53	GACTCCAGTGGTAATCTAC
human shATM #34	CCTTTCATTCAGCCTTTAGAA
human shATM #36	TGATGGTCTTAAGGAACATCT
mouse shCtrl	CGAAATTGGATCACAGCGATA
mouse shp53 #1	CCGACCTATCCTTACCATCAT
mouse shp53 #2	CTACAAGAAGTCACAGCACAT
mouse shp53 #3	CGGGCGTAAACGCTTCGAGAT

Supplementary Table 2: List of antibodies

Protein	Name/ cat. #	Company
Hdmx	A300-287A	Bethyl Laboratories, Montgomery TX, USA
Hdm2 * / Mdm2	4B2	Chen *et al*., 1993
Hdm2 *	SMP14 sc-6965	Santa Cruz Biotechnology, Santa Cruz, CA, USA
p53 °	DO-1 / sc-126	Santa Cruz Biotechnology, Santa Cruz, CA, USA
p53 °	18O1 / sc-98	Santa Cruz Biotechnology, Santa Cruz, CA, USA
mouse p53	1C12 / 2524	Cell signalling Technology, Beverly, MA, USA
p-p53 Ser46	2521	Cell signalling Technology, Beverly, MA, USA
p-p53 Ser15	9284	Cell signalling Technology, Beverly, MA, USA
PUMA N-terminal	P4743	Sigma-Aldrich, St Louis, MO, USA
p21	CP74 / 05-655	Upstate Biotechnology, Lake Placid, NY, USA
mouse p21	F5 / sc-6246	Santa Cruz Biotechnology, Santa Cruz, CA, USA
vinculin	hVIN-1 / V9131	Sigma-Aldrich, St Louis, MO, USA
γ-tubulin	GTU-88 / T6557	Sigma-Aldrich, St Louis, MO, USA
HAUSP USP7	A300-033A	Bethyl Laboratories, Montgomery TX, USA
PARP	9542	Cell signalling Technology, Beverly, MA, USA
cleaved caspase 3 (Asp175)	9661	Cell signalling Technology, Beverly, MA, USA
HIPK2	F-189 / sc-100383	Santa Cruz Biotechnology, Santa Cruz, CA, USA
HIF-1α	610958	BD Biosciences, San Diego, CA, USA
HIF-2α	NB100-122	Novus Biologicals, Littleton, CO, USA
p-ATM S1981	EP1890Y / 2152-1	Epitomics,California, USA
ATM	Y170 / 1549-1	Epitomics,California, USA
p-Kap1 S824	A300-767A	Bethyl Laboratories, Montgomery TX, USA
Kap1	A300-274A	Bethyl Laboratories, Montgomery TX, USA
p-Chk2 S19	2666	Cell signalling Technology, Beverly, MA, USA
Chk2	EPR4325 / 3428-1	Epitomics,California, USA

For detection of human Hdm2 we used a mix of 4B2 and SMP14 (*), for detection of human p53 we used a mix of DO-1 and 1801 (°).

Ref) Chen J *et al.* **Mapping of the p53 and mdm-2 interaction domains**. *Mol Cell Biol* 1993, **13:**4107-4114.

Supplementary Table 3: Primer sequences used for qRT-PCR reactions.

Human gene	Forward primer	Reverse primer
p21	AGCAGAGGAAGACCATGTGGA	AATCTGTCATGCTGGTCTGCC
Hdm2 Exon 2	ACGCACGCCACTTTTTCTCT	TCCGAAGCTGGAATCTGTGAG
PUMA	GACCTCAACGCACAGTA	CTAATTGGGCTCCATCT
VEGF	GCCTTGCCTTGCTGCTCTACC	GTGATGATTCTGCCTCCTCCTTC
Glut1	CCCGCTTCCTGCTCATCAACC	GCCGACTCTCTTCCTTCATCTCC
Enolase-γ	TAGAATGGGAAGGGTCATAGAAAGGG	AGAGGTGGTGGCAACTGTGG
CAPNS1	ATGGTTTTGGCATTGACACATG	GCTTGCCTGTGGTGTCGC
Beta-Actin	CGGGACCTGACTGACTACCTC	CTCCTTAATGTCACGCACGATTTC
ARP	CACCATTGAAATCCTGAGTGATGT	ACCAGCCGAAAGGAGAAG
RPS11	AAGCAGCCGACCATCTTTCA	CGGGAGCTTCTCCTTGCC
Mouse gene	**Forward primer**	**Reverse primer**
p21	CCTGACAGATTTCTATCACTCCA	AGGCAGCGTATATCAGGAG
Mdm2	CGGCCTAAAAATGGTTGCAT	TTTGCACACGTGAAACATGACA
β2-Microglobulin	CGGTCGCTTCAGTCGTCAG	GCAGTTCAGTATGTTCGGCTTCC

Chapter 5

Chk2 mediates RITA-induced apoptosis

J. de Lange, M. Verlaan-de Vries, A.F.A.S. Teunisse, A.G. Jochemsen

Department of Molecular Cell Biology, Leiden University Medical Center, 2300 RC Leiden, The Netherlands

Cell Death and Differentiation 2012, *in press*

Abstract

Reactivation of the p53 tumor suppressor protein by small-molecules like Nutlin-3 and RITA (reactivation of p53 and induction of tumor cell apoptosis) is a promising strategy for cancer therapy. The molecular mechanisms involved in the responses to RITA remain enigmatic. Several groups reported the induction of a p53-dependent DNA damage response. Furthermore, the existence of a p53-dependent S-phase checkpoint has been suggested, involving the checkpoint kinase Chk1. We have recently shown synergistic induction of apoptosis by RITA in combination with Nutlin-3, and we observed concomitant Chk2 phosphorylation. Therefore, we investigated whether Chk2 contributes to the cellular responses to RITA. Strikingly, the induction of apoptosis seemed entirely Chk2-dependent. Transcriptional activity of p53 in response to RITA required the presence of Chk2. A partial rescue of apoptosis observed in Noxa knockdown cells emphasized the relevance of p53 transcriptional activity for RITA-induced apoptosis. In addition, we observed an early p53- and Chk2-dependent block of DNA replication upon RITA treatment. Replicating cells seemed more prone to entering RITA-induced apoptosis. Furthermore, the RITA-induced DNA damage response, which was not a secondary effect of apoptosis induction, was strongly attenuated in cells lacking p53 or Chk2. In conclusion, we identified Chk2 as an essential mediator of the cellular responses to RITA.

Introduction

The human transcription factor p53 provides an essential roadblock against cancer. The *TP53* gene is mutated in ~ 50% of all human cancers; the remaining tumors are assumed to have attenuated wild-type p53 activity (1). Reactivation of p53 in tumors with intact, but functionally impaired, p53 using non-genotoxic drugs is a promising anti-cancer strategy. Such strategies generally rely on inhibiting the interaction of p53 with its main negative regulators, human double minute 2 (Hdm2) and human double minute x (Hdmx). In addition, RITA (reactivation of p53 and induction of tumor cell apoptosis) was identified to directly bind and activate human p53 and to suppress *in vivo* growth of transformed cells in a p53-dependent manner (2).

Understanding factors that determine the outcome of p53 activation is the aim of many investigators, as specifically directing the cellular response towards apoptosis is crucial for successful cancer treatment. Interestingly, distinct p53-activating drugs have strongly divergent effects. For example, Nutlin-3 (3) and MI-219 (4) mainly induce G1 and G2-arrest, resulting in depletion of S-phase cells, whereas the induction of apoptosis by these compounds varies greatly between cell lines. On the other hand, RITA does not induce G1-arrest, but in general is more capable of inducing apoptosis (5). The mechanistic properties of RITA seem complex. RITA was proposed to induce a conformational change in p53 that prevents its binding to Hdm2 (2). NMR studies did not support this mechanism (6), but a later study suggested a role for the released pool of Hdm2 to promote degradation of p21 and the p53 cofactor hnRNP K (5). Furthermore, induction of pro-apoptotic homeodomain-interacting protein kinase-2 levels (7), inhibition of pro-survival TrxR1 activity (8) and reduced expression of Wip1 phosphatase and Hdmx (9) have been described as contributing to the RITA effects. RITA has also been implicated in inhibition of angiogenesis-promoting HIF-1α protein synthesis by increasing the phosphorylation of eIF2α (10). Importantly, several groups recently reported the induction of a DNA damage response by RITA (9-12)

The canonical DNA damage response network is traditionally divided into two major pathways, involving the sensor kinases ataxia telangiectasia mutated (ATM) and ataxia telangiectasia and Rad3-related (ATR) that activate their respective effector kinases, Chk2 and Chk1. ATR phosphorylates Chk1 on Ser317 and Ser345 (13, 14). The best characterized activating phosphorylation site of Chk2 is Thr68 (15), but phosphorylation of residues Ser19, Ser33 and Ser35 has been described to contribute to Chk2 activation (16). The p53 pathway is strongly affected at multiple levels by DNA damage signaling. ATM, ATR, Chk1

and Chk2 were all reported to directly mediate N-terminal phosphorylation on p53. In addition, both Hdm2 and Hdmx are downstream targets of the DNA damage response, including phosphorylation by ATM, ATR, Chk2 and Chk1 (Meek DW (17) and references therein).

The intensive interactions described above predict a great impact of DNA damage signaling on the biochemical and biological effects of small-molecule p53 activators. Indeed, when combined with genotoxic drugs like doxorubicin or topotecan, Nutlin-3 synergistically induced apoptosis in certain experimental settings (12, 18-20). We along with others showed synergistic tumor cell killing when Nutlin-3 and RITA are combined (12, 21), suggesting the induction of distinct pathways, as enhanced activation of the same pathway would expected to be additive at the best. Recently, RITA was proposed to induce p53-dependent replication stalling, with a role for Chk1 in maintaining DNA integrity, but not in the induction of apoptosis (11). In this study, we focused on the role of Chk2 in the RITA response and found that Chk2 is essential for the induction of replication arrest and apoptosis by RITA.

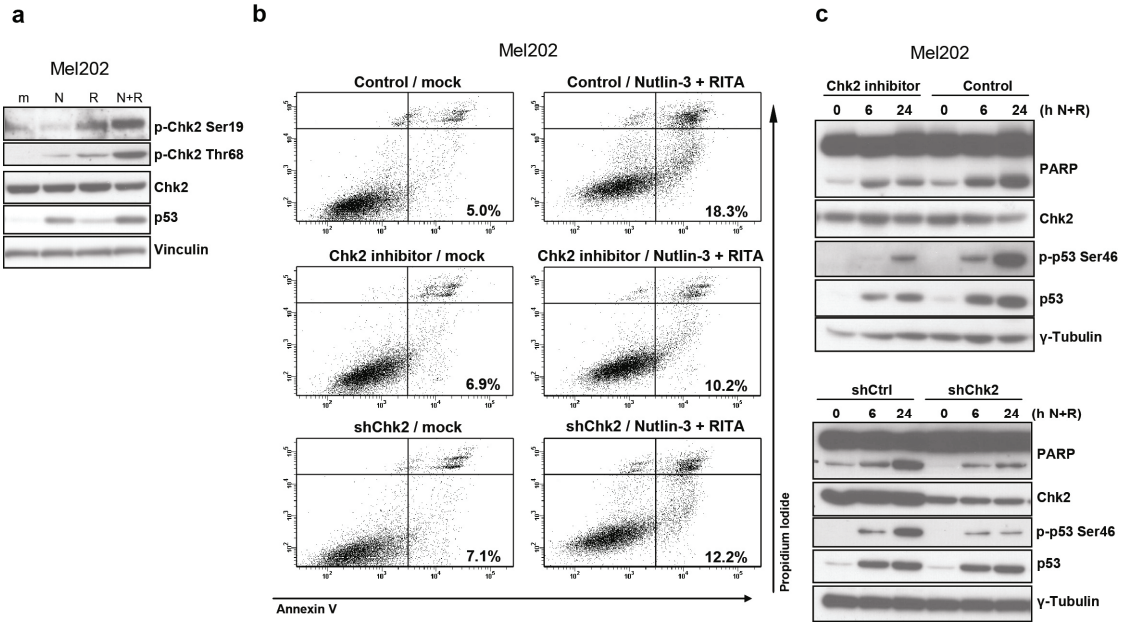

Figure 1 Chk2 inhibition attenuates apoptosis induction by RITA in Mel202 cells. (**a**) Mel202 cells were treated as indicated for 24 h and protein extracts were analyzed by western blotting using the indicated antibodies. (**b**) Mel202 cells were stably transduced with shCtrl or shChk2 constructs. Control cells were pre-treated for 2 h with the 10 μM Chk2 inhibitor II where indicated. Subsequently, cells were mock-treated or treated with a combination of Nutlin-3 and RITA. Apoptosis was assessed after 48 h by Annexin V staining. (**c**) Protein extracts from the same cells as in panel **b** were isolated after 24 h and analyzed by western blot using the indicated antibodies

Results

We recently reported that Nutlin-3 and RITA synergistically induce apoptosis in uveal melanoma cells, correlating with induction of ATM signaling and enhanced p53-Ser46 phosphorylation (12). An important downstream target of ATM is the checkpoint kinase Chk2. Indeed, Chk2 was phosphorylated on Thr68 and Ser19 upon RITA treatment in the uveal melanoma cell line Mel202 (Figure 1a). Therefore, we investigated whether Chk2 contributes to the RITA response, using a specific inhibitor of Chk2 kinase activity, and by short-hairpin RNA (shRNA)-mediated Chk2 knockdown. Interestingly, both approaches markedly reduced apoptosis induction by Nutlin-3 plus RITA in Mel202 cells, shown by Annexin V staining (Figure 1b) and poly [ADP-ribose] polymerase (PARP) cleavage (Figure 1c). Reduced apoptosis correlated with reduced p53-Ser46 phosphorylation. Similar results were obtained in 92.1, another uveal melanoma cell line (data not shown).

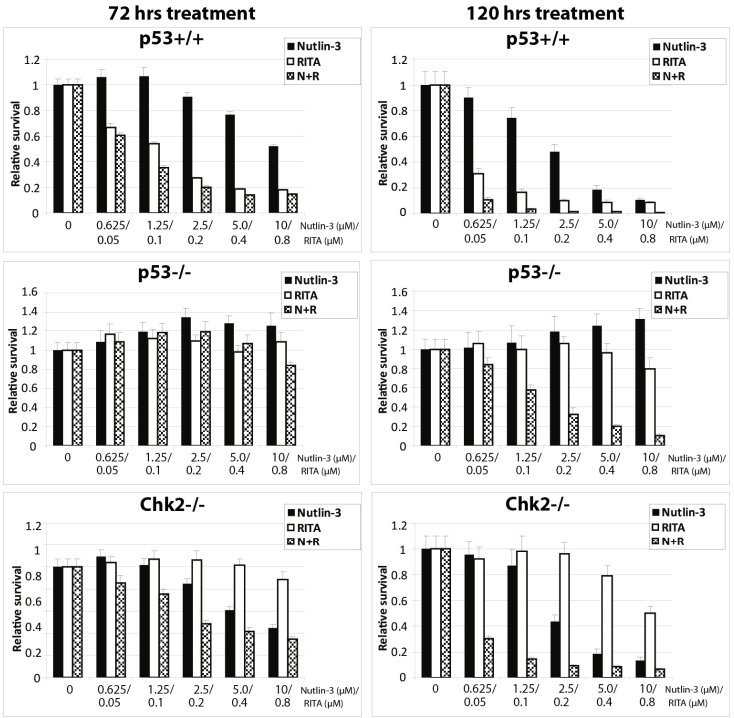

Drug concentrations		Combination Index	
Nutlin-3 (μM)	RITA (μM)	72h	120h
0.625	0.05	0.885	0.234
1.25	0.1	0.569	0.109
2.5	0.2	0.496	0.093
50	0.4	0.644	0.160
10	0.8	1.308	0.224

Figure 2 HCT116 $p53^{-/-}$ and HCT116 $Chk2^{-/-}$ cells show reduced sensitivity to RITA-induced growth inhibition. HCT116 $p53^{+/+}$, $p53^{-/-}$ and $Chk2^{-/-}$ cells were continuously treated for 72 h or 120 h as indicated with different concentrations of Nutlin-3 and RITA, alone or in constant ratio combinations. Cell viability was measured using the WST-1 proliferation assay. The effects of drug treatment as fraction of mock-treated control cells were calculated. The combination index (CI), reflecting the extent of synergy or antagonism for two drugs, was derived for HCT116 $p53^{+/+}$ cells after 72 h and 120 h treatments for each concentration of drug combination using Compusyn software (38). CI<0.9, synergy; 0.9<CI<1.1, additive effect; CI>1.1, antagonism

To further study the role of Chk2 in the responses to Nutlin-3 and RITA, we used the isogenic $p53^{+/+}$, $p53^{-/-}$ and $Chk2^{-/-}$ HCT116 colon carcinoma cell lines. We confirmed synergy between Nutlin-3 and RITA in wild-type HCT116 cells (Figure 2). Calculated combination index (CI) values indicated synergy at most concentrations. Notably, CI calculations as defined by Chou (22) require experimentally derived values describing the dose-response curves for each single drug, which is not possible if the drug has no detectable effect at all. As expected, $p53^{-/-}$ cells were largely insensitive to both treatments. Interestingly, whereas the sensitivity of $Chk2^{-/-}$ cells to Nutlin-3 was comparable to $p53^{+/+}$ cells, they were hardly affected by RITA. Only after 5 days of continuous RITA treatment, we could observe a clear effect in $Chk2^{-/-}$ cells at the highest concentrations. Remarkably, at this time point also the $p53^{-/-}$ cells were growth inhibited by the combination treatment, indicating activation of p53-independent pathways.

To obtain more insight into the effects of RITA and Nutlin-3 alone and in combination, we investigated the effects on cell cycle profiles (Figure 3a). In wild-type HCT116 cells, Nutlin-3 treatment induced both a G1 and a G2 arrest, whereas RITA treatment resulted in decreased G1 and increased S and G2/M fractions. RITA also prevented the S-phase depletion by Nutlin-3, suggesting an S-phase arrest by RITA. In $p53^{-/-}$ cells, Nutlin-3 alone had no effect, but RITA clearly decreased G1 and increased G2/M fractions. Combining Nutlin-3 and RITA dramatically elevated the G2/M fraction, which can explain the growth inhibition observed in the WST-1 assay (Figure 2). These findings indicate that Nutlin-3 and RITA exert some p53-independent effects, although the effect of Nutlin-3 is only revealed in the presence of RITA. In $Chk2^{-/-}$ cells, Nutlin-3 depleted the S phase and increased G1, but not G2/M, suggesting that Nutlin-3 induced G2-arrest is Chk2 dependent. In contrast to Nutlin-3, RITA decreased G1 and increased G2/M fractions, similar as observed in $p53^{-/-}$ cells. The combined treatment depleted S phase and arrested $Chk2^{-/-}$ cells in both G1 and G2. Notably, RITA alone hardly changed the percentage of cells in the S phase in $p53^{-/-}$ and $Chk2^{-/-}$ cells, whereas the G2/M increase was transient (data not shown). In conclusion, the cell-cycle profiles suggest that Nutlin-3 induces a p53-dependent G1 arrest and a p53- and Chk2-dependent G2 arrest. However, RITA induces a p53- and Chk2-dependent S arrest and a p53- and Chk2-independent G2 arrest, but no G1 arrest.

We also examined apoptosis induction using sub-G1 evaluation (Figure 3b) and Annexin V staining (Figure 3c). Nutlin-3 induced a mild, p53-dependent apoptotic response in HCT116. Importantly, RITA strongly induced apoptosis in a p53- and Chk2-dependent manner. Combination treatments, as compared with single RITA treatments, slightly increased apoptosis in all cell lines.

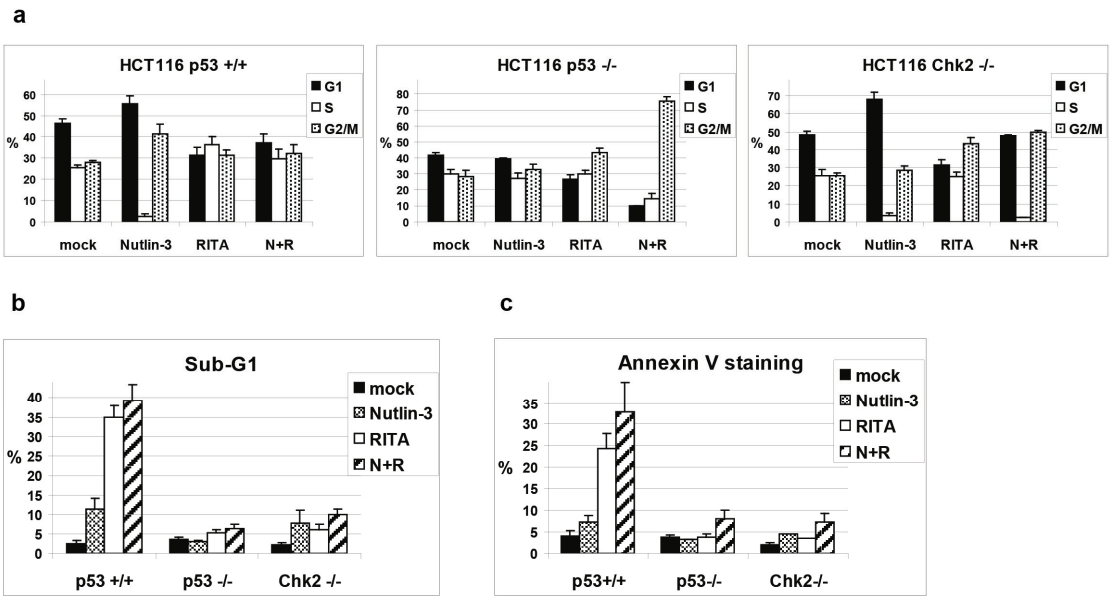

Figure 3 p53- and Chk2-dependent and -independent effects of Nutlin-3 and RITA on cell cycle profiles and apoptosis. (**a** and **b**) HCT116 $p53^{+/+}$, $p53^{-/-}$ and $Chk2^{-/-}$ cells were treated as indicated for 24 h, harvested and analyzed by flow cytometry. Bars represent means and s.e. of three independent experiments. (**c**) Cells were treated as indicated for 48 h, harvested and analyzed by Annexin V staining. Bars represent means and s.e. of three independent experiments

To obtain more insight into the pathways by which RITA affects cell-cycle progression and apoptosis, we analyzed the levels and phosphorylation status of a number of proteins (Figure 4a). Supporting the observed effects on apoptosis, RITA induced PARP cleavage in $p53^{+/+}$ cells, but not in $p53^{-/-}$ and $Chk2^{-/-}$ cells. As reported before (9-12), RITA also induced a DNA damage response, evidenced by phosphorylation of ATM-Ser1981, KRAB-interacting protein 1 (KAP1)-Ser824, Chk2-Thr68, p53-Ser15 and p53-Ser46, as well as by downregulation of Hdmx. Interestingly, these effects were strongly attenuated in $p53^{-/-}$ and $Chk2^{-/-}$ cells. In addition, Chk1-Ser345 phosphorylation, recently implicated in RITA response (11), and Hdm2 downregulation were all p53 and Chk2 dependent (Figure 4b). It is important to note that not only stress-induced p53 phosphorylation is strongly reduced in $Chk2^{-/-}$ cells, but also p53 stabilization (Figure 4b). We further analyzed the DNA damage response in HCT116 $p53^{+/+}$ cells in a RITA time course, in comparison with the known DNA-damaging agent etoposide (Figure 4c). RITA-induced phosphorylations clearly occurred with slower kinetics. Notably, phosphorylation of ATM, KAP1 and Chk2 induced by etoposide was comparable in $p53^{+/+}$, $p53^{-/-}$ and $Chk2^{-/-}$ cells (Supplementary Figure 1 and not shown), suggesting that the mechanisms by which RITA and etoposide elicit DNA damage response are distinct.

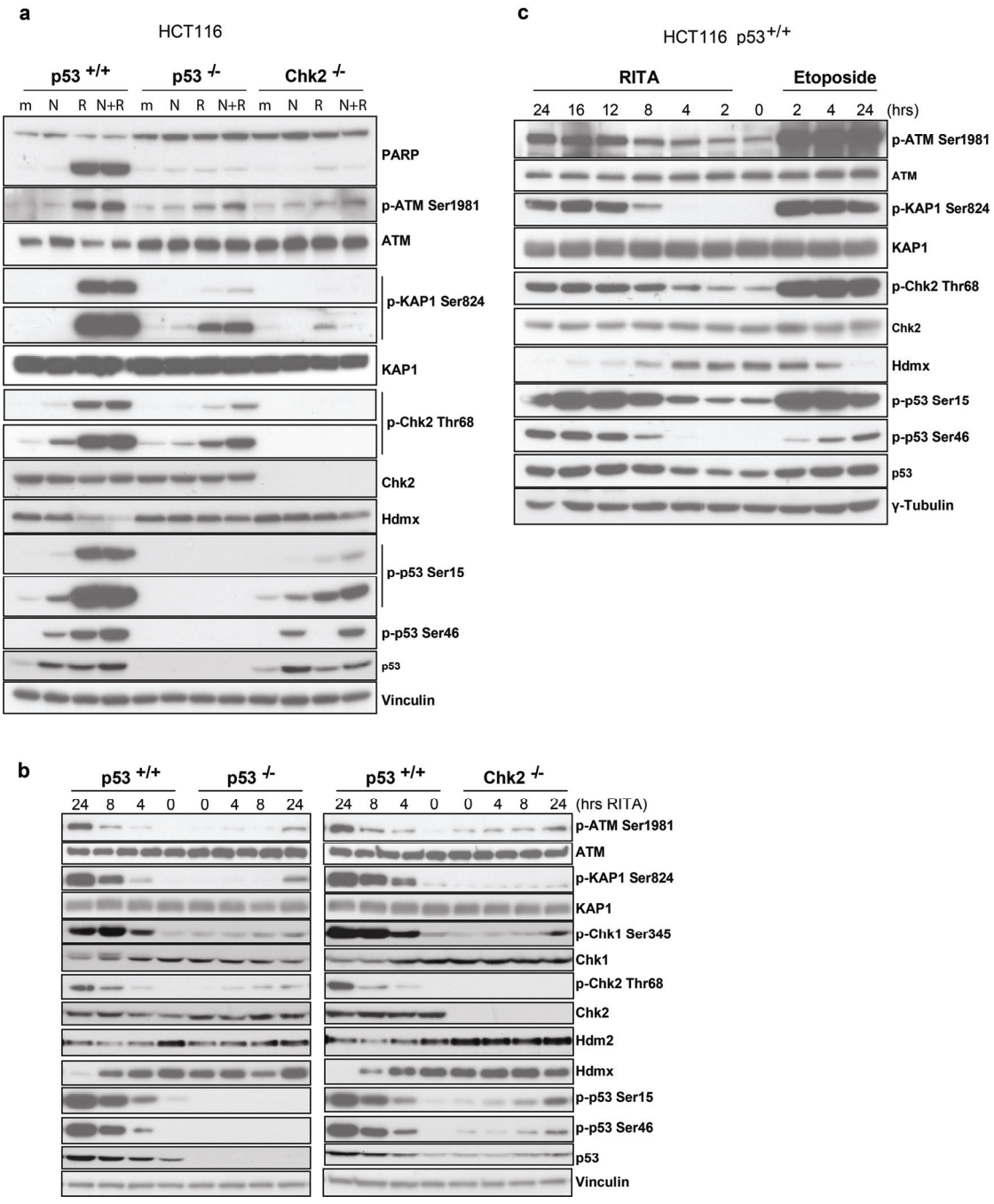

Figure 4 Activation of DNA damage response by RITA is p53- and Chk2-dependent and occurs with slower kinetics compared to etoposide. (**a**) HCT116 $p53^{+/+}$, $p53^{-/-}$ and $Chk2^{-/-}$ cells were treated as indicated for 24 h, and protein extracts were analyzed by western blot using the indicated antibodies. (**b**) HCT116 $p53^{+/+}$, $p53^{-/-}$ and $Chk2^{-/-}$ cells were treated as indicated, and protein extracts were analyzed by western blot using the indicated antibodies. (**c**) HCT116 $p53^{+/+}$ cells were treated with 1 μM RITA or 10 μM etoposide for the indicated periods, and protein extracts were analyzed by western blot using the indicated antibodies.

As the observed DNA damage response might be a secondary result of apoptosis-associated DNA fragmentation, we treated HCT116 cells with RITA in the presence of the pan-caspase inhibitor Z-VAD-FMK. Annexin V staining (Supplementary Figure 2a) and PARP cleavage (Supplementary Figure 2b) showed that Z-VAD-FMK efficiently blocked apoptosis induction by RITA and Nutlin-3 plus RITA. However, the inductions of ATM, KAP1, Chk2 and p53 phosphorylation, as well as Hdmx downregulation, were not influenced by Z-VAD-FMK. Furthermore, the RITA time course showed that PARP cleavage only became apparent after induction of the DNA damage response (compare Supplementary Figure 2c and Figure 4c).

Recently, it has been demonstrated that RITA blocks DNA replication in a p53-dependent manner (11). To test whether this effect depends on Chk2 expression, we analyzed 5-ethynyl-2'-deoxyuridine (EdU) incorporation in HCT116 $p53^{+/+}$, $p53^{-/-}$ and $Chk2^{-/-}$ cells in a RITA time course (Figure 5a). In $p53^{+/+}$ cells, 4-h RITA treatment already effectively blocked

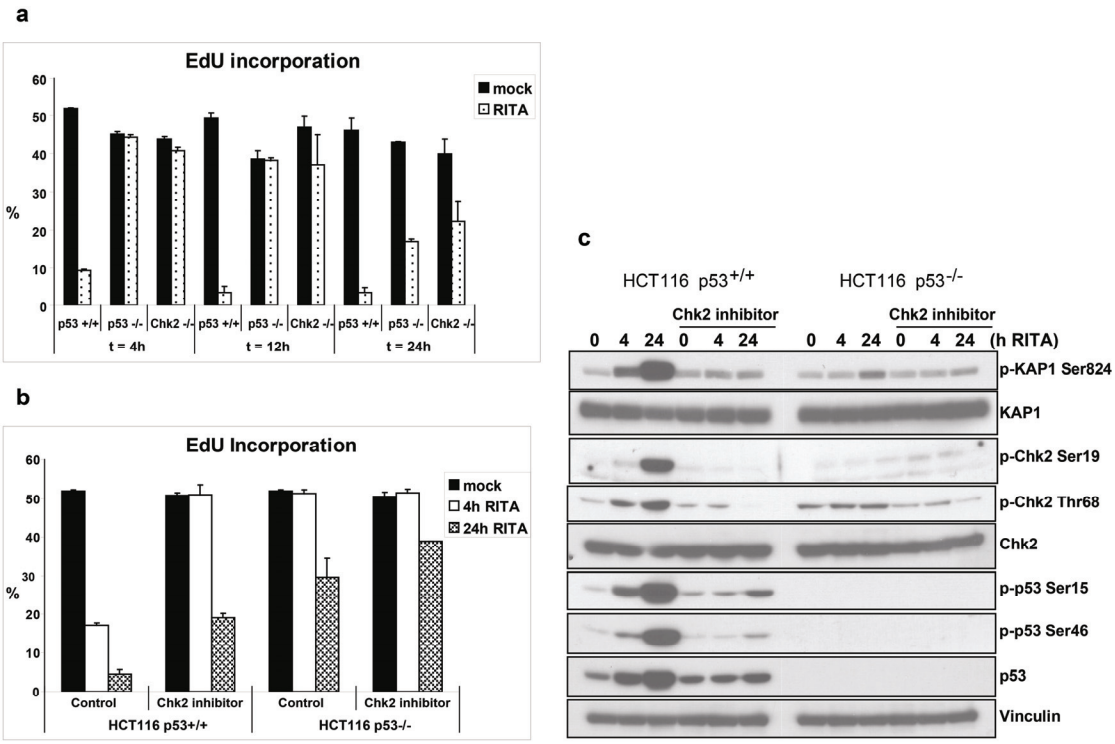

Figure 5 The rapid replication block in response to RITA treatment is p53- and Chk2 dependent. (**a**) HCT116 $p53^{+/+}$, $p53^{-/-}$ and $Chk2^{-/-}$ cells were treated with RITA for the indicated periods. Subsequently, 2.0 μM 5-ethynyl-2'-deoxyuridine (EdU) was added for 1 h to allow incorporation into newly synthesized DNA. Cells were harvested and percentages EdU positive cells were determined using flow cytometry. Bars represent means and s.e. of two independent experiments. (**b**) HCT116 $p53^{+/+}$ and $p53^{-/-}$ cells were pre-treated for 2 h with 10 μM Chk2 inhibitor II where indicated, and subsequently mock-treated or treated with RITA for 4 or 24 h. EdU incorporation was analyzed as described in panel **a**. (**c**) Protein extracts of cells treated as mentioned in panel **b** were analyzed by western blot using the indicated antibodies.

replication. The effects in $p53^{-/-}$ and $Chk2^{-/-}$ cells were much weaker; only after 24-h RITA treatment, a significant reduction in EdU-positive cells could be observed. A closer examination of the EdU profile at the 12-h time point (Supplementary Figure 3a) revealed that in $p53^{-/-}$ and $Chk2^{-/-}$ cells, RITA shifted the EdU-positive peak somewhat to the left, suggesting a slower DNA replication in these cells. To investigate whether Chk2 inhibition would modulate the effect of RITA on S-phase progression even in $p53^{-/-}$ cells, we chemically inhibited Chk2 kinase activity in HCT116 $p53^{+/+}$ and $p53^{-/-}$ cells and analyzed EdU incorporation (Figure 5b and Supplementary Figure 3b). In $p53^{+/+}$ cells, Chk2 inhibition prevented the replication block at 4 h, resembling the observations in $Chk2^{-/-}$ cells. In addition, the Chk2 inhibitor prevented phosphorylation of KAP1, Chk2 and p53, as well as p53 accumulation (Figure 5c). In $p53^{-/-}$ cells, Chk2 inhibition still partially rescued the effects of RITA on replication at later time points.

We hypothesized that RITA-induced apoptosis could be a secondary event of the replication block. If so, this could implicate that non-replicating cells are less prone to enter RITA-induced apoptosis. Therefore, we reduced the number of replicating cells by serum starvation (Figure 6a). Indeed, replicating cells seemed more sensitive to RITA treatment, as indicated by reduced Annexin V staining (Figure 6b, P=0.00284) and sub-G1 fraction (Figure 6c) in serum-deprived cells. Interestingly, reduced apoptosis did not coincide with lower induction of DNA damage response by RITA, with the exception of p53-Ser46 phosphorylation (Figure 6d). Notably, we found no protection from RITA by pre-treatment with Nutlin-3 in HCT116 cells (Supplementary Figure 4). In fact, in our hands, apoptosis induction by RITA was significantly enhanced by pre-treatment with Nutlin-3. This suggests that synergy between Nutlin-3 and RITA in apoptosis induction does not depend on DNA replication.

RITA promotes p53 transcriptional activity, including towards pro-apoptotic targets (5, 21). We analyzed the levels of several p53 target genes in response to RITA in different HCT116 cells (Figure 7a). RITA induced messenger RNA (mRNA) levels of p21 and Noxa and reduced MCL1 in HCT116 $p53^{+/+}$ cells. These alterations were not observed in $p53^{-/-}$ and $Chk2^{-/-}$ cells, indicating that the activation of p53-dependent transcription by RITA requires Chk2. Nutlin-3 induced transcription of p21, p53-upregulated modulator of apoptosis (PUMA) and Bax in $Chk2^{-/-}$ cells, indicating that these cells are still responsive to p53 activation (Supplementary Figure 5). It must be noted that we found only very low PUMA induction and no increase of Bax upon RITA treatment in HCT116 cells (Figure 7a), in line with our observation that HCT116 $PUMA^{-/-}$ and HCT116 $Bax^{-/-}$ cells were equally sensitive to RITA as were wild-type HCT116 cells (data not shown). To address the relevance of Noxa induction for RITA-induced apoptosis, we applied shRNA-mediated knockdown of Noxa expression. Noxa mRNA levels were efficiently

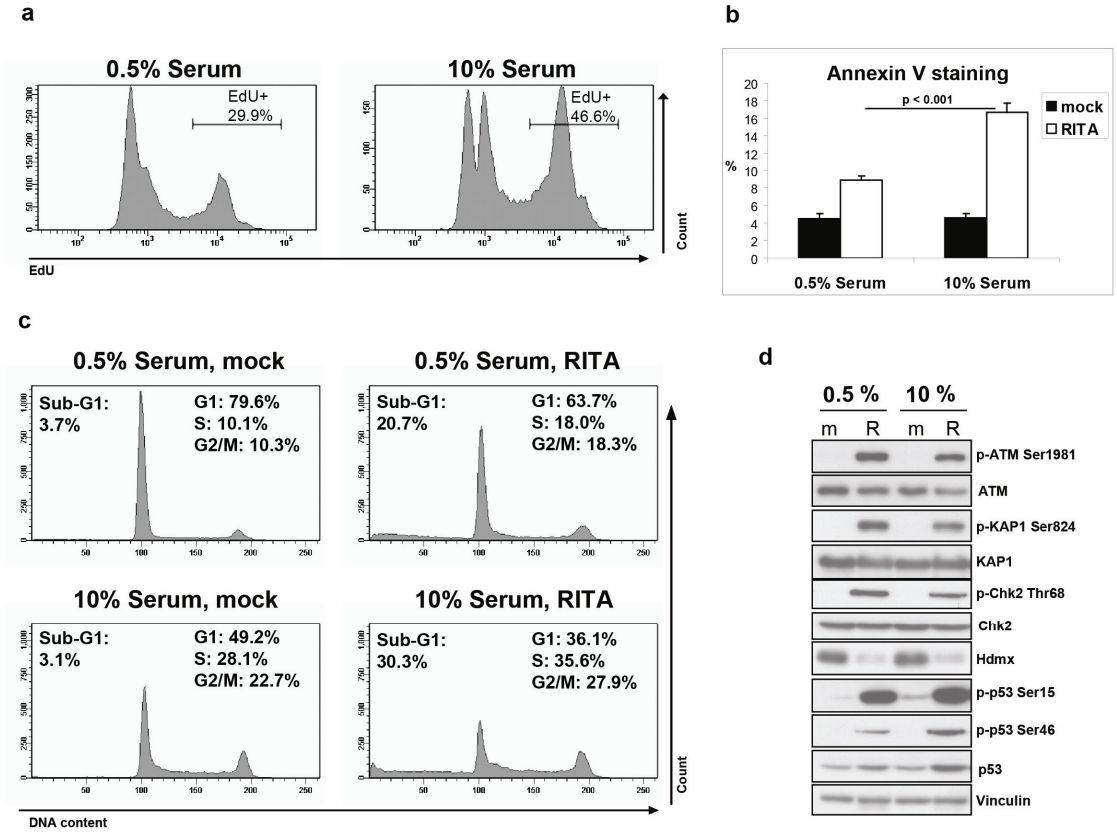

Figure 6 Serum-deprived cells show reduced RITA sensitivity. (**a**) HCT116 $p53^{+/+}$ cells were cultured in 0.5% serum for 48 h and DNA replication was analyzed using EdU incorporation. (**b-d**) Cells treated as mentioned in panel **a** were subsequently incubated with RITA for 24 h while maintaining initial serum conditions. (**b**) Apoptosis induction was assessed by Annexin V staining; bars represent means and s.e. of three independent experiments. Statistical analysis was performed using a two-tailed *t* test. (**c**) Cells were analyzed by flow cytometry. (**d**) Protein extracts were analyzed by western blot using the indicated antibodies.

reduced (Figure 7b), and RITA-induced apoptosis was significantly lower (P=0.0046, Figure 7c). These results suggest that the partial rescue of RITA-induced apoptosis by simultaneous knockdown of PUMA and Noxa (5) can be mainly attributed to the loss of Noxa-mediated effects.

We next investigated a causal link between RITA-induced DNA damage response and apoptosis by using two kinase inhibitors: KU-55933, which specifically inhibits ATM, and caffeine, which inhibits ATM, ATR and DNA-PK. Both diminished most of the RITA- and Nutlin-3 plus RITA-induced phosphorylation of ATM, KAP1, Chk2 and p53, as well as Hdmx downregulation (Supplementary Figure 6a). Interestingly, whereas KU-55933 efficiently blocked RITA-induced phosphorylation of ATM, Chk2 and KAP1, caffeine more efficiently inhibited p53-Ser46 phosphorylation. However, neither drug could rescue RITA-induced

cell death, as exemplified by PARP cleavage (Supplementary Figure 6a) and sub-G1 evaluation (Supplementary Figure 6b). In fact, both KU-55933 and caffeine enhanced induction of apoptosis. Treatment with either KU-55933 or caffeine did not affect RITA-induced mRNA levels of p21 and Noxa (data not shown).

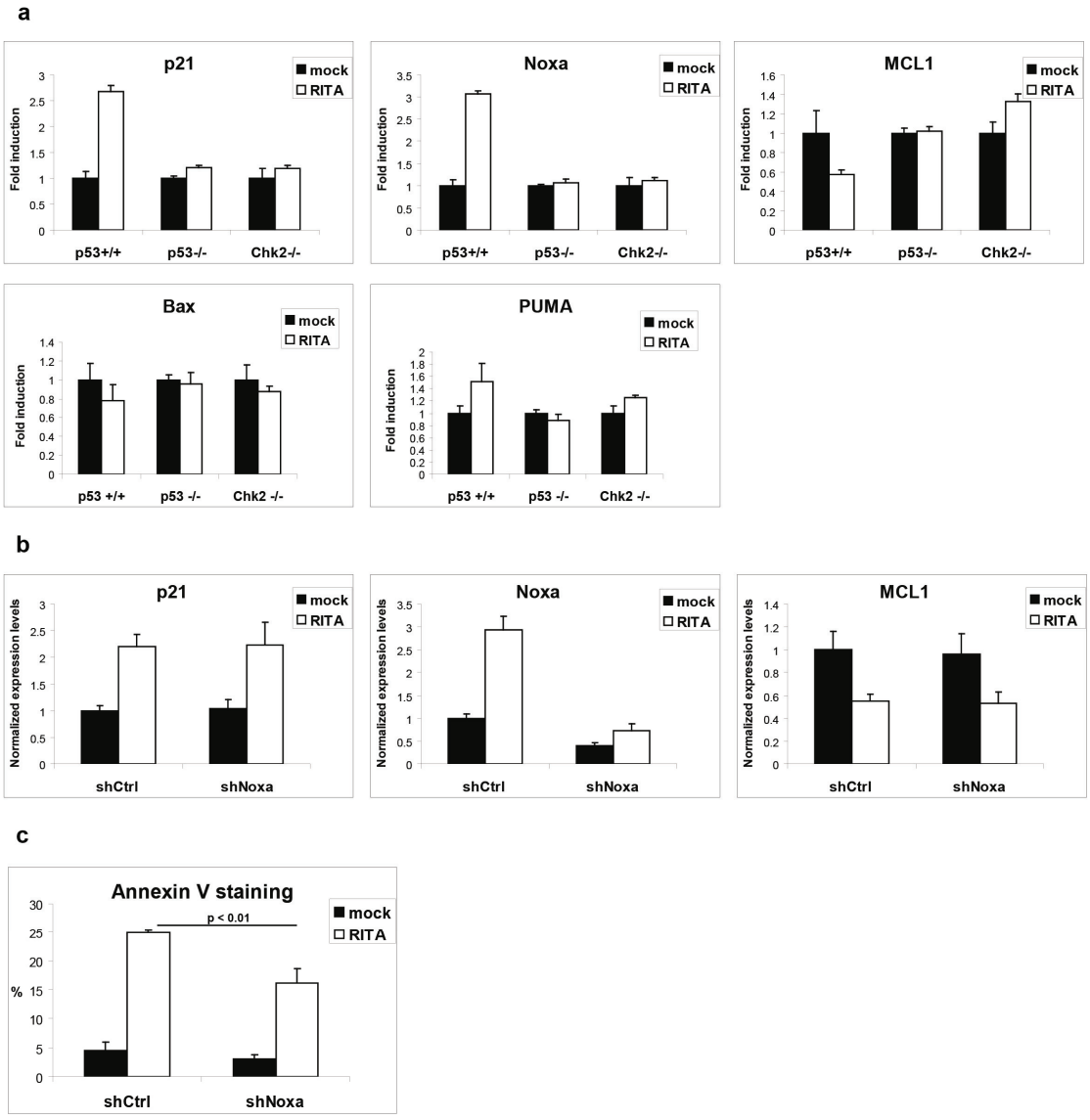

Figure 7 p53-dependent Noxa upregulation by RITA requires Chk2 and contributes to apoptosis induction. (**a**) HCT116 $p53^{+/+}$, $p53^{-/-}$ and $Chk2^{-/-}$ cells were treated with RITA for 6 h, and analyzed by qRT-PCR for p21, Noxa, MCL1, Bax and PUMA mRNA expression levels. (**b**) HCT116 cells stably expressing shCtrl or shNoxa constructs were treated with RITA for 6 h and analyzed by qRT-PCR. (**c**) HCT116 cells stably expressing shCtrl or shNoxa constructs were treated with RITA for 48 h and apoptosis was assessed using Annexin V staining. Bars represent means and s.e. of three independent experiments. Statistical analysis was performed using a two-tailed *t* test.

Recently, Wip1 downregulation was shown to contribute to RITA-induced apoptosis, at least partly through destabilization of Hdmx (9). We analyzed Wip1 mRNA expression in HCT116 cells (Figure 8a) and found that its reduction by RITA was both p53 and Chk2 dependent, correlating with Hdmx protein levels (Figure 4a). We further examined the role of Wip1 in RITA response using stable Wip1 knockdown in MCF7 cells and doxycycline-inducible Wip1 overexpression in U2OS cells. In MCF7 (Figure 8b), Wip1 knockdown indeed enhanced RITA--induced PARP cleavage, KAP1-Ser824 phosphorylation and Hdmx downregulation. *Vice versa*, Wip1 overexpression in U2OS indeed diminished RITA-induced PARP cleavage and phosphorylation of ATM, KAP1 and Chk2 (Figure 8c). Together, these results indicate that Chk2 contributes to the reduction of Wip1 levels after RITA treatment, and that Wip1 contributes to the modulation of the RITA response, as reported previously (9).

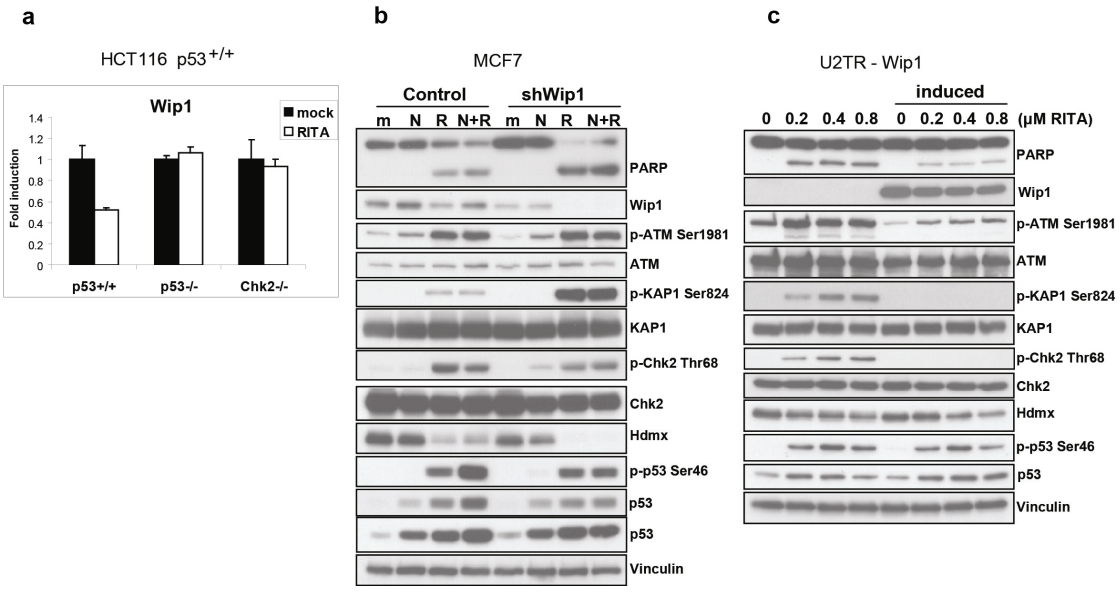

Figure 8 Chk2 contributes to the reduction of Wip1 levels after RITA treatment. (**a**) HCT116 $p53^{+/+}$, $p53^{-/-}$ and $Chk2^{-/-}$ cells were treated with RITA for 6 h, and RNA extracts were analyzed by qRT-PCR for Wip1 expression levels. (**b**) MCF7 cells stably transduced with an empty pRS vector or pRS-shWip1 were treated as indicated for 24 h, and protein extracts were analyzed by western blot using the indicated antibodies. (**c**) U2TR-Wip1 cells were pre-treated with 1 μg/ml doxycycline for 2 h to induce Wip1 expression, and subsequently treated for 6 h with the indicated doses RITA. Protein extracts were analyzed by western blot using the indicated antibodies.

Discussion

Several compounds have been developed for p53 reactivation in tumor cells to synergize with or even substitute conventional cancer therapies, including the small molecules Nutlin-3 (3) and RITA (2). They bind Hdm2 and p53, respectively, and interfere with the p53-Hdm2 interaction. However, the molecular changes that may be relevant for the cellular response, particularly those induced by RITA, stretch well beyond p53 stabilization. This is illustrated by the effects of RITA on the cell-cycle profile in HCT116 $p53^{-/-}$ cells, which was strongly enhanced by combination with Nutlin-3. However, the majority of RITA effects occur through p53, although the underlying mechanisms have not yet been completely elucidated.

Surprisingly, here we show that HCT116 $Chk2^{-/-}$ cells largely mimicked $p53^{-/-}$ cells in their RITA response: lack of immediate replication block, activation of DNA damage signaling, reduction of Hdm2 and Hdmx protein levels, transcriptional regulation of p53-responsive genes and, most importantly, induction of apoptosis. In contrast, $Chk2^{-/-}$ cells were still responsive to p53 activation by Nutlin-3 , although Nutlin-3 induced G2 arrest seemed Chk2 dependent. The absence of G2 arrest in $Chk2^{-/-}$ cells was restricted to Nutlin-3; RITA clearly (although transiently) elevated the G2/M fraction. This G2/M increase upon RITA treatment may appear stronger in $p53^{-/-}$ and $Chk2^{-/-}$ cells just because they lack an S-phase arrest. It has recently been demonstrated that RITA induces a p53-dependent S-phase checkpoint via stalling of replication fork elongation (11). The authors showed phosphorylation of Chk1 on Ser345 and proposed a functional contribution of Chk1, although this appeared to be restricted to maintaining DNA integrity upon short-term exposure, and the relevance of Ser345 phosphorylation remained unclear. Our data indicate that Chk2 is essential for both Chk1 phosphorylation and efficient activation of an S-phase checkpoint by RITA. It seems plausible that RITA-induced DNA damage signaling results from replication stalling. We found that RITA-induced phosphorylations occur with much slower kinetics as compared with a classical DNA damaging agent like etoposide. Furthermore, the DNA damage response is not just a result of apoptosis induction, as it was still observed in the presence of Z-VAD-FMK.

Which pathway does RITA use to trigger apoptosis? Although the mechanism by which RITA activates Chk2 has still to be solved, our data indicate that Chk2 is required for Hdm2 degradation and full p53 stabilization. This could implicate that RITA partly stabilizes p53 indirectly, by reducing Hdm2 levels. In addition, the partial rescue observed in Noxa knockdown experiments defined p53 transcriptional activity as an important contributor to

apoptosis induction upon RITA treatment. Furthermore, serum-starved cells displayed reduced sensitivity to RITA, suggesting that replicating cells are particularly prone to RITA-induced apoptosis. This may provide a valuable aspect of RITA as cancer treatment, as tumor cells generally replicate faster than normal cells. On the other hand, DNA replication seems not to be an absolute requirement for RITA-induced apoptosis. Pre-treatment of HCT116 cells with Nutlin-3 for 24 h, which effectively depleted S-phase cells, did not protect cells from RITA-induced apoptosis, in contrast to an earlier report in which U2OS cells were used (7). Replication blockage and apoptosis induction required the presence of both p53 and Chk2. These findings suggest that RITA activates a p53- and Chk2-dependent S-phase checkpoint that signals back to p53, possibly through Chk2, to activate a pro-apoptotic transcriptional program. However, DNA damage signaling may not be required for apoptosis induction, as serum starvation partially prevented apoptosis, but not the DNA damage response. Furthermore, the use of PIKK-inhibitors KU-55933 and caffeine revealed no evidence for a contribution of ATM/ATR/DNA-PK activity in RITA-induced apoptosis, supporting the findings of Ahmed *et al.* (11) obtained using Wortmannin. It must be noted that caffeine seemed much more efficient in inhibiting RITA-induced p53-Ser46 phosphorylation as compared with KU-55933, suggesting that this depends on ATR and/or DNA-PK activity, rather than on ATM. Interestingly, DNA-PK was reported to synergistically act with Chk2 to activate p53-dependent apoptosis (23).

We found that Chk2 kinase activity is required for activating both the early replication block and apoptosis after RITA treatment. Comparison of several time-course analyses suggests that phosphorylation of Chk2 is not necessary for inhibiting replication. Its contribution to apoptosis induction remains elusive. In addition, the relevant Chk2 substrate(s) need to be identified. An obvious candidate is p53-Ser46, which is believed to specifically lead to apoptosis (24, 25) and correlated with Nutlin-3 plus RITA-induced apoptosis in uveal melanoma (12). Indeed, RITA-induced p53-Ser46 phosphorylation was almost absent in HCT116 Chk2$^{-/-}$ cells. However, additional targets may be involved as well. Chk2 is known to phosphorylate proteins involved in cell cycle arrest, such as Cdc25C (26) and Cdc25A (27), and DNA repair, including BRCA1 (28). The most interesting Chk2 targets are those involved in apoptosis, which might include not only p53 and Hdmx but also E2F1 (29) and PML (30). However, we detected a reduction of E2F1 and its targets p73 and APAF1 on the mRNA level in response to RITA treatment in wild-type HCT116 cells, ruling out a putative involvement of E2F1.

Collective literature indicates that *Chk2* is a cancer-susceptibility gene, possibly acting in synergy with other factors to cause cancer (31). Patients with Chk2-deficient tumors might

be treated with inhibitors of other DNA-repair proteins, whereas patients with tumors harboring functional Chk2 may benefit from Chk2 inhibition. This relies on the observation that cancer cells often contain an impaired checkpoint machinery, which results in a greater dependence on the remaining functional processes that ensure cell survival. Indeed, Chk1 inhibitors aiming at potentiating DNA damaging chemotherapy have reached clinical trials (32). However, Chk2 inhibition is not always a good anti-cancer strategy. In fact, Chk2 activation in the absence of DNA damage was proposed as cancer therapy (33). In addition, Chk2 inhibition can protect cells from radiation toxicity; the Chk2 inhibitor VRX0466617 attenuated IR-induced apoptosis (34), and an earlier report showed that Chk2-deficient mice are radio resistant and exhibit impaired IR-induced p53-activation (35). This may be exploited to improve the therapeutic index of radiotherapy in Chk2-deficient tumors, as Chk2 could have a radio-protective effect on normal tissues.

Here, we show that Chk2 loss protects cells from RITA, indicating that RITA will be particularly useful in tumors harboring functional Chk2. Interestingly, we also found that Chk2 inhibition diminished apoptosis in uveal melanoma cell lines induced by a combination of Nutlin-3 and the topoisomerase I inhibitor Topotecan (data not shown). By contrast, inhibition of the ATR-Chk1 axis has been demonstrated to potentiate the effects of topoisomerase I inhibitors (36). Thus, Chk1 and Chk2 clearly exhibit distinct roles in the responses to replicative stress. Our data place Chk2 in a central position in mediating the cellular responses to RITA. Future work should focus on the mechanism by which RITA activates Chk2, as well as on precisely defining the S-phase checkpoint induced by RITA, which is confusing because its induction is p53 dependent. Another challenge is finding out through which substrate(s) Chk2 contributes to apoptosis induction. Convincing evidence that replication stalling really is the (only) trigger for apoptosis is still lacking, so in theory RITA might induce two separate events. Elucidating these issues will help understanding the mechanistic properties of RITA and the evaluation of its utility as anti-cancer drug.

Materials and Methods

Cell lines, lentiviral transductions

Human uveal melanoma cell line Mel202 was cultured in RPMI + F10 medium (1:1 ratio) with 10% fetal bovine serum (FBS) and antibiotics. Human colorectal carcinoma HCT116, human breast cancer cell line MCF7 and human osteosarcoma U2OS were cultured in Dulbecco's modified Eagle medium supplemented with 10% FBS and antibiotics. HCT116 $p53^{+/+}$, $p53^{-/-}$ and $Chk2^{-/-}$ cell lines were a kind gift from Dr. B. Vogelstein. The generation of U2OS cells with inducible Wip1 expression (U2TR) has

been described before (37). U2TR cells, as well as MCF7 cell lines stably transduced with empty pRS or pRS-shWip1 vectors, were kindly provided by Dr. R. Medema. Lentiviral constructs targeting Noxa (TRCN0000153637), Chk2 (TRCN0000010314) and a non-targeting control construct (SHC002) were obtained from the Mission shRNA library (Sigma-Aldrich, St Louis, MO, USA). Cells were transduced using MOI = 1.0 in a medium containing 8.0 μg/ml polybrene and puromycin selected for stable expression.

Drug treatments

HCT116 cells were seeded in 6-wells plates at a density of $5.0*10^5$ cells per well, Mel202 at $1.0*10^6$ cells per 6-cm dish, MCF7 at $9.0*10^5$ cells per 6-cm dish and U2TR at $6.0*10^5$ cells per 6-cm dish. Unless differently stated, final drug concentrations were 1.0 μM RITA and 10 μM Nutlin-3 in HCT116 and MCF7, and 0.25 μM RITA and 3.0 μM Nutlin-3 in Mel202. Nutlin-3 was purchased from Cayman Chemical (Ann Arbor, MI, USA) and RITA was kindly provided by Galina Selivanova. KU-55933 was a kind gift of Graeme Smith and Steve Jackson, and provided to us by Yosef Shiloh. Caffeine (C0750), Chk2 inhibitor II (C3742) and Z-VAD-FMK (V116) were purchased from Sigma-Aldrich.

Immunoblotting

Cells were lysed in Giordano buffer (50 mM Tris-HCl, pH 7.4, 250 mM NaCl, 0.1% Triton X-100, 5 mM EDTA) with protease- and phosphatase inhibitors. Proteins were separated by SDS-PAGE, blotted onto polyvinylidene fluoride transfer membranes, incubated with the appropriate primary (listed in Supplementary Table 1) and secondary antibodies, and bands were visualized by chemoluminescence (West Dura, Pierce Biotechnology, Rockford, IL, USA).

RNA isolation, quantitative real-time PCR

RNA was isolated using the SV Total RNA isolation kit (Promega, Madison, WI, USA). cDNA was synthesized using 2.0 μg RNA in a total volume of 30 μl reverse transcriptase reaction mixture (Promega). Samples were analyzed in triplicate using SYBR Green mix (Roche Biochemicals, Indianapolis, IN, USA) in a 7900ht Fast Real-Time PCR System (Applied Biosystems, Foster City, CA, USA). For normalization, the geometric mean of two housekeeping genes (*RPS11* and *CAPNS1*) was used. Expression levels were calculated relative to untreated samples. Primer sequences are listed in Supplementary Table 2.

Flow cytometry

Cells were harvested, washed in PBS and fixed in ice-cold 70% EtOH. Before to FACS analysis, cells were washed in PBS and resuspended in PBS containing 50 μg/ml RNase A and 50 μg/ml propidium iodide (PI). Flow cytometry was performed in the BD LSR II system (BD Biosciences, San Diego, CA, USA). For Annexin V staining, cells were washed twice in PBS and resuspended in Annexin V-binding buffer containing Fluorescein isothyocyanate (FITC)-labeled Annexin-V (Sigma-Aldrich) and PI. After 10-min RT incubation cells were analyzed by flow cytometry. Positive PI staining, indicating necrotic or late apoptotic cells were excluded from the analysis. PI-negative, Annexin V-positive cells represent early apoptotic cells.

For EdU incorporation, we used the Click-iT EdU flow cytometry assay kit (Invitrogen, Grand Island, NY, USA). In short, cells were 1h pulse-labeled with 2.0 μM EdU, harvested, fixed with 4% paraformaldehyde and permeabilized with a saponin-based reagent. Cells were stained with Alexa Fluor 488 azide and analyzed by flow cytometry to detect EdU positive cells.

WST-1 proliferation assay, calculation of synergism

HCT116 cells were counted and seeded in triplicate in 96-well plates at a density of 4000 cells per well, in a total volume of 100 μl medium. Cells were incubated with 10 μl WST-1 (Roche) for two hours and absorbance (450 nm) was measured in a microplate reader (Victor; Perkin Elmer, San Jose, CA, USA). For synergy studies, drug effects were calculated as 'affected fraction' of treated *versus* untreated cells. Dose-effect analyses and calculation of CI were performed using CompuSyn software (Paramus, NJ, USA (38)). CI reflects the extent of synergy or antagonism for two drugs: CI<0.9, synergy; 0.9<CI<1.1, additive effect; CI>1.1, antagonism.

Acknowledgements

We thank Prof. B.R. Ksander for providing the Mel202 cell line, Dr. B Vogelstein for providing the HCT116 cell lines, Dr. R. Medema for the MCF-7/pRS, MCF-7/pRS-shWip1 cells and the Wip1-inducible U2OS cells U2TR, as well as Dr. G. Selivanova for providing RITA.

Reference List

(1) Vogelstein B, Lane D, Levine AJ. Surfing the p53 network. *Nature* 2000; **408**: 307-310.

(2) Issaeva N, Bozko P, Enge M, Protopopova M, Verhoef LG, Masucci M, et al. Small molecule RITA binds to p53, blocks p53-HDM-2 interaction and activates p53 function in tumors. *Nat Med* 2004; **10**: 1321-1328.

(3) Vassilev LT, Vu BT, Graves B, Carvajal D, Podlaski F, Filipovic Z, et al. In vivo activation of the p53 pathway by small-molecule antagonists of MDM2. *Science* 2004; **303** :844-848.

(4) Ding K, Lu Y, Nikolovska-Coleska Z, Wang G, Qiu S, Shangary S, et al. Structure-based design of spiro-oxindoles as potent, specific small-molecule inhibitors of the MDM2-p53 interaction. *J Med Chem* 2006; **49**: 3432-3435.

(5) Enge M, Bao W, Hedstrom E, Jackson SP, Moumen A, Selivanova G. MDM2-dependent downregulation of p21 and hnRNP K provides a switch between apoptosis and growth arrest induced by pharmacologically activated p53. *Cancer Cell* 2009; **15**: 171-183.

(6) Krajewski M, Ozdowy P, D'Silva L, Rothweiler U, Holak TA. NMR indicates that the small molecule RITA does not block p53-MDM2 binding in vitro. *Nat Med* 2005;**11**: 1135-1136.

(7) Rinaldo C, Prodosmo A, Siepi F, Moncada A, Sacchi A, Selivanova G, et al. HIPK2 regulation by MDM2 determines tumor cell response to the p53-reactivating drugs nutlin-3 and RITA. *Cancer Res* 2009; **69**: 6241-6428.

(8) Hedstrom E, Eriksson S, Zawacka-Pankau J, Arner ES, Selivanova G. p53-dependent inhibition of TrxR1 contributes to the tumor-specific induction of apoptosis by RITA. *Cell Cycle* 2009 ;**8**: 3576-3583.

(9) Spinnler C, Hedstrom E, Li H, De Lange J, Nikulenkov F, Teunisse AF, et al. Abrogation of Wip1 expression by RITA-activated p53 potentiates apoptosis induction via activation of ATM and inhibition of HdmX. *Cell Death Differ* 2011; **18**:1736-1745.

(10) Yang J, Ahmed A, Poon E, Perusinghe N, de Haven BA, Box G, et al. Small-molecule activation of p53 blocks hypoxia-inducible factor 1alpha and vascular endothelial growth factor expression in vivo and leads to tumor cell apoptosis in normoxia and hypoxia. *Mol Cell Biol* 2009; **29**: 2243-2253.

(11) Ahmed A, Yang J, Maya-Mendoza A, Jackson DA, Ashcroft M. Pharmacological activation of a novel p53-dependent S-phase checkpoint involving CHK-1. *Cell Death Dis* 2011; May 19; 2 :e160.

(12) De Lange J, Ly LV, Lodder K, Verlaan-de Vries M, Teunisse AF, Jager MJ, et al. Synergistic growth inhibition based on small-molecule p53 activation as treatment for intraocular melanoma. *Oncogene* 2011; Jul 18.

(13) Liu Q, Guntuku S, Cui XS, Matsuoka S, Cortez D, Tamai K, et al. Chk1 is an essential kinase that is regulated by Atr and required for the G(2)/M DNA damage checkpoint. *Genes Dev* 2000; **14**: 1448-1459.

(14) Zhao H, Piwnica-Worms H. ATR-mediated checkpoint pathways regulate phosphorylation and activation of human Chk1. *Mol Cell Biol* 2001; **21**: 4129-4139.

(15) Ahn JY, Schwarz JK, Piwnica-Worms H, Canman CE. Threonine 68 phosphorylation by ataxia telangiectasia mutated is required for efficient activation of Chk2 in response to ionizing radiation. *Cancer Res* 2000; **60**: 5934-5936.

(16) Buscemi G, Carlessi L, Zannini L, Lisanti S, Fontanella E, Canevari S, et al. DNA damage-induced cell cycle regulation and function of novel Chk2 phosphoresidues. *Mol Cell Biol* 2006; **26**: 7832-7845.

(17) Meek DW. Tumour suppression by p53: a role for the DNA damage response? *Nat Rev Cancer* 2009; **9**: 714-723.

(18) Coll-Mulet L, Iglesias-Serret D, Santidrian AF, Cosialls AM, de FM, Castano E, et al. MDM2 antagonists activate p53 and synergize with genotoxic drugs in B-cell chronic lymphocytic leukemia cells. *Blood* 2006; **107**: 4109-4114.

(19) Lam S, Lodder K, Teunisse AF, Rabelink MJ, Schutte M, Jochemsen AG. Role of Mdm4 in drug sensitivity of breast cancer cells. *Oncogene* 2010; **29**: 2415-2426.

(20) Laurie NA, Donovan SL, Shih CS, Zhang J, Mills N, Fuller C, et al. Inactivation of the p53 pathway in retinoblastoma. *Nature* 2006; **444**: 61-66.

(21) Saha MN, Jiang H, Mukai A, Chang H. RITA inhibits multiple myeloma cell growth through induction of p53-mediated caspase-dependent apoptosis and synergistically enhances nutlin-induced cytotoxic responses. *Mol Cancer Ther* 2010; **9**: 3041-3051.

(22) Chou TC. Theoretical basis, experimental design, and computerized simulation of synergism and antagonism in drug combination studies. *Pharmacol Rev* 2006; **58**: 621-681.

(23) Jack MT, Woo RA, Motoyama N, Takai H, Lee PW. DNA-dependent protein kinase and checkpoint kinase 2 synergistically activate a latent population of p53 upon DNA damage. *J Biol Chem* 2004; **279**: 15269-15273.

(24) Bulavin DV, Saito S, Hollander MC, Sakaguchi K, Anderson CW, Appella E, et al. Phosphorylation of human p53 by p38 kinase coordinates N-terminal phosphorylation and apoptosis in response to UV radiation. *EMBO J* 1999; **18**: 6845-6854.

(25) Saito S, Goodarzi AA, Higashimoto Y, Noda Y, Lees-Miller SP, Appella E, et al. ATM mediates phosphorylation at multiple p53 sites, including Ser(46), in response to ionizing radiation. *J Biol Chem* 2002; **277**: 12491-12494.

(26) Blasina A, de W, IV, Laus MC, Luyten WH, Parker AE, McGowan CH. A human homologue of the checkpoint kinase Cds1 directly inhibits Cdc25 phosphatase. *Curr Biol* 1999; **9**: 1-10.

(27) Falck J, Mailand N, Syljuasen RG, Bartek J, Lukas J. The ATM-Chk2-Cdc25A checkpoint pathway guards against radioresistant DNA synthesis. *Nature* 2001; **410**: 842-847.

(28) Lee JS, Collins KM, Brown AL, Lee CH, Chung JH. hCds1-mediated phosphorylation of BRCA1 regulates the DNA damage response. *Nature* 2000; **404**: 201-204.

(29) Stevens C, Smith L, La Thangue NB. Chk2 activates E2F-1 in response to DNA damage. *Nat Cell Biol* 2003; **5**: 401-409.

(30) Yang S, Kuo C, Bisi JE, Kim MK. PML-dependent apoptosis after DNA damage is regulated by the checkpoint kinase hCds1/Chk2. *Nat Cell Biol* 2002; **4**: 865-870.

(31) Antoni L, Sodha N, Collins I, Garrett MD. CHK2 kinase: cancer susceptibility and cancer therapy - two sides of the same coin? *Nat Rev Cancer* 2007; 7: 925-936.

(32) Ma CX, Janetka JW, Piwnica-Worms H. Death by releasing the breaks: CHK1 inhibitors as cancer therapeutics. *Trends Mol Med* 2011; **17**: 88-96.

(33) Chen CR, Wang W, Rogoff HA, Li X, Mang W, Li CJ. Dual induction of apoptosis and senescence in cancer cells by Chk2 activation: checkpoint activation as a strategy against cancer. *Cancer Res* 2005; **65**: 6017-6021.

(34) Carlessi L, Buscemi G, Larson G, Hong Z, Wu JZ, Delia D. Biochemical and cellular characterization of VRX0466617, a novel and selective inhibitor for the checkpoint kinase Chk2. *Mol Cancer Ther* 2007; **6**: 935-944.

(35) Takai H, Naka K, Okada Y, Watanabe M, Harada N, Saito S, et al. Chk2-deficient mice exhibit radioresistance and defective p53-mediated transcription. *EMBO J* 2002; **21**: 5195-5205.

(36) Flatten K, Dai NT, Vroman BT, Loegering D, Erlichman C, Karnitz LM, et al. The role of checkpoint kinase 1 in sensitivity to topoisomerase I poisons. *J Biol Chem* 2005; **280**: 14349-14355.

(37) Macurek L, Lindqvist A, Voets O, Kool J, Vos HR, Medema RH. Wip1 phosphatase is associated with chromatin and dephosphorylates gammaH2AX to promote checkpoint inhibition. *Oncogene* 2010; **29**: 2281-2291.

(38) CompuSyn software for drug combinations and for general dose-effect analysis, and user's guide [computer program]. ComboSyn, Inc.Paramus, NJ; 2007.

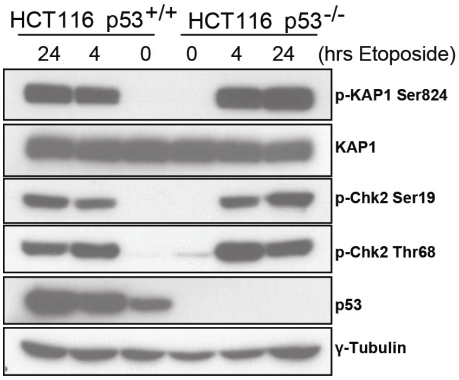

Supplementary Figure 1 Similar inductions of KAP1 and Chk2 phosphorylations in HCT116 $p53^{+/+}$ and $p53^{-/-}$ cells. HCT116 $p53^{+/+}$ and $p53^{-/-}$ cells were mock treated or treated with 10 μM etoposide for 4 or 24 h, and protein extracts were analyzed by western blot using the indicated antibodies.

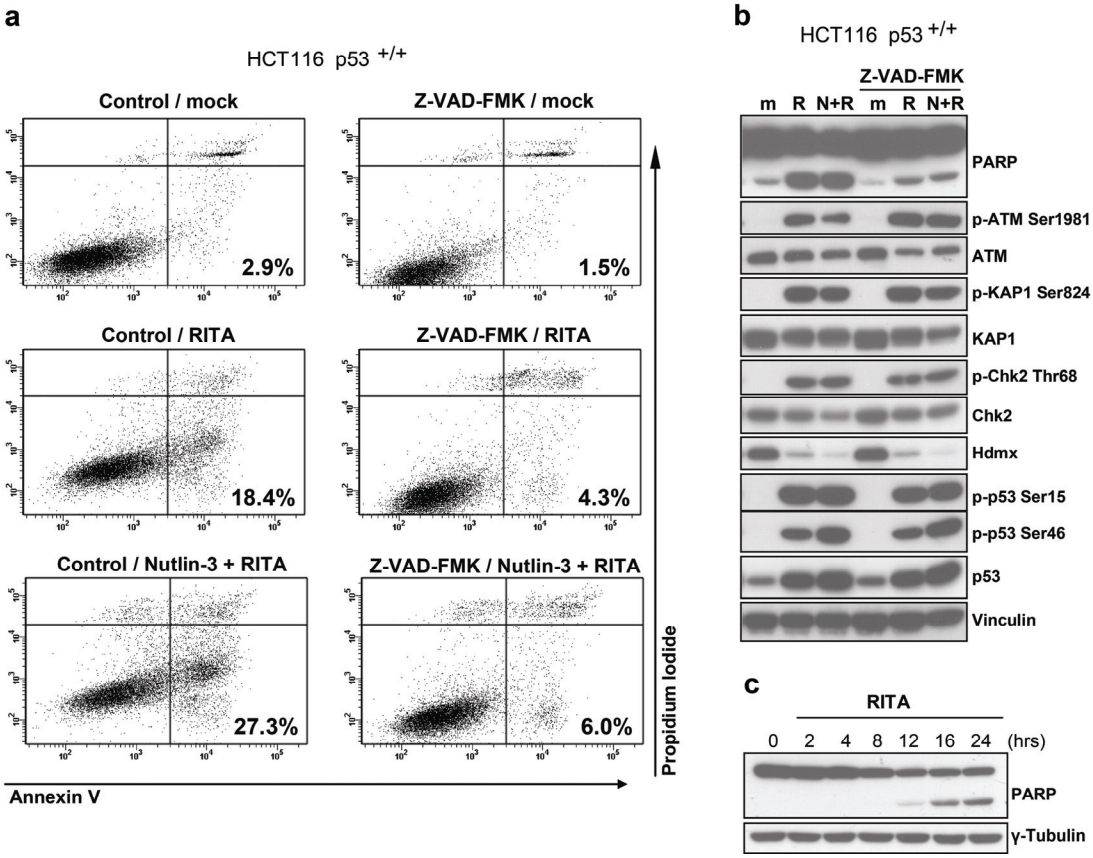

Supplementary Figure 2 Activation of DNA damage response by RITA is not a secondary effect caused by apoptosis induction. HCT116 $p53^{+/+}$, $p53^{-/-}$ and $Chk2^{-/-}$ cells were 2 h pre-treated with 20 μM Z-VAD-FMK and subsequently treated as indicated. (**a**) Apoptosis was assessed after 48 h using Annexin V staining. (**b**) Protein extracts were isolated after 24 h and analyzed by western blot using the indicated antibodies. (**c**) HCT116 $p53^{+/+}$ cells were treated with RITA for the indicated periods, and proteins were analyzed by western blot using the indicated antibodies.

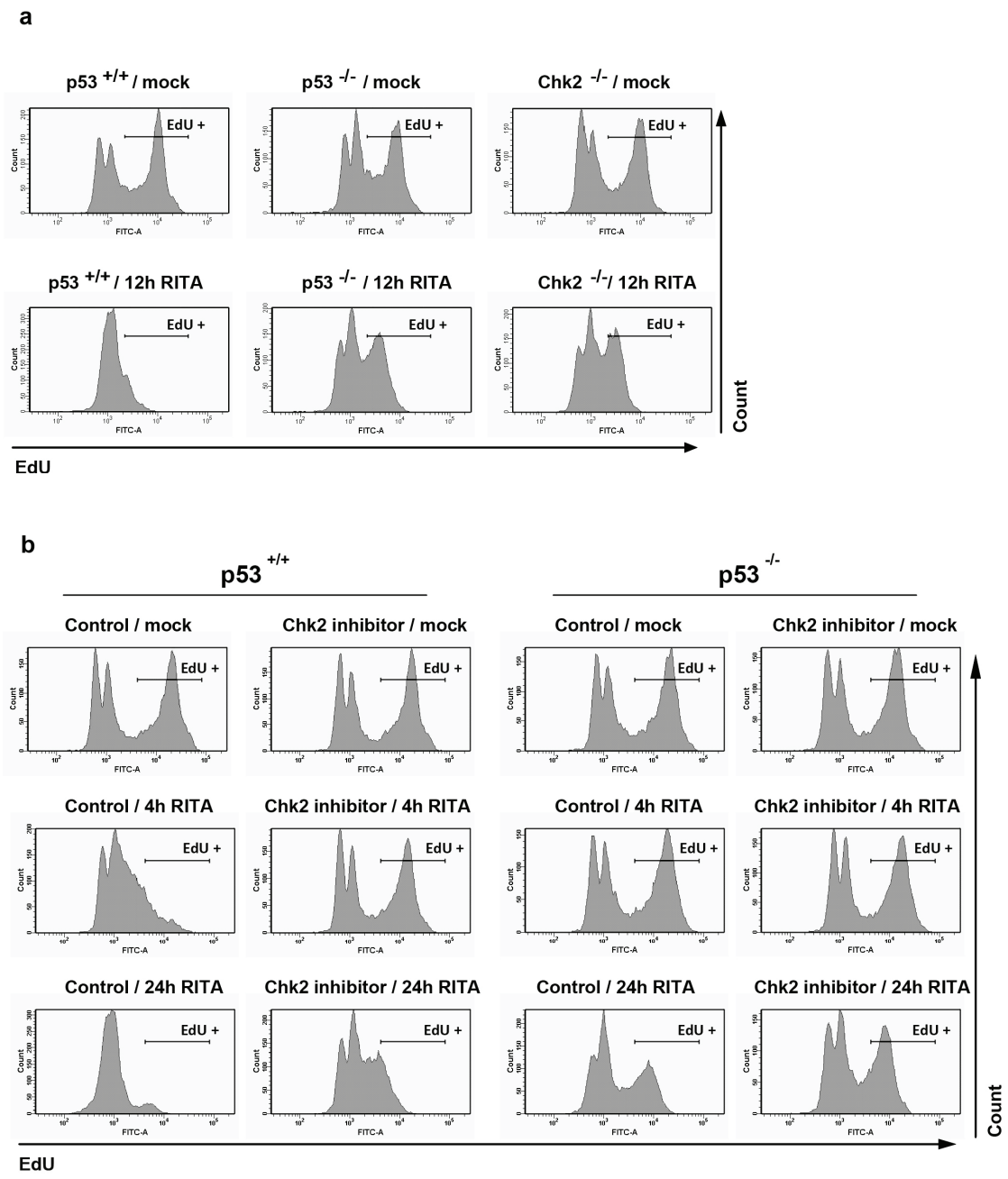

Supplementary Figure 3 RITA slows down DNA replication of p53- and Chk2-deficient HCT116 cells at later time points. (**a**) HCT116 $p53^{+/+}$, $p53^{-/-}$ and $Chk2^{-/-}$ cells were treated with RITA for 12 h. Subsequently, 5-ethynyl-2'-deoxyuridine (EdU) was added (final concentration 2.0 μM) for 1 h to allow incorporation into newly synthesized DNA. Cells were harvested and analyzed for EdU content using flow cytometry. (**b**) HCT116 $p53^{+/+}$ and $p53^{-/-}$ cells were pre-treated for 2 h with 10 μM Chk2 inhibitor II where indicated, and subsequently mock-treated or treated with RITA for 4 or 24 h. Cells were harvested and analyzed for EdU content using flow cytometry.

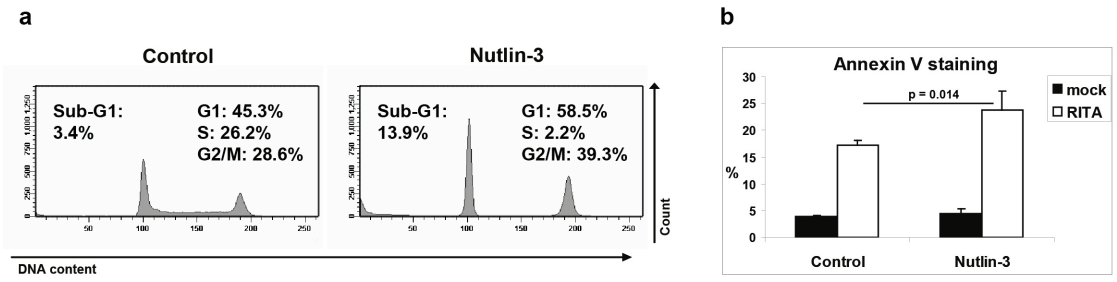

Supplementary Figure 4 Pre-treatment with Nutlin-3 does not protect HCT116 cells from apoptosis induction by RITA. (**a**) HCT116 $p53^{+/+}$ cells were 24 h pre-treated with 10 μM Nutlin-3 and the effect on cell-cycle distribution was analyzed using flow cytometry. (**b**) Cells were subsequently incubated with RITA for 24 h in the presence of Nutlin-3. Apoptosis induction was assessed by Annexin V staining; bars represent means and s.e. of four independent experiments. Statistical analysis was performed using a two-tailed *t* test.

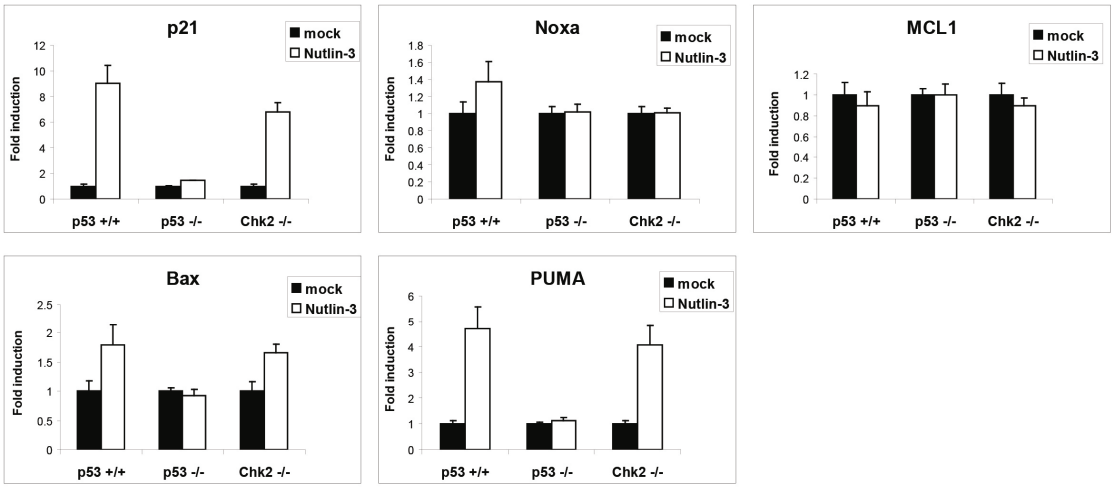

Supplementary Figure 5 Nutlin-3 induces transcription of p53 target genes in HCT116 $p53^{+/+}$ and $Chk2^{-/-}$ cells. HCT116 $p53^{+/+}$, $p53^{-/-}$ and $Chk2^{-/-}$ cells were treated with 10 μM Nutlin-3 for 6 h, and analyzed by qRT-PCR for p21, Noxa, MCL1, Bax and PUMA expression levels.

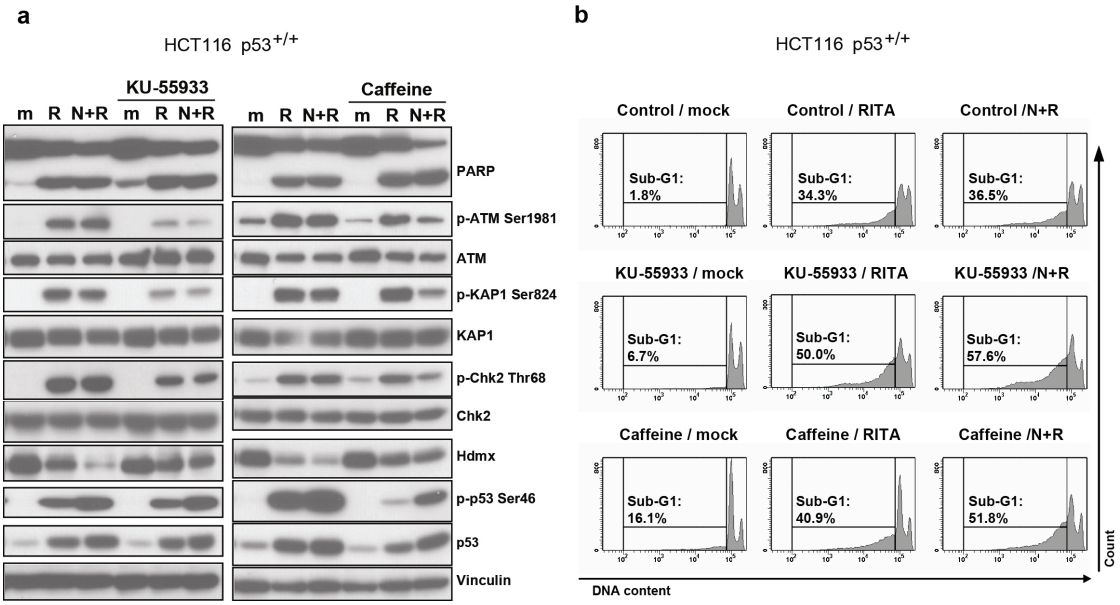

Supplementary Figure 6 Inhibition of RITA-induced DNA damage signaling fails to prevent apoptosis. HCT116 cells were 2 h pre-treated with 10 μM KU-55933 or 5 mM caffeine and subsequently treated for 24 h as indicated. (**a**) Protein extracts were analyzed by western blot using the indicated antibodies. (**b**) Cells were harvested and analyzed by flow cytometry for sub-G1 evaluation.

Supplementary Table 1: List of antibodies

Protein	Name/ cat. #	Company
PARP	9542	Cell signalling Technology, Beverly, MA, USA
p-ATM Ser1981	EP1890Y / 2152-1	Epitomics, California, USA
ATM	Y170 / 1549-1	Epitomics, California, USA
p-KAP1 Ser824	A300-767A	Bethyl Laboratories, Montgomery TX, USA
KAP1	A300-274A	Bethyl Laboratories, Montgomery TX, USA
p-Chk1 Ser345	2348	Cell signalling Technology, Beverly, MA, USA
Chk1	FL-476 / sc-7898	Santa Cruz Biotechnology, Santa Cruz, CA, USA
p-Chk2 Ser19	2666S	Cell signalling Technology, Beverly, MA, USA
p-Chk2 Thr68	C13C1 / 2197	Cell signalling Technology, Beverly, MA, USA
Chk2	EPR4325 / 3428-1	Epitomics, California, USA
Wip1	A300-664A	Bethyl Laboratories, Montgomery TX, USA
Hdm2 *	4B2	Chen *et al*., 1993
Hdm2 *	SMP14 sc-6965	Santa Cruz Biotechnology, Santa Cruz, CA, USA
Hdmx	A300-287A	Bethyl Laboratories, Montgomery TX, USA
p-p53 Ser46	2190-1 / EP42Y	Epitomics, California, USA
p-p53 Ser15	9284	Cell signalling Technology, Beverly, MA, USA
p53 °	DO-1 / sc-126	Santa Cruz Biotechnology, Santa Cruz, CA, USA
p53 °	PAb1801 / sc-98	Santa Cruz Biotechnology, Santa Cruz, CA, USA
Vinculin	hVIN-1 / V9131	Sigma-Aldrich, St Louis, MO, USA
γ-Tubulin	GTU-88 / T6557	Sigma-Aldrich, St Louis, MO, USA

For detection of human Hdm2 we used a mix of 4B2 and SMP14 (*), for detection of human p53 we used a mix of DO-1 and 1801 (°).

Ref) Chen J *et al.* Mapping of the p53 and mdm-2 interaction domains. *Mol Cell Biol* 1993, **13:**4107-4114.

Supplementary Table 2: Primer sequences used for qRT-PCR reactions.

Gene	Forward primer	Reverse primer
p21	5'-AGCAGAGGAAGACCATGTGGA-3'	5'-AATCTGTCATGCTGGTCTGCC-3'
Noxa	5'-ACTGTTCGTGTTCAGCTC-3'	5'-GTAGCACACTCGACTTCC-3'
PUMA	5'-GACCTCAACGCACAGTA-3'	5'-CTAATTGGGCTCCATCT-3'
Bax	5'-ATGTTTTCTGACGGCAACTTC-3'	5'-ATCAGTTCCGGCACCTTG-3'
MCL1	5'-TAAGGACAAAACGGGACTGG-3'	5'-AACCAGCTCCTACTCCAGCA-3'
Wip1	5'-ATACCTGAACCTGACTGAC-3'	5'-CTCCTCCAGTGACTTGAC-3'
CAPNS1	5'-ATGGTTTTGGCATTGACACATG-3'	5'-GCTTGCCTGTGGTGTCGC-3'
RPS11	5'-AAGCAGCCGACCATCTTTCA-3'	5'-CGGGAGCTTCTCCTTGCC-3'

Chapter 6

General Discussion

It has been long recognized that the p53 tumor suppressor protein plays a key role in cancer and its direct or indirect inactivation is an almost universal feature of human tumors. Collective studies in the last decades have resulted in a profound understanding of p53's regulation and function, and p53 is now placed in a central position in the prevention of genomic instability and protection of tumorigenesis, therefore nicknamed "guardian of the genome" [1]. Clinical application of the obtained knowledge about p53 appears promising; however, there are still many challenges that remain to be addressed. This thesis has essentially focused on two different arms in p53 research, one involving the role of the p53 regulator Hdmx in cancer development (chapter 2 and 3) and the second exploring several aspects of the use of small-molecule p53 activators as cancer treatment (chapter 4 and 5).

Hdmx in oncogenic transformation

Designing future anticancer strategies that target the p53 pathway requires a detailed understanding of the functional properties of Mdm2 and Mdmx (in humans named Hdm2 and Hdmx) and the mechanisms controlling them. Hdm2 is mostly regarded the more general regulator of p53, with Hdmx being its little brother. This is exemplified by the notions that unlike Hdm2, Hdmx on its own cannot degrade p53 or facilitate its nuclear export [2;3]. Hdmx blocks p53 transcriptional activity and may serve as a cofactor for Hdm2-mediated p53 ubiquitination. Furthermore, Hdmx loss as compared with Hdm2 loss generally appears to exhibit less severe effects, in terms of the timing of embryonic lethality in mice [4-6] as well as the toxicity in adult tissues [7;8]. In addition, Mdm2 overexpression rescues the lethal phenotype of Mdmx knockout in mice [9], whereas widespread Mdmx overexpression appears not to compensate for Mdm2 loss [10]. Nevertheless, a subset of human cancers relies on Hdmx overexpression to inactivate the p53 tumor suppressor pathway [11-14]. This suggests that increased Hdmx levels are sufficient to counteract the oncogene-induced p53 activity during neoplastic transformation. Indeed, this has been shown for murine cells [11]. Importantly, chapter 2 of this thesis also provides evidence for such a direct role of Hdmx in cultured human cells. When combined with other defined genetic changes, constitutive Hdmx overexpression contributed to the oncogenic transformation of both foreskin fibroblasts (VH10) and human embryonic retinoblasts (HER). The choice for retinoblasts was based on the frequent Hdmx overexpression observed in retinoblastoma. Like most Hdmx overexpressing cancers, retinoblastoma retains wild-type p53. This suggests that the oncogenic function of Hdmx is based on p53 inhibition, which is supported by the observations in chapter 2 that cells with increased Hdmx levels functionally resembled the

p53 knockdown cells. The most transformed HER cells, with either Hdmx overexpression or p53-knockdown, also showed *in vivo* growth capacity, although limited.

The principal effector linking upstream oncogenic signals and p53 activation is the tumor suppressor protein $p14^{ARF}$, a direct target of the Rb-repressed transcription factor E2F1, which antagonizes Hdm2 function [15-17]. This pathway may be particularly relevant in retinoblastomas, which harbor direct Rb gene inactivation. Importantly, $p14^{ARF}$ does not directly prevent p53 inhibition by Hdmx [18], although it has been proposed that $p14^{ARF}$ stimulates Hdm2-mediated Hdmx degradation [19]. This suggests that in $p14^{ARF}$-proficient tumor cells, Hdmx has the capacity to bind and inhibit p53 without the help of functional Hdm2, but only when being sufficiently abundant. Hdmx overexpression does not reduce p53 protein levels, which is indeed observed in the transformed fibroblasts and retinoblasts in chapter 2. However, Hdmx effectively inhibited p53 activity, visualized by reduced basal mRNA and protein levels of p53 targets, except for Hdm2 protein, which is directly stabilized by Hdmx.

Hdmx in uveal melanoma

A proportion of human cancers contains increased Hdmx expression, mostly correlating with wild-type p53 status [11-14]. Chapter 3 investigated the role of Hdmx in uveal melanoma and showed Hdmx overexpression in a subset of cell lines and fresh-frozen tumor samples. Proliferation of some of these cell lines depended on Hdmx expression, as Hdmx reduction resulted in growth inhibition. Since uveal melanomas rarely contain p53 mutations, these cells most likely selected for high Hdmx levels because of its capacity to control p53 activity. Interestingly, however, the experiments in uveal melanoma cell lines indicated the existence of an additional growth promoting role of Hdmx. Such a p53-independent function of Hdmx may only become apparent when being overexpressed during tumorigenesis and not in normal development, as p53 deletion is known to prevent the effects of Mdmx knockout in mouse embryos [4-6]. The results in chapter 3 suggested the involvement of the Cdk inhibitor p27. Hdmx affected p27 at the post-transcriptional level, although the exact mechanism remains to be determined. Depletion of p27 partially rescued the induction of G1 arrest in response to Hdmx knockdown. The supposed p53-independent activity of Hdmx probably involves additional factors, although other contributors besides p27 could not yet be identified, including p73, Rb, p21, Survivin and a range of genes presented on an apoptosis-specific gene expression array. Therefore, further investigations are required to uncover the molecular basis of a p53-independent function of Hdmx in uveal melanoma. In addition, it is important to analyze the relevance

of such a role of Hdmx in other cell types as well. This will teach us more about Hdmx overexpressing tumors and ultimately may result in novel strategies to target such tumors.

Effect of Hdmx on the responses to Nutlin-3 treatment

The development of specific drugs that reactivate p53 in tumor cells is a promising strategy to treat cancer. A well-studied example is the non-genotoxic Hdm2 antagonist Nutlin-3, which disrupts the Hdm2-p53 interaction and has already shown therapeutic potential in both *in vitro* and *in vivo* experiments [20]. The affinity of Nutlin-3 for Hdmx is much lower as compared to Hdm2 [12;21]. It has been argued that Hdmx levels dictate a cells' sensitivity to Nutlin-3 [22-24], because high levels of Hdmx may still be capable of binding and inhibiting p53 even in the presence of Nutlin-3. The established transformation models in chapter 2 provided a nice opportunity to investigate the effects of Hdmx overexpression on the outcome of Nutlin-3 treatment, in addition to assessing the role of Hdmx in neoplastic transformation. Indeed, Hdmx overexpression in skin fibroblasts was sufficient to attenuate p53 activation and growth inhibition mediated by Nutlin-3. However, Hdmx overexpression in HER cells could not prevent p53 induction and growth inhibition by Nutlin-3. Most likely, the lower Hdmx levels in the HER cells underlie this difference between VH10 and HER cells. Upon Nutlin-3 treatment, Hdmx levels were further reduced, due to Hdm2-mediated degradation. Retinoblastoma cell lines also show sensitivity to Nutlin-3, despite the presence of high Hdmx levels [12], indicating that the transformed HER cell lines provided a physiologically relevant model. Chapter 3 and 4 showed that Nutlin-3 efficiently induces p53-dependent growth inhibition in uveal melanoma cell lines. Interestingly, cell lines expressing high (92.1 and Mel202) and low levels of Hdmx (Mel270 an Mel285) displayed similar sensitivity to Nutlin-3. Thus, the results in HER cells and uveal melanoma cell lines suggest that patholigical Hdmx expression *per se* is not an all determing single determinant for the efficacy of Nutlin-3 treatment.

Use of Nutlin-3 in combination treatments

Nutlin-3 alone is probably not sufficient as cancer treatment, since in many wild-type p53 expressing tumors the Nutlin-3-activated p53 mainly leads to a reversible cell cycle arrest. Obviously, induction of apoptosis would lead to a more effective eradication of tumor cells. Chapter 4 investigated whether the therapeutic potential of Nutlin-3 could be increased by combination with other drugs. Calculated combination index values [25] demonstrated that Nutlin-3 synergized with both the topoisomerase I inhibitor Topotecan and with the small-molecule p53-activator RITA [26] to inhibit uveal melanoma growth,

correlating with enhanced apoptosis induction. Growth inhibition by Nutlin-3 and Topotecan was confirmed *in vivo* in a mouse model for ocular melanoma [27]. Importantly, low oxygen levels, often occurring *in vivo*, were found to not interfere with the efficacy of the proposed treatments. Thus, chapter 4 holds a strong case for using small-molecule p53 activators in combination therapy as treatment for ocular melanomas.

DNA damage response and p53-Ser46 phosphorylation

Chapter 4 also describes attempts to find a mechanistic explanation for the enhanced induction of apoptosis when combining Nutlin-3 with Topotecan or RITA. In chapter 5, the focus gradually shifted toward the mechanistic properties of RITA alone, which appeared to be very complex (discussed below). The increased p53-Ser46 phosphorylation as observed in both combination therapies was remarkable. This particular modification has been reported to contribute to directing the p53 response to apoptosis induction. The use of PIKK inhibitors and knockdown constructs against ATM in chapter 4 demonstrated that p53-Ser46 phosphorylation is a result of DNA damage signaling. Both Topotecan and RITA are known to induce a DNA damage response; Topotecan via inducing double strand DNA breaks and RITA via a poorly understood p53-dependent mechanism. However, ATM inhibition as described in chapter 4 and 5, in order to reduce DNA damage signaling and p53-Ser46 phosphorylation, on itself appeared to affect cell viability, and no rescue of apoptosis could be observed. Therefore, a functional contribution of the DNA damage response in general and p53-Ser46 phosphorylation in particular to the enhanced induction of apoptosis by the combination treatments remained unclear. An additional experiment in chapter 5, which focuses on RITA and no longer on Topotecan, further questioned the relevance of DNA damage signaling for apoptosis induction. Serum starvation partially prevented the induction of apoptosis by RITA, but not the DNA damage response. Therefore, the DNA damage response may just be an irrelevant side effect of RITA treatment.

Role of Chk2 in mediating the responses to RITA

Despite the fact that both Nutlin-3 and RITA were identified as p53-activating molecules, they exhibit very different effects on cell cycle progression (G1 arrest vs. S and G2 arrest). This may be an important contribution to the observed synergy, as only a stronger activation of the same pathway would probably at best be additive, but not synergistic. It is becoming increasingly clear that RITA has a much broader impact than just stabilizing p53, which is best shown by the reported p53-dependent induction of DNA damage response

[28-31]. Indeed, the proposed mechanism, i.e. RITA binds directly to p53 and disrupts the p53-Hdm2 interaction, is controversial [32]. The necessity of Chk2 for the RITA-induced responses, presented in Chapter 5, adds another level of complexity. Chemical inhibition of Chk2 kinase activity in uveal melanoma cell lines provided the initial clue for a contribution of Chk2 to the responses to Nutlin-3 plus RITA. Similar to ATM inhibition, inhibiting Chk2 using drugs or knockdown reduced p53-Ser46 phosphorylation, suggesting the classical activation of Chk2 function as part of the DNA damage response. However, the RITA-induced DNA damage response itself appeared to be Chk2-dependent, indicating that Chk2 acts upstream of ATM. Moreover, the findings in chapter 5 indicated that Chk2, unlike ATM, has a crucial contribution to the biological effects of RITA. In fact, Chk2-null HCT116 cells largely mimicked the p53-null HCT116 cells in their RITA response: lack of replication stalling, DNA damage response, apoptosis induction, reduction of Hdm2 and Hdmx protein levels, full p53 stabilization and transcriptional regulation of p53-responsive genes. These data place Chk2 in a central position in mediating the cellular responses to RITA.

Although chapter 5 represents an important step forward with regard to the understanding of RITA's mechanism of action, many questions remain unanswered. First, it would be intriguing to find out in detail how RITA triggers p53 and Chk2 activity. The data in chapter 5 could implicate that p53 stabilization is partially indirect, via Hdm2 degradation. Identifying additional players that directly interact with RITA might provide important new insights. An early study investigating RITA (initially named NSC-652287) suggested the induction of both DNA-protein and DNA-DNA cross-links, correlating with cytotoxicity [33]. In addition, RITA was reported to bind multiple, not further characterized proteins and its differential cytotoxic activities in different cell lines were attributed to differences in cellular drug accumulation and the cell´s capacity to metabolize RITA into reactive species [34]. Fitting these observations with later findings that RITA selectively kills transformed cells in a p53-dependent fashion [26] is a major challenge. Interestingly, chapter 5 suggested that Chk2 is essential for efficient activation of a previously reported p53-dependent S-phase checkpoint by RITA, involving Chk1 [28]. The induction of crosslinks may be relevant in this respect, however the nature of this checkpoint remains enigmatic and needs to be elucidated. In addition, it will be important to identify the substrate(s) of Chk2 that are relevant for the observed effects. Lastly, it is unclear whether Chk2 phosphorylation contributes to apoptosis induction by RITA, or whether this is a secondary effect of DNA damage signaling, resulting from replication stalling. Of note, the DNA damage response triggered by Nutlin-3 plus Topotecan (chapter 4) may be more relevant for the biological effects, as the induction of DNA damage signaling by Topotecan was much stronger as compared with RITA when the drugs were used at around IC50

concentrations. On the other hand, Chk2 inhibition also diminished apoptosis induced by Nutlin-3 plus Topotecan. This indicates that Chk2 may have an important role in translating replicative stress into an apoptotic response.

Future directions

Rapid advances are currently being made in drug-development aiming at reactivation of the p53 pathway [35]. Analogs of the Hdm2-antagonists Nutlin-3 and MI-219 have processed to advanced preclinical development or early phase clinical trials [36]. A key issue for p53-activating anti-cancer strategies that still requires better understanding involves how to achieve a maximal apoptotic response in cancer cells and a mild, reversible growth arrest in normal tissues. The realization that a subset of cancers relies on Hdmx overexpression to inactivate p53, including retinoblastoma and uveal melanoma, may have important implications for the treatment of those tumors. Whereas Hdm2 inhibition may trigger pathological p53 function in normal tissues, the targeting of Hdmx will probably have a milder impact [7], thereby possibly increasing the therapeutic window of specific Hdmx inhibitors. Indeed, such compounds are now being developed [37]. As discussed in this thesis, the use of specific drug combinations could also be an effective method to increase the therapeutic efficacy of p53 activating drugs while reducing the toxic effects of the individual compounds. However, this will require a labor-intensive determination of a fixed ratio of the different compounds to work optimally together taking into account the variable pharmacological properties of the individual molecules. Combination therapy using non-genotoxic activation of p53 might also be useful in what is named cyclotherapy. In such a strategy, normal cells undergo a protective cell cycle arrest, whereas mutant-p53 expressing cells continue to proliferate and are more sensitive to subsequent treatment with anti-mitotic agents [38]. The use of RITA will be particularly useful in tumors harboring wild-type p53 and functional Chk2. However, a better understanding of RITA's molecular mode of action will help defining the optimal conditions for its efficient application in patients. Eventually, this will bring us closer to developing personalized and effective cancer treatments with reduced toxicity.

Reference List

1. Vogelstein,B., Lane,D., and Levine,A.J. (2000) Surfing the p53 network. *Nature*, **408**, 307-310.

2. Jackson,M.W. and Berberich,S.J. (2000) MdmX protects p53 from Mdm2-mediated degradation. *Mol.Cell Biol.*, **20**, 1001-1007.

3. Stad,R., Ramos,Y.F., Little,N., Grivell,S., Attema,J., van der Eb,A.J., and Jochemsen,A.G. (2000) Hdmx stabilizes Mdm2 and p53. *J.Biol.Chem.*, **275**, 28039-28044.

4. Finch,R.A., Donoviel,D.B., Potter,D., Shi,M., Fan,A., Freed,D.D., Wang,C.Y., Zambrowicz,B.P., Ramirez-Solis,R., Sands,A.T., and Zhang,N. (2002) mdmx is a negative regulator of p53 activity in vivo. *Cancer Res.*, **62**, 3221-3225.

5. Migliorini,D., Lazzerini,D.E., Danovi,D., Jochemsen,A.G., Capillo,M., Gobbi,A., Helin,K., Pelicci,P.G., and Marine,J.C. (2002) Mdm4 (Mdmx) regulates p53-induced growth arrest and neuronal cell death during early embryonic mouse development. *Mol.Cell Biol.*, **22**, 5527-5538.

6. Parant,J., Chavez-Reyes,A., Little,N.A., Yan,W., Reinke,V., Jochemsen,A.G., and Lozano,G. (2001) Rescue of embryonic lethality in Mdm4-null mice by loss of Trp53 suggests a nonoverlapping pathway with MDM2 to regulate p53. *Nat.Genet.*, **29**, 92-95.

7. Garcia,D., Warr,M.R., Martins,C.P., Brown,S.L., Passegue,E., and Evan,G.I. (2011) Validation of MdmX as a therapeutic target for reactivating p53 in tumors. *Genes Dev.*, **25**, 1746-1757.

8. Marine,J.C., Francoz,S., Maetens,M., Wahl,G., Toledo,F., and Lozano,G. (2006) Keeping p53 in check: essential and synergistic functions of Mdm2 and Mdm4. *Cell Death.Differ.*, **13**, 927-934.

9. Steinman,H.A., Hoover,K.M., Keeler,M.L., Sands,A.T., and Jones,S.N. (2005) Rescue of Mdm4-deficient mice by Mdm2 reveals functional overlap of Mdm2 and Mdm4 in development. *Oncogene*, **24**, 7935-7940.

10. De Clercq,S., Gembarska,A., Denecker,G., Maetens,M., Naessens,M., Haigh,K., Haigh,J.J., and Marine,J.C. (2010) Widespread overexpression of epitope-tagged Mdm4 does not accelerate tumor formation in vivo. *Mol.Cell Biol.*, **30**, 5394-5405.

11. Danovi,D., Meulmeester,E., Pasini,D., Migliorini,D., Capra,M., Frenk,R., de Graaf,P., Francoz,S., Gasparini,P., Gobbi,A., Helin,K., Pelicci,P.G., Jochemsen,A.G., and Marine,J.C. (2004) Amplification of Mdmx (or Mdm4) directly contributes to tumor formation by inhibiting p53 tumor suppressor activity. *Mol.Cell Biol.*, **24**, 5835-5843.

12. Laurie,N.A., Donovan,S.L., Shih,C.S., Zhang,J., Mills,N., Fuller,C., Teunisse,A., Lam,S., Ramos,Y., Mohan,A., Johnson,D., Wilson,M., Rodriguez-Galindo,C., Quarto,M., Francoz,S., Mendrysa,S.M., Guy,R.K., Marine,J.C., Jochemsen,A.G., and Dyer,M.A. (2006) Inactivation of the p53 pathway in retinoblastoma. *Nature*, **444**, 61-66.

13. Ramos,Y.F., Stad,R., Attema,J., Peltenburg,L.T., van der Eb,A.J., and Jochemsen,A.G. (2001) Aberrant expression of HDMX proteins in tumor cells correlates with wild-type p53. *Cancer Res.*, **61**, 1839-1842.

14. Riemenschneider,M.J., Knobbe,C.B., and Reifenberger,G. (2003) Refined mapping of 1q32 amplicons in malignant gliomas confirms MDM4 as the main amplification target. *Int.J.Cancer*, **104**, 752-757.

15. Honda,R. and Yasuda,H. (1999) Association of p19(ARF) with Mdm2 inhibits ubiquitin ligase activity of Mdm2 for tumor suppressor p53. *EMBO J.*, **18**, 22-27.

16. Tao,W. and Levine,A.J. (1999) P19(ARF) stabilizes p53 by blocking nucleo-cytoplasmic shuttling of Mdm2. *Proc.Natl.Acad.Sci.U.S.A*, **96**, 6937-6941.

17. Weber,J.D., Taylor,L.J., Roussel,M.F., Sherr,C.J., and Bar-Sagi,D. (1999) Nucleolar Arf sequesters Mdm2 and activates p53. *Nat.Cell Biol.*, **1**, 20-26.

18. Wang,X., Arooz,T., Siu,W.Y., Chiu,C.H., Lau,A., Yamashita,K., and Poon,R.Y. (2001) MDM2 and MDMX can interact differently with ARF and members of the p53 family. *FEBS Lett.*, **490**, 202-208.

19. Pan,Y. and Chen,J. (2003) MDM2 promotes ubiquitination and degradation of MDMX. *Mol.Cell Biol.*, **23**, 5113-5121.

20. Vassilev,L.T., Vu,B.T., Graves,B., Carvajal,D., Podlaski,F., Filipovic,Z., Kong,N., Kammlott,U., Lukacs,C., Klein,C., Fotouhi,N., and Liu,E.A. (2004) In vivo activation of the p53 pathway by small-molecule antagonists of MDM2. *Science*, **303**, 844-848.

21. Joseph,T.L., Madhumalar,A., Brown,C.J., Lane,D.P., and Verma,C.S. (2010) Differential binding of p53 and nutlin to MDM2 and MDMX: computational studies. *Cell Cycle*, **9**, 1167-1181.

22. Patton,J.T., Mayo,L.D., Singhi,A.D., Gudkov,A.V., Stark,G.R., and Jackson,M.W. (2006) Levels of HdmX expression dictate the sensitivity of normal and transformed cells to Nutlin-3. *Cancer Res.*, **66**, 3169-3176.

23. Wade,M., Wong,E.T., Tang,M., Stommel,J.M., and Wahl,G.M. (2006) Hdmx modulates the outcome of p53 activation in human tumor cells. *J.Biol.Chem.*, **281**, 33036-33044.

24. Hu,B., Gilkes,D.M., Farooqi,B., Sebti,S.M., and Chen,J. (2006) MDMX overexpression prevents p53 activation by the MDM2 inhibitor Nutlin. *J.Biol.Chem.*, **281**, 33030-33035.

25. Chou,T.C. (2006) Theoretical basis, experimental design, and computerized simulation of synergism and antagonism in drug combination studies. *Pharmacol.Rev.*, **58**, 621-681.

26. Issaeva,N., Bozko,P., Enge,M., Protopopova,M., Verhoef,L.G., Masucci,M., Pramanik,A., and Selivanova,G. (2004) Small molecule RITA binds to p53, blocks p53-HDM-2 interaction and activates p53 function in tumors. *Nat.Med.*, **10**, 1321-1328.

27. Ly,L.V., Baghat,A., Versluis,M., Jordanova,E.S., Luyten,G.P., van Rooijen,N., van Hall,T., van der Velden,P.A., and Jager,M.J. (2010) In aged mice, outgrowth of intraocular melanoma depends on proangiogenic M2-type macrophages. *J.Immunol.*, **185**, 3481-3488.

28. Ahmed,A., Yang,J., Maya-Mendoza,A., Jackson,D.A., and Ashcroft,M. (2011) Pharmacological activation of a novel p53-dependent S-phase checkpoint involving CHK-1. *Cell Death.Dis.*, **2**, e160.

29. De Lange,J., Ly,L.V., Lodder,K., Verlaan-de Vries,M., Teunisse,A.F., Jager,M.J., and Jochemsen,A.G. (2011) Synergistic growth inhibition based on small-molecule p53 activation as treatment for intraocular melanoma. *Oncogene*.

30. Spinnler,C., Hedstrom,E., Li,H., De Lange,J., Nikulenkov,F., Teunisse,A.F., Verlaan-de Vries,M., Grinkevich,V., Jochemsen,A.G., and Selivanova,G. (2011) Abrogation of Wip1 expression by RITA-activated p53 potentiates apoptosis induction via activation of ATM and inhibition of HdmX. *Cell Death.Differ.*.

31. Yang,J., Ahmed,A., Poon,E., Perusinghe,N., de Haven,B.A., Box,G., Valenti,M., Eccles,S., Rouschop,K., Wouters,B., and Ashcroft,M. (2009) Small-molecule activation of p53 blocks hypoxia-inducible factor 1alpha and vascular endothelial growth factor expression in vivo and leads to tumor cell apoptosis in normoxia and hypoxia. *Mol.Cell Biol.*, **29**, 2243-2253.

32. Krajewski,M., Ozdowy,P., D'Silva,L., Rothweiler,U., and Holak,T.A. (2005) NMR indicates that the small molecule RITA does not block p53-MDM2 binding in vitro. *Nat.Med.*, **11**, 1135-1136.

33. Nieves-Neira,W., Rivera,M.I., Kohlhagen,G., Hursey,M.L., Pourquier,P., Sausville,E.A., and Pommier,Y. (1999) DNA protein cross-links produced by NSC 652287, a novel thiophene derivative active against human renal cancer cells. *Mol.Pharmacol.*, **56**, 478-484.

34. Rivera,M.I., Stinson,S.F., Vistica,D.T., Jorden,J.L., Kenney,S., and Sausville,E.A. (1999) Selective toxicity of the tricyclic thiophene NSC 652287 in renal carcinoma cell lines: differential accumulation and metabolism. *Biochem.Pharmacol.*, **57**, 1283-1295.

35. Lane,D.P., Cheok,C.F., and Lain,S. (2010) p53-based cancer therapy. *Cold Spring Harb.Perspect.Biol.*, **2**, a001222.

36. Shangary,S. and Wang,S. (2009) Small-molecule inhibitors of the MDM2-p53 protein-protein interaction to reactivate p53 function: a novel approach for cancer therapy. *Annu.Rev.Pharmacol.Toxicol.*, **49**, 223-241.

37. Reed,D., Shen,Y., Shelat,A.A., Arnold,L.A., Ferreira,A.M., Zhu,F., Mills,N., Smithson,D.C., Regni,C.A., Bashford,D., Cicero,S.A., Schulman,B.A., Jochemsen,A.G., Guy,R.K., and Dyer,M.A. (2010) Identification and characterization of the first small molecule inhibitor of MDMX. *J.Biol.Chem.*, **285**, 10786-10796.

38. Blagosklonny,M.V. and Darzynkiewicz,Z. (2002) Cyclotherapy: protection of normal cells and unshielding of cancer cells. *Cell Cycle*, **1**, 375-382.

Nederlandse samenvatting

Het menselijk lichaam is opgebouwd uit miljarden cellen. Cellen hebben het vermogen om zich te delen, wat nodig is voor groei en ontwikkeling en voor het herstellen van beschadigde weefsels. Het wel of niet delen van een cel is een zeer strak gereguleerd proces. Wanneer cellen aan deze regulatie ontsnappen, kan een tumor ontstaan. Tumorcellen verliezen hun normale functie, worden ongevoelig voor groeiremmende signalen van buitenaf en kunnen het orgaan beschadigen waarin ze zijn ontstaan. Bovendien kunnen (kwaadaardige) tumorcellen zich verspreiden door invasie van omringende weefsels en uitzaaiing via bloed- en lymfestromen. Elke cel bevat de complete set genetische informatie, het DNA. Daarvan wordt slechts een gedeelte gebruikt, afhankelijk van de functie van de cel en de specifieke omstandigheden. Wanneer nodig, wordt een stukje DNA (een gen) overgeschreven in messenger RNA en vervolgens vertaald in eiwit. Eiwitten zijn betrokken bij zeer uiteenlopende processen om de cel goed te laten functioneren, zoals transport, celstructuur, communicatie met andere cellen, signaaloverdracht en modificatie van andere eiwitten. De precieze volgorde van de bouwstenen van het DNA bepaalt de precieze volgorde van de bouwstenen van een eiwit. Een fout in het DNA kan dus leiden tot een fout in het eiwit, waardoor het eiwit en vervolgens de cel mogelijk niet meer naar behoren functioneert. Het is daarom van groot belang dat fouten of beschadigingen in het DNA snel worden opgespoord en adequaat worden bestreden. Het eiwit p53 speelt hierbij een cruciale rol. In gewone en gezonde cellen is p53 een grotendeels inactief eiwit, met name door toedoen van twee belangrijke p53-remmers, de eiwitten Hdm2 en Hdmx. Diverse omstandigheden die een potentieel risico vormen voor het ontstaan van kanker, bijvoorbeeld DNA schade, zuurstofgebrek of de aanwezigheid van ongewenste groeisignalen in de cel, leiden tot activering van p53. P53 zet vervolgens in de cel een heel proces in gang waarbij een groot aantal genen ‘aan’ dan wel ‘uit’ worden gezet. Dit proces kan leiden tot een tijdelijke stop van de celdeling en herstel van de schade, of tot het in gang zetten van geprogrammeerde celdood (apoptose genoemd). Dit gebeurt om te voorkomen dat de beschadigde cel een bedreiging gaat vormen voor de rest van het lichaam. Een tumor kan alleen ontstaan wanneer p53 om de een of andere reden niet werkt. Ongeveer de helft van alle menselijke tumoren heeft directe mutaties in het p53 gen, terwijl in de overige tumoren de functie van het p53 eiwit op een indirecte manier is geblokkeerd. Die cellen kunnen bijvoorbeeld een overmaat (‘overexpressie’) hebben van de p53-remmers Hdm2 en Hdmx. Dit proefschrift richt zich hoofdzakelijk op tumoren met ‘wildtype‘ p53, d.w.z. er zijn geen mutaties in het p53 gen.

Na een algemene inleiding in **hoofdstuk 1** van dit proefschrift, zoomt **hoofdstuk 2** verder in op de rol van Hdmx in het ontstaan van kanker. Van een aantal soorten kanker is bekend dat Hdmx overexpressie relatief vaak voorkomt. Een bekend voorbeeld is retinoblastoma,

een tumor die ontstaat in cellen van het netvlies en bij kinderen voorkomt. Het was nog niet zeker of Hdmx overexpressie inderdaad voldoende is om p53 te remmen in het proces van normale cellen naar tumorcellen. Dit hebben wij onderzocht. Uitgangspunt van onze studie waren twee soorten 'normale' (niet tumor) cellen: embryonale retinoblasten (cellen waaruit retinoblastoma kan ontstaan) en huidcellen. Het bleek dat verhoogde Hdmx expressie in beide celtypen inderdaad kan bijdragen aan de zogenoemde 'oncogene transformatie' van deze cellen: ze gaan zich meer gedragen als tumorcellen. Een belangrijke bevinding is dat de effecten van Hdmx overexpressie vergelijkbaar zijn met die van verlies van p53.

In **hoofdstuk 3** wordt een andere oogtumor onder de loep genomen: uveale melanoma. Aangezien deze melanomen (net zoals huidmelanomen) meestal geen p53-mutaties bevatten, zou Hdmx hier een belangrijke rol kunnen spelen. Onze analyse van tumoren van deze patiënten en van cellijnen die van dergelijke tumoren zijn afgeleid, wees uit dat Hdmx overexpressie inderdaad vaak voorkomt. Het experimenteel uitschakelen ('knockdown') van Hdmx blokkeerde bovendien de groei van de cellen met hoge Hdmx expressie, maar niet van cellen met lagere Hdmx expressie. Verrassend genoeg bleek knockdown van p53 niet zo goed het groeiremmende effect van Hdmx knockdown te kunnen voorkomen. Dit duidt erop dat Hdmx niet alleen p53 remt, maar daarnaast ook nog een andere, p53-onafhankelijke functie heeft die nodig is voor de groei van de onderzochte uveale melanoma cellen en wellicht ook in andere kankersoorten van belang is. Nader onderzoek naar deze nieuwe functie van Hdmx leverde aanwijzingen op voor een mogelijke betrokkenheid van het eiwit p27, dat de groei van cellen kan remmen, maar de precieze werking blijft vooralsnog onbekend.

Hoofdstuk 4 focust op het gebruik van specifieke p53-activators als methode om tumoren te bestrijden. In tumorcellen waarin het p53 gen zelf nog intact is, maar de functie van het p53 eiwit is geblokkeerd, kan p53 op een slimme manier worden gereactiveerd. Nutlin-3 is een klein molecuul dat speciaal ontworpen is om te binden aan Hdm2 en daardoor de Hdm2-p53 binding te voorkomen. Hierdoor wordt p53 niet langer geblokkeerd door Hdm2 en kan het zijn groeiremmende taak gaan uitvoeren. Inderdaad bleek Nutlin-3 in staat de groei van de eerder genoemde uveale melanoma cellen te stoppen. Nutlin-3 kon tevens *in vivo* de tumorgroei afremmen in een muismodel voor uveale melanoma. Echter, de groeiremming na behandeling met Nutlin-3 kwam vooral doordat de celdeling tijdelijk stopte, terwijl voor een echt effectieve tumorbestrijding de cellen zouden moeten doodgaan. Nutlin-3 bleek veel beter te werken in combinatie met een andere drug. Zowel Topotecan, een middel dat al gebruikt wordt in chemotherapie voor sommige tumoren, als

RITA, een andere experimentele p53-activator, bleek 'synergistisch' te werken met Nutlin-3. Dit betekent dat het effect van de combinatiebehandeling sterker was dan mocht worden verwacht op basis van de opgetelde individuele effecten. Dit kwam doordat de gebruikte combinatiebehandelingen meer celdood tot gevolg hadden. Deze toename van apoptose hield verband met de toename van een bepaalde modificatie van het p53 eiwit (fosforylering van serine 46). Deze modificatie, waarvan is geclaimd dat het specifiek leidt tot p53-geïnduceerde apoptose, bleek het resultaat te zijn van een cascade van reacties die wordt gestart als gevolg van DNA schade. Het is echter onzeker of deze DNA schaderespons en p53 modificatie ook daadwerkelijk de oorzaak zijn van de toegenomen apoptose.

Hoofdstuk 5 beschrijft een nader onderzoek naar het werkingsmechanisme van het eerder genoemde stofje RITA. RITA is een aantal jaren geleden in een grote screen opgepikt op basis van zijn vermogen om celgroei te remmen op een p53-afhankelijke manier. RITA veroorzaakt een relatief hoog percentage celdood in vergelijking met andere p53 activators, en gewone cellen lijken veel minder gevoelig dan tumorcellen. Dit zijn veelbelovende eigenschappen, maar hoe RITA precies werkt op moleculair niveau is nog heel onduidelijk. Wij hebben onderzoek gedaan naar het eiwit Chk2, waarvan bekend is dat het betrokken is bij de respons op DNA schade en mogelijke problemen bij de replicatie (het verdubbelen van het DNA). Mutaties in het Chk2 gen verhogen de kans op kanker. Onze experimenten laten zien dat Chk2 een cruciale rol speelt in de effecten van RITA op de cel. Onder meer de activering van p53, inductie van DNA schaderespons en inductie van apoptose door RITA zijn vrijwel volledig afhankelijk van de aanwezigheid van Chk2 in de cel. Deze bevindingen zijn belangrijk voor het beter begrijpen van het mechanisme dat ten grondslag ligt aan de uitwerking van RITA en dus voor de bruikbaarheid ervan als potentieel medicijn tegen kanker, aangezien Chk2 niet actief is in een deel van bepaalde kankersoorten.

Hoofdstuk 6 beziet de resultaten van dit proefschrift in een bredere context. De reactivering van p53 als behandelmethode voor kanker krijgt wereldwijd veel aandacht. Ons onderzoek heeft geleid tot waardevolle nieuwe inzichten, die kunnen bijdragen aan de ontwikkeling van nieuwe, effectievere tumorbehandelingen. Hdmx lijkt een belangrijke rol te spelen in meerdere soorten kanker met wildtype p53, waaronder de oogtumoren retinoblastoma en uveale melanoma. Dit maakt Hdmx een interessant eiwit om therapieën op te richten. De effectiviteit van p53-activering door Nutlin-3 kan sterk verbeterd worden door het te gebruiken in slimme drugcombinaties, zoals met Topotecan of RITA. De tumorgroei-remmende effecten van de experimentele p53-activator RITA blijken

grotendeels afhankelijk te zijn van het Chk2 eiwit. Deze waarneming benadrukt het belang van een snelle analyse van een tumor voordat besloten kan worden welke behandeling van de patiënt waarschijnlijk het meest effectief zal zijn.

Curriculum Vitae

Job de Lange was born on the 26th of November 1982 in Zwolle. After finishing the gymnasium at the Carolus Clusius College in Zwolle in 2001, he studied Biotechnology at Wageningen University. From July 2006 until January 2007 he did a research internship at the lab of Prof. Moshe Oren at the Weizmann Institute of Science in Rehovot, Israel. This internship stimulated his interest in cancer research in general and the p53 field in particular. Therefore, after obtaining the Master degree Medical Biotechnology, in July 2007 he joined the lab of Dr. AG Jochemsen at the LUMC in Leiden for his PhD training. Since November 2011 he is working as a postdoc in the lab of Dr. Johan de Winter at the VUMC in Amsterdam.

List of publications

Lenos K*, **De Lange J***, Teunisse AF, Lodder K, Verlaan - De Vries M, Wiercinska E, Van der Burg MJ, Szuhai K and Jochemsen AG (2011). Oncogenic functions of hMDMX in *in vitro* transformation of primary human fibroblasts and embryonic retinoblasts. *Molecular Cancer* **10**, 111

De Lange J, Teunisse AF, Verlaan - De Vries M, Lodder K, Lam S, Luyten GPM, Jager MJ and Jochemsen AG (2012). High levels of Hdmx promote cell growth in a subset of uveal melanomas. *Submitted manuscript*

De Lange J, Ly LV, Lodder K, Verlaan - De Vries M, Teunisse AF, Jager MJ and Jochemsen AG (2012). Synergistic growth inhibition based on small-molecule p53 activation as treatment for intraocular melanoma. *Oncogene* **31**, 1105-1116

De Lange J, Verlaan - De Vries M, Teunisse AF and Jochemsen AG (2012). Chk2 mediates RITA-induced apoptosis. *Cell Death and Differentiation, in press*

Gembarska A, Luciani F, Russell E, **De Lange J**, Yip D, Goydos J, Haigh JJ, Larue L, Jochemsen AG, Ghanem G, Bernal F and Marine JC (2012). MDM4 is a key therapeutic target in Melanoma. *Submitted manuscript*

Liang CY, **De Lange J**, Chen XW, Van Oers MM, Vlak JM and Westenberg M (2012). Functional analysis of two inhibitor of apoptosis (*iap*) orthologs from *Helicoverpa armigera* nucleopolyhedrovirus. *Virus Research, in press*

Spinnler C, Hedstrom E, Li H, **De Lange J**, Nikulenkov F, Teunisse AF, Verlaan - De Vries M, Grinkevich V, Jochemsen AG and Selivanova G (2011). Abrogation of Wip1 expression by RITA-activated p53 potentiates apoptosis induction via activation of ATM and inhibition of HdmX. *Cell Death and Differentiation* **18**, 1736-1745.

Phillips A, Teunisse A, Lam S, Lodder K, Darley M, Emaduddin M, Wolf A, Richter J, **De Lange J**, Verlaan - De Vries M, Lenos K, Bohnke A, Bartel F, Blaydes JP and Jochemsen AG (2010). HDMX-L is expressed from a functional p53-responsive promoter in the first intron of the HDMX gene and participates in an autoregulatory feedback loop to control p53 activity. *Journal of Biological Chemistry* **285**, 29111-29127